Deciphering the Metabolic Determinants of *Listeria monocytogenes* Virulence in the Host

By

Matthew J. Freeman

A dissertation submitted in partial fulfillment of

the requirements for the degree of:

Doctor of Philosophy

(Cellular and Molecular Biology)

at the

UNIVERSITY OF WISCONSIN-MADISON

2025

Date of final oral examination: 05/07/2025

The dissertation is approved by the following members of the Final Oral Committee:

John-Demian Sauer, Associate Professor, Medical Microbiology and Immunology

Laura Knoll, Professor, Medical Microbiology and Immunology

Jeniel Nett, Associate Professor, Medical Microbiology and Immunology

Johanna Elfenbein, Associate Professor, Pathobiological Sciences

Jason Cantor, Assistant Professor, Biochemistry

ACKNOWLEDGEMENTS

To Those Who Supported Me,

First, I want to acknowledge my space is limited here to thank all the people who made this work possible, if I have forgotten anyone – forgive me. In deepest appreciation I want to thank...

My PhD advisor, JD: Thank you so much. I wish words could really capture how grateful I am that I had the opportunity to learn from you. Undoubtably, I am both a better scientist and person from having been your student. You have given me balance during my PhD: When I spiraled - you picked me up; When I triumphed - you kept me humble. Most importantly you didn't just teach me hot to do science, you taught me how to love doing science. Thank you for being an awesome mentor. I will cherish and miss our chance to touch base casually and think about scientific problems together. I hope I can repay you by doing what you have done for me for my own student one day. Thank you for everything.

My Committee, Jason, Jeniel, Laura, Johanna: Thank you all for the time and dedication you put into guiding me through this work. Your hours spent in committee meetings, and answering my requests for help, and emails are deeply appreciated. I could not have done without all your ideas and mentorship.

My Clinical Mentors, Cristina and Jeniel: Dr. Sanger and Dr. Nett, thank you both for continuing to encourage the clinical part of my training during the PhD. You all always kept me passionate about caring for patients and making me a better future physician. You both have supported my love of science and medicine.

My undergrad, Noah: Noah, what can I say, you really are an amazing undergrad, scientist, and person. I want to thank you for teaching me as much, if not more, than I have taught you these two years. You have taught me the lingo of the young kids, but also how to be a better mentor. I also want to thank you for your diligent work in lab, while maintaining such a positive spirit. Right when I needed it you often rekindled my joy of coming into lab and being excited to do all things science. Your excitement for science is infectious, and I hope you will keep that passion going in wherever your life brings you. You *are* going to go on to do great things in your life and I can't wait to see them.

Past Sauer lab members, Zach M., Hans, Kim, Simone, Jess, Caroline, Kijeong, John, Grace: First, I really want to thank John. John we only overlapped for a year, but you have become a really close friend. I love being able to brainstorm about wild scientific ideas and philosophize about stuff that means absolutely nothing with you. I hope we will continue to connect and maybe get some backpacking and skiing in together. Zach, you also deserve a special thanks. I loved our late nights and early mornings in the lab and just being there and willing to work together on wild scientific ideas. Your willingness to push back always gave me perspective that I needed. Kijeong, I will always be grateful to have had to opportunity to get to know you – you were always quiet but somehow always knew the right words. Hans and Simone, thank you both for being models of diligent and thorough scientists – I was always envy your work ethic. Jess, I want to thank you for being such an exemplary role model. I hope I continue to work to be the type of scientist you are. Thank you to each one of you for teaching me so many life lessons and how to be a better scientist. For everyone mentioned or not here, I hope you all continue to go on to do great things.

Current lab members, Delanie, Abby, Alyssa, Chris, and Kevin: Honestly, I don't think I got to know you all as well as I would like given how hectic and busy the last year has been. What I can say is there is a time in every graduate student's experience where the lab entirely changes around them, and you all have been that change – and it has been an awesome one. I couldn't be more grateful and hopeful for the future of the lab thanks to your caring approach, scientific minds, and positive attitude. Keep it going, remember

to participate in team science, and help each other continue to build an amazing culture of science and friendship!

My undergraduate mentors: Drs. Linden, Marthaler, and Hallstrom: You all encouraged me to pursue science in my future, and I guess I have done that now? Seriously though, you all were so patient and caring to foster my scientific interest as an undergraduate. Thank you for all your advising, mentoring, and guidance that helped bring me to this place.

The UW-Madison MSTP: To all the friends and colleagues in the UW-Madison MSTP, thank you. This program has been so supportive through the trials of this type of program. You all have been so brilliant to learn from. Thank you for answering those late nights texts and helping build a strong program that trains great physician-scientists.

My family, Mom and Dad in particular: I want to thank all my brothers and sister (Phil, Al, Laura, Steve, John, and James) – you all have been great supports listening to my ranting calls or family dinners about my work. I am so thankful you all imparted advice from your lived experiences in my journey. Mom and Dad, you both deserve a very, very important thank you. You have supported me at every step of the way through my life. When I had a crazy goal or ideas your response was not whether I should go for it, but how could you help me go for it. Your love and caring means the world to me. I could not have asked for better parents and friends to bring me through life. I also need to thank you for all the encouragement when I needed it. In everyone's life there are dark days, you both somehow knew how to help me navigate those struggles. Thank you to my entire family, I love you all.

My pups, Morse and Rumble: You both are dogs and will never read this, but you deserve a thanks. You two have been loyal and loving without fault. I will cherish the nights spent with you on my lap while I was writing, reading, or working on a presentation. You both have had your little paws all over my thesis work and heart. You both probably deserve honorary doctorates for all the presentation you listened to me practice. Thank you pups!

My wife, Madi: I love you. Thank you for being the best life partner I could ask for. You have been such a diligent supporter of all my ambitions, and for that I will forever be grateful. I know at times my work has pushed and pulled us in many directions, but I want to tell you that I love you more than science and medicine, combined. I truly could not have done any of this without you. You brought me balance when I didn't know how to find it. You reminded me to breathe, to rest, and to laugh—especially when I felt overwhelmed. You've always seen the version of me I sometimes forget to believe in or embrace, and your love gave me strength on the hardest days. Through every draft, deadline, and detour, you've been there with patience, encouragement, and quiet strength. On that note, I also want to thank Lance and Heather for letting me into their family and being ardent supporters of me for years as I grew—it has been an honor and a privilege.

Finally Madi, you are my inspiration and my muse for everything I do. I will always be indebted to you for the love, grace, and joy you've brought into my life. I want to continue to grow and love with you, to keep the biggest experiment of my life alive – our relationship. I can't wait to take results, refine hypotheses, and write of a thesis of love and life together. Thank you so much for everything, and I hope I can repay all of this with a life of love and support together.

Again, to anyone not mentioned – thank you.

DISSERTATION ABSTRACT

All bacteria must carefully regulate carbon acquisition and utilization to meet their metabolic demands. Uniquely, bacterial pathogens such as *Listeria monocytogenes* (*L.* monocytogenes) face the additional challenge of acquiring host-derived nutrients while avoiding detection by the host immune system. *L. monocytogenes* represents an exceptional model for studying host-pathogen metabolic interactions, as it is both genetically tractable and a professional cytosolic pathogen. However, a comprehensive understanding of *L. monocytogenes*—and other intracellular pathogens'—carbon metabolism has been limited by technical constraints and an incomplete characterization of metabolic genetic determinants. Unraveling these metabolic strategies may provide critical insight into novel antimicrobial targets and undiscovered host immune pathways.

It has been widely accepted that *L. monocytogenes* primarily utilizes host-derived glycerol and hexose phosphates during intracellular infection, as demonstrated by isotopologue analyses from the Goebel and Eisenreich labs. However, *L. monocytogenes* mutants lacking the ability to catabolize glycerol (*ΔglpD/ΔgolD*) and/or import hexose phosphates (*ΔuhpT*) display near wild-type levels of intracellular growth and only modest virulence defects. These findings suggest that *L. monocytogenes* must exploit alternative cytosolic carbon sources to sustain intracellular replication and pathogenesis.

In support of this hypothesis, we have demonstrated that mutants lacking key components of the phosphotransferase system (PTS), specifically *ΔptsI* and *ΔptsH*, are unable to grow in the macrophage cytosol and exhibit significant attenuation *in vivo*. Strikingly, when we simultaneously disrupt all known major carbon acquisition pathways

(*ΔuhpT/ΔglpD/ΔgolD/ΔptsI*), the resulting strain is completely defective for cytosolic replication and is nearly avirulent *in vivo*. These results reveal that *L. monocytogenes* relies on a previously underappreciated metabolic strategy and depends heavily on PTS-mediated carbon uptake to support intracellular proliferation. More broadly, these findings highlight the potential for pathogens to use PTS as a critical mechanism for nutrient acquisition in the host cytosol. This discovery may inform our understanding of other bacterial pathogens' metabolic strategies and reveal novel vulnerabilities for therapeutic intervention. Additionally, our data suggest that previously described attenuation in *pdh* mutants is, in part, due to a loss of PTS function and associated redox imbalance. Together our work centralizes that PTS are both an essential acquisition tool for cytosolic pathogens and *L. monocytogenes* must be metabolically primed to be able to use these in the restrictive host cell environment.

While our work defines a broad role for PTS in supporting cytosolic growth, the specific carbon substrates imported via these systems remain unknown. Furthermore, how PTS interact with transcriptional regulation and mediate bacterial adaptation to the host environment is not yet fully understood. Given the high diversity of PTS systems among *L. monocytogenes* strains, these differences may contribute to variation in disease severity, host cell tropism, and persistence in food production environments. Understanding the specific roles of these systems may offer valuable insights for improving food safety and developing strain-specific interventions against *L. monocytogenes*.

TABLE OF CONTENTS

CHAPTER 1: Metabolic Determinants of Bacterial Pathogenesis and the strategies of *Listeria monocytogenes*

Authors and their contributions:

Matthew J. Freeman: Wrote and edited.

John-Demian Sauer, PhD: Supervised writing and editing.

*ChatGPT-4o was used for copy editing of my original ideas and writings using the prompt: “Can you copy edit part of my thesis to use correct scientific nomenclature and formatting while improving flow?”

Introduction and *Listeria monocytogenes* as a model organism and bacterial pathogen

Mortality caused by infectious diseases is projected to become the leading cause of death by 2050 (1). A subset of these infectious agents includes bacterial pathogens, which persist in various environmental reservoirs until an opportunity arises to infect a suitable host, save for those which are obligate human pathogens (2). One significant reservoir for bacterial pathogens is the food processing and production industry (3). Despite rigorous screening and treatment measures, certain pathogens, including *Escherichia coli*, *Salmonella* spp., *Campylobacter* spp., and *Listeria monocytogenes* (*L. monocytogenes*), are capable of surviving in these environments and causing disease (4). Notably, *L. monocytogenes* is the only Gram-positive bacterium among this group and is unique in its ability to exploit the host cytosol as a replicative niche (5,6). It is classified as a zero-tolerance pathogen in the food chain due to its significant public health implications (7). Even in the face of this classification *L. monocytogenes* is the source of multiple deadly outbreaks worldwide with some of the most notable being the 2011 U.S. cantaloupe outbreak, the 2017-2018 South African polony outbreak, and most recently the 2024 U.S. Boar's Head outbreak (8–10).

L. monocytogenes is a ubiquitous organism found in soil and the gastrointestinal tracts of various animals (11). It has been implicated in significant disease outbreaks in wildlife, particularly in Canidae, based on necropsy findings from infected animals (12,13). In addition, it is found to both colonized and infected livestock such as cattle, sheep, and goats (14). Beyond this list, *L. monocytogenes* is known to cause disease in a wide range of wildlife and pets in isolated case reports (15–17). Due to its public health significance, *L. monocytogenes* has been extensively

studied as a foodborne pathogen, a model for intracellular pathogenesis, and a tool for examining the innate and adaptive immune response.

Clinically, *L. monocytogenes* can cause the severe illness known as listeriosis, which is associated with high morbidity and mortality (18). Upon ingestion, *L. monocytogenes* must first withstand the highly bactericidal acidic environment of the stomach (19,20). Once in the intestines the exact mechanism by which *L. monocytogenes* gains access to the intracellular environment and disseminates within the host is still debated. Some evidence show that the bacterium gains access to colonic epithelial cells at the tips of villi through exposed E-cadherin, replicates, and disseminates via cell-to-cell spread (21,22). Other evidence suggests that it gains access to goblet cells and transcytoses into the lamina propria and where it is subsequently phagocytosed by resident macrophages in which it can replicate and disseminate (23). Finally, some work suggest that M cell may phagocytose *L. monocytogenes* allowing it to cross the epithelial barrier (23). Once across the epithelium, an essential part of its pathogenesis is to enter macrophages or dendritic cells through phagocytosis, facilitating its transport to mesenteric lymph nodes and systemic dissemination via hematogenous spread (24). Primary sites of infection include the spleen and liver, where *L. monocytogenes* predominantly infects splenocytes, macrophages, hepatocytes, and Kupffer cells (21,25). In severe cases, *L. monocytogenes* can breach the placental and blood-brain barriers, leading to severe outcomes such as fetal loss or neonatal infections and cerebellar meningitis, respectively (26,27). In response to the former, pregnant people are advised to avoid pre-processed meats, soft cheese, and unpasteurized dairy products (28). Because of the latter, when patients present with severe meningitis of unknown origin they are prophylactically treated with ampicillin to treat potential *L. monocytogenes* infection (29). While the precise mechanism by which *L.*

monocytogenes crosses the blood-brain barrier remains unclear, hypotheses include monocyte-mediated trojan horse entry, direct infection via cranial nerve V following oral ingestion, or dissemination through the vagus nerve after colonic colonization (26). The latter hypotheses is supported by evidence demonstrating bacterial migration along nerve axons at a rate of approximately one inch per hour, though this route has yet to be definitively confirmed experimentally (30). Despite appropriate diagnosis and treatment, listeriosis carries a case fatality rate of 20–30%, though this figure may be inflated due to underreporting of mild gastroenteritis cases that do not require medical intervention (31,32). Notably, humans may ingest *L. monocytogenes* more frequently than previously assumed, with studies suggesting an average annual exposure of four instances per person and detection in approximately 1-14% of raw sushi samples (33–35). This is exemplified by seminal work showing that 10% of human fecal samples show shedding of *L. monocytogenes* (36). Therefore, despite frequent exposure*, L. monocytogenes* can cause severe, often fatal listeriosis by surviving gastric acidity, invading intestinal and immune cells, and disseminating to organs including the liver, spleen, placenta, and brain, highlighting its complex and multifaceted pathogenesis.

Beyond its role as a significant public health threat, *L. monocytogenes* serves as a well-established model organism due to its defined intracellular lifecycle, genetic tractability, and robust infection models. This research has enabled robust characterization of *L. monocytogenes*' intracellular pathogenesis, particularly its master virulence regulator PrfA and its associated regulon (37,38). PrfA, a member of the Crp/Fnr family, senses the host cytosolic environment via glutathione binding and regulates virulence gene expression by recognizing a 14-base pair palindrome (PrfA box) within the -40 region of PrfA-dependent promoters (39,40). Mutations

that uncouple PrfA activation from glutathione binding, such as the Gly-145Ser mutation, lead to constitutive virulence gene expression known as PrfA* (41).

To successfully invade host cells, *L. monocytogenes* utilizes the PrfA regulated proteins internalin A (InlA) and internalin B (InlB) to bind host cell receptors E-cadherin and hepatocyte growth factor receptor (Met), respectively (42). Other tissue and cell specific internalins have been identified, but they do not appear to be conclusively essential for systemic *L. monocytogenes* infection and are most specific to complicating events such as placental or neurologic invasion (43,44). Alternatively, *L. monocytogenes* can be phagocytosed by immune cells, where it enters through an acidified phagolysosome. In either case, *L. monocytogenes* employs listeriolysin O (LLO), a pore-forming toxin encoded by *hly*, to escape into the host cytosol. Notably, LLO is specifically activated in acidic environments due to a pH-sensing acidic triad (E247, D208, D320), preventing inadvertent host cell damage (45–49). Additionally, LLO targets cholesterol-containing membranes, avoiding pore formation in bacterial membranes that lack cholesterol (50). Together this shows that to initiate infection, *L. monocytogenes* employs distinct invasion strategies and tightly regulated expression of virulence factors like internalins and listeriolysin O, enabling host cell entry and phagosomal escape while minimizing host damage.

Once in the cytosol, *L. monocytogenes* encounters a highly reducing environment enriched with glutathione, further promoting PrfA activation (39). This regulation is reinforced by a temperature-sensitive riboswitch that unfolds at 37°C, ensuring virulence factor expression occurs only at host physiologic temperatures (51). Since glutathione is essential for activating wild-type PrfA, *L. monocytogenes* imports it via oligopeptide permeases with cysteine

transporters (Opp/Ctp) or synthesizes it through glutathione synthetase (gshF), a PrfA-regulated gene critical for cytosolic survival (52–54). Current work suggests that *L. monocytogenes* is likely more reliant on the self-production of glutathione as opposed to acquiring it from the host (53). Finally, a well-characterized PrfA-regulated metabolic gene is *uhpT*, which encodes a hexose phosphate:phosphate antiporter thought to be important for *L. monocytogenes* to acquire host derived hexose phosphates (55).

Concurrent with cytosolic replication, *L. monocytogenes* exploits ActA, an additional PrfA regulated protein that recruits the host Arp2/3 complex to initiate actin polymerization, enabling intracellular motility and cell-to-cell spread via actin rockets (56–58). This process is facilitated by phospholipases PlcA and PlcB which degrade host membranes to promote dissemination to neighboring cells (59,60). Emerging evidence suggests that *L. monocytogenes* subpopulations within infected cells exhibit distinct roles, with pioneering bacteria prioritizing cell-to-cell spread while others remain metabolically active in the primary infected cell (61,62). This emerging perspective of bacteria population level division of labor is reminiscent of *Salmonella* spp. intracellular dynamics described by the Helaine lab (63,64).

L. monocytogenes has evolved sophisticated mechanisms to circumvent host immune defenses. For instance, it employs peritrichous flagella at lower temperatures for motility, yet represses flagellar expression at 37°C to evade cytosolic Toll-like receptor 5 (TLR5) detection (65). Extensive research into these virulence strategies has enabled the use of *L. monocytogenes* mutants as valuable controls in experimental models and has paved the way for novel therapeutic applications. Fo example, despite *L. monocytogenes*' evolved traits to avoid host cell detection it has been shown to be a potent activator of TLRs and STING, which does

permit robust protective responses (66,67). Further, our lab has shown that *L. monocytogenes* infection results in substantial, but transient, increase in prostaglandin-E2 production which is essential for robust T-cell mediate immunity and memory (68). One notable example is the development of live-attenuated *L. monocytogenes*-based vaccines, such as the Listeria-based attenuated double-deletion (LADD) strain, which lacks ActA and InlB to limit cell-to-cell spread and hepatocyte invasion. These mutations lead to approximately 1000-fold attenuation making it a stable platform (69,70). This platform has been explored for inducing potent T-cell responses against tumor antigens, demonstrating potential as an immunotherapeutic strategy against cancer (71). Through evolved immune evasion strategies and robust immunostimulatory properties, *L. monocytogene*s has become both a model for studying host-pathogen interactions and a promising platform for vaccine and cancer immunotherapy development.

Given its dual role as a model pathogen and a tool for studying intracellular survival strategies, *L. monocytogenes* remains a crucial focus of microbiological research. While many of its virulence determinants are well characterized, substantial gaps remain in understanding its metabolic adaptations to the cytosolic environment. Investigating these factors is particularly challenging due to the intricate interplay between host and bacterial metabolism, compounded by the limitations of *ex vivo* cell culture systems. Nevertheless, further exploration of *L. monocytogenes*' metabolic and genetic determinants promises to enhance our broader understanding of intracellular bacterial pathogenesis, with implications for developing novel therapeutics against not only *L. monocytogenes* but related pathogens.

The host cytosol as a restrictive replicative niche

For many years, it was believed that if a pathogen could access the host cytosol, it would encounter a highly protected, nutrient-replete, and privileged environment conducive to survival and replication. However, over the past two decades, this notion has been challenged (72). It is now clear that the cytosol is not merely a safe haven, but rather a hostile compartment that demands specialized machinery and evolutionary adaptations for access and survival.

Initial evidence suggesting that the cytosol constituted a permissive replicative niche emerged in the 1990s, when Bielecki et al. engineered a nonpathogenic *Bacillus subtilis* strain to express the pore-forming toxin listeriolysin O (LLO) from *L. monocytogenes*, enabling cytosolic entry. Once inside, *B. subtilis* proliferated readily, suggesting that the key limitation to cytosolic pathogenesis was the absence of virulence factors facilitating access (73). This conclusion was later refuted by Goebel and colleagues, who bypassed natural entry mechanisms by directly microinjecting bacteria into the cytosol of Caco-2 cells (74). Notably, bacterial species not specifically adapted to cytosolic life, such as *Bacillus* and *Salmonella*, were unable to survive and replicate; in fact, *Bacillus* was rapidly cleared. In contrast, other pathogens such as *Shigella* spp. and enteroinvasive *Escherichia coli* (EIEC) could replicate within single cells, while *L. monocytogenes* uniquely replicated and spread to neighboring cells (74). In partial reconciliation of these disparate findings, Goebel showed that rare replication of *B. subtillis* does occur in dead or dying cells (74). These findings underscored that cytosolic survival is a selective trait requiring distinct evolutionary adaptations. Moreover, they affirmed a critical distinction: cytosolic replication is mechanistically separate from the capacity to spread intercellularly—each requiring specific bacterial machinery.

While *Salmonella* spp. have since been recognized as capable of cytosolic replication under certain conditions, discrepancies between studies likely stem from differences in mode of entry and the transcriptional programs activated upon cytosolic exposure (75). The early work of Bielecki et al. has been further challenged by findings that *L. monocytogenes* mutants lacking ActA—a protein not encoded in *B. subtilis*—exhibit increased co-localization with polyubiquitin, the autophagy receptor p62, and LC3, a marker of mature autophagosomes, during macrophage infection (76,77). This autophagy-mediated targeting significantly reduces *L. monocytogenes* replication in the cytosol. Further evidence of host cell killing of pathogens not specifically adapted to the restrictive host cytosol include that *sifA* mutants of *Salmonella enterica* serovar Typhimurium are able to replicate in the cytosol of epithelial cells but are killed in the macrophage cytosol (78). Finally, *sdhA* mutants of *Legionella pneumophilia* cannot maintain vacuolar integrity and are killed once released into the cytosol (79). In sum, Cytosolic replication is tightly restricted by host defenses, with pathogens like *L. monocytogenes*, *Salmonella*, and *Legionella* requiring specific adaptations to avoid autophagy and cytosolic killing across different host cell types.

The work by Goebel et al. helped define a crucial subfield in bacterial pathogenesis: that cytosolic pathogens are a distinct class of bacterial pathogens warranting dedicated study, and that the cytosol is an environment with diverse defensive properties. Although we have thus far referred to the cytosol as a uniform compartment, research has shown that neither cytosolic composition nor access pathways to the cytosol are homogenous. In particular, cytosols of cells specialized in pathogen detection and clearance—such as macrophages and neutrophils—are particularly inhospitable to bacteria (80,81). For instance, phagosomes in neutrophils and macrophages mature rapidly and deploy toxic mechanisms to eliminate invaders, whereas

dendritic cells delay phagosomal maturation to preserve antigenic peptides for presentation (82,83). Further, our lab has previously shown that some *L. monocytogenes* mutants killed in the macrophage cytosol are not kill in the cytosol of Caco-2 cells (84). Finally, many myeloid cells that are interferon-γ stimulated produce guanylate binding proteins (GBPs) that can assemble of the surface of bacteria to activate the downstream inflammasome limiting bacterial survival (85,86). Taken together these findings show that not all cytosols are the same in their properties and so pathogens must be specifically adapted to the cytosol of each type of host cell they infect.

Multiple pattern recognition receptors (PRRs) monitor the cytosol for pathogen-associated molecular patterns (PAMPs), including AIM2-like receptors (ALRs), NOD-like receptors (NLRs), and the stimulator of interferon genes (STING), which detect bacterial double-stranded DNA, peptidoglycan fragments, and cyclic di-nucleotides, respectively, all of which have been implicated is *L. monocytogenes* pathogenesis (67,87–90). Despite these robust defenses, it has paradoxically been observed that intracellular bacteria often exploit cytosols of bactericidal immune cells—particularly macrophages—as replicative niches. This phenomenon, termed the "macrophage paradox," reflects the tendency of bacterial pathogens to preferentially target the macrophage cytosol despite its potent antimicrobial capabilities (91). It has been hypothesized that the reason for this is that macrophage cytosol serves as a "great filter" such that if a bacterial pathogen evolutionarily attempts to establish the cytosol as a replicative niche its must be able to do so in macrophages due to their role as key sentinels of bacterial invaders (91).

Further, multiple studies have revealed that cytosolic detection extends beyond structural recognition of PAMPs. Host cells can sense bacterial behavior—such as metabolic activity—within the cytosol (92,93). While many molecular mechanisms underpinning cytosolic immunity

have been characterized, much less is understood about how host metabolic state, host sub-tissues, and immune activation affect the shared metabolism between host and pathogen. A central theme in host-pathogen interactions is the co-evolution of metabolic strategies that permit survival without mutual destruction. One critical facet of this relationship is host-pathogen metabolic interplay. Host cells and bacteria have developed competing strategies: hosts utilize "nutritional immunity" to restrict access to key metabolites, while pathogens evolve mechanisms to circumvent or exploit these defenses (94–97). A well-known example of nutritional immunity is natural resistance-associated macrophage protein 1 (NRAMP1), which facilitates iron and manganese export during phagosomal maturation, thus limiting bacterial access to these essential cofactors (98,99). In another example of nutritional immunity, host-derived itaconate, produced by IRG1 in response to inflammation, inhibits bacterial succinate dehydrogenase (SDH), an essential component of the tricarboxylic acid (TCA) cycle (100,101). Intriguingly, many intracellular pathogens, including *L. monocytogenes*, lack SDH and exhibit a disrupted TCA cycle—possibly as an evolutionary adaptation to evade such inhibition (102). However, not all host attempts at nutrient sequestration hinder pathogens. In another example of nutritional immunity, the host expression of interferon-γ–induced indoleamine 2,3-dioxygenase (IDO) which limits intracellular tryptophan (103), however, in response to IDO activation, *Mycobacterium tuberculosis* upregulates its *de novo* tryptophan biosynthesis pathway (103). For instance, *L. monocytogenes* mutants deficient in riboflavin transporter RibU are unable to grow extracellularly and become obligate intracellular pathogens that scavenge riboflavin that has been sequestered into host cytosol (104). Similarly, *L. monocytogenes* must acquire host-derived lipoic acid from lipoyl peptides to support key dehydrogenase complexes (105). In summary, host-pathogen interactions in the cytosol are shaped by a dynamic metabolic arms race, where

hosts deploy nutritional immunity to restrict key nutrients and pathogens like L. monocytogenes evolve diverse strategies to evade or exploit these defenses for survival.

Macrophage polarization is another key component in shaping the metabolic environment during infection. The classical M1 vs. M2 paradigm reflects both functional and metabolic divergence: M1 macrophages, activated by IFN-γ, LPS, or GM-CSF, are pro-inflammatory and exhibit a glycolytic "Warburg-like" metabolic profile (106). M2 macrophages, induced by IL-4, IL-10, or IL-13, are anti-inflammatory and rely more on fatty acid oxidation and oxidative phosphorylation (107). Wild-type *L. monocytogenes* infection typically promotes an M1 phenotype, while attenuated strains have been shown to shift macrophages toward an M2 state (108,109). Interestingly, Miskoci et al. reported that *L. monocytogenes* infection in a zebrafish tail wound model recruited both M1- and M2-like macrophages (110). The rationale for promoting M1 polarization remains speculative, but may relate to the metabolic environment needed to support cytosolic bacterial growth. To date, no experiments in the literature have shown how M2-like macrophage polarization may differentially impact *L. monocytogenes*' ability to grow in the host cytosol. However, intriguing evidence that tangentially supports that M2-macrophages may be more restrictive to *L. monocytogenes* include that Hofbauer cells, a form of placental macrophages that display an M2-like phenotype basally, display low susceptibility to *L. monocytogenes* (111).

Although nutritional immunity is well characterized, a major emerging question is whether host cells can detect pathogen derived metabolism itself. Supporting this concept, groundbreaking work from the Bogyo lab (2016) showed that macrophages monitor their own metabolic flux using mitochondrial NAD^+/NADH ratios. Inhibition of flux—either via chemical inhibitors or *Salmonella* infection—triggered cell death and reduced infection. Supplementing

exogenous pyruvate rescued host mitochondrial function and redox balance (112). Similarly, Tucey et al. (2018) demonstrated competition for sugars between Candida spp. and host macrophages, where metformin-mediated increases in free sugar improved host survival (113). While bacterial metabolite theft can be detected, so to can the secretion of metabolites. For example, the Brodsky lab has shown that *Salmonella* spp. lacking aconitase induce rapid inflammasome activation via NLRP3 detection of altered mitochondrial activity secondary to excess secretion of citrate by the pathogen (114). These findings support the idea that bacterial pathogens must both carefully modulate their metabolic intake and outputs to prevent host cell detection and subsequent elimination.

Ultimately, regardless of the pathogen or host cell type, bacterial survival and replication hinge on metabolic adaptability. The ability to acquire or synthesize necessary nutrients is fundamental to intracellular pathogenesis. What remains to be fully understood is this metabolic interplay is a determinant of *L. monocytogenes* cytosolic survival and replication—both from the perspective of the pathogen and the host—with a particular focus on metabolism (93).

Use of forward genetic screens to identify metabolic genes essential for growth and virulence

Despite the significant selective pressures imposed by the host cytosol, bacterial pathogens—including *Listeria monocytogenes*—have evolved an array of tools to navigate these challenges and persist in this hostile environment. This phenomenon can be understood through the lens of the "Red Queen hypothesis," which posits that in predator-prey dynamics, such as host-pathogen interactions, both organisms undergo continual evolutionary changes to outcompete the other. This perpetual arms race continues until one party is driven to extinction (115–117).

While this co-evolutionary arms race may be more apparent in organisms that interact frequently, it is still critical determinant of pathogenesis for facultative intracellular pathogens like *L. monocytogenes*, which divides its life cycle between environmental reservoirs (as a saprophyte) and mammalian hosts (as a pathogen) (118). Although the specific environmental reservoir for *L. monocytogenes* remains poorly defined beyond detection in soil and decaying organic matter, the bacterium stably maintains all virulence determinants and pathogenic potential (119,120). This stability suggests frequent enough host interactions to preserve these traits under selective pressure.

A complementary, though not mutually exclusive, framework is the "Black Queen hypothesis." This theory proposes that evolutionary pressures may favor genome reduction, whereby organisms lose genes that are no longer essential due to reliance on shared functions provided by their environment or microbial community (121,122). Applying both hypotheses in parallel, one can posit that professional cytosolic pathogens such as *L. monocytogenes* possess streamlined genomes containing specialized genes finely tuned to withstand host-derived pressures. This insight opens the door for leveraging bacterial genetics and forward genetic screens to identify the determinants required for cytosolic survival and, in turn, uncover novel host defense mechanisms.

Forward genetic screens offer a powerful strategy to identify genes responsible for virulence phenotypes. These screens typically involve introducing random mutations across the bacterial genome and subjecting the resulting mutant library to a selective pressure—often within a host or host-derived environment—to pinpoint genes critical for survival. The conceptual foundation for bacterial genetic screening predates molecular genetics. In 1928, Frederick

Griffith performed a landmark experiment in which he co-injected mice with a non-virulent rough strain of *Streptococcus pneumoniae* and heat-killed cells from a virulent smooth strain. Remarkably, he recovered viable smooth strain bacteria from the mice's hearts, demonstrating that bacteria could exchange genetic material and that this material encoded virulence (123). The significance of genetic determinants in pathogenesis was further formalized by Stanley Falkow, who adapted Koch's postulates into a molecular framework. Falkow's molecular Koch's postulates state:

1. The virulence phenotype should be associated with pathogenic strains of a species;
2. Disruption of the gene responsible for the virulence trait should attenuate pathogenicity; and
3. Restoration of the gene should restore virulence (124).

These principles have underpinned the use of forward genetic screens as one of the most robust tools available for interrogating bacterial and host determinants of infection. Early screens relied on random mutagenesis via chemical agents (e.g., ethyl methanesulfonate) or ultraviolet radiation, with mutant libraries then challenged under selective conditions to identify phenotypes of interest—typically survival or loss thereof, the breadth of which is beyond the scope of this thesis.

A major advancement in bacterial forward genetics was the development of the Himar1 transposon system (125,126). Himar1 is a Class II DNA transposon from the mariner family that randomly inserts at TA dinucleotides, allowing high-density mutagenesis across the genome and enabling nearly comprehensive interrogation of non-essential genes. Transposon mutagenesis has been widely applied to numerous bacterial pathogens, including *L. monocytogenes*, and was

pivotal in the discovery of key virulence genes such as *prfA*, *hly* (encoding LLO), and *inlA/B* (127).

Our lab and others have employed Himar1 transposon mutagenesis to identify *L. monocytogenes* genes essential for cytosolic survival. In one early example, Zemanksy et al., (2009) utilized a Himar 1 mariner transposon to screen ~50,000 mutants for hypohemolytic phenotypes (126). This screen unveiled 8 mutants defect for hemolysis by *L. monocytogenes* and resulted in the characterization of *prsA2*-mediated LLO folding (126). More recently, the Woodward group (2024) utilized RECON-deficient mice—known to be hypersusceptible to *L. monocytogenes* infection—to screen an incomplete transposon library for virulence determinants during *in vivo* infection using Tn-Seq (128).

Notably, our lab designed and performed an unbiased forward genetic screen in 2017 aimed specifically at identifying *L. monocytogenes* genes required for survival in the cytosol (84). In brief, a gridded transposon-mutagenized library of *L. monocytogenes* was engineered to carry a plasmid encoding luciferase under control of a eukaryotic cytomegalovirus (CMV) promoter. These strains were then screened using immortalized bone marrow-derived macrophages (BMDMs) to identify bacterial mutants prone to cytosolic killing. Because wild-type (WT) *L. monocytogenes* only rarely lyses in the cytosol, mutants that exhibit increased lysis must harbor physiological defects that compromise intracellular survival. Upon lysis, the plasmid-encoded luciferase is released and expressed by the host cell, allowing mutant detection luminescence-based readouts (84). Screening thousands of mutants identified several genes critical for cytosolic survival. Intriguingly, the majority of mutants exhibiting increased bacteriolysis were disrupted in genes associated with key metabolic pathways. These included

genes involved in central carbon metabolism (e.g., pyruvate metabolism), anaerobic nucleotide biosynthesis, and menaquinone production. Additionally, this screen identified several mutants defective for cell wall biosynthesis, which we have now repeatedly shown to be an essential component of *L. monocytogenes* pathogenesis. Importantly, these mutants did not show increased lysis under *in vitro* conditions, underscoring that their defects were specific to the cytosolic host environment (84). Ongoing work in our lab and others continues to investigate these mutants to determine the underlying physiological mechanisms that govern *L. monocytogenes* survival in the cytosol. Together, these studies illustrate the power of forward genetic screens in uncovering bacterial factors essential for navigating host defenses, with metabolism emerging as a recurring and central theme.

Intracellular carbon metabolism of bacterial pathogens including *L. monocytogenes*

For bacterial pathogens to achieve their virulence goals and replicate, they—like all life—require access to sufficient carbon sources and metabolites within their respective niches. For intracellular pathogens, I posit three key tenets must be met:

1. The pathogen must acquire essential metabolites, either through auto-synthesis or via auxotrophic acquisition form the host.
2. It must compete with the host for specific resources when biosynthesis is not possible; and
3. It must avoid host detection, either during metabolite acquisition or through secretion of metabolic byproducts.

Failure to satisfy any of these requirements can compromise the pathogen's ability to meet its metabolic needs or may lead to immune recognition and elimination. Importantly, pathogens must meet these requirements for all metabolite classes—including metals, vitamins, amino acids, lipids, and carbohydrates.

Although technical limitations, non-physiologic models, and the dynamic metabolic landscape during infection have made it difficult to comprehensively define carbon source usage by intracellular pathogens, several broadly accepted models have emerged. One of the most studied frameworks is the concept of bipartite metabolism, in which intracellular pathogens partition carbon flux into catabolic and anabolic pathways, utilizing distinct substrates for energy production and biosynthesis, respectively (129,130). This model is supported by both isotopolog-based metabolic flux analysis and bacterial genetic studies. Notably, not all intracellular pathogens reside in the cytosol—many have adapted to life within pathogen-containing vacuoles, where nutrients are delivered via host solute carrier (SLC) transporters. Examples of vacuolar pathogens thought to use bipartite metabolism include *Legionella pneumophila*, *Coxiella burnetii*, and *Chlamydia trachomatis* (129,131–133). In several of these pathogens, bipartite metabolic strategies appear to be temporally regulated, with carbon source preference shifting according to growth phase during infection. For example, *L. pneumophila* preferentially utilizes the amino acids serine, cysteine, and alanine for energy production during exponential growth, while switching to carbohydrate metabolism during the post-exponential phase to fuel anabolic needs. Interestingly, *L. pneumophila* is also capable of scavenging host-derived pyruvate, though the relevance of this activity to virulence remains unclear (131,134–136). Similar patterns of partitioned carbon utilization have been reported in *C. burnetii* and *Salmonella enterica* serovar Typhimurium (132,137,138). *Mycobacterium tuberculosis*, another primarily vacuolar pathogen,

uses amino acids and performs fatty acid β-oxidation to generate acetyl-CoA and fuel the tricarboxylic acid (TCA) cycle (139,140).

Among other intracellular pathogens, *C. trachomatis* consumes host malate to support its TCA cycle and encodes a hexose phosphate transporter functionally analogous to *L. monocytogenes* UhpT, enabling the uptake of host-derived hexose phosphates for cell wall biosynthesis (133). In *L. monocytogenes*, isotope-based flux studies suggest utilization of host-derived glycerol and hexose phosphates during intracellular growth (129). Glycerol is thought to enter the cell via diffusion or through two independent transport facilitators, after which it is funneled through parallel pathways that converge at dihydroxyacetone phosphate (DHAP), feeding into the lower half of glycolysis for catabolic purposes (141,142). Hexose phosphates are imported via UhpT and routed into the pentose phosphate pathway to support anabolic processes such as nucleotide and cell wall biosynthesis (55,129). However, at the start of this thesis work it remained undetermined whether these metabolite are essential for *L. monocytogenes* pathogenesis. The reason for why these incorrect conclusions were made is difficult to assess, but is likely influenced by the complexity of isotopologue tracing of intracellular pathogens due to host metabolism of fed carbon sources and distortion of original carbon source. This observation underscores the need to further dissect *L. monocytogenes*' metabolic capabilities in the cytosol.

While the bipartite metabolism model provides a compelling explanation for how intracellular pathogens balance metabolic demands and immune evasion, it does not universally apply. A notable exception is *Shigella flexneri*, which has been shown to rely heavily on host-derived pyruvate for fueling its TCA cycle and supporting gluconeogenesis, with minor

contributions from glycerol and potentially glycolytic carbohydrates (143). Nonetheless, *S. flexneri* mutants deficient in pyruvate import remain virulent, implying the pathogen can access alternative carbon sources within the cytosol (143). This finding highlights the metabolic redundancy and adaptability of intracellular pathogens that requires further studies for a global understanding of metabolic pathogenicity.

Taken together, these studies illustrate that intracellular pathogens deploy diverse strategies to access carbon sources and meet their metabolic demands. The specific substrates used likely depend on several factors, including metabolic demand, nutrient availability, and the pathogen's enzymatic capacity to acquire and process particular metabolites. For instance, *L. monocytogenes* lacks a functional fatty acid degradation pathway and has never been shown to consume fatty acids *in vitro* or *in vivo* (102). Similarly, it lacks both the glyoxylate shunt and Entner–Doudoroff pathway, limiting its ability to convert two-carbon compounds into carbohydrates or metabolize sugars into pyruvate outside of central glycolysis (102). Curiously, *L. monocytogenes* and multiple other intracellular pathogen encode a "broken" TCA cycle, but the significance of this metabolic adaption remains unclear (102).

Beyond the capacity to utilize certain metabolites for anabolic or catabolic purposes, some metabolites can be inherently toxic or serve as signals that affect virulence gene regulation. This is best exemplified by sugar phosphate toxicity in a variety of bacteria, where accumulation of sugar-phosphate in the bacterial cytosol activates inhibitory enzymes or induces generalized stress responses (144,145). Thus, carbon metabolism is not only a matter of nutrient availability but also a key interface for immune evasion and virulence control. The field's current understanding of intracellular metabolism—and its integration with host responses—remains

limited. Addressing this knowledge gap will require new genetic approaches and more tractable *in vivo* systems to monitor metabolite dynamics during infection. Ultimately, a deeper understanding of how bacterial metabolism interfaces with the host environment holds the potential to advance our knowledge of pathogenesis, reveal new antimicrobial targets, and inform the development of attenuated bacterial strains for therapeutic purposes, including applications in cancer immunotherapy.

Role and function of phosphotransferase systems (PTS) in carbon acquisition and pathogenesis

As discussed previously, most bacterial pathogens must survive in both host associated and saprophytic conditions; as such, bacterial metabolism must be well adapted to both environments (92,130,146). One way bacterial pathogens have been primarily thought to acquire carbohydrates in the environment is using Phosphotransferase systems (PTS) (147,148). PTS are carbon import and metabolite uptake systems that are nearly universal in prokaryotes but notably absent in eukaryotes (147). More specifically, PTS are predominantly found in anaerobic and facultatively anaerobic bacteria, with fewer occurrences in obligate aerobes(149). This evolutionary divergence supports the idea that PTS, being unique to a subset of prokaryotes—and particularly to some bacterial pathogens—may represent valuable targets for future antimicrobial therapies (150–152).

PTS can mediate the uptake of a wide range of carbon substrates, including monosaccharides, disaccharides, amino sugars, and polyols, by catalyzing their import into the bacterial cytosol in a phosphorylated form (149). Interestingly, PTS have also been implicated in other cellular processes, such as peptidoglycan shedding and recycling, and in metabolite sharing

between co-inhabiting pathogens—for example, *Pseudomonas* and *Staphylococcus* species in cystic fibrosis lung infections (153). The phosphorylation and intake of sugars through PTS are driven by the conversion of phosphoenolpyruvate (PEP) to pyruvate. The phosphate from PEP is initially transferred to enzyme I (EI, encoded by *ptsI*), which then passes it to the HPr protein (encoded by *ptsH*), specifically at its phosphorylatable histidine residue. These initial steps are conserved across all known PTS systems. The phosphoryl group is subsequently transferred from HPr to a carbohydrate-specific permease complex, comprising components referred to as EIIA, EIIB, EIIC, and occasionally EIID. Once phosphorylated, these EII components facilitate sugar import and concomitant phosphorylation (149). The EII complexes are highly variable depending on the carbohydrate substrate (154). They are often redundant and may exhibit partial substrate promiscuity (155). There is substantial evidence that EII subunits can be shared across different PTS systems to compensate for incomplete complexes, albeit inefficiently (155,156). Together, these modular systems operate in a coordinated fashion to support carbohydrate import and central metabolism in many bacterial species (147).

Because multiple carbon sources may be available in most ecological niches, bacteria have evolved carbon catabolite repression (CCR) to prioritize the most energetically favorable substrates—typically via PTS (157,158). This hierarchical usage is exemplified by enteric bacteria preferentially consuming glucose before switching to secondary carbon sources, often producing a classic diauxic growth curve (149). One mechanism underlying this preference is known as inducer exclusion. When glucose is actively transported and phosphorylated via PTS, fewer EII proteins remain in their phosphorylated state. These dephosphorylated forms inhibit the uptake and metabolism of non-PTS carbohydrates. In parallel, decreased phosphorylation of EII components reduces activation of adenylate cyclase, thereby decreasing intracellular cAMP

levels—further modulating the expression of catabolic genes. Thus, while PTS systems are principally involved in carbohydrate acquisition, they also play a broader regulatory role in coordinating bacterial metabolism and gene expression (148,149,159).

PTS systems are increasingly recognized for their role in regulating bacterial virulence (92,102,141,160). For example, *Streptococcus pyogenes* mutants lacking *ptsI* (EI) exhibit increased skin lesion sizes and murine mortality despite lower bacterial loads, suggesting dysregulated virulence expression (161). Another proposed mechanism involves the phosphorylation of HPr at a conserved serine residue (HPr-Ser), a modification dependent on metabolic cues such as fructose-1,6-bisphosphate and ATP (149,162). This phosphorylation is mediated by HPr kinase (HPrK), generating HPr-Ser-P. Although the downstream regulatory targets remain unclear, it has been hypothesized that this modified form of HPr may directly influence virulence regulators such as PrfA in *Listeria monocytogenes* (163). Additionally, in *L. monocytogenes*, mutants with defective *ptsH* or *hprK* exhibit elevated expression of *prfA* and enhanced listeriolysin O (LLO)-mediated hemolytic activity (164,165).

Interestingly, the inverse relationship between PTS and virulence is not universally conserved. In *Salmonella enterica*, transposon insertions in *ptsI* lead to reduced expression of virulence genes associated with quorum sensing, SPI-3, type III secretion systems, flagella, and the PhoPQ regulon, as revealed by transcriptomic analyses (166). Notably, while core PTS components such as EI and HPr have not been comprehensively evaluated in *Salmonella*, some data suggest that PTS are important for intracellular nutrient acquisition. For example, deletion of the glucose-specific PTS results in moderate attenuation of virulence (138,160). In contrast, deletion of the 6-phosphofructokinase, responsible for the upper glycolytic conversion of

fructose-6-phosphate to fructose-1,6-bisphosphate, results in near full intracellular attenuation and clearance. This suggestes that other carbon sources, potentially some being PTS mediated, are feeding upper glycolysis to support *Salmonella*'s intracellular replication (138). However, due to the high redundancy of PTS systems, it remains challenging to isolate the contribution of individual transporters to pathogenesis.

Large-scale genomic analyses have provided further insight into the distribution and diversity of PTS systems across bacterial species. Several microbial lineages—including Actinobacteria (*Mycobacterium*, *Tropheryma*), Cyanobacteria, certain Proteobacteria (e.g., the cytosolic pathogen *Rickettsia*), and all known Archaea—lack PTS entirely (154). Others, such as *Burkholderia pseudomallei*, encode only a single PTS system, which has not yet been studied in the context of its cytosolic pathogenesis (154). In stark contrast, *L. monocytogenes* encodes 29 complete PTS systems involving 84 distinct genes. Moreover, PTS content can vary by clonal complex. For instance, clonal complex 4 (CC4), a hypervirulent lineage, encodes a cluster of six cellobiose-family PTS that appear to contribute to its enhanced pathogenicity (119). Nevertheless, the importance of PTS during infection remains variable. For example, *Shigella* species lacking *ptsI* can still grow intracellularly using imported pyruvate as a carbon source (143).

Taken together, PTS represent a highly diverse and adaptable set of carbohydrate import systems that support both nutrient acquisition and virulence gene regulation. The distribution of PTS across bacterial pathogens is heterogeneous, and their modularity allows for functional interchangeability of components. Surprisingly, despite their prevalence among intracellular and cytosolic pathogens, relatively few PTS systems have been studied in the context of infection.

We argue that a deeper understanding of PTS will improve our grasp of the carbon sources available inside host cells, reveal how host cells respond to bacterial metabolism, and identify new therapeutic avenues for disrupting bacterial nutrient acquisition.

Role and function of pyruvate dehydrogenase (PDH) physiological and during pathogenesis

Carbon acquisition is only one aspect of bacterial metabolism during infection. An additional key question—and a major focus of our work—is how these acquired carbon sources are funneled through available metabolic pathways to support the unique demands of the cytosolic niche. As described above, our lab performed a large-scale forward genetic screen in *Listeria monocytogenes* to identify transposon mutants that exhibit increased susceptibility to bacteriolysis in the cytosol of bone marrow-derived macrophages (84). While multiple genes and metabolic pathways were identified, one mutant of particular interest remains uncharacterized: a disruption in the pyruvate dehydrogenase complex (*pdhC::Tn*). Notably, although this mutant is killed at a higher rate in macrophages compared to wild type (WT), it grows readily in rich broth without lysis. This indicates that the defect is not due to a general physiological impairment, but rather reflects increased sensitivity to specific pressures encountered within the host cytosol (84).

The pyruvate dehydrogenase (PDH) complex operates at a critical metabolic junction between glycolysis and the tricarboxylic acid (TCA) cycle (149). It catalyzes the irreversible conversion of pyruvate to acetyl-CoA, a process essential for aerobic metabolism. This reaction plays a key role in the respiro-fermentative metabolism of *L. monocytogenes*, which our lab has previously shown to be important for the fitness of respiration-defective mutants (167–169). Although *L. monocytogenes* also encodes pyruvate formate lyase (PFL), which can convert pyruvate to acetyl-CoA under anaerobic conditions, this enzyme is highly sensitive to oxygen

due to its glycyl radical cofactor and produces formate—a toxic metabolic byproduct (141,165,169). Under aerobic or respiro-fermentative conditions, *L. monocytogenes* predominantly generates acetate from acetyl-CoA to regenerate NAD^+, and secondarily converts pyruvate to lactate (169).

The PDH complex itself is composed of multiple subunits with distinct roles. The E1 component (*pdhA* and *pdhB*) decarboxylates pyruvate, forming a reactive acetyl group bound to thiamine pyrophosphate (TPP) (149). This intermediate is then oxidized by the disulfide moiety in lipoic acid, which is covalently attached to the E2 subunit (*pdhC*). Of note, *L.* monocytogenes must acquire this lipoic acid from host cells and does not have its own lipoic acid biosynthesis pathway further supporting the metabolic interplay between *L. monocytogenes* and the host (105). The acetyl group is then transferred to coenzyme A (CoASH), generating acetyl-CoA and reduced lipoic acid. The E3 component (*pdhD*, also referred to as dihydrolipoamide dehydrogenase) subsequently reoxidizes the lipoic acid, passing electrons to FAD and ultimately reducing NAD^+ to NADH (149). Throughout this multistep reaction, metabolic intermediates remain tightly bound to the enzyme complex, likely to prevent dilution and unwanted side reactions. The net result of PDH activity is the generation of acetyl-CoA, NADH, and CO_2, using NAD^+ and CoASH as cofactors (149,170). Because PDH serves as a gatekeeper between glycolysis and the TCA cycle, its activity is tightly regulated. Known inhibitors of PDH include acetyl-CoA and NADH, which signal sufficient energy or metabolic flux. Conversely, the enzyme can be activated by high levels of phosphoenolpyruvate (PEP) and AMP, which serve as indicators of glycolytic flux and energy demand, respectively (170). In *Escherichia coli*, mutations that alter NADH sensitivity in PDH have been shown to restore activity under

otherwise inhibitory conditions (171). Despite the centrality of PDH in bacterial metabolism, relatively little is known about its role during pathogenesis—especially within the host cytosol.

Nonetheless, emerging studies are beginning to shed light on PDH's importance during infection (172,173). In *Shigella flexneri*, which relies on host-derived pyruvate that is ultimately converted to acetate, PDH is essential for intracellular survival and virulence (143). In contrast, pathogens that can bypass PDH through the uptake and metabolism of acetate or malate—feeding directly into the TCA cycle—may be less dependent on this complex. One instance where pathogens require the PDH complex is *Vibrio cholerae* requires PDH to metabolize host mucins and successfully colonize the gut (174). On instance where the PDH complex can be bypassed in in *Legionella pneumophila* where TCA metabolite are supplemented from fatty acid and amino acid degradation (134). However, other pathogens can bypass this need Beyond its metabolic function, recent work suggests that PDH may also influence host immune responses. In a striking example, *Staphylococcus aureus* was shown to suppress macrophage activation through the release of lipoylated E2-PDH subunits, indicating potential immunomodulatory roles beyond metabolic flux (175).

Taken together, these findings highlight that while PDH is a well-characterized metabolic enzyme, its role in *L. monocytogenes'*, and more generally bacterial pathogens', virulence and intracellular survival remains poorly understood. Studying the *pdhC::Tn* mutant and its associated phenotypes may uncover novel metabolic requirements for bacterial persistence in the host cytosol and provide insight into how intracellular pathogens adapt their core metabolism to evade host defenses.

Conclusions and relevance to this thesis

In aggregate, it is clear that *L. monocytogenes*, like many other bacterial pathogens, has evolved specifically to withstand the pressures of its replicative niche during infection. Understanding how *L. monocytogenes* adapts to and overcomes these pressures not only provides deeper insight into its unique biology but also offers broader insights into our understanding of other intracellular pathogens and how to effectively treat the infections they cause. In studying bacterial pathogenesis, we also gain valuable perspective on the host—how it detects, responds to, and defends itself against microbial invaders—and how both host and pathogen continually adapt within the ongoing evolutionary arms race.

This thesis approaches these questions through the lens of shared host–pathogen metabolism. More specifically, I examine current understanding of cytosolic bacterial carbon acquisition and metabolic adaptation. We aim to define the systems that *L. monocytogenes* uses to acquire carbon within the host cytosol and how these systems support its intracellular survival and virulence. To address this, we first utilized targeted mutagenesis to disrupt genes involved in the utilization of previously hypothesized cytosolic carbon sources—namely glycerol and hexose phosphates. Surprisingly, deletion of these pathways resulted in only modest impairment of *L. monocytogenes* virulence suggesting that additional, unidentified carbon sources are critical for intracellular replication. To identify these sources, we turned to an unbiased metabolic screen and found evidence that *L. monocytogenes* relies on phosphotransferase systems (PTS) as a major route for cytosolic carbon acquisition. We further investigated this through deletion of universally conserved PTS components (*ptsI* and *ptsH*), and found that without functional PTS, *L. monocytogenes* is unable to grow in the macrophage cytosol and is significantly

attenuated *in vivo*—especially when hexose phosphate and glycerol metabolism are also disrupted.

Next, we sought to understand the physiological basis for the virulence defects observed in pyruvate dehydrogenase (PDH) mutants, which are rapidly killed in the host cytosol (84). Using both hypothesis-driven experiments and unbiased metabolomics, we found that PDH mutants are globally starved for carbon and unable to utilize PTS-mediated carbon sources unless redox balance is restored or growth occurs under anaerobic conditions. To further probe this relationship, we performed a suppressor screen by growing PDH mutants on defined media containing PTS-dependent carbon sources and identified suppressor mutations that partially restored growth and virulence. These findings strongly suggest that a central defect in PDH mutants is the loss of access to PTS-acquired carbon sources—a phenotype that is genetically suppressible.

Together, this work advances our understanding of how *L. monocytogenes* acquires and metabolizes carbon within host cells. While these findings are novel, many questions remain. The specific carbon sources transported by PTS systems during infection are still undefined, and although the inability to utilize these sources explains a major component of the PDH mutant phenotype, these defects are likely pleiotropic. Further research is needed to understand the full range of physiological disruptions caused by PDH deficiency. Finally, one of the key open questions motivating this work is how host cells respond to and potentially detects metabolically perturbed bacteria. While this question lies beyond the scope of the current thesis, answering it will be critical to fully understanding *L. monocytogenes* pathogenesis—and more broadly, the pathogenesis of cytosolic and intracellular pathogens.

REFERENCES

1. Naghavi M, Vollset SE, Ikuta KS, Swetschinski LR, Gray AP, Wool EE, et al. Global burden of bacterial antimicrobial resistance 1990–2021: a systematic analysis with forecasts to 2050. The Lancet. 2024 Sep;404(10459):1199–226.

2. Thakur A, Mikkelsen H, Jungersen G. Intracellular Pathogens: Host Immunity and Microbial Persistence Strategies. Journal of Immunology Research. 2019 Apr 14;2019:1–24.

3. Alves VF, Tadielo LE, Pires ACMDS, Pereira MG, Bersot LDS, De Martinis ECP. Hidden Places for Foodborne Bacterial Pathogens and Novel Approaches to Control Biofilms in the Meat Industry. Foods. 2024 Dec 11;13(24):3994.

4. Abebe E, Gugsa G, Ahmed M. Review on Major Food-Borne Zoonotic Bacterial Pathogens. Journal of Tropical Medicine. 2020 Jun 29;2020:1–19.

5. Pizarro-Cerdá Javier, Cossart Pascale, Fischetti Vincent A., Novick Richard P., Ferretti Joseph J., Portnoy Daniel A., et al. Listeria monocytogenes: cell biology of invasion and intracellular growth. Microbiology Spectrum. 2018 Dec 7;6(6):6.6.05.

6. Slaghuis J, Goetz M, Engelbrecht F, Goebel W. Inefficient Replication of *Listeria innocua* in the Cytosol of Mammalian Cells. J INFECT DIS. 2004 Feb;189(3):393–401.

7. Pohl AM, Pouillot R, Van Doren JM. Changing US Population Demographics: What Does This Mean for Listeriosis Incidence and Exposure? Foodborne Pathogens and Disease. 2017 Sep;14(9):524–30.

8. Thomas J, Govender N, McCarthy KM, Erasmus LK, Doyle TJ, Allam M, et al. Outbreak of Listeriosis in South Africa Associated with Processed Meat. N Engl J Med. 2020 Feb 13;382(7):632–43.

9. Multistate outbreak of listeriosis associated with Jensen Farms cantaloupe--United States, August-September 2011. MMWR Morb Mortal Wkly Rep. 2011 Oct 7;60(39):1357–8.

10. Mohapatra RK, Mishra S, Tuglo LS, Sarangi AK, Kandi V, Al Ibrahim AA, et al. Recurring food source-based *Listeria* outbreaks in the United States: An unsolved puzzle of concern? Health Science Reports. 2024 Feb;7(2):e1863.

11. Vivant AL, Garmyn D, Piveteau P. Listeria monocytogenes, a down-to-earth pathogen. Front Cell Infect Microbiol [Internet]. 2013 [cited 2025 Apr 5];3. Available from: http://journal.frontiersin.org/article/10.3389/fcimb.2013.00087/abstract

12. Heiderich E, Origgi FC, Pisano SRR, Kittl S, Oevermann A, Ryser-Degiorgis† MP, et al. LISTERIA MONOCYTOGENES INFECTION IN FREE-RANGING RED FOXES (VULPES VULPES) AND EURASIAN LYNX (LYNX LYNX) IN SWITZERLAND. Journal of Zoo and Wildlife Medicine [Internet]. 2024 Mar 5 [cited 2025 Apr 5];55(1). Available from: https://bioone.org/journals/journal-of-zoo-and-wildlife-medicine/volume-55/issue-1/2022-0144/LISTERIA-MONOCYTOGENES-INFECTION-IN-FREE-RANGING-RED-FOXES-VULPES-VULPES/10.1638/2022-0144.full

13. Weyna AAW, Niedringhaus KD, Kunkel MR, Fenton HMA, Keel MK, Webb AH, et al. Listeriosis with viral coinfections in 8 gray foxes, 8 wild turkeys, and 2 young cervids in the southeastern United States. J VET Diagn Invest. 2022 Jul;34(4):654–61.

14. Zhao Q, Hu P, Li Q, Zhang S, Li H, Chang J, et al. Prevalence and transmission characteristics of *Listeria* species from ruminants in farm and slaughtering environments in China. Emerging Microbes & Infections. 2021 Jan 1;10(1):356–64.

15. Palacios-Gorba C, Moura A, Leclercq A, Gómez-Martín Á, Gomis J, Jiménez-Trigos E, et al. *Listeria* spp. Isolated from Tonsils of Wild Deer and Boars: Genomic Characterization. Dudley EG, editor. Appl Environ Microbiol. 2021 Feb 26;87(6):e02651-20.

16. Schoder D, Guldimann C, Märtlbauer E. Asymptomatic Carriage of Listeria monocytogenes by Animals and Humans and Its Impact on the Food Chain. Foods. 2022 Nov 1;11(21):3472.

17. Sévellec Y, Torresi M, Félix B, Palma F, Centorotola G, Bilei S, et al. First Report on the Finding of Listeria mnocytogenes ST121 Strain in a Dolphin Brain. Pathogens. 2020 Sep 28;9(10):802.

18. Scobie A, Kanagarajah S, Harris RJ, Byrne L, Amar C, Grant K, et al. Mortality risk factors for listeriosis - A 10 year review of non-pregnancy associated cases in England 2006-2015. J Infect. 2019 Mar;78(3):208–14.

19. O'Driscoll B, Gahan CG, Hill C. Adaptive acid tolerance response in Listeria monocytogenes: isolation of an acid-tolerant mutant which demonstrates increased virulence. Appl Environ Microbiol. 1996 May;62(5):1693–8.

20. Wemekamp-Kamphuis HH, Wouters JA, Sleator RD, Gahan CGM, Hill C, Abee T. Multiple Deletions of the Osmolyte Transporters BetL, Gbu, and OpuC of *Listeria monocytogenes* Affect Virulence and Growth at High Osmolarity. Appl Environ Microbiol. 2002 Oct;68(10):4710–6.

21. Pizarro-Cerda J, Kuhbacher A, Cossart P. Entry of Listeria monocytogenes in Mammalian Epithelial Cells: An Updated View. Cold Spring Harbor Perspectives in Medicine. 2012 Nov 1;2(11):a010009–a010009.

22. Pentecost M, Otto G, Theriot JA, Amieva MR. Listeria monocytogenes Invades the Epithelial Junctions at Sites of Cell Extrusion. Cossart P, editor. PLoS Pathog. 2006 Jan 27;2(1):e3.

23. Nikitas G, Deschamps C, Disson O, Niault T, Cossart P, Lecuit M. Transcytosis of *Listeria monocytogenes* across the intestinal barrier upon specific targeting of goblet cell accessible E-cadherin. Journal of Experimental Medicine. 2011 Oct 24;208(11):2263–77.

24. Nowacki JS, Jones GS, D'Orazio SEF. *Listeria monocytogenes* use multiple mechanisms to disseminate from the intestinal lamina propria to the mesenteric lymph nodes. Blondel CJ, editor. Microbiol Spectr. 2025 Feb 4;13(2):e02595-24.

25. Swaminathan B, Gerner-Smidt P. The epidemiology of human listeriosis. Microbes and Infection. 2007 Aug 1;9(10):1236–43.

26. Lecuit M. Understanding how Listeria monocytogenes targets and crosses host barriers. Clinical Microbiology and Infection. 2005 Jun;11(6):430–6.

27. Cossart P. Illuminating the landscape of host–pathogen interactions with the bacterium *Listeria monocytogenes*. Proc Natl Acad Sci USA. 2011 Dec 6;108(49):19484–91.

28. Caro R, Fast J. Pregnancy Myths and Practical Tips. 2020;102(7).

29. Mount HR, Boyle SD. Aseptic and Bacterial Meningitis: Evaluation, Treatment, and Prevention. 2017;96(5).

30. Henke D, Rupp S, Gaschen V, Stoffel MH, Frey J, Vandevelde M, et al. Listeria monocytogenes Spreads within the Brain by Actin-Based Intra-Axonal Migration. Blanke SR, editor. Infect Immun. 2015 Jun;83(6):2409–19.

31. Vázquez E, de Gregorio-Vicente O, Soriano V, Álvarez-Domínguez C, Corral O, Moreno-Torres V. Increased incidence and mortality from Listeria monocytogenes infection in Spain. Int J Infect Dis. 2024 Aug;145:107089.

32. Huang C, Lu TL, Yang Y. Mortality risk factors related to listeriosis — A meta-analysis. Journal of Infection and Public Health. 2023 May 1;16(5):771–83.

33. Stout A, Van Stelten-Carlson A, Marquis H, Ballou M, Reilly B, Loneragan GH, et al. Public health impact of foodborne exposure to naturally occurring virulence-attenuated *Listeria*

monocytogenes: inference from mouse and mathematical models. Interface Focus. 2020 Feb 6;10(1):20190046.

34. Atanassova V, Reich F, Klein G. Microbiological Quality of Sushi from Sushi Bars and Retailers. Journal of Food Protection. 2008 Apr 1;71(4):860–4.

35. Miya S, Takahashi H, Ishikawa T, Fujii T, Kimura B. Risk of *Listeria monocytogenes* Contamination of Raw Ready-To-Eat Seafood Products Available at Retail Outlets in Japan. Appl Environ Microbiol. 2010 May 15;76(10):3383–6.

36. Hafner L, Pichon M, Burucoa C, Nusser SHA, Moura A, Garcia-Garcera M, et al. Listeria monocytogenes faecal carriage is common and depends on the gut microbiota. Nat Commun. 2021 Nov 24;12(1):6826.

37. Leimeister-Wächter M, Haffner C, Domann E, Goebel W, Chakraborty T. Identification of a gene that positively regulates expression of listeriolysin, the major virulence factor of listeria monocytogenes. Proc Natl Acad Sci USA. 1990 Nov;87(21):8336–40.

38. Mengaud J, Dramsi S, Gouin E, Vazquez-Boland JA, Milon G, Cossart P. Pleiotropic control of *Listeria monocytogenes* virulence factors by a gene that is autoregulated. Molecular Microbiology. 1991 Sep;5(9):2273–83.

39. Hall M, Grundström C, Begum A, Lindberg MJ, Sauer UH, Almqvist F, et al. Structural basis for glutathione-mediated activation of the virulence regulatory protein PrfA in *Listeria*. Proc Natl Acad Sci USA. 2016 Dec 20;113(51):14733–8.

40. Scortti M, Monzó HJ, Lacharme-Lora L, Lewis DA, Vázquez-Boland JA. The PrfA virulence regulon. Microbes and Infection. 2007 Aug;9(10):1196–207.

41. Vega Y, Rauch M, Banfield MJ, Ermolaeva S, Scortti M, Goebel W, et al. New *Listeria monocytogenes prfA* * mutants, transcriptional properties of PrfA* proteins and structure–function of the virulence regulator PrfA. Molecular Microbiology. 2004 Jun;52(6):1553–65.

42. Gaillard JL, Berche P, Frehel C, Gouln E, Cossart P. Entry of L. monocytogenes into cells is mediated by internalin, a repeat protein reminiscent of surface antigens from gram-positive cocci. Cell. 1991 Jun;65(7):1127–41.

43. Conner KN, Burke JT, Ravi J, Hardy JW. Novel internalin P homologs in Listeria. Microbial Genomics [Internet]. 2022 Jul 29 [cited 2025 Apr 5];8(7). Available from: https://www.microbiologyresearch.org/content/journal/mgen/10.1099/mgen.0.000828

44. Ghosh P, Halvorsen EM, Ammendolia DA, Mor-Vaknin N, O'Riordan MXD, Brumell JH, et al. Invasion of the Brain by *Listeria monocytogenes* Is Mediated by InlF and Host Cell Vimentin. Freitag NE, editor. mBio. 2018 Mar 7;9(1):e00160-18.

45. Beauregard KE, Lee KD, Collier RJ, Swanson JA. pH-dependent Perforation of Macrophage Phagosomes by Listeriolysin O from *Listeria monocytogenes*. The Journal of Experimental Medicine. 1997 Oct 6;186(7):1159–63.

46. Henry R, Shaughnessy L, Loessner MJ, Alberti-Segui C, Higgins DE, Swanson JA. Cytolysin-dependent delay of vacuole maturation in macrophages infected with Listeria monocytogenes. Cell Microbiol. 2006 Jan;8(1):107–19.

47. Gaillard JL, Berche P, Mounier J, Richard S, Sansonetti P. In vitro model of penetration and intracellular growth of Listeria monocytogenes in the human enterocyte-like cell line Caco-2. Infect Immun. 1987 Nov;55(11):2822–9.

48. Mengaud J, Chenevert J, Geoffroy C, Gaillard JL. Identification of the Structural Gene Encoding the SH-Activated Hemolysin of Listeria monocytogenes: Listeriolysin 0 Is Homologous to Streptolysin 0 and Pneumolysin.

49. Vazquez-Boland JA, Kocks C, Dramsi S, Ohayon H, Geoffroy C, Mengaud J, et al. Nucleotide sequence of the lecithinase operon of Listeria monocytogenes and possible role of lecithinase in cell-to-cell spread. Infect Immun. 1992 Jan;60(1):219–30.

50. Seveau S. Multifaceted Activity of Listeriolysin O, the Cholesterol-Dependent Cytolysin of Listeria monocytogenes. In: Anderluh G, Gilbert R, editors. MACPF/CDC Proteins - Agents of Defence, Attack and Invasion [Internet]. Dordrecht: Springer Netherlands; 2014 [cited 2025 Apr 5]. p. 161–95. (Subcellular Biochemistry; vol. 80). Available from: https://link.springer.com/10.1007/978-94-017-8881-6_9

51. Loh E, Dussurget O, Gripenland J, Vaitkevicius K, Tiensuu T, Mandin P, et al. A trans-Acting Riboswitch Controls Expression of the Virulence Regulator PrfA in Listeria monocytogenes. Cell. 2009 Nov;139(4):770–9.

52. Berude JC, Kennouche P, Reniere ML, Portnoy DA. *Listeria monocytogenes* utilizes glutathione and limited inorganic sulfur compounds as sources of essential cysteine. Bäumler AJ, editor. Infect Immun. 2024 Mar 12;92(3):e00422-23.

53. Reniere ML, Whiteley AT, Portnoy DA. An In Vivo Selection Identifies Listeria monocytogenes Genes Required to Sense the Intracellular Environment and Activate Virulence Factor Expression. Brodsky IE, editor. PLoS Pathog. 2016 Jul 14;12(7):e1005741.

54. Portman JL, Dubensky SB, Peterson BN, Whiteley AT, Portnoy DA. Activation of the *Listeria monocytogenes* Virulence Program by a Reducing Environment. Miller JF, editor. mBio. 2017 Nov 8;8(5):e01595-17.

55. Chico-Calero I, Suárez M, González-Zorn B, Scortti M, Slaghuis J, Goebel W, et al. Hpt, a bacterial homolog of the microsomal glucose- 6-phosphate translocase, mediates rapid intracellular proliferation in Listeria. Proc Natl Acad Sci USA. 2002 Jan 8;99(1):431–6.

56. Kocks C, Gouin E, Tabouret M, Berche P, Ohayon H, Cossart P. L. monocytogenes-induced actin assembly requires the actA gene product, a surface protein. Cell. 1992 Feb;68(3):521–31.

57. Domann E, Wehland J, Rohde M, Pistor S, Hartl M, Goebel W, et al. A novel bacterial virulence gene in Listeria monocytogenes required for host cell microfilament interaction with homology to the proline-rich region of vinculin. The EMBO Journal. 1992 May;11(5):1981–90.

58. Tilney LG, Portnoy DA. Actin filaments and the growth, movement, and spread of the intracellular bacterial parasite, Listeria monocytogenes. Journal of Cell Biology. 1989 Oct 1;109(4):1597–608.

59. Camilli A, Tilney LG, Portnoy DA. Dual roles of plcA in Listeria monocytogenes pathogenesis. Mol Microbiol. 1993 Apr;8(1):143–57.

60. Smith GA, Marquis H, Jones S, Johnston NC, Portnoy DA, Goldfine H. The two distinct phospholipases C of Listeria monocytogenes have overlapping roles in escape from a vacuole and cell-to-cell spread. Infect Immun. 1995 Nov;63(11):4231–7.

61. Ortega FE, Koslover EF, Theriot JA. Listeria monocytogenes cell-to-cell spread in epithelia is heterogeneous and dominated by rare pioneer bacteria. eLife. 2019 Feb 5;8:e40032.

62. Radhakrishnan P, Theriot JA. *Listeria monocytogenes* cell-to-cell spread bypasses nutrient limitation for replicating intracellular bacteria [Internet]. 2025 [cited 2025 Apr 5]. Available from: http://biorxiv.org/lookup/doi/10.1101/2025.01.31.635960

63. Stapels DAC, Hill PWS, Westermann AJ, Fisher RA, Thurston TL, Saliba AE, et al. *Salmonella* persisters undermine host immune defenses during antibiotic treatment. Science. 2018 Dec 7;362(6419):1156–60.

64. Helaine S, Holden DW. Heterogeneity of intracellular replication of bacterial pathogens. Current Opinion in Microbiology. 2013 Apr 1;16(2):184–91.

65. Oh HB, Lee S jin, Yoon S il. Structural and biochemical analyses of the flagellar expression regulator DegU from Listeria monocytogenes. Sci Rep. 2022 Jul 7;12(1):10856.

66. Torres D, Barrier M, Bihl F, Quesniaux VJF, Maillet I, Akira S, et al. Toll-Like Receptor 2 Is Required for Optimal Control of *Listeria monocytogenes* Infection. Infect Immun. 2004 Apr;72(4):2131–9.

67. Sauer JD, Sotelo-Troha K, Von Moltke J, Monroe KM, Rae CS, Brubaker SW, et al. The *N* -Ethyl- *N* -Nitrosourea-Induced *Goldenticket* Mouse Mutant Reveals an Essential Function of *Sting* in the *In Vivo* Interferon Response to *Listeria monocytogenes* and Cyclic Dinucleotides. Flynn JL, editor. Infect Immun. 2011 Feb;79(2):688–94.

68. McDougal CE, Morrow ZT, Christopher T, Kim S, Carter D, Stevenson DM, et al. Phagocytes produce prostaglandin E2 in response to cytosolic Listeria monocytogenes. Coers J, editor. PLoS Pathog. 2021 Sep 23;17(9):e1009493.

69. Brockstedt DG, Giedlin MA, Leong ML, Bahjat KS, Gao Y, Luckett W, et al. *Listeria* -based cancer vaccines that segregate immunogenicity from toxicity. Proc Natl Acad Sci USA. 2004 Sep 21;101(38):13832–7.

70. Shahabi V, Reyes-Reyes M, Wallecha A, Rivera S, Paterson Y, Maciag P. Development of a Listeria monocytogenes based vaccine against prostate cancer. Cancer Immunol Immunother. 2008 Sep;57(9):1301–13.

71. Deng W, Lira V, Hudson TE, Lemmens EE, Hanson WG, Flores R, et al. Recombinant *Listeria* promotes tumor rejection by $CD8^+$ T cell-dependent remodeling of the tumor microenvironment. Proc Natl Acad Sci USA. 2018 Aug 7;115(32):8179–84.

72. O'Riordan M, Portnoy DA. The host cytosol: front-line or home front? Trends in Microbiology. 2002 Aug 1;10(8):361–4.

73. Bielecki J, Youngman P, Connelly P, Portnoy DA. Bacillus subtilis expressing a haemolysin gene from Listeria monocytogenes can grow in mammalian cells. Nature. 1990 May;345(6271):175–6.

74. Goetz M, Bubert A, Wang G, Chico-Calero I, Vazquez-Boland JA, Beck M, et al. Microinjection and growth of bacteria in the cytosol of mammalian host cells. Proc Natl Acad Sci USA. 2001 Oct 9;98(21):12221–6.

75. Drecktrah D, Knodler LA, Ireland R, Steele-Mortimer O. The Mechanism of *Salmonella* Entry Determines the Vacuolar Environment and Intracellular Gene Expression. Traffic. 2006 Jan;7(1):39–51.

76. Yoshikawa Y, Ogawa M, Hain T, Yoshida M, Fukumatsu M, Kim M, et al. Listeria monocytogenes ActA-mediated escape from autophagic recognition. Nat Cell Biol. 2009 Oct;11(10):1233–40.

77. Mitchell G, Ge L, Huang Q, Chen C, Kianian S, Roberts MF, et al. Avoidance of Autophagy Mediated by PlcA or ActA Is Required for Listeria monocytogenes Growth in Macrophages. Roy CR, editor. Infect Immun. 2015 May;83(5):2175–84.

78. Beuzón CR, Salcedo SP, Holden DW. Growth and killing of a Salmonella enterica serovar Typhimurium sifA mutant strain in the cytosol of different host cell lines. Microbiology. 2002 Sep 1;148(9):2705–15.

79. Creasey EA, Isberg RR. The protein SdhA maintains the integrity of the *Legionella* -containing vacuole. Proc Natl Acad Sci USA. 2012 Feb 28;109(9):3481–6.

80. O'Riordan M, Yi CH, Gonzales R, Lee KD, Portnoy DA. Innate recognition of bacteria by a macrophage cytosolic surveillance pathway. Proc Natl Acad Sci USA. 2002 Oct 15;99(21):13861–6.

81. Weinrauch Y, Drujan D, Shapiro SD, Weiss J, Zychlinsky A. Neutrophil elastase targets virulence factors of enterobacteria. Nature. 2002 May;417(6884):91–4.

82. Westcott MM, Henry CJ, Amis JE, Hiltbold EM. Dendritic Cells Inhibit the Progression of *Listeria monocytogenes* Intracellular Infection by Retaining Bacteria in Major Histocompatibility Complex Class II-Rich Phagosomes and by Limiting Cytosolic Growth. Infect Immun. 2010 Jul;78(7):2956–65.

83. Alloatti A, Kotsias F, Magalhaes JG, Amigorena S. Dendritic cell maturation and cross-presentation: timing matters! Immunological Reviews. 2016 Jul;272(1):97–108.

84. Chen GY, McDougal CE, D'Antonio MA, Portman JL, Sauer JD. A Genetic Screen Reveals that Synthesis of 1,4-Dihydroxy-2-Naphthoate (DHNA), but Not Full-Length Menaquinone, Is Required for *Listeria monocytogenes* Cytosolic Survival. Swanson MS, editor. mBio [Internet]. 2017 May 3 [cited 2021 Dec 14];8(2). Available from: https://journals.asm.org/doi/10.1128/mBio.00119-17

85. Wandel MP, Kim BH, Park ES, Boyle KB, Nayak K, Lagrange B, et al. Guanylate-binding proteins convert cytosolic bacteria into caspase-4 signaling platforms. Nat Immunol. 2020 Aug;21(8):880–91.

86. Hayward JA, Mathur A, Ngo C, Man SM. Cytosolic Recognition of Microbes and Pathogens: Inflammasomes in Action. Microbiol Mol Biol Rev. 2018 Dec;82(4):e00015-18.

87. Sauer JD, Pereyre S, Archer KA, Burke TP, Hanson B, Lauer P, et al. *Listeria monocytogenes* engineered to activate the Nlrc4 inflammasome are severely attenuated and are poor inducers of protective immunity. Proc Natl Acad Sci USA. 2011 Jul 26;108(30):12419–24.

88. Sauer JD, Witte CE, Zemansky J, Hanson B, Lauer P, Portnoy DA. Listeria monocytogenes Triggers AIM2-Mediated Pyroptosis upon Infrequent Bacteriolysis in the Macrophage Cytosol. Cell Host & Microbe. 2010 May;7(5):412–9.

89. Warren SE, Mao DP, Rodriguez AE, Miao EA, Aderem A. Multiple Nod-Like Receptors Activate Caspase 1 during *Listeria monocytogenes* Infection. The Journal of Immunology. 2008 Jun 1;180(11):7558–64.

90. Louie A, Bhandula V, Portnoy DA. Secretion of c-di-AMP by Listeria monocytogenes Leads to a STING-Dependent Antibacterial Response during Enterocolitis. Freitag NE, editor. Infect Immun. 2020 Nov 16;88(12):e00407-20.

91. Price JV, Vance RE. The Macrophage Paradox. Immunity. 2014 Nov;41(5):685–93.

92. Bhagwat A, Haldar T, Kanojiya P, Saroj SD. Bacterial metabolism in the host and its association with virulence. Virulence. 2025 Dec 31;16(1):2459336.

93. Chen GY, Pensinger DA, Sauer JD. *Listeria monocytogenes* cytosolic metabolism promotes replication, survival, and evasion of innate immunity. Cellular Microbiology. 2017 Oct;19(10):e12762.

94. Hood MI, Skaar EP. Nutritional immunity: transition metals at the pathogen–host interface. Nat Rev Microbiol. 2012 Aug;10(8):525–37.

95. Passalacqua KD, Charbonneau ME, O'Riordan MXD. Bacterial Metabolism Shapes the Host–Pathogen Interface. Kudva IT, Cornick NA, editors. Microbiol Spectr. 2016 May 6;4(3):4.3.13.

96. Olive AJ, Sassetti CM. Metabolic crosstalk between host and pathogen: sensing, adapting and competing. Nat Rev Microbiol. 2016 Apr;14(4):221–34.

97. Flannagan RS, Farrell TJ, Trothen SM, Dikeakos JD, Heinrichs DE. Rapid removal of phagosomal ferroportin in macrophages contributes to nutritional immunity. Blood Advances. 2021 Jan 26;5(2):459–74.

98. Barton CH, Biggs TE, Baker ST, Bowen H, Atkinson PGP. *Nrampl* : a link between intracellular iron transport and innate resistance to intracellular pathogens. Journal of Leukocyte Biology. 1999 Nov 1;66(5):757–62.

99. Jabado N, Jankowski A, Dougaparsad S, Picard V, Grinstein S, Gros P. Natural Resistance to Intracellular Infections: Natural Resistance–associated Macrophage Protein 1 (NRAMP1) Functions as a pH-dependent Manganese Transporter at the Phagosomal Membrane.

100. Peace CG, O'Neill LAJ. The role of itaconate in host defense and inflammation. Journal of Clinical Investigation. 2022 Jan 18;132(2):e148548.

101. Luan HH, Medzhitov R. Food Fight: Role of Itaconate and Other Metabolites in Antimicrobial Defense. Cell Metabolism. 2016 Sep;24(3):379–87.

102. Eisenreich W, Dandekar T, Heesemann J, Goebel W. Carbon metabolism of intracellular bacterial pathogens and possible links to virulence. Nat Rev Microbiol. 2010 Jun;8(6):401–12.

103. Schmidt SV, Schultze JL. New Insights into IDO Biology in Bacterial and Viral Infections. Front Immunol [Internet]. 2014 Aug 11 [cited 2025 Apr 5];5. Available from: http://journal.frontiersin.org/article/10.3389/fimmu.2014.00384/abstract

104. Rivera-Lugo R, Light SH, Garelis NE, Portnoy DA. RibU is an essential determinant of *Listeria* pathogenesis that mediates acquisition of FMN and FAD during intracellular growth. Proc Natl Acad Sci USA. 2022 Mar 29;119(13):e2122173119.

105. Keeney KM, Stuckey JA, O'Riordan MXD. LplA1-dependent utilization of host lipoyl peptides enables *Listeria* cytosolic growth and virulence. Molecular Microbiology. 2007 Nov;66(3):758–70.

106. Kelly B, O'Neill LA. Metabolic reprogramming in macrophages and dendritic cells in innate immunity. Cell Res. 2015 Jul;25(7):771–84.

107. Strizova Z, Benesova I, Bartolini R, Novysedlak R, Cecrdlova E, Foley LK, et al. M1/M2 macrophages and their overlaps – myth or reality? Clinical Science. 2023 Aug 14;137(15):1067–93.

108. D'Orazio SEF. Innate and Adaptive Immune Responses during *Listeria monocytogenes* Infection. Fischetti VA, Novick RP, Ferretti JJ, Portnoy DA, Braunstein M, Rood JI, editors. Microbiol Spectr. 2019 May 31;7(3):7.3.12.

109. Li X, Lyons AB, Woods GM, Körner H. The absence of TNF permits myeloid Arginase 1 expression in experimental L. monocytogenes infection. Immunobiology. 2017 Aug;222(8–9):913–7.

110. Miskolci V, Tweed KE, Lasarev MR, Britt EC, Walsh AJ, Zimmerman LJ, et al. In vivo fluorescence lifetime imaging of macrophage intracellular metabolism during wound responses in zebrafish. eLife. 2022 Feb 24;11:e66080.

111. Azari S, Johnson LJ, Webb A, Kozlowski SM, Zhang X, Rood K, et al. Hofbauer Cells Spread Listeria monocytogenes among Placental Cells and Undergo Pro-Inflammatory Reprogramming while Retaining Production of Tolerogenic Factors. Vazquez-Boland JA, editor. mBio. 2021 Aug 31;12(4):e01849-21.

112. Sanman LE, Qian Y, Eisele NA, Ng TM, van der Linden WA, Monack DM, et al. Disruption of glycolytic flux is a signal for inflammasome signaling and pyroptotic cell death. eLife. 2016 Mar 24;5:e13663.

113. Tucey TM, Verma J, Harrison PF, Snelgrove SL, Lo TL, Scherer AK, et al. Glucose Homeostasis Is Important for Immune Cell Viability during Candida Challenge and Host Survival of Systemic Fungal Infection. Cell Metabolism. 2018 May;27(5):988-1006.e7.

114. Wynosky-Dolfi MA, Snyder AG, Philip NH, Doonan PJ, Poffenberger MC, Avizonis D, et al. Oxidative metabolism enables Salmonella evasion of the NLRP3 inflammasome. Journal of Experimental Medicine. 2014 Apr 7;211(4):653–68.

115. Clay K, Kover PX. THE RED QUEEN HYPOTHESIS AND PLANT/PATHOGEN INTERACTIONS. Annu Rev Phytopathol. 1996 Sep;34(1):29–50.

116. Brockhurst MA, Chapman T, King KC, Mank JE, Paterson S, Hurst GDD. Running with the Red Queen: the role of biotic conflicts in evolution. Proc R Soc B. 2014 Dec 22;281(1797):20141382.

117. Stockmann C, Ampofo K, Pavia AT, Blaschke AJ, Mason EO, Presson AP, et al. Clinical and Epidemiological Evidence of the Red Queen Hypothesis in Pneumococcal Serotype Dynamics. Clin Infect Dis. 2016 Sep 1;63(5):619–26.

118. Freitag NE, Port GC, Miner MD. Listeria monocytogenes — from saprophyte to intracellular pathogen. Nat Rev Microbiol. 2009 Sep;7(9):623–8.

119. Maury MM, Bracq-Dieye H, Huang L, Vales G, Lavina M, Thouvenot P, et al. Hypervirulent Listeria monocytogenes clones' adaption to mammalian gut accounts for their association with dairy products. Nat Commun. 2019 Jun 6;10(1):2488.

120. Bécavin C, Bouchier C, Lechat P, Archambaud C, Creno S, Gouin E, et al. Comparison of Widely Used Listeria monocytogenes Strains EGD, 10403S, and EGD-e Highlights Genomic Differences Underlying Variations in Pathogenicity. Casadevall A, editor. mBio. 2014 May;5(2):e00969-14.

121. Morris JJ, Lenski RE, Zinser ER. The Black Queen Hypothesis: Evolution of Dependencies through Adaptive Gene Loss. mBio. 2012 May 2;3(2):e00036-12.

122. Souza LS, Irie Y, Eda S. Black Queen Hypothesis, partial privatization, and quorum sensing evolution. Taylor TB, editor. PLoS ONE. 2022 Nov 30;17(11):e0278449.

123. Müller GA. The Transformation Experiment of Frederick Griffith I: Its Narrowing and Potential for the Creation of Novel Microorganisms. Bioengineering. 2025 Mar 20;12(3):324.

124. Falkow S. Molecular Koch's postulates applied to microbial pathogenicity. Rev Infect Dis. 1988 Aug;10 Suppl 2:S274-276.

125. Simon R, Priefer U, Puhler A. A BROAD HOST RANGE MOBILIZATION SYSTEM FOR IN VIVO GENETIC ENGINEERING: TRANSPOSON MUTAGENESIS IN GRAM NEGATIVE BACTERIA. :8.

126. Zemansky J, Kline BC, Woodward JJ, Leber JH, Marquis H, Portnoy DA. Development of a *mariner* -Based Transposon and Identification of *Listeria monocytogenes* Determinants, Including the Peptidyl-Prolyl Isomerase PrsA2, That Contribute to Its Hemolytic Phenotype. J Bacteriol. 2009 Jun 15;191(12):3950–64.

127. Gaillard JL, Berche P, Sansonetti P. Transposon mutagenesis as a tool to study the role of hemolysin in the virulence of Listeria monocytogenes. Infect Immun. 1986 Apr;52(1):50–5.

128. Stamm CE, McFarland AP, Locke MN, Tabakh H, Tang Q, Thomason MK, et al. RECON gene disruption enhances host resistance to enable genome-wide evaluation of intracellular pathogen fitness during infection. Kline KA, editor. mBio. 2024 Aug 14;15(8):e01332-24.

129. Grubmuller S, Schauer K, Goebel W, Fuchs TM, Eisenreich W. Analysis of carbon substrates used by Listeria monocytogenes during growth in J774A.1 macrophages suggests a bipartite intracellular metabolism. Front Cell Infect Microbiol [Internet]. 2014 Nov 3 [cited 2022 Jun 2];4. Available from: http://journal.frontiersin.org/article/10.3389/fcimb.2014.00156/abstract

130. Best A, Abu Kwaik Y. Nutrition and Bipartite Metabolism of Intracellular Pathogens. Trends in Microbiology. 2019 Jun 1;27(6):550–61.

131. Häuslein I, Manske C, Goebel W, Eisenreich W, Hilbi H. Pathway analysis using^{13} C-glycerol and other carbon tracers reveals a bipartite metabolism of *Legionella pneumophila*. Molecular Microbiology. 2016 Apr;100(2):229–46.

132. Häuslein I, Cantet F, Reschke S, Chen F, Bonazzi M, Eisenreich W. Multiple Substrate Usage of Coxiella burnetii to Feed a Bipartite Metabolic Network. Front Cell Infect Microbiol. 2017 Jun 29;7:285.

133. Mehlitz A, Eylert E, Huber C, Lindner B, Vollmuth N, Karunakaran K, et al. Metabolic adaptation of *Chlamydia trachomatis* to mammalian host cells. Molecular Microbiology. 2017 Mar;103(6):1004–19.

134. Eylert E, Herrmann V, Jules M, Gillmaier N, Lautner M, Buchrieser C, et al. Isotopologue Profiling of Legionella pneumophila. Journal of Biological Chemistry. 2010 Jul;285(29):22232–43.

135. Schunder E, Gillmaier N, Kutzner E, Herrmann V, Lautner M, Heuner K, et al. Amino Acid Uptake and Metabolism of Legionella pneumophila Hosted by Acanthamoeba castellanii. Journal of Biological Chemistry. 2014 Jul;289(30):21040–54.

136. Oliva G, Sahr T, Buchrieser C. The Life Cycle of L. pneumophila: Cellular Differentiation Is Linked to Virulence and Metabolism. Front Cell Infect Microbiol. 2018 Jan 19;8:3.

137. Das P, Lahiri A, Lahiri A, Sen M, Iyer N, Kapoor N, et al. Cationic Amino Acid Transporters and Salmonella Typhimurium ArgT Collectively Regulate Arginine Availability towards Intracellular Salmonella Growth. Ahmed N, editor. PLoS ONE. 2010 Dec 3;5(12):e15466.

138. Bowden SD, Rowley G, Hinton JCD, Thompson A. Glucose and Glycolysis Are Required for the Successful Infection of Macrophages and Mice by *Salmonella enterica* Serovar Typhimurium. Infect Immun. 2009 Jul;77(7):3117–26.

139. Lee W, VanderVen BC, Fahey RJ, Russell DG. Intracellular Mycobacterium tuberculosis Exploits Host-derived Fatty Acids to Limit Metabolic Stress. Journal of Biological Chemistry. 2013 Mar;288(10):6788–800.

140. Mashabela GT, De Wet TJ, Warner DF. *Mycobacterium tuberculosis* Metabolism. Fischetti VA, Novick RP, Ferretti JJ, Portnoy DA, Braunstein M, Rood JI, editors. Microbiol Spectr. 2019 Jul 19;7(4):7.4.18.

141. Joseph B, Mertins S, Stoll R, Schär J, Umesha KR, Luo Q, et al. Glycerol Metabolism and PrfA Activity in *Listeria monocytogenes*. J Bacteriol. 2008 Aug;190(15):5412–30.

142. Crespo Tapia N, den Besten HMW, Abee T. Glycerol metabolism induces Listeria monocytogenes biofilm formation at the air-liquid interface. International Journal of Food Microbiology. 2018 May 20;273:20–7.

143. Kentner D, Martano G, Callon M, Chiquet P, Brodmann M, Burton O, et al. *Shigella* reroutes host cell central metabolism to obtain high-flux nutrient supply for vigorous intracellular growth. Proc Natl Acad Sci USA. 2014 Jul 8;111(27):9929–34.

144. Richards GR, Patel MV, Lloyd CR, Vanderpool CK. Depletion of Glycolytic Intermediates Plays a Key Role in Glucose-Phosphate Stress in Escherichia coli. J Bacteriol. 2013 Nov;195(21):4816–25.

145. Boulanger EF, Sabag-Daigle A, Baniasad M, Kokkinias K, Schwieters A, Wrighton KC, et al. Sugar-Phosphate Toxicities Attenuate Salmonella Fitness in the Gut. O'Toole G, editor. J Bacteriol. 2022 Dec 20;204(12):e00344-22.

146. Rohmer L, Hocquet D, Miller SI. Are pathogenic bacteria just looking for food? Metabolism and microbial pathogenesis. Trends in Microbiology. 2011 Jul;19(7):341–8.

147. Postma PW. Phosphoenolpyruvate:Carbohydrate Phosphotransferase Systems of Bacteria. MICROBIOL REV. 1993;57.

148. Saier Jr. MH. The Bacterial Phosphotransferase System: New Frontiers 50 Years after Its Discovery. Microb Physiol. 2015;25(2–3):73–8.

149. White D, Drummond JT, Fuqua C. The Physiology and Biochemistry of Prokaryotes [Internet]. Oxford University Press; 2012. Available from: https://books.google.com/books?id=ToF6pwAACAAJ

150. Oftedal TF, Ovchinnikov KV, Hestad KA, Goldbeck O, Porcellato D, Narvhus J, et al. Ubericin K, a New Pore-Forming Bacteriocin Targeting mannose-PTS. Howell KS, editor. Microbiol Spectr. 2021 Oct 31;9(2):e00299-21.

151. Simons A, Alhanout K, Duval RE. Bacteriocins, Antimicrobial Peptides from Bacterial Origin: Overview of Their Biology and Their Impact against Multidrug-Resistant Bacteria. Microorganisms. 2020 Apr 27;8(5):639.

152. Tymoszewska A, Aleksandrzak-Piekarczyk T. Subclass IId bacteriocins targeting mannose phosphotransferase system—Structural diversity and implications for receptor interaction and antimicrobial activity. Brenner D, editor. PNAS Nexus. 2024 Sep 2;3(9):pgae381.

153. Pajon C, Fortoul MC, Diaz-Tang G, Marin Meneses E, Kalifa AR, Sevy E, et al. Interactions between metabolism and growth can determine the co-existence of Staphylococcus aureus and Pseudomonas aeruginosa. eLife. 2023 Apr 20;12:e83664.

154. Barabote RD, Saier MH. Comparative Genomic Analyses of the Bacterial Phosphotransferase System. Microbiol Mol Biol Rev. 2005 Dec;69(4):608–34.

155. McCoy JG, Levin EJ, Zhou M. Structural insight into the PTS sugar transporter EIIC. Biochimica et Biophysica Acta (BBA) - General Subjects. 2015 Mar;1850(3):577–85.

156. Roth P, Jeckelmann JM, Fender I, Ucurum Z, Lemmin T, Fotiadis D. Structure and mechanism of a phosphotransferase system glucose transporter. Nat Commun. 2024 Sep 12;15(1):7992.

157. Görke B, Stülke J. Carbon catabolite repression in bacteria: many ways to make the most out of nutrients. Nat Rev Microbiol. 2008 Aug;6(8):613–24.

158. Behari J, Youngman P. A Homolog of CcpA Mediates Catabolite Control in Listeria monocytogenes but Not Carbon Source Regulation of Virulence Genes. J BACTERIOL. 1998;180.

159. Hogema BM, Arents JC, Bader R, Eijkemans K, Inada T, Aiba H, et al. Inducer exclusion by glucose 6-phosphate in *Escherichia coli*. Molecular Microbiology. 1998 May;28(4):755–65.

160. Pokorzynski ND, Groisman EA. How Bacterial Pathogens Coordinate Appetite with Virulence. Microbiol Mol Biol Rev. 2023 Sep 26;87(3):e00198-22.

161. Gera K, Le T, Jamin R, Eichenbaum Z, McIver KS. The Phosphoenolpyruvate Phosphotransferase System in Group A Streptococcus Acts To Reduce Streptolysin S Activity and Lesion Severity during Soft Tissue Infection. Camilli A, editor. Infect Immun. 2014 Mar;82(3):1192–204.

162. Choe M, Park YH, Lee CR, Kim YR, Seok YJ. The general PTS component HPr determines the preference for glucose over mannitol. Sci Rep. 2017 Feb 22;7(1):43431.

163. Woo JKK, Zimnicka AM, Federle MJ, Freitag NE. Novel motif associated with carbon catabolite repression in two major Gram-positive pathogen virulence regulatory proteins. Kolodkin-Gal I, editor. Microbiol Spectr. 2024 Nov 5;12(11):e00485-24.

164. Mertins S, Joseph B, Goetz M, Ecke R, Seidel G, Sprehe M, et al. Interference of Components of the Phosphoenolpyruvate Phosphotransferase System with the Central Virulence Gene Regulator PrfA of *Listeria monocytogenes*. J Bacteriol. 2007 Jan 15;189(2):473–90.

165. Liu Y, Ceruso M, Jiang Y, Datta AR, Carter L, Strain E, et al. Construction of *Listeria monocytogenes* Mutants with In-Frame Deletions in the Phosphotransferase Transport

System (PTS) and Analysis of Their Growth under Stress Conditions. Journal of Food Science [Internet]. 2013 Sep [cited 2024 Jul 7];78(9). Available from: https://ift.onlinelibrary.wiley.com/doi/10.1111/1750-3841.12181

166. Lim S, Seo HS, Jeong J, Yoon H. Understanding the multifaceted roles of the phosphoenolpyruvate: Phosphotransferase system in regulation of Salmonella virulence using a mutant defective in ptsI and crr expression. Microbiological Research. 2019 Jun 1;223–225:63–71.

167. Smith HB, Li TL. Listeria monocytogenes MenI Encodes a DHNA-CoA Thioesterase Necessary for Menaquinone Biosynthesis, Cytosolic Survival, and Virulence. Infection and Immunity. 2021;89(5):12.

168. Smith HB, Lee K, Freeman MJ, Stevenson DM, Amador-Noguez D, Sauer JD. Listeria monocytogenes requires DHNA-dependent intracellular redox homeostasis facilitated by Ndh2 for survival and virulence. Infection and Immunity. 2023;91(10):e00022-23.

169. Rivera-Lugo R, Deng D, Anaya-Sanchez A, Tejedor-Sanz S, Tang E, Reyes Ruiz VM, et al. Listeria monocytogenes requires cellular respiration for NAD+ regeneration and pathogenesis. eLife. 2022 Apr 5;11:e75424.

170. Patel MS, Nemeria NS, Furey W, Jordan F. The Pyruvate Dehydrogenase Complexes: Structure-based Function and Regulation. Journal of Biological Chemistry. 2014 Jun;289(24):16615–23.

171. Kim Y, Ingram LO, Shanmugam KT. Dihydrolipoamide Dehydrogenase Mutation Alters the NADH Sensitivity of Pyruvate Dehydrogenase Complex of *Escherichia coli* K-12. J Bacteriol. 2008 Jun;190(11):3851–8.

172. Wang Y, Wang Y, Liu B, Wang S, Li J, Gong S, et al. *pdh* modulate virulence through reducing stress tolerance and biofilm formation of *Streptococcus suis* serotype 2. Virulence. 2019 Jan 1;10(1):588–99.

173. Venugopal A, Bryk R, Shi S, Rhee K, Rath P, Schnappinger D, et al. Virulence of Mycobacterium tuberculosis Depends on Lipoamide Dehydrogenase, a Member of Three Multienzyme Complexes. Cell Host & Microbe. 2011 Jan;9(1):21–31.

174. Van Alst AJ, DiRita VJ. Aerobic Metabolism in Vibrio cholerae Is Required for Population Expansion during Infection. Groisman EA, editor. mBio. 2020 Oct 27;11(5):e01989-20.

175. Grayczyk JP, Harvey CJ, Laczkovich I, Alonzo F. A Lipoylated Metabolic Protein Released by Staphylococcus aureus Suppresses Macrophage Activation. Cell Host & Microbe. 2017 Nov;22(5):678-687.e9.

CHAPTER 2: *Listeria monocytogenes* Requires Phosphotransferase Systems to Facilitate Intracellular Growth and Virulence

Authors and their contributions:

Matthew J. Freeman: Planned and conducted experiments, wrote, and edited this manuscript.

Noah J. Eral: Planned and conducted experiments and edited this manuscript.

John-Demian Sauer: Supervised all research and contributed to the design of experiments, edited this manuscript.

As published from Freeman *et. al*., *PLOS Pathogens*, May 2025

ABSTRACT

The metabolism of bacterial pathogens is exquisitely evolved to support virulence in the nutrient-limiting host. Many bacterial pathogens utilize bipartite metabolism to support intracellular growth by splitting carbon utilization between two carbon sources and dividing flux to distinct metabolic needs. For example, previous studies suggest that the professional cytosolic pathogen Listeria monocytogenes (L. monocytogenes) utilizes glycerol and hexose phosphates (e.g. Glucose-6-Phosphate) as catabolic and anabolic carbon sources in the host cytosol, respectively. However, the role of this putative bipartite metabolism in L. monocytogenes virulence has not been fully assessed. Here, we demonstrate that when L. monocytogenes is unable to consume either glycerol (Δ*glpD*/Δ*golD*), hexose phosphates (Δ*uhpT*), or both (Δ*glpD*/Δ*golD*/Δ*uhpT*), it is still able to grow in the host cytosol and is 10- to 100-fold attenuated in vivo suggesting that L. monocytogenes consumes alternative carbon source(s) in the host. An in vitro metabolic screen using BioLog's phenotypic microarrays unexpectedly demonstrated that WT and PrfA* (G145S) L. monocytogenes, a strain with constitutive virulence gene expression, use phosphotransferase system (PTS) mediated carbon sources. These findings contrast with the existing metabolic model that cytosolic L. monocytogenes expressing PrfA does not use PTS mediated carbon sources. We next demonstrate that two independent and universal phosphocarrier proteins (PtsI [EI] and PtsH [HPr]), essential for the function of all PTS, are critical for intracellular growth and virulence in vivo. Constitutive virulence gene expression using a PrfA* (G145S) allele in Δ*glpD*/Δ*golD*/Δ*uhpT* and Δ*ptsI* failed to rescue in vivo virulence defects suggesting phenotypes are due to metabolic disruption and not virulence gene regulation. Finally, in vivo attenuation of Δ*ptsI* and Δ*ptsH* was additive to Δ*glpD*/Δ*golD*/Δ*uhpT*, suggesting that hexose phosphates and glycerol and PTS mediated carbon

source are relevant metabolites. Taken together, these studies indicate that PTS are critical virulence factors for the cytosolic growth and virulence of L. monocytogenes.

AUTHOR SUMMARY

Listeria monocytogenes is an important bacterial pathogen and the causative agent of listeriosis, a foodborne infection associated with significant morbidity and mortality. *L. monocytogenes* lives in a diverse set of environments including as a saprophyte in the soil and in the cytosol of host cells during infection. Understanding the metabolic crosstalk between host cells and their bacterial invaders can illuminate mechanisms of bacterial pathogenesis and the host response and could lead to the development of novel treatments in a world of ever-increasing antibiotic resistance. Here we use bacterial genetics combined with metabolic screens to identify how *L. monocytogenes* acquires nutrients from the host during infection. We find that *L. monocytogenes* uses a combination of host cell derived hexose phosphates, glycerol, and free sugars to support its metabolic needs during infection. Specifically, we find *L. monocytogenes* requires its arsenal of phosphotransferase systems (PTS), a set of free sugar importers, to survive and replicate during infection. Together our results broaden our understanding of how cytosolic pathogens acquire nutrients to support their metabolic needs during infection and highlight novel targets for future therapeutic intervention.

INTRODUCTION

The mammalian cytosol is a stringent and hostile environment that restricts the growth of bacteria not specifically adapted to that niche (1–5). One mediator of bacterial growth restriction in the host cytosol is nutrient availability whereby cells actively or passively limit access to vital nutrient resources preventing bacterial growth. For example, intracellular pathogens are metabolically restricted through limited access to metal ions, vitamin cofactors, and amino acid pools (6–9). More specifically, macrophages contribute to this metabolic foray by shifting metabolism between M1 or M2 states, altering concentrations of metals, and rewiring glycolysis and the tricarboxylic acid cycle to control bacterial pathogens (10–12). Despite this well-orchestrated defense, canonical cytosolic pathogens such as *Listeria monocytogenes* (*L. monocytogenes*) can replicate in this environment at a rate equivalent to that in rich media (13). This rapid growth allows *L. monocytogenes* to overtake host defenses and disseminate to distant sites of infection from the intestine (spleen, liver, & meninges), resulting in a mortality rate approaching 30% (14–16). Defining bacterial metabolism can reveal novel targets for antibiotics and a better understanding of host-pathogen interactions. Despite significant progress, there are significant unknowns about what metabolites pathogens such as *L. monocytogenes* are using in their respective host environments, how these nutrients are acquired, and what impact this has on the host response to infection (17–20). Key challenges to progress in understanding host-pathogen metabolisms include an incomplete understanding of the metabolic profile of host cells during infection and redundant metabolic pathways in both the host and the pathogen.

In addition to *L. monocytogenes'* role as an important pathogen, it serves as a powerful model organism to answer questions about host-pathogen interactions (21). *L. monocytogenes*' virulence genes and intracellular lifecycle have been well studied including in macrophages

which serve as a primary replicative niche and host dissemination vehicle (13,22). *L. monocytogenes* encodes the master transcriptional virulence regulator, PrfA, that controls many key virulence factors to mediate the *L. monocytogenes* cytosolic lifecycle including Listeriolysin O (LLO) that facilitates cytosolic access, the phospholipase Cs (PLCs) that contribute to secondary vacuole escape, ActA which mediates intracellular motility and cell-to-cell spread, and the hexose phosphate transporter UhpT which contributes to cytosolic metabolism (13,22). PrfA is activated upon entry into the cytosol via allosteric regulation by glutathione, however PrfA* mutations such as the G145S mutation result in constitutive virulence gene expression and upregulation of *uhpT,* the *L. monocytogenes* hexose phosphate transporter (23–25). Finally, well-defined *ex vivo* and *in vivo* models of *L. monocytogenes* infection and its genetic tractability allow for a thorough examination of how metabolic perturbation might impact its virulence and host response to that metabolic perturbation (26).

Previously, *L. monocytogenes* has been employed as a tool to understand bacterial cytosolic metabolism through isotopologue analysis. Specifically, this work examined the metabolism of *L. monocytogenes* during the infection of macrophages, a necessary step in disseminated infection *in vivo* (27,28). The Eisenreich and Goebel groups previously identified glycerol and hexose phosphates (e.g. Glucose-6-Phosphate) as the primary carbon metabolites used by *L. monocytogenes* during cytosolic replication (29–32). These findings were supported by the fact that *Listeria innocua*, a non-pathogenic *Listeria* species, lacks the transporter necessary for use of hexose phosphates (UhpT) and that glycerol is a common metabolite used by a variety of intracellular pathogens (33,34). Further, these analyses suggested that glycerol and hexose phosphates are primarily funneled into lower glycolytic catabolism and pentose phosphate pathway anabolism, respectively. Despite this, *L. monocytogenes* mutants lacking the

ability to use glycerol (Δ*glpD*) or hexose phosphates (Δ*uhpT*) individually maintain intracellular growth and significant virulence (29,32). The lack of robust virulence phenotypes could be due to incomplete perturbation of specific carbon source use, a lack of physiologic relevancy of the *ex vivo* models, or the ability of *L. monocytogenes* to utilize alternative, yet to be defined carbon sources (35–39).

In addition to being able to replicate in the host cytosol following infection, *L. monocytogenes* also lives as a saprophyte in the environment and in food production facilities where its metabolic potential has also been studied intensely (40–42). Like many other bacteria, *L. monocytogenes* can utilize phosphotransferase systems (PTS) in these environments to acquire free sugar (43). The *L. monocytogenes* 10403s strain used in this study encodes 29 complete PTS, encoded by a collection of 86 genes (39,44,45). Interestingly, other *L. monocytogenes* strains as well as different *Listeria* species such as *L. innocua* and *L. welshimeri* vary in the specific PTS they encode suggesting flexibility in the use of PTS (46–49). Early work has shown these differences may be important for virulence, but a global understanding of their importance remains unknown (46,49,50). Mechanisms of PTS function are well-defined and reviewed elsewhere (51); yet, there are many open questions about the relationship between PTS components' structure, sugar specificity, regulatory inputs/outputs, and ultimately their importance during infection (51). PTS mediate carbon source import and phosphorylation, with secondary functions on transcriptional regulation having been reported (52). PTS import free sugars following binding of a sugar to pre-phosphorylated import permeases. This pre-phosphorylation is tied to the lower glycolytic conversion of phosphoenolpyruvate (PEP) to pyruvate through two phosphocarrier proteins (PtsI [EI] & PtsH [HPr-His]). The result of this phospho-cycling is that free sugars are phosphorylated during import and readied for direct

funneling to glycolysis. It has previously been reported that PrfA-dependent virulence gene expression is repressed when *L. monocytogenes* is utilizing primarily PTS-dependent carbon sources (42,53,54). Conversely, when PTS function is blocked via deletion of the HPr phosphocarrier protein (Δ*ptsH*), PrfA-dependent virulence gene expression is significantly increased *in vitro* (20,32,54,55). Because of these observations, PTS have been widely believed to be inactive during *L. monocytogenes* intracellular growth and virulence (39,44,45,56,57).

In this work, we assessed the contribution of glycerol and hexose phosphate metabolism to *L. monocytogenes* virulence *in vivo* finding that glycerol and hexose phosphates are neither sufficient nor essential to support intra-macrophage growth and although they do contribute to virulence of *L. monocytogenes in vivo*. A metabolic screen of carbon sources revealed highly similar metabolite utilization between WT and PrfA* (G145S) *L. monocytogenes,* including the use of PTS mediated carbon sources. Ablation of all PTS-mediated carbon acquisition via deletion of the phosphocarrier proteins EI (Δ*ptsI*) or HPr (Δ*ptsH*) revealed that *L. monocytogenes* requires PTS function to support intracellular growth and virulence. *In vivo* virulence defects could not be rescued by constitutive virulence gene expression with the PrfA* (G145S) allele in Δ*ptsI* or Δ*glpD*/Δ*golD*/Δ*uhpT* suggesting that the virulence defects are due to metabolic disruption and not altered virulence gene expression. Further, Δ*ptsI* and Δ*glpD*/Δ*golD*/Δ*uhpT* mutants both showed basally increased levels of hemolytic activity relative to WT *L. monocytogenes* suggesting increased PrfA activity. Finally, the phenotypes associated with loss of PTS function are additive with the inability to utilize glycerol and hexose phosphates (Δ*glpD*/Δ*golD*/Δ*uhpT/ΔptsI or* Δ*glpD*/Δ*golD*/Δ*uhpT/ΔptsH*) demonstrating that *L. monocytogenes* uses a highly complex and varied network of metabolites to promote rapid intracellular replication during infection.

RESULTS

glpD/*golD* and *uhpT* genes are required for *L. monocytogenes* to consume glycerol and hexose phosphate, respectively

L. monocytogenes uses host-derived glycerol and hexose phosphates during cytosolic replication, as defined using isotopologue metabolomics analysis by the Goebel and Eisenreich labs (29,31,32), however whether these are the predominant carbon sources used during *in vivo* infection has not been fully explored. Although *uhpT, glpD* and *golD* mutants have been studied in isolation, the phenotype of combination metabolic mutants of parallel glycerol utilization pathways (Δ*glpD*/Δ*golD*) and of glycerol with hexose phosphate pathways (Δ*glpD*/Δ*golD*/Δ*uhpT*) have not been assessed (**Fig 1A**). We aimed to test the hypothesis that combination metabolic mutants of Δ*glpD*/Δ*golD*, Δ*uhpT*, and combination Δ*glpD*/Δ*golD*/Δ*uhpT* would completely ablate *L. monocytogenes* growth on glycerol, hexose phosphates, and both, respectively. To do this we generated these metabolic mutants and assessed growth in *Listeria* synthetic media (LSM) with glucose, glycerol, glucoe-6-phosphate (+glutathione), or glycerol/glucose-6-phosphate (+glutathione) as the sole carbon source (**Fig 1B-E.**). LSM with defined sole carbon sources was inoculated with WT *L. monocytogenes* or the indicated mutants, and growth was assessed via OD_{600} absorbance every 15 minutes. Importantly, any LSM containing hexose phosphates required further supplementation with 10 mM reduced glutathione to induce *prfA,* and therefore *uhpT*, expression (23,58). Of note, we found that a Δ*glpD* mutant was still able to grow in LSM supplemented with glycerol and a second glycerol utilization pathway required ablation (Δ*golD*) to limit *in vitro* growth (38). We found that glycerol (Δ*glpD*/Δ*golD*), hexose phosphate (Δ*uhpT*), and combined (Δ*glpD*/Δ*golD*/Δ*uhpT*) mutants were not defective for *in vitro* growth when compared to WT *L. monocytogenes* in LSM with glucose

as the sole carbon source (**Fig 1B**). In contrast, when Δ*glpD*/Δ*golD* or Δ*uhpT* mutants were supplied with glycerol and hexose phosphates, respectively, they were unable to grow while WT *L. monocytogenes* sustained growth (**Fig 1E**). Mutants lacking only the hexose phosphate transporter (Δ*uhpT*) showed sustained growth in LSM with glycerol alone, but they were only able to growth modestly in LSM with glycerol and hexose phosphates (**Fig 1C and 1E**). Finally, a mutant defective for glycerol and hexose phosphate (Δ*glpD*/Δ*golD/*Δ*uhpT*) utilization was fully capable of growing in defined media with glucose as the carbon source but was unable to grow on glycerol, hexose phosphates, or glycerol/hexose phosphates combined when compared to WT *L. monocytogenes* (**Fig 1B-E**). Taken together, these data demonstrate that there are not additional unknown glycerol or hexose-phosphate utilization pathways and that the Δ*glpD*/Δ*golD/*Δ*uhpT* mutant is incapable of growing on glycerol and hexose phosphates as primary carbon sources. Similarly, the Δ*glpD*/Δ*golD/*Δ*uhpT* mutant shows no growth defects when supplied with glucose as its sole carbon source.

Δ*glpD*/Δ*golD*/Δ*uhpT L. monocytogenes* mutants unable to use hexose phosphates and glycerol replicate in macrophages and are attenuated in vivo

Glycerol and hexose phosphates have been demonstrated via isotopologue metabolomic flux analysis to be utilized by *L. monocytogenes* during intra-macrophage replication (30,31). We hypothesized that mutants deficient in both pathways would be attenuated for virulence. To determine if glycerol, hexose phosphates, or both were necessary for cytosolic replication of *L. monocytogenes* we performed intra-macrophage growth curves in murine bone marrow-derived macrophages (BMDMs). Intracellular growth curves in BMDM demonstrated that individual (Δ*glpD*/Δ*golD* and Δ*uhpT*) and combined (Δ*glpD*/Δ*golD/*Δ*uhpT*) metabolic mutants unable to

use glycerol and/or hexose phosphates were still able to grow in the host cytosol with kinetics like WT *L. monocytogenes* (**Fig 2A)**. This data suggests that in a single cycle infection in primary BMDMs, *L. monocytogenes* does not require glycerol or hexose phosphate to support cytosolic replication. Further, this data suggests that *L. monocytogenes* must be able to use alternate undefined carbon source(s) to support cytosolic growth.

In vivo, *L. monocytogenes* not only replicates in the primary infected cell but must spread to neighboring cells using ActA mediated actin-based motility (22). This intracellular replication and spread is modeled *ex vivo* using a plaquing assay (59,60). Mutants with replication defects, impaired cytosolic survival, or defects in actin-based motility and secondary vacuole escape all produce small plaques as this assay measures both replication and cell-to-cell spread over multiple infectious cycles and days. Thus, plaque assays can further elucidate minor defects due to their more stringent conditions. To further test the hypothesis that glycerol and hexose phosphates contribute to cytosolic replication and cell-to-cell spread, we measured the plaque sizes of the metabolic mutants relative to WT *L. monocytogenes*. Hexose phosphate acquisition deficient *L. monocytogenes* (Δ*uhpT*) formed statistically significantly smaller plaques (**Fig 2B**). In contrast, mutants defective for glycerol utilization (Δ*glpD*/Δ*golD*) generated plaques indistinguishable from WT. *L. monocytogenes*. Finally, a mutant defective for both glycerol and hexose phosphate utilization (Δ*glpD*/Δ*golD/*Δ*uhpT*) phenocopied a hexose phosphate mutant (Δ*uhpT*) alone suggesting no additive role for glycerol in the context of multicycle infection and cell to cell spread in fibroblasts (**Fig 2B**). This data indicates that while glycerol utilization is dispensable in single cycle infections in BMDMs and plaque multi-cycle plaque assays, hexose phosphates contribute to *L. monocytogenes* fitness in the context of multi-cycle infections and/or cell-to-cell spread, but not single cycle BMDM growth curves.

Given the apparent role for hexose phosphates in multicycle infections in the plaquing assay, we wanted to test the hypothesis that glycerol and hexose phosphates would be required for virulence *in vivo*. Mutants with replication and survival defects will sometimes show more robust virulence defects in murine models compared to *ex vivo* assays given the more restrictive physiology and multicycle infectious nature (61). To test this hypothesis, we utilized a murine disseminated listeriosis model and assessed virulence via bacterial burdens in the spleen and liver 48 hours after intravenous infection (**Fig 2C**). Consistent with results from the intracellular growth curves and the plaquing assay, glycerol mutants (Δ*glpD*/Δ*golD*) were not statistically significantly attenuated, although there was a trend towards lower bacterial burdens 48 hours post infection. Additionally, hexose phosphate mutants (Δ*uhpT*) showed statistically significant attenuation in both organs with approximately 1.5-2 logs of virulence reduction. Finally, failure to use glycerol in addition to hexose phosphates (Δ*glpD*/Δ*golD*/Δ*uhpT*) resulted in more significant attenuation than hexose phosphate mutants alone (Δ*uhpT*) in the spleen, while a similar trend was observed in the liver (**Fig 2C**). Taken together this data suggests that hexose phosphates, and not glycerol, are essential for multi-cycle replication *ex vivo* and full virulence during *in vivo* infection. Importantly, even though a mutant defective for utilization of both glycerol and hexose phosphates is attenuated *in vivo* relative to wild-type *L. monocytogenes,* it is unexpected that it can grow the host cytosol, productively invade neighboring cells, and maintain significant bacterial burdens in a murine model. These observations suggest that additional, yet to be defined, carbon source(s) are major contributors to replication and virulence of *L. monocytogenes in vivo*.

BioLog phenotype microarray screening reveals WT and PrfA* (G145S) *L. monocytogenes* equivalently respire on PTS mediated carbon sources

The unexpected results that Δ*glpD*/Δ*golD*/Δ*uhpT L. monocytogenes* can grow the host cytosol and maintain virulence in a murine model led us to hypothesize that *L. monocytogenes* must use additional carbon sources during infection. To identify potential metabolites used by *L. monocytogenes* that could support cytosolic growth, we employed BioLog's phenotypic carbon microarrays (PM1 and PM2A) to screen for differential carbon source respiration between WT and PrfA* (G145S) *L. monocytogenes* (25). PrfA* mutants contain a G145S mutation in the virulence regulator PrfA that results in constitutive virulence gene expression, including upregulation of *uhpT* for the use of hexose phosphates (23–25). We hypothesized that PrfA* (G145S) *L. monocytogenes* may differentially use carbon sources relative to WT *L. monocytogenes*, similar to its differential use of hexose phosphates, which could reveal targets used to support cytosolic growth. Inoculation and setup of phenotypic microarray plates were performed as previously described, assays were performed in triplicate and plates were incubated at 37° stationary for 48 hours (62,63). At 48 hours post-inoculation, plates were assessed for change in tetrazolium dye color, indicating bacterial respiration on the carbon source. OD_{490} values were normalized to glucose, a carbon source known to be used by both strains, for each respective strain to account for potential global metabolic variance between strains. 190 total carbon sources were assessed for use by *L. monocytogenes* relative to glucose respiration (**Fig 3, Table 1, and Table 2**). WT *L. monocytogenes* was able to use 51 carbon sources at or above the level of glucose, of which, 35 are hypothesized to be available in the host cytosol according to the human metabolome database (64). PrfA* was able to consume all these same carbon sources and had significantly increased respiration on hexose phosphates as expected based on its known

upregulation of *uhpT* (**Fig 3 and Table 1**). PrfA* also showed a statistically significant decreased respiration on a single PTS mediated carbon source, α-D-Lactose. Notably, PrfA* *L. monocytogenes* had overall similar use of most carbon sources, including PTS mediated carbon sources (**Fig 3 and Table 1**). The glycerol and hexose phosphate (Δ*glpD*/Δ*golD*/Δ*uhpT*) mutant was similarly tested using PM1 and PM2A and phenocopied WT *L. monocytogenes* except for the loss of the ability to respire glycerol and α-Methyl-D-Glucoside (**Fig 3, S4 Table, and Table 2**). Contrary to our hypothesis that PrfA* mutants would utilize metabolites differentially relative to WT *L. monocytogenes*, the only metabolites utilized more readily in PrfA* *L. monocytogenes* were hexose phosphates. Nevertheless, we were surprised to find that PrfA* *L. monocytogenes* readily utilized PTS-dependent carbon sources nearly identically to WT *L. monocytogenes.* This was striking given the established model in the field that PTS are not used during infection. However, PrfA* *L. monocytogenes* using PTS-mediated carbon sources is not mutually exclusive to the existing literature, in which, PTS transcripts are repressed during PrfA activation and use of PTS-mediated carbon sources' reciprocally repress *prfA* expression (42,54).

PTS are necessary for intracellular *L. monocytogenes* growth and virulence *in vivo*

Based on the similar utilization of PTS-mediated carbon sources between WT and PrfA* *L. monocytogenes* and the incomplete attenuation of the Δ*glpD*/Δ*golD*/Δ*uhpT* mutant, we hypothesized that PTS-dependent sugars could be an alternative carbon source during infection. The *L. monocytogenes* strain 10403s used in this study encodes 29 complete PTS systems encoded by 86 genes making it difficult to test individual PTS for importance during infection(44). Therefore, to test the hypothesis that PTS contribute to *L. monocytogenes* virulence we instead targeted the universally conserved phosphocarrier proteins essential for the

function of all PTS, HPr (*ptsH*) and EI (*ptsI*) (**Fig 4A**). Δ*ptsI* mutants were constructed in WT and *ΔglpD/ΔgolD/ΔuhpT L. monocytogenes* backgrounds to assess the relative contribution of hexose phosphates and glycerol vs PTS-dependent metabolites during cytosolic growth and virulence. To assess the role of PTS in cytosolic growth we infected primary murine BMDMs with WT, *ΔglpD/ΔgolD/ΔuhpT,* Δ*ptsI*, *and ΔglpD/ΔgolD/ΔuhpT*/Δ*ptsI L. monocytogenes*. While *ΔglpD/ΔgolD/ΔuhpT* and WT *L. monocytogenes* were able to replicate in the macrophage cytosol as previously demonstrated (**Fig 2B and Fig 4B**), PTS deficient strains were completely unable to replicate, independent of the presence or absence of glycerol and hexose phosphate utilization pathways. Taken together these data demonstrate that PTS-dependent metabolites are both necessary and sufficient to support replication in the cytosol of BMDMs.

The striking lack of cytosolic replication of PTS deficient *L. monocytogenes* in BMDMs, led us to ask whether PTS systems were similarly required for replication and cell-to-cell spread in more protracted multi-cycle infections by performing a plaquing assay in L2 fibroblasts. As previously demonstrated, *ΔglpD/ΔgolD/ΔuhpT* mutants had a statistically significant plaquing defect relative to WT *L. monocytogenes*; however, in contrast to the BMDM growth phenotype of PTS deficient mutants, *L. monocytogenes* strains lacking only *ptsI* demonstrated no plaquing defects (**Fig 4C**). Combining PTS deficiency with glycerol and hexose phosphate deficiency led to a complete loss of plaque formation (**Fig 4C**). Taken together these data suggest that while PTS are absolutely required for replication in the macrophage cytosol, PTS are only conditionally required in fibroblasts when glycerol and hexose phosphates are not available. These data suggest that there are differences in nutrient availability in different cell types, and further, that *L. monocytogenes* uses metabolic flexibility to grow in diverse cell types.

Given the differential requirements of PTS in macrophages versus fibroblasts *ex vivo*, we wanted to determine the role of PTS during *in vivo* infection in a murine disseminated listeriosis model. As we previously demonstrated, *ΔglpD/ΔgolD/ΔuhpT* mutants had 10-100-fold lower bacterial burdens relative to wild type *L. monocytogenes* 48 hours post infection (**Fig 4D**). In contrast, Δ*ptsI* mutants were 500-fold and 5000-fold attenuated in the spleens and livers of infected mice respectively (**Fig 4D**). Furthermore, loss of PTS function in the absence of glycerol and hexose phosphate utilization led to an additive virulence defect whereby the *ΔglpD/ΔgolD/ΔuhpT/*Δ*ptsI* mutants were more attenuated than the *ΔglpD/ΔgolD/ΔuhpT* mutants or the Δ*ptsI* mutants alone (**Fig 4D**). Intra-macrophage growth, cell-to-cell spread, and virulence *in vivo* were proportionally rescued with constitutive overexpression trans-complementation of *ptsI* (**Fig 4C and 4D)**. Together this data suggests that PTS mediated carbon acquisition is an important contributor to *in vivo* virulence. Furthermore, the additive attenuation of the *ΔglpD/ΔgolD/ΔuhpT/*Δ*ptsI* mutant relative to *ΔptsI* mutant alone demonstrates that glycerol, hexose phosphates and PTS mediated carbon sources are all significant contributors to *L. monocytogenes* virulence *in vivo*.

Virulence defects of Δ*glpD*/Δ*golD*/Δ*uhpT* and Δ*ptsI* mutants are not due to lack of PrfA activation

Given the intertwined nature of *L. monocytogenes*' metabolism and its virulence gene regulation it is possible that all or part of Δ*glpD*/Δ*golD*/Δ*uhpT* and Δ*ptsI* virulence defects could be attributed to virulence gene mis-regulation. To test the hypothesis that Δ*glpD*/Δ*golD*/Δ*uhpT* and Δ*ptsI* are attenuated due to incomplete PrfA activation, a constitutively active PrfA* (G145S) allele was cloned *in situ* into WT, Δ*glpD*/Δ*golD*/Δ*uhpT* and Δ*ptsI L. monocytogenes*. These strains

[PrfA* (G145S), Δ*glpD*/Δ*golD*/Δ*uhpT*::PrfA* (G145S) and Δ*ptsI*::PrfA* (G145S)] were compared to each other and their isogenic counterparts (WT, Δ*glpD*/Δ*golD*/Δ*uhpT* and Δ*ptsI*) in a murine burden assay. As previously demonstrated, Δ*glpD*/Δ*golD*/Δ*uhpT* mutants display a 1-2 log defect in both the spleen and liver, while Δ*ptsI* mutants were 500-fold and 5000-fold attenuated in the spleens and livers of infected mice respectively (**Fig 5A**). Meanwhile, PrfA* (G145S), Δ*glpD*/Δ*golD*/Δ*uhpT*::PrfA* (G145S), and Δ*ptsI*::PrfA* (G145s) strain showed no restoration of virulence compared to WT *L. monocytogenes* and no statistically significant benefit compared to their isogenic counterparts (**Fig 5A**). Taken together this suggests that defective PrfA-regulon expression does not account for the virulence defects observed in Δ*glpD*/Δ*golD*/Δ*uhpT* and Δ*ptsI L. monocytogenes* and supports that these virulence defects are due to metabolic deficiencies.

Overall, the lack of rescue associated with the PrfA* (G145S) allele in a Δ*ptsI* mutant was consistent with prior literature showing that disruption of PTS should result in increased PrfA-regulon expression and terminal activity (54). In contrast, based on the literature suggesting that PTS function is inversely related to PrfA activation, it was somewhat surprising that Δ*glpD*/Δ*golD*/Δ*uhpT L. monocytogenes*, a strain dependent on PTS for virulence (**Fig 4C, D**), showed no benefit from the PrfA* (G145S) allele (23,32,54). To assess PrfA activation in our metabolic mutants we assessed Listeriolysin-O (LLO)-dependent hemolysis of sheep red blood cells (RBCs), an established surrogate of PrfA activity (65), using supernatants from Δ*glpD*/Δ*golD*/Δ*uhpT* and Δ*ptsI L. monocytogenes* compared to WT as previously described (65). Strains were grown overnight at 37°C shaking to overcome RNA thermosensor repression of PrfA, supernatants harvested, serially diluted and incubated with sheep RBCs, and hemoglobin release quantified via OD_{420} (65,66). A standard curve of detergent driven hemolysis was used to calculate percent hemolysis across dilutions of each strain in each biological replicate. From these values,

percent hemolysis was interpolated as a function of OD_{600} for each strain and the resultant equation was used to calculate percent hemolysis at an OD_{600} of 0.025. An OD_{600} of 0.025 was selected as it was where ~50% hemolysis occurred in our experimental strains. Hemolysis from the supernatants of Δ*glpD*/Δ*golD*/Δ*uhpT* and Δ*ptsI L. monocytogenes* showed significantly more activity than that of WT *L. monocytogenes* (**Fig 5B)**. This was further visualized and verified by left shift of toxin dose-response curves from a single representative biological replicate relative to WT *L. monocytogenes* (**Fig 5C**). Taken together these data indicate that both Δ*glpD*/Δ*golD*/Δ*uhpT* and Δ*ptsI L. monocytogenes* have excess LLO activity, and therefore PrfA activity, relative to WT. Further this demonstrates why PrfA* alleles did not rescue virulence of these strains and indicates that the primary defect of these mutants is metabolic in nature.

Loss of HPr (*ptsH*) phenocopies loss of EI (*ptsI*)

To further confirm that the loss of virulence in the Δ*ptsI* mutant was due to loss of function of PTS and not another unknown function of EI, we created deletion mutants in the other conserved essential phosphocarrier protein HPr (*ptsH*). HPr is known to have a secondary role in genetic regulation via CcpA through phosphorylation by HPr kinase, therefore we hypothesized that Δ*ptsH* should, at minimum, phenocopy Δ*ptsI,* with the potential for further attenuation. Consistent with PTS being essential for growth in the macrophage cytosol, Δ*ptsH* mutants were unable to replicate in BMDM alone or when combined with hexose phosphate and glycerol (*ΔglpD/ΔgolD/ΔuhpT*/Δ*ptsH*) mutants (**Fig 6A**). Similarly, Δ*ptsH* mutants were significantly attenuated for virulence *in vivo* and when combined with glycerol and hexose phosphate mutants, *ΔglpD/ΔgolD/ΔuhpT*/Δ*ptsH* mutants were essentially avirulent *in vivo* (**Fig 6B)**. Taken together, these data suggest that PTS are major contributors to virulence of *L.*

monocytogenes in vivo and that a loss of PTS combined with loss of glycerol and hexose phosphate utilization leads to almost complete attenuation of *L. monocytogenes in vivo.*

DISCUSSION

Mechanisms of carbon acquisition, catabolism, and anabolism by cytosolic pathogens remain incompletely defined, but are vitally important virulence factors in driving pathogenesis. A mechanistic understanding of bacterial metabolism during infection can help identify novel anti-microbial targets and host targeted metabolic interventions. Despite *L. monocytogenes* being both an important pathogen and a model organism that has been studied for decades, we still have a relatively limited understanding of its metabolism during infection. In this work, we demonstrated that although hexose phosphate and glycerol contribute to *L. monocytogenes* infection *in vivo,* they are dispensable for cytosolic replication in macrophages in contrast to previous suggestions from isotopologue metabolomics. Further, combining an unbiased screen using BioLog's Carbon Phenotypic Microarrays (PM1 and PM2A) with genetic deletions of conserved PTS phosphocarrier proteins, we demonstrate that PTS are essential for replication in the macrophage cytosol and are critical for virulence *in vivo*. We then separated *L. monocytogenes'* metabolism from virulence gene regulation using a PrfA* (G145S) allele in the Δ*glpD*/Δ*golD*/Δ*uhpT* and Δ*ptsI* backgrounds and found no rescue of *in vivo* virulence and further demonstrate that Δ*glpD*/Δ*golD*/Δ*uhpT* and Δ*ptsI* mutants have increased LLO mediated hemolytic activity relative to WT *L.* monocytogenes. Together our data suggest that *L. monocytogenes* is utilizing a previously underappreciated and more diverse metabolic strategy to replicate in the cytosolic environment and potentiate infection. These findings illuminate a

generally overlooked contributor to virulence, PTS, and point to a system not previously identified as necessary for successful intracellular growth and virulence.

Despite PTS' broad and well-defined role in carbon acquisition and previous demonstrated roles in the growth of *Shigella flexneri* and *Streptococcus pyogenes* during infection, they have largely been viewed as either minor contributors or in some cases active inhibitors of bacterial pathogenesis more broadly (40,42,44,52,54,67–69). In *L. monocytogenes,* work demonstrating that PTS activity represses *prfA* expression lead to a widespread and often repeated assumption that PTS are not used during infection, as virulence gene repression was considered detrimental to pathogenesis (39,44,45,56). Nevertheless*,* our findings demonstrate that a Δ*glpD*/Δ*golD/*Δ*uhpT* mutant *L. monocytogenes* with presumed obligate use of PTS, can still readily cause infection (32,54). Interestingly, this mutant even showed increased LLO-mediated hemolysis relative to WT *L. monocytogenes,* however the mechanism by which this is mediated remains unclear. These results indicate that more must be done for the field to understand how more specific metabolic mutants', such as Δ*uhpT* or metabolite-specific PTS mutants, regulate their virulence gene expression through PrfA. Our results demonstrate that over reliance on PTS, and consequential PrfA regulon repression is not the driver of virulence defects of Δ*glpD*/Δ*golD/*Δ*uhpT L. monocytogenes* observed *in vivo* as a PrfA* (G145S) allele does not rescue *in vivo* virulence. Like Δ*glpD*/Δ*golD/*Δ*uhpT*, Δ*ptsI* mutant *L. monocytogenes* shows elevated PrfA-regulon activity and are not rescued by PrfA* (G145S) allele. Interestingly while not statistically significant, Δ*ptsI* mutant *L. monocytogenes* subjectively appear harmed by PrfA-regulon over expression. We hypothesize this may be due to the substantial metabolic demand of constitutive PrfA activity, hexose phosphate toxicity as described in other organisms, or some unknown regulatory effects of PrfA* on bacterial metabolism (70). One remaining question is

why *L. monocytogenes* would use this complex metabolic strategy utilizing such a wide array of carbon sources including those with potentially negative impacts on virulence gene expression? We hypothesize that *L. monocytogenes* may be using a balance of carbon sources to optimize virulence gene expression while maximizing carbon acquisition for metabolism and growth potential while avoiding host cell detection. One indicator in our data that this hypothesis might be correct is that Δ*glpD*/Δ*golD*/Δ*uhpT* mutants show mild declines during intra-macrophage growth and virulence defects in plaque assays and murine burdens, This strain may be attenuated later during its intracellular life cycle due to starvation from depletion of host metabolites through PTS, resultant host cell death, bacterial physiologic defects, or even host cell detection and elimination. As such, we conclude the phenotypes uncovered through these studies represent the relative metabolic insufficiencies due to failure of glycerol, hexose phosphates, and PTS mediated carbon source acquisition and use in the host.

Bacterial PTS encode two phosphocarrier proteins that are necessary for the function of all PTS regardless of sugar: PtsI (EI) and PtsH (HPr) (43). Despite these two proteins sharing universal roles in PTS carbon acquisition, they have diverse functions, and per our results, phenotypes. Δ*ptsI L. monocytogenes* are defective for only carbon acquisition through PTS as PtsI has no described role as a transcriptional regulator. In contrast, HPr (*ptsH*) has been shown previously to not only impact carbon acquisition through PTS but also to play a central role in transcriptional regulation of virulence through the phosphorylation of the HPr-Ser-46 residue (54,69). The HPr-Ser residue is phosphorylated by HPr Kinase (HprK) dependent on upper glycolytic flux and the abundance of fructose-1,6-bisphosphate and ATP. Importantly, these functions are not linked to lower glycolytic PEP to pyruvate conversion or PtsI (EI) function (68). The exact mechanism by which HPr-Ser-P enacts this repression is unknown (42,53).

Consistent with this, Δ*ptsH* (HPr) mutants in the WT and *ΔglpD/ΔgolD/ΔuhpT L. monocytogenes* backgrounds show decreased virulence relative to those of Δ*ptsI* in an isogenic background suggesting that that the transcriptional dysregulation due to loss of *ptsH* is key to the additional virulence defects. Our favored hypothesis is that Δ*ptsH L. monocytogenes* is failing to modulate expression of genes necessary for alternate carbon source acquisition and/or deal with stresses unique to the host cytosol and these functions are retained in Δ*ptsI*. For example prior work has shown that HprK mediated phosphorylation of CcpA plays an important role in hierarchal carbon source utilization and stress responses in *L. monocytogenes* (71,72). Because the exact transcriptional changes mediated by HPr-Ser-P are not well defined, it would be valuable to test how phospho-ablative and -mimetic HPr-Ser and HPr-His mutants behave differently through virulence assays and transcriptomic profiling. Overall, PtsI (EI) and PtsH (HPr) have separate but overlapping, functions that once characterized could unveil how and why bacteria connect the function of PTS to gene expression.

Previous isotopologue analysis by the Eisenreich and Goebel groups have shown that *L. monocytogenes* uses hexose phosphates and glycerol to support its cytosolic growth (29–33,73). These carbon substrates are logical carbon sources for an intracellular pathogen such as *L. monocytogenes* because not only does *L. monocytogenes* have dedicated transporters for these carbon sources but, equally importantly, they are available in the host cytosol (29,32). Nearly all sugar that is brought into eukaryotic cells is phosphorylated to prevent backward diffusion to the extracellular space. Once a sugar is phosphorylated it has two primary fates: 1. Funneling into glycolysis. 2. De-phosphorylation for use as a moiety/metabolite component in more complex forms, such as glycogen in the liver (74–76). Nevertheless, for PTS to be essential for *L. monocytogenes* growth in the cytosol, free sugars (monomers or polymers) must be present in

abundance to support bacterial growth. Consistent with existing literature that PTS cannot facilitate transport of phosphorylated sugars, the Δ*glpD*/Δ*golD*/Δ*uhpT* mutant relying on PTS was unable to grow hexose phosphates *in vitro* but retained ability to grow in the host cytosol. Therefore, *L. monocytogenes* must have access to unphosphorylated sugar in the cytosol. Whether these unphosphorylated, free sugars are liberated by the host or bacteria during the course of *L. monocytogenes* infection remains an unknown and critical component in understanding the use of PTS. One hypothesis is that *L. monocytogenes* is using a yet to be defined phosphatase to dephosphorylate and liberate free sugars. These putative phosphatases could represent high value targets for the development of antivirulence based antimicrobials (77). Alternatively, host cells could attempt to dephosphorylate sugars to allow sugar diffusion in an act of nutritional immunity, a process that *L. monocytogenes* might have evolved to take advantage of. Ultimately, understanding how *L. monocytogenes* accesses free sugars in the cytosol of an infected cell could inform whether other cytosolic pathogens could have access to and use similar carbon sources during infection.

Answering what specific PTS and corresponding carbon source might be used by *L. monocytogenes* is extremely challenging given the intertwined nature of the *L. monocytogenes*-macrophage metabolism and the redundancy of PTS systems in the *L. monocytogenes* genome (78). Importantly, while our work shows that the carbon acquisition function of PTS is an important contributor to *L. monocytogenes* cytosolic growth, we do not know specifically what PTS mediated sugars might be consumed. Because of the diverse arsenal of PTS encoded by *L. monocytogenes,* it is possible that there are multiple redundant carbon sources consumed by *L. monocytogenes* in the cytosol (44). Additionally, our observation that *L. monocytogenes* PTS mutants have unique host cell and organ specific phenotypes suggests the presence of divergent

metabolites within host cells that *L. monocytogenes* might be consuming. For example, Δ*ptsI* mutants show very different phenotypes in BMDMs where no growth occurs compared to the L2 fibroblast plaquing assay where Δ*ptsI* mutants are indistinguishable from wild type *L. monocytogenes*. Similarly, there are subjectively different bacterial burdens in spleens versus liver for Δ*ptsI* during *in vivo* murine infection. Comparison of these growth conditions through advancing techniques in metabolomics may unveil the metabolic underpinning of these phenotypes. Identifying what specific carbon sources *L. monocytogenes* acquires from the host via PTS may unveil unique metabolic strategies to avoid host cell detection and support cytosolic bacterial physiology.

It is challenging to develop a complete picture of cytosolic pathogen metabolism given the ill-defined composition of the host cytosol, challenging technical methods, inherent metabolic redundancy, and diverse environments encountered in the host in different tissues. Our work demonstrates for the first time that PTS are essential for *L. monocytogenes* cytosolic growth and critical for virulence in contrast with the current dogma in the field (39,45,56). These highly conserved and redundant systems are understudied, and therefore their role in carbon acquisition by bacterial pathogens within the host cell is not well understood. Further work is needed to elucidate if PTS are critical for the cytosolic growth of other pathogens. Additionally, more work is needed to identify the preferred sugars for cytosolic pathogens and how these sugars are liberated. Finally, how differential carbon source availability across cell types, organ systems and even host species impacts bacterial pathogenesis remains to be elucidated.

MATERIALS AND METHODS

Ethics Statement

All animal-based experiments were performed using the protocol (M005916-R01-A01) approved by the Animal Use and Care Committee of the University of Wisconsin—Madison and consistent with the standards of the National Institutes of Health.

Bacterial strains and culture

All *Listeria monocytogenes* strains used for experiments in this study were in a 10403s background. All *L. monocytogenes* strains were grown overnight in BHI and at 30°C stationary for all experiments, except as described. *Escherichia coli* strains were grown in Luria broth (LB) at 37°C shaking. Antibiotics used on *E. coli* were at a concentration of 100 μg/ml carbenicillin or 30 μg/ml kanamycin when appropriate. Antibiotics used on *L. monocytogenes* were at a concentration of 200 μg/mL streptomycin and/or 10 μg/mL chloramphenicol, when appropriate. Plasmids were transformed into chemically competent *E. coli* and further conjugated in *L. monocytogenes* using SM10 or S17 *E.coli*.

Construction of strains

pLIM (from Arne Rietsche at Case Western) suicide plasmid or pKSV7 plasmid was used for generation of in frame deletions (61,79). The pPL2 integrative vector pIMK2 was used for constitutive expression of *L. monocytogenes* genes (80). pLIM and pKSV7 knockout constructs were cloned in XL1-Blue *E. coli* with 100 μg/ml carbenicillin (30μg/mL Kanamycin for pIMK2) and grown for plasmid harvest using Promega MiniPrep Kit. Harvested plasmid sequences were confirmed using was performed by Plasmidsaurus using Oxford Nanopore Technology with custom analysis and annotation. Plasmid were then shuttled into *L. monocytogenes* through

conjugation with SM10 (pLIM1 and pKSV7) or S17 (pIMK2) *E. coli*. In-frame deletions of genes in *L. monocytogenes* were performed by allelic exchange using suicide plasmid pLIM as previously described with p-chlorophenylalanine as a counter selectable marker (81). *De novo* PrfA* (G145S) allele introduction was performed by amplifying the PrfA* allele and flanking regions and assembling into pLIM (25). Following initial homologous recombination, enrichment of PrfA* (G145S) mutants was by performed by passaging merodiploid strains at 30°C shaking in selective *Listeria* Synthetic Media (LSM) with 55mM glucose-6-phosphate without glutathione (Sigma-Aldrich G7879) and plated on p-chlorophenylalanine as a counter selectable marker. Generated strains were frozen in 50:50 (glycerol:overnight culture) solution at -80°C. All mutants were confirmed via PCR, plasmid sequencing, and whole-genome sequencing using Oxford Nanopore technology from Plasmidsaurus with custom analysis and annotation.

In vitro Growth Assays

Bacteria were grown overnight in BHI at 30°C stationary. Overnight cultures were used to generate inoculums with ~$3.7x10^8$ CFU in PBS. 100 µLs per well of a flat bottom clear 96-well plate of *Listeria* synthetic media (LSM) with carbons source (supplied in 55 mM glucose carbon equivalents) was inoculated with 2 µL of inoculums. Plates were parafilmed on the edge to prevent evaporation and evaluated for OD_{600} in plate reader at 37°C shaking (250 r.p.m.) and reads every 15 minutes for times displayed.

Intra-macrophage growth curves

Bone marrow-derived macrophages were isolated from CL57/BL6 mice and cultured as previously described in Roswell Park Memorial Institute Medium (RPMI) based media (Invitrogen: 11875093) (82). BMDMs were plated into 60 mm dishes contain 13 degassed

coverslips. BMDMs cells were infected with *L. monocytogenes* strains at a multiplicity of infection [MOI] of 0.2. Inoculums of *L. monocytogenes* were grown in 3mL of BHI at 30°C stationary until all strains had reach stationary phase. Colony forming units to OD_{600} ratios were determined for each strain and adjusted to ensure infection results in a comparable MOI across strains. After 30 minutes BMDM media was exchanged for media containing 50 μg/ml Gentamycin. Coverslips were harvested, cells lysed in pure water, bacteria rescued isotonically, and plated to quantify CFU at displayed time points. All strains were assayed in biological triplicate and data displayed is one representative biologic replicate.

Plaque Assay

Plaque assays were conducted using a L2 fibroblast cell line grown in Dulbecco's Minimal Essential Media (DMEM) based media (Thermo Fischer: 11965092) as previously described with minor modifications for visualization and quantification of plaques (59,60). L2 fibroblasts were seeded at 1.2×10^6 per well of a 6-well plate, then infected at an MOI of 0.5 to obtain approximately 10-30 PFU per dish. Inoculums of *L. monocytogenes* were grown in 3mL of BHI at 30°C stationary until all strains had reached stationary phase. Colony forming units to OD_{600} ratios were determined for each strain and adjusted to ensure infection results in a comparable MOI across strains. At 4 days postinfection, cells were stained with 0.3% crystal violet for 10 min and washed twice with deionized water. Stained wells were scanned, uploaded, and areas of plaque formation were measured on ImageJ analysis software. All strains were assayed in biological triplicate and the average plaque areas of each strain (one-well per strain were normalized to wild-type plaque size within each replicate.

Murine Infection and Organ Burdens

Infections were performed as previously described (83). Briefly, 6 to 12-week-old female and male C57BL/6 mice were infected IV with 1×10^5 CFU logarithmically growing *L. monocytogenes* (optical density at 600 nm [OD600] = 0.5) in 200 μL of PBS. Colony forming units to OD600 ratios were determined for each strain and adjusted to ensure infection results in a comparable MOI across strains. 48 hours post-infection, mice were euthanized, and livers and spleens were harvested, homogenized in water with 0.1% NP-40, and plated for CFU. Two independent replicates of each experiment with 5 mice per group were performed.

Cell Culture

L2 cells were all kind gifts from Daniel Portnoy (UC Berkeley) (60). Bone marrow-derived macrophages (BMDM) were prepared from 6-to-8-week-old mice as previously described (82).

Phenotypic Microarrays

Phenotype Microarrays 1 (Cat. #12111) and 2A (Cat. #12112) were obtained from BioLog (BioLog). Plates were prepared and inoculated as previously described (63,84). OmniLog incubation was substituted with incubation at 37°C stationary. OD490 was collected for each plate at 24 and 48 hours. Data was then normalized to consumption of α-D-glucose for each strain and replicate, and averaged across triplicate. Value were clustered based on similarity using clustergrammer and plotted as a heat-map in Prism 6 (85). Data normalized to glucose was used for statistical analysis and displayed in tables. Statistics are representative of a student's T-test between two strains.

Hemolysis Assays

Hemolysis assays were performed as described previously with minor modification to optimize assay utility and interpretation. In short, overnight cultures were grown at 37°C in a 50:50 mixture of Luria Broth (LB) and Brain Heart Infusion (BHI) to optimize growth of metabolic mutants while maintaining PrfA expression. Supernatants containing *L. monocytogenes'* primary hemolytic toxin, Listeriolysin-O (LLO), were harvested by pelleting overnight cultures (15000 rcf for 1.5 minutes) and supernatants taken. These were 2-fold serially diluted with un-inoculated overnight broth 10 times to obtain robust dynamic range of sheep red blood cell (RBC) lysis. Simultaneously, a standard curve was generated by taking un-inoculated overnight broth and adding 0.1% Triton-100 and mixing in 1:1 ratio with washed 5% RBC solution and serially diluting as described above. Samples were then mixed in a 50:50 with washed 5% RBC solution and incubated for 30 minutes at 37°C stationary in round-bottom 96-well plates. After incubation, this mixture was centrifugated at 500 r.p.m. for 10 minutes to pellet unlysed RBCs. 75 µL of supernatants were transferred to a flat-bottom 96-well plate for measurement of free hemoglobin at OD_{420} in a plate reader. Percent hemolysis of each strains' dilution was calculated using each biological replicates' standard curve. Percent homolysis was then graphed as a function of OD600. Graphs for each replicate and each strain were individually interpolated using Prism 6's (GraphPad Software) non-linear Sigmoidal, 4PL, X analysis. This provided values to fill in the sigmoidal equation and calculate percent hemolysis ('Y') for any given OD_{600} ('X'):

$$Y = \frac{(Bottom\ + (X^{Hillslope}) * (Top - Bottom))}{(X^{Hillslope} + IC50^{Hillslope})}$$

The closest mid-inflection point for the majority of strains was identified (OD_{600} = 0.025) and input into the above equation with individual replicate values to calculate interpolated percent hemolysis for 3 replicates, averaged, and evaluated using one-way ANOVA.

Statistical Analysis

Prism 6 (GraphPad Software) was used for statistical analysis of data. Means from two groups of BioLog plates were compared with unpaired two-tailed Student's T-test. Means from more than two groups for all other assays were analyzed by one-way ANOVA test. Independently, Mann-Whitney Test was used to analyze two group comparison of non-normal data from animal experiments. * $p < 0.05$, ** $p < 0.01$, *** $p < 0.001$ for all statistical tests displayed.

FIGURES

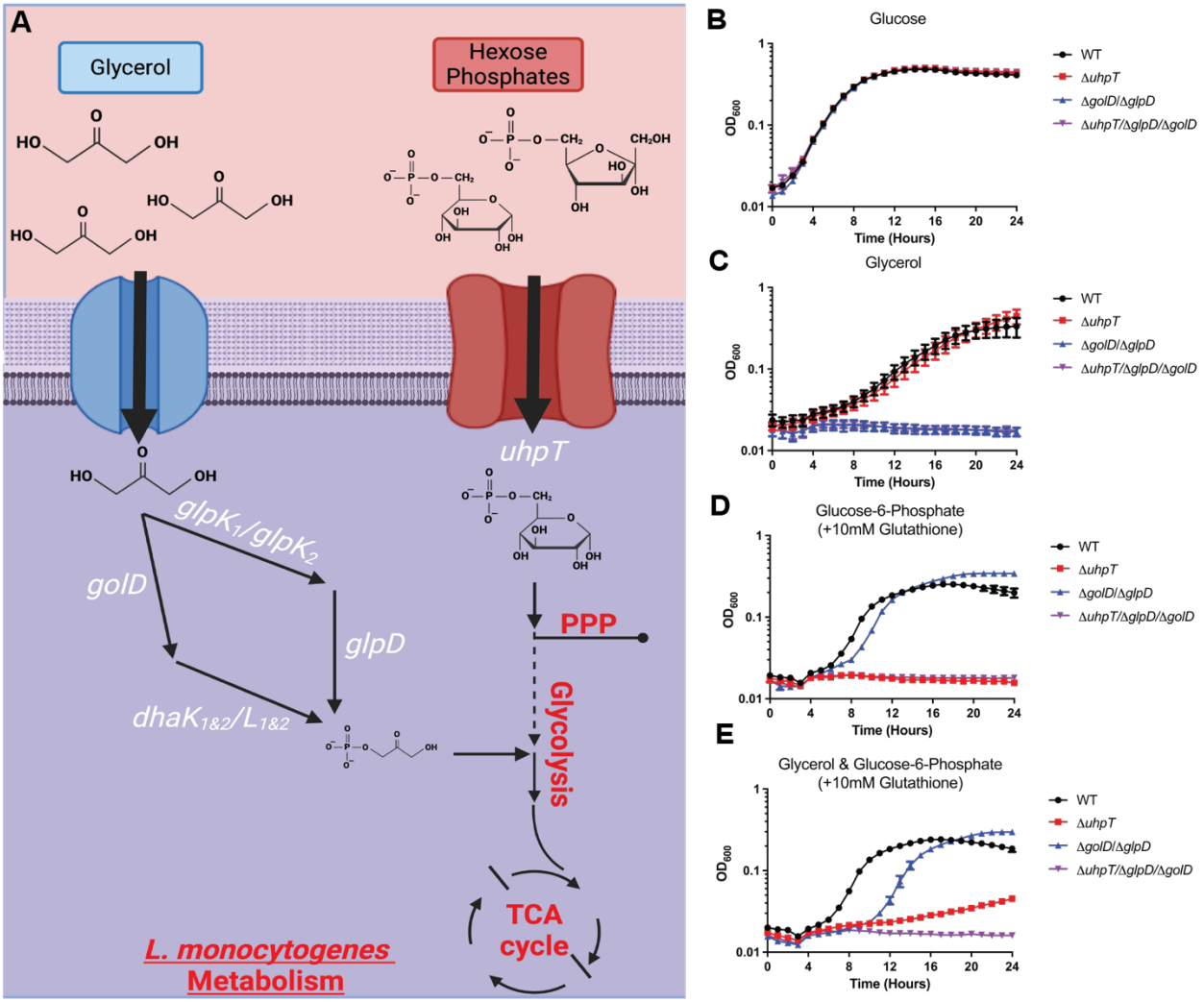

Figure 1. Mutants defective for consumption of glycerol (Δ*glpD*/Δ*golD*) and/or hexose phosphates (Δ*uhpT*) require alternative carbon sources to support growth in a defined medium. (A) Simplified model of glycerol being imported and funneled into two parallel glycerol utilization pathways (*glpD* and *golD*) for entry into central catabolic glycolysis. Hexose phosphate imported and funneled into the anabolic pentose phosphate pathway. Indicated strains were grown in LSM at 37°C, shaking at 250 r.p.m. with the addition of 55mM glucose (B) or carbon equivalent amounts of glycerol (C), hexose phosphates (+10mM glutathione) (D), and glycerol and hexose phosphates (+10mM glutathione) (E). OD_{600} was monitored every 15

minutes for 24 hours. Data represents average of three technical replicates from one representative of three biological replicates.

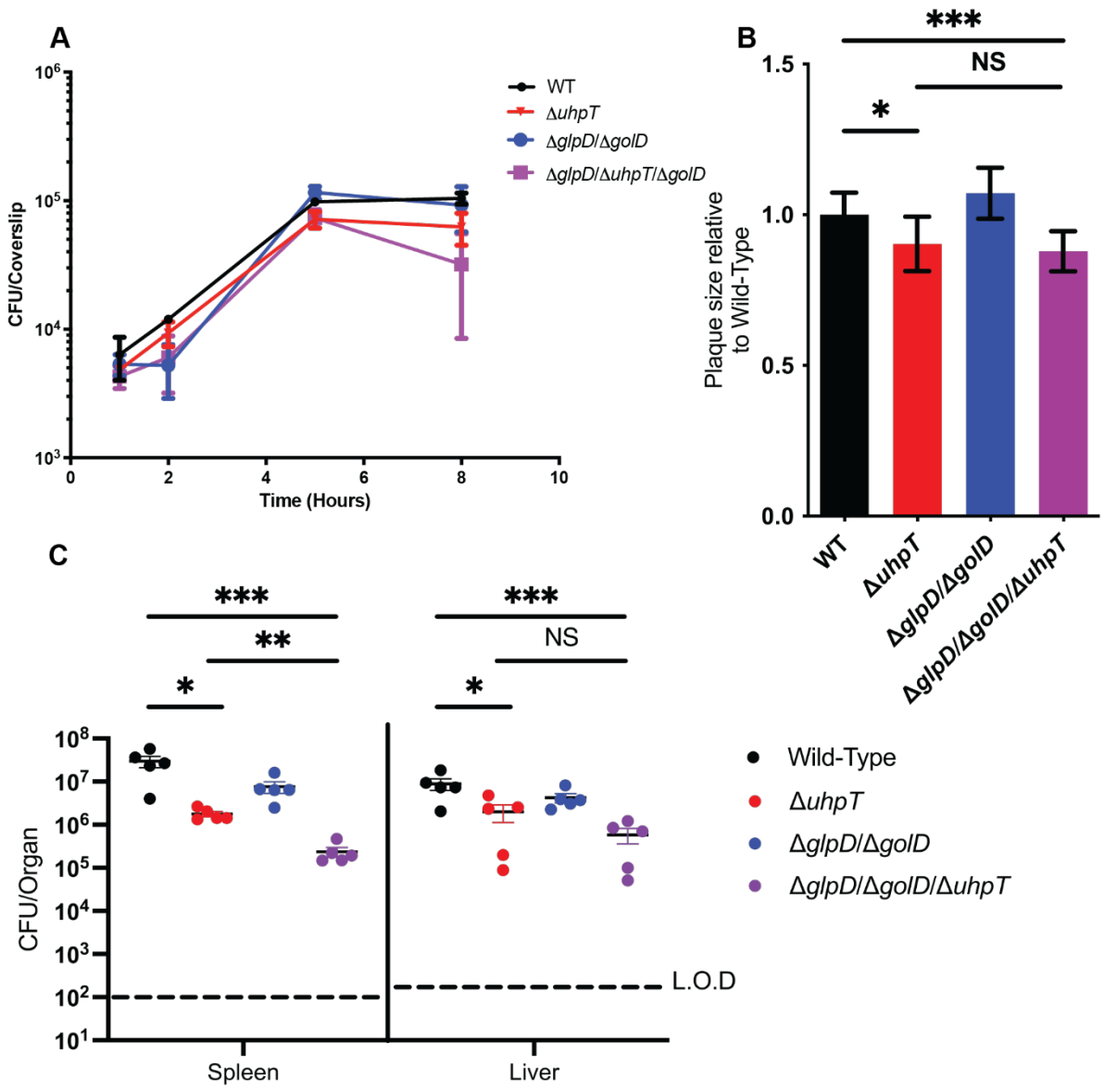

Figure 2. Mutants defective for metabolism of glycerol (Δ*glpD*/Δ*golD*) and/or hexose phosphates (Δ*uhpT*) are readily able to grow in the host cytosol and maintain virulence. (A) Intracellular growth of WT, Δ*glpD*/Δ*golD*, Δ*uhpT,* Δ*glpD*/Δ*golD*/Δ*uhpT* was determined in BMDMs following infection at an MOI of 0.2. Growth curves are representative of at least three independent experiments. Error bars represent the standard deviation of the means of technical triplicates within the representative experiment. (B) L2 fibroblasts were infected with indicated *L. monocytogenes* strains at an MOI of 0.5 and were examined for plaque formation 4 days post

infection. Assays were performed in biological triplicate and data displayed is the median and SEM of a strain's plaque size relative to WT in one of three representative biological replicates. (C) Bacterial burdens from the spleen and liver were enumerated at 48 hours post-intravenous infection with $1x10^5$ bacteria. Data are representative of results from two separate experiments. Horizontal dashed lines represent the limits of detection, and the bars associated with the individual strains represents the mean and SEM of the group.

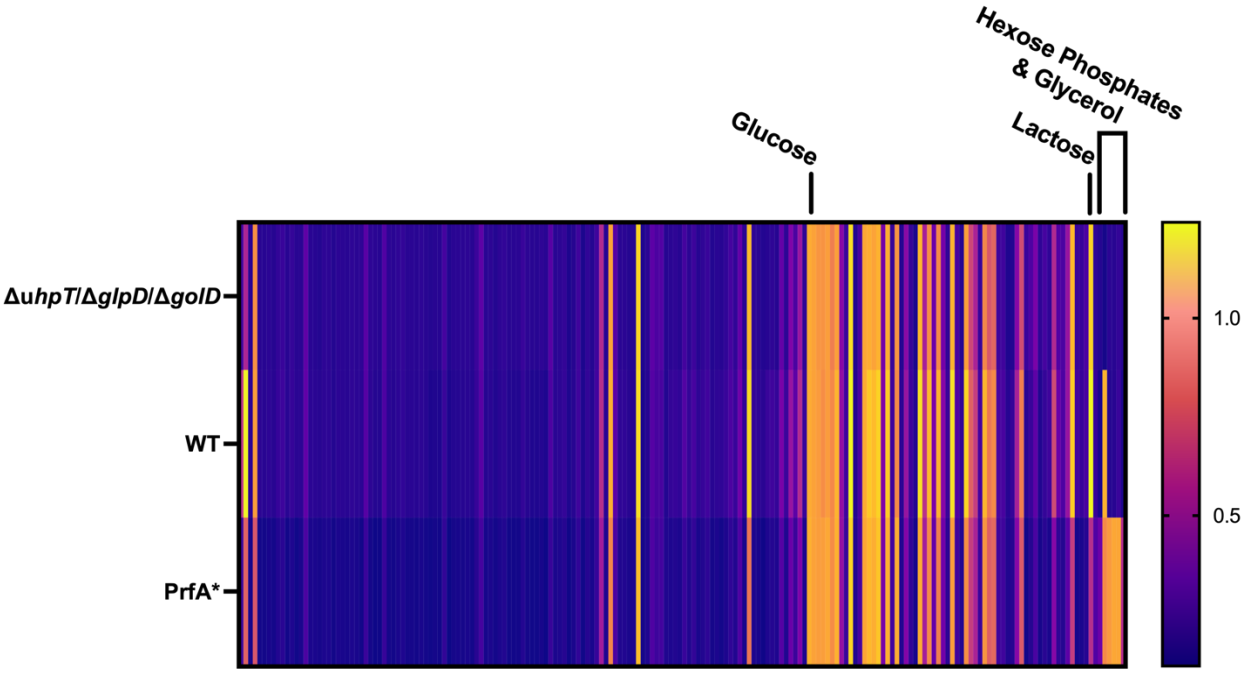

<u>Figure 3.</u> Carbon metabolite respiration of WT, Δ*glpD*/Δ*golD*/Δ*uhpT*, and PrfA* L. monocytogenes is globally similar, identified using Biolog's Phenotypic Microarrays. Clustered heatmaps indicating level of tetrazolium dye color change as measured by OD_{490} at 48 hours in response to Δ*glpD*/Δ*golD*/Δ*uhpT* (Top), WT (Middle), and PrfA* (Bottom) respiration of carbon metabolites (PM1 & PM2A) at 37°C stationary. Each bar indicates the average of 3 biologic replicates. Samples were normalized to readings of a α-D-glucose control (~1 on scale and labeled) and sorted based on cluster analysis. Select differentially used metabolites from Table 1 and Table 2 of hexose phosphates, glycerol, and lactose are labeled above.

Table 1. Statistically significant and greater than 2-fold differentially used metabolites between WT and PrfA* *L. monocytogenes*

Metabolite	Fold Change (WT/PrfA*)	P-Value
D-Glucose-6-Phosphate	0.16	<0.001
D-Glucose-1-Phosphate	0.16	<0.001
D-Fructose-6-Phosphate	0.21	<0.001
alpha-D-Lactose	2.12	0.002

Purple highlights indicate metabolites used more in PrfA* strains compared to wild-type and gold highlights are less used by PrfA*.

Table 2. Statistically significant and greater than 2-fold differentially used metabolites between WT and Δ*glpD*/Δ*golD*/Δ*uhpT L. monocytogenes*

Metabolite	Fold Change (WT/Δ*glpD*/Δ*golD*/Δ*uhpT*)	P-Value
Glycerol	7.97	0.001
alpha-Methyl-D-Glucoside	2.25	0.005

Purple highlights indicate metabolites used more in WT strains compared to Δ*glpD*/Δ*golD*/Δ*uhpT L. monocytogenes.*

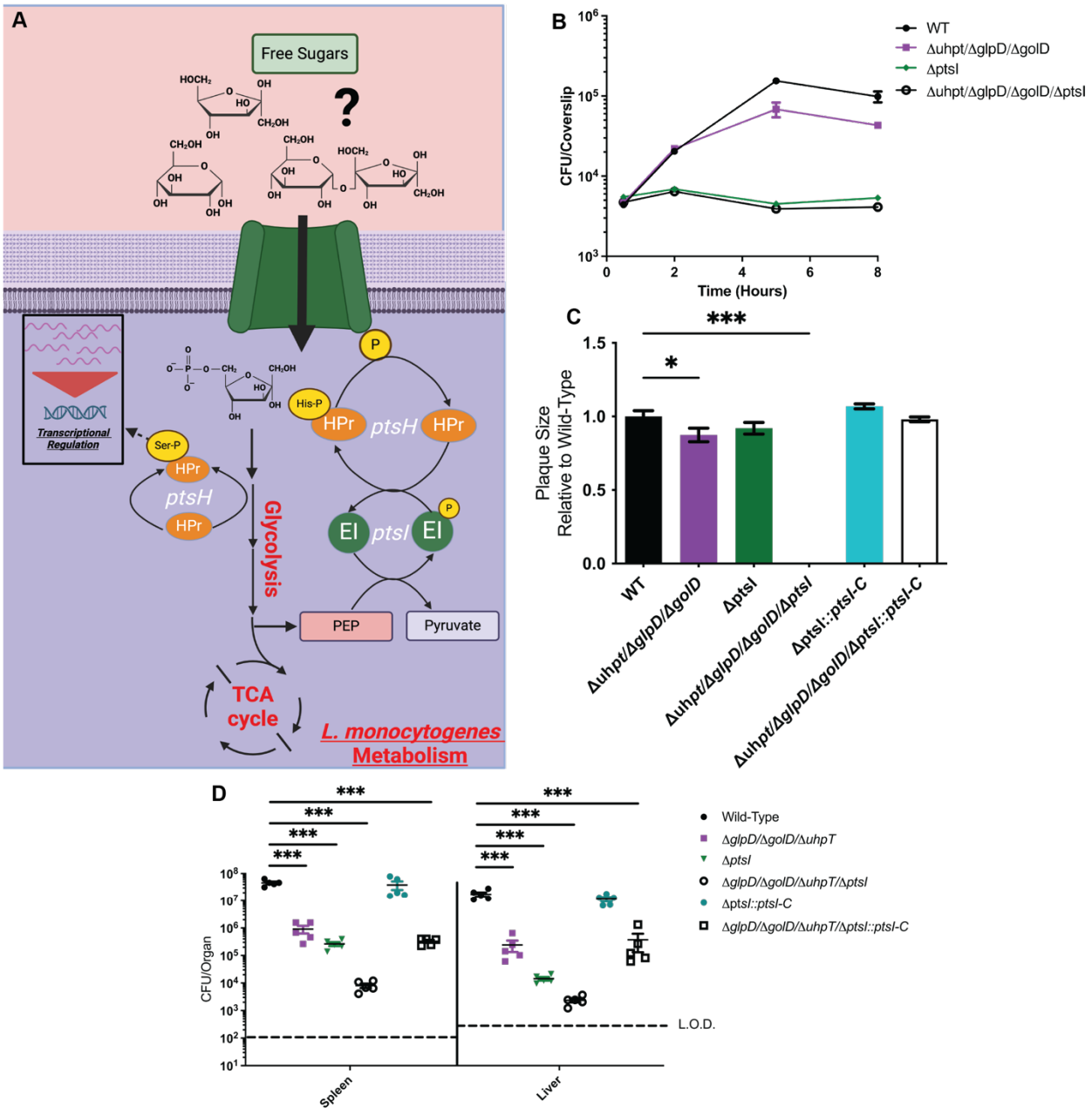

Figure 4. Δ*ptsI* mutants are impaired for intramacrophage growth and virulence, with more decreased virulence in a Δ*glpD*/Δ*golD*/Δ*uhpT* background and can be trans-complemented with *ptsI* over expression for intracellular growth and virulence. (A) PTS mediated free sugar import and phosphorylation by phosphocarrier protein phospho-cycling from the terminal conversion of phosphoenol-pyruvate (PEP) to pyruvate. (B) Intracellular growth of WT, Δ*glpD*/Δ*golD*/Δ*uhpT*, Δ*ptsI*, and Δ*glpD*/Δ*golD*/Δ*uhpT*/Δ*ptsI* was determined in

BMDMs following infection at an MOI of 0.2. Growth curves are representative of at least three independent experiments. Error bars represent the standard deviation of the means of technical triplicates within the representative experiment. (C) L2 fibroblasts were infected with indicated *L. monocytogenes* strains at an MOI of 0.5 and were examined for plaque formation 4 days post infection. Assays were performed in biological triplicate and data displayed is the median and SEM of a strain's plaque size relative to WT in one of three representative biological replicates. (D) Bacterial burdens from the spleen and liver were enumerated at 48 hours post-intravenous infection with $1x10^5$ bacteria. Data are representative of results from two separate experiments. Horizontal dashed lines represent the limits of detection, and the bars associated with the individual strains represents the mean and SEM of the group.

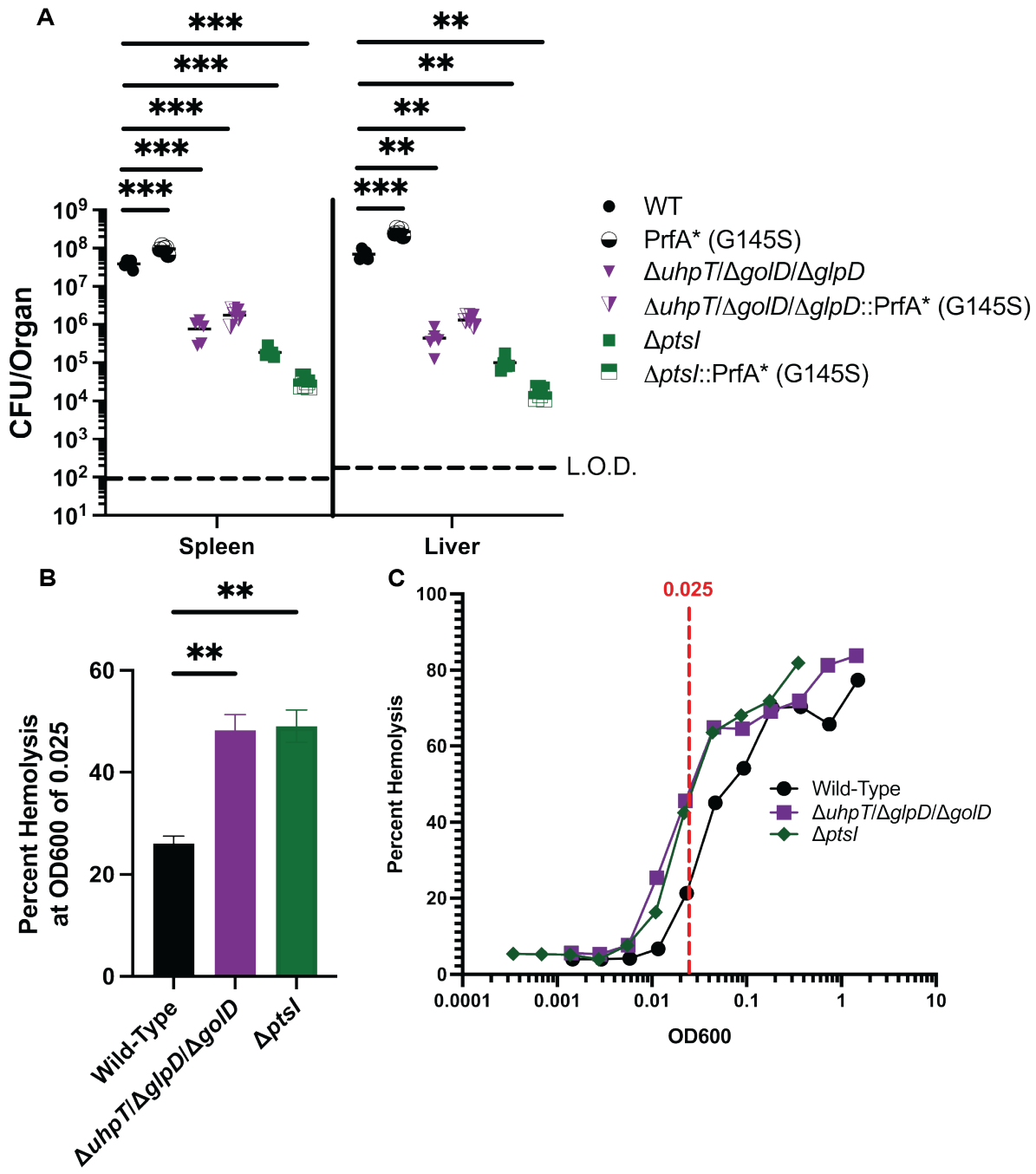

Figure 5. Δ*glpD*/Δ*golD*/Δ*uhpT* and Δ*ptsI* mutants are not rescued by constitutively active PrfA and show basally higher levels of virulence protein activity. (A) Bacterial burdens from the spleen and liver were enumerated at 48 hours post-intravenous infection with $1x10^5$ bacteria. Data are representative of results from two separate experiments. Horizontal dashed lines represent the limits of detection, and the bars associated with the individual strains represents the

mean and SEM of the group. (B) Median and SEMs of percent hemolysis interpolated at OD600 of 0.025 from biological triplicate for displayed strains. (C) Representative toxin dose-response curves from a single biological replicate used for interpolation and generation of continuous percent hemolysis data as a function of OD600.

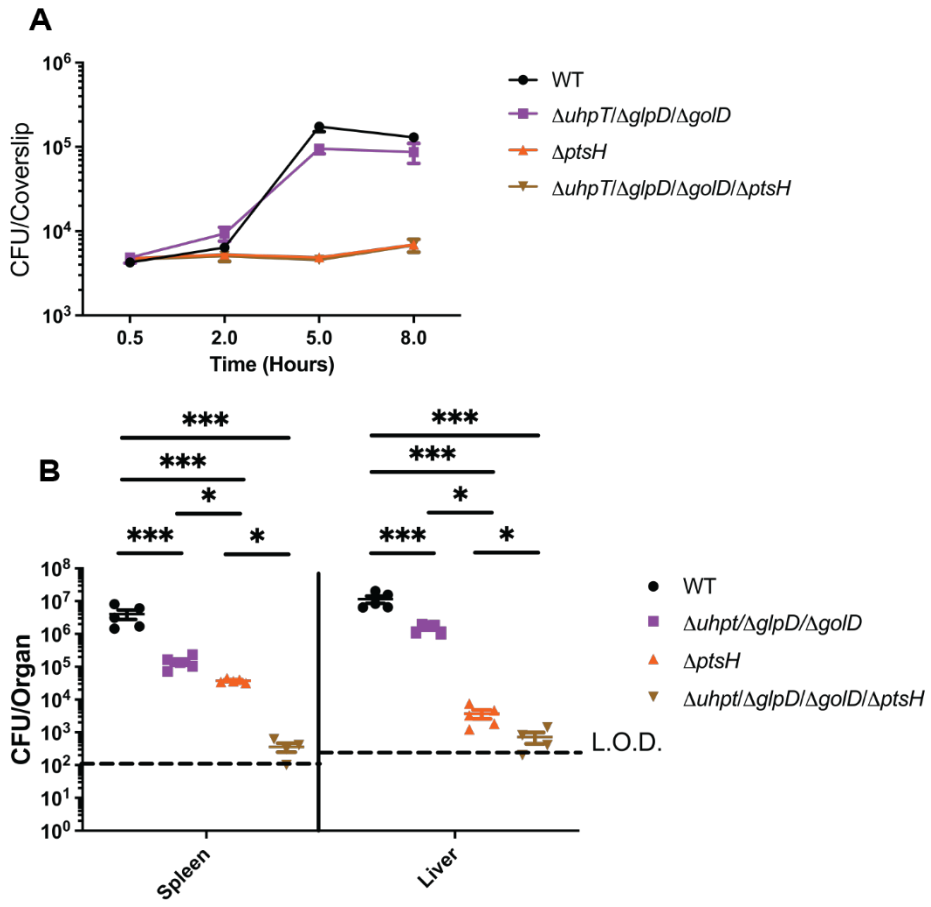

Figure 6. Δ*ptsH* mutants are more attenuated for intracellular growth and virulence than in Δ*ptsI* in all backgrounds. (A) Intracellular growth of wild-type, Δ*glpD*/Δ*golD*/Δ*uhpT*, Δ*ptsH*, and Δ*glpD*/Δ*golD*/Δ*uhpT*/Δ*ptsH* was determined in BMDMs following infection at an MOI of 0.2. Growth curves are representative of at least three independent experiments. Error bars represent the standard deviation of the means of technical triplicates within the representative experiment. (B) Bacterial burdens from the spleen and liver were enumerated at 48 hours post-intravenous infection with $1x10^5$ bacteria. Data are representative of results from two separate experiments. Horizontal dashed lines represent the limits of detection, and the bars associated with the individual strains represents the mean and SEM of the group.

SUPPLEMENTARY INFORMATION

Supplemental Table 1. Bacterial strains used in this study. Listed here are all bacterial strains used in this work. Those derived from prior works have been cited and those generated by us have been labeled under the 'Reference' column as 'This Work'. Relevant strain numbers have been so that if others wish to use one of these strains in their own work it can be sourced from our strain repository.

Strain	Description	Reference
XL1-Blue	competent *E. coli* strain	(61)
SM10	*E. coli* strain for conjugations into *L. monocytogenes;* Km^R	(61)
S17	*E. coli* strain for conjugations into *L. monocytogenes;* Sp^R	(80)
10403S [JDS1]	Background *L. monocytogenes* 10403s strain	(86)
JDS237	PrfA* (G145S)	(25)
JDS2641 & MJF35	Δ*uhpT*	This Work & (29)
JDS2642 & MJF112	Δ*glpD*/Δ*golD*	This Work
JDS2643 & MJF121	*ΔglpD/ΔgolD/ΔuhpT*	This Work
JDS2644 & MJF279	Δ*ptsI*	This Work
JDS2645 & MJF281	*ΔglpD/ΔgolD/ΔuhpT*/Δ*ptsI*	This Work
JDS2646 & MJF286	Δ*ptsI::ptsI-C (pIMK2)*	This Work
JDS2647 & MJF288	*ΔglpD/ΔgolD/ΔuhpT*/Δ*ptsI::ptsI-C (pIMK2)*	This Work
JDS2648 & MJF223	Δ*ptsH*	This Work & (54)
JDS2649 & MJF225	*ΔglpD/ΔgolD/ΔuhpT*/Δ*ptsH*	This Work
JDS2650 & MJF346	PrfA* (G145S) Cleanly generated in JDS1 background	This Work
JDS2651 & MJF342	*ΔglpD/ΔgolD/ΔuhpT*::PrfA* (G145S)	This Work
JDS2652 & MJF348	Δ*ptsI*::PrfA* (G145S)	This Work

Supplemental Table 2. Primers used in this study. Below are primers used to generate the complement and clean-deletion constructs in pIMK2 or pLIM and pKSV7, respectively. Restriction enzyme cut sites used for homologous overlaps for Gibson Assembly have been provided.

Primers Sequence	Description	Restriction Sites
TACGAATTCGAGCTCGGTACCCGGG GATCCTTTGAATATAGCGATGGAAA AAATGTTCTA	pKSV7 Construct *uhpT* deletion; Fragment 1 Forward	BamHI
TCT TCA CTC ATT GTT TTC AAC TTA TAG ATG TAA TGA CAT TAT AAT TTT CCT TTC CAG TGT	Construct *uhpT* deletion; Fragment 1 Reverse	N/A
ACACTGGAAAGGAAAATTATAATG TCATTACATCTATAAGTTGAAAACA ATGAGTGAAGA	Construct *uhpT* deletion; Fragment 2 Forward	N/A
GAC GGC CAG TGC CAA GCT TGC ATG CCT GCA GGT GCG GGC GCT GCG CTT GGT CCA GCT TTC G	pKSV7 Construct *uhpT* deletion; Fragment 2 Reverse	PstI
GGTACCCGGGGATCCCTACCAGCAA TGAAAGC	pKSV7 Construct *glpD* deletion; Fragment 1 Forward	BamHI
TTGAATTTTAATTATCTATCGTGTTG TACCATTTTGTTTGC	Construct *glpD* deletion; Fragment 1 Reverse	N/A
GCAAACAAAATGGTACAACACGAT AGATAATTAAAATTCAA	Construct *glpD* deletion; Fragment 2 Forward	N/A
CTTGCATGCCTGCAGGCTTCGGTAG TACTAACACC	pKSV7 Construct *glpD* deletion; Fragment 2 Reverse	PstI
GAGCTCGGTACCCGGGGATCCTAGA ATCAATCATTGATCTAAGC	pKSV7 Construct *golD* deletion; Fragment 1 Forward	BamHI
GAACTTTAAAGCTGAATACTTTATT TAATAAAAGTCATTTTTCATTACCT CC	Construct *golD* deletion; Fragment 1 Reverse	N/A
GGAGGTAATGAAAAATGACTTTTAT TAAATAAAGTATTCAGCTTTAAAGT TC	Construct *golD* deletion; Fragment 2 Forward	N/A
CAGTGCCAAGCTTGCATGCCTGCAG GGCGTTTTACTGCCAG	pKSV7 Construct *golD* deletion; Fragment 2 Reverse	PstI

ATTCGAGCTCGGTACCCGGGGATCC TAGAGCATTGTCACTCGG	pLIM Construct *ptsI* deletion; Fragment 1 Forward	BamHI
GTCTTTATTCAGATATTATTCTGCAG TCTCTTTAGCCATTATTCAGCC	Construct *ptsI* deletion; Fragment 1 Reverse	N/A
GGCTGAATAATGGCTAAAGAGACT GCAGAATAATATCTGAATAAAGAC	Construct *ptsI* deletion; Fragment 2 Forward	N/A
CAAGCTTGCATGCCTGCAGGGATCC TGCACCAATCCCTTGAC	pLIM Construct *ptsI* deletion; Fragment 2 Reverse	BamHI
CCCATGGAAAAGGATCCATGGCTA AAGAGTTGAAAGGTATC	Construct *ptsI* complement; pIMK2 Vector Foreward	BamHI
ATATCGAATTCCTGCAGGTCTAGGT CTTTATTCAGATATTATTCTGC	Construct *ptsI* complement; pIMK2 Vector Reverse	PstI
ATTCGAGCTCGGTACCCGGGGATCC TGTTGCCTCTATCTTGCTG	pLIM Construct *ptsH* deletion; Fragment 1 Forward	BamHI
CCATTATTCAGCCAATCCTTCAAAA CTTGCTTGTTCCATAATTTAC	Construct *ptsH* deletion; Fragment 1 Reverse	N/A
GTAAATTATGGAACAAGCAAGTTTT GAAGGATTGGCTGAATAATGG	Construct *ptsH* deletion; Fragment 2 Forward	N/A
GCAGGTCGACTCTAGAGGATCCAG ATTCAAACATACCAATAAACATGTC	pLIM Construct *ptsH* deletion; Fragment 2 Reverse	BamHI
AGCTCGGTACCCGGGGATCCagactgct tatcaagcttccaaag	pLIM Construct PrfA* (G145S) Revertant FWD	BamHI
TTGCATGCCTGCAGGGATCCgtgatgatc tagtagtggtttcacc	pLIM Construct PrfA* (G145S) Revertant RVS	BamHI

Supplemental Table 3. Results of BioLog PM1 and PM2A at 48 hours for WT, Δ*glpD*/Δ*golD*/Δ*uhpT*, and PrfA*. The 'Metabolite' column shows scientific names for all metabolites screened using BioLog Phenotypic Microarrays. Fold usage of each metabolite for each strain [WT, Δ*glpD*/Δ*golD*/Δ*uhpT*, and PrfA* (G145S)] is displayed relative the α-D-Glucose usage. Finally, p-values from comparisons of average metabolite usage per strain is shown for all metabolites. Comparison data was limited to WT v.s. Δ*glpD*/Δ*golD*/Δ*uhpT and* WT v.s. PrfA*.

	Fold Usage Normalized to α-D-Glucose			P-value (Student's T-Test)	
Metabolite	WT	Δ*glpD*/Δ*golD*/Δ*uhpT*	PrfA*	WT v.s. Δ*glpD*/Δ*golD*/Δ*uhpT*	WT v.s. PrfA*
Amygdalin	1.24	1.18	1.15	0.25	0.10
N-Acetyl-D-Glucosamine	1.06	0.99	1.05	0.30	0.76
Maltotriose	1.08	1.01	1.04	0.22	0.18
D-Trehalose	0.93	0.96	1.03	0.39	0.01
D-Glucose-6-Phosphate	0.17	0.17	1.02	0.97	<0.01
D-Fructose-6-Phosphate	0.21	0.19	1.01	0.68	<0.01
Beta-Methyl-D-Glucoside	1.03	1.02	1.01	0.78	0.72
alpha-Cyclodextrin	1.14	1.05	1.11	0.41	0.71
alpha-D-Glucose	1.00	1.00	1.00	N/A	N/A
D-Mannose	1.18	1.06	0.99	0.14	0.01
D-Cellobiose	0.98	0.96	0.99	0.70	0.83
Arbutin	1.17	1.15	1.08	0.53	0.06
D-Glucose-1-Phosphate	0.16	0.17	0.98	0.58	<0.01
Beta-Cyclodextrin	1.12	1.04	1.07	0.24	0.30
D-Fructose	1.06	0.91	0.96	0.25	0.38
Beta-D-Allose	1.12	1.04	1.04	0.25	0.16
Xylitol	1.18	1.06	1.03	0.30	0.24
Sailcin	1.03	1.03	1.05	0.98	0.63
Gamma-Cyclodextrin	0.98	0.99	1.02	0.88	0.55
N-Acetyl-Beta-D-Mannosamine	0.92	0.88	0.93	0.23	0.82
Glycerol	1.05	0.13	0.92	<0.01	0.31
L-Rhamnose	1.07	0.94	0.92	0.35	0.32
Gentiobiose	0.94	0.96	0.99	0.55	0.05

D-Psicose	1.05	0.92	0.89	0.31	0.20
Dihydroxy Acetone	1.15	0.99	0.94	0.24	0.14
D-Glucosamine	1.04	1.00	0.91	0.71	0.12
Uridine	0.93	0.80	0.81	0.45	0.48
Alpha-Methyl-D-Mannoside	1.17	1.08	0.86	0.36	0.12
L-Lyxose	0.89	0.70	0.75	0.21	0.36
2-Deoxy-D-Ribose	0.86	0.74	0.77	0.34	0.44
alpha-Methyl-D-Glucoside	1.23	0.55	0.79	<0.01	0.02
D-Arabitol	0.99	0.95	0.74	0.77	0.01
D-Ribose	0.78	0.68	0.65	0.41	0.27
Maltose	1.12	1.07	0.64	0.25	<0.01
alpha-D-Lactose	1.24	1.14	0.59	0.30	<0.01
D-Malic Acid	0.14	0.16	0.58	0.09	0.39
D-Xylose	0.65	0.54	0.54	0.47	0.49
Acetic Acid	0.59	0.57	0.51	0.69	0.35
5-Keto-D-Gluconic Acid	0.60	0.53	0.52	0.27	0.20
Capric Acid	0.46	0.43	0.46	0.85	0.98
Inosine	0.57	0.48	0.40	0.51	0.23
N-Acetyl-D-Glucosaminitol	0.53	0.43	0.43	0.27	0.25
Acetoacetic Acid	0.41	0.37	0.38	0.73	0.80
Sorbic Acid	0.48	0.44	0.42	0.39	0.23
Dextrin	0.70	0.57	0.42	0.33	0.07
L-Arabinose	0.42	0.37	0.36	0.51	0.47
m-Tartaric Acid	0.14	0.16	0.35	0.08	0.42
Adenosine	0.40	0.35	0.34	0.57	0.48
D-Arabinose	0.48	0.40	0.34	0.21	0.04
alpha-keto-Butyric Acid	0.48	0.48	0.30	1.00	<0.01
Palatinose	0.38	0.33	0.28	0.25	0.02
Mucic Acid	0.31	0.39	0.25	0.50	0.59
D-Fucose	0.28	0.30	0.27	0.69	0.78
Beta-Methyl-D-Galactoside	0.30	0.28	0.26	0.81	0.54
Putrescine	0.20	0.18	0.27	0.71	0.28
D-Tagatose	0.36	0.32	0.26	0.59	0.18
Thymidine	0.24	0.27	0.23	0.50	0.73
3-Methyl Glucose	0.32	0.31	0.25	0.94	0.50
Adonitol	0.25	0.23	0.22	0.70	0.66
Oxalic Acid	0.29	0.31	0.24	0.79	0.22
Glyoxylic Acid	0.24	0.26	0.22	0.88	0.65
Sedoheptulosan	0.25	0.24	0.24	0.88	0.84

Glucuronamide	0.27	0.24	0.21	0.15	0.03
D,L-Octopamine	0.22	0.20	0.23	0.65	0.90
2-Deoxy-Adenosine	0.26	0.29	0.20	0.56	0.29
Pyruvic Acid	0.26	0.27	0.20	0.69	0.01
Oxalomalic Acid	0.27	0.24	0.22	0.59	0.31
2,3-Butanedione	0.25	0.22	0.22	0.38	0.37
Mannan	0.24	0.21	0.22	0.57	0.67
L-Histidine	0.23	0.21	0.21	0.57	0.41
Turanose	0.31	0.25	0.21	0.30	0.09
Pectin	0.29	0.29	0.21	0.86	0.06
Sebacic Acid	0.60	0.22	0.20	0.21	0.19
L-Sorbose	0.23	0.22	0.20	0.88	0.56
alpah-Keto-Valeric Acid	0.24	0.21	0.19	0.60	0.35
Sec-Butylamine	0.22	0.22	0.19	0.94	0.37
Beta-Methyl-D-Xyloside	0.21	0.24	0.19	0.54	0.66
L-Fucose	0.22	0.21	0.17	0.80	0.27
N-Acetyl-Neuaminic Acid	0.21	0.20	0.19	0.48	0.31
Methyl Pyruvate	0.20	0.21	0.17	0.46	0.02
Propionic Acid	0.20	0.24	0.17	0.32	0.20
3-0-Beta-D-Galactopyranosyl-D-Arabinose	0.26	0.24	0.18	0.67	0.07
L-Alanyl-Glycine	0.25	0.26	0.16	0.34	<0.01
L-Galactonic Acide-gamma-lactone	0.19	0.19	0.16	0.80	0.23
Inulin	0.34	0.27	0.18	0.46	0.11
L-Pyroglutamic Acid	0.21	0.19	0.17	0.49	0.30
D-Melezitose	0.23	0.21	0.18	0.67	0.31
L-Lactic Acid	0.26	0.25	0.16	0.83	0.03
L-Alanine	0.19	0.21	0.16	0.59	0.26
Tween 40	0.18	0.19	0.15	0.51	0.14
D-Sorbitol	0.21	0.18	0.15	0.08	0.02
D-Galactose	0.20	0.17	0.15	0.57	0.29
D,L-alpha-glycerol-phosphate	0.17	0.17	0.15	0.85	0.38
D-Galactonic Acid-gamma-Lactone	0.16	0.16	0.15	0.55	0.57
alpha-Methyl-D-Galactoside	0.18	0.18	0.15	0.99	0.49
D-Glucuronic Acid	0.19	0.19	0.15	0.89	0.20
L-Alaninamide	0.20	0.19	0.16	0.94	0.23
Butyric Acid	0.20	0.26	0.16	0.47	0.19
2-Aminoethanol	0.17	0.18	0.14	0.44	0.14
L-Methionine	0.20	0.16	0.16	0.46	0.55

alpha-Hydroxy Butyric Acid	0.21	0.21	0.14	0.96	0.13
D-Galacturonic Acid	0.18	0.18	0.14	0.93	0.04
L-Arabitol	0.19	0.16	0.16	0.34	0.26
Maltitol	0.22	0.18	0.16	0.47	0.29
D-Mannitol	0.17	0.17	0.14	0.83	0.20
Tween 80	0.17	0.17	0.14	1.00	0.09
m-Hydroxy Phenyl Acetic Acid	0.17	0.18	0.14	0.57	0.06
Glycogen	0.21	0.19	0.15	0.49	0.09
Dulcitol	0.17	0.16	0.14	0.69	0.19
Glycyl-L-Proline	0.22	0.19	0.14	0.17	0.02
Beta-Methyl-D-Glucuronic Acid	0.20	0.18	0.15	0.64	0.24
Lactitol	0.20	0.19	0.15	0.81	0.26
Delta-Amino Valeric Acid	0.16	0.15	0.15	0.70	0.75
L-Glucose	0.20	0.18	0.15	0.58	0.23
L-Leucine	0.16	0.15	0.15	0.55	0.62
Glycine	0.18	0.17	0.15	0.68	0.27
Caproic Acid	0.18	0.17	0.15	0.58	0.20
L-Proline	0.18	0.18	0.14	0.94	0.07
Succinic Acid	0.17	0.18	0.14	0.72	0.06
D-Gluconic Acid	0.17	0.18	0.14	0.61	0.12
Negative Control	0.18	0.17	0.14	0.84	0.03
Negative Control	0.18	0.16	0.15	0.49	0.43
3-Hydroxy-2-Butanone	0.21	0.17	0.15	0.41	0.27
Bromo Succinic Acid	0.15	0.18	0.13	0.35	0.21
D-Alanine	0.16	0.17	0.13	0.55	0.21
2-Hydroxy Benzoic Acid	0.16	0.17	0.15	0.62	0.39
L-Aspartic Acid	0.17	0.16	0.13	0.50	0.03
Apha-Hydroxy Glutaric Acid-gamma-lactone	0.16	0.18	0.13	0.33	0.24
p-Hydroxy Phenyl Acetic Acid	0.16	0.17	0.13	0.58	0.01
i-Erythritol	0.19	0.17	0.15	0.26	0.05
Beta-Hydroxy Butyric Acid	0.20	0.19	0.15	0.91	0.16
Sucrose	0.16	0.17	0.13	0.65	0.22
D-Threonine	0.14	0.15	0.13	0.63	0.51
D-Ribono-1,4-Lactone	0.16	0.16	0.15	0.96	0.26
Tyramine	0.16	0.17	0.13	0.57	0.18
Glycolic Acid	0.15	0.17	0.13	0.16	0.10
Chondroitin Sulfate C	0.19	0.16	0.15	0.33	0.18
L-Threonine	0.16	0.18	0.13	0.44	0.08

D-Saccharic Acid	0.17	0.18	0.13	0.87	0.11
D-Melibiose	0.17	0.18	0.13	0.91	0.10
4-Hydroxy Benzoic Acid	0.21	0.19	0.14	0.46	0.06
D-Raffinose	0.19	0.16	0.14	0.34	0.11
Alpha-Keto-Glutaric Acid	0.17	0.16	0.13	0.86	0.17
Gelatin	0.21	0.18	0.14	0.42	0.11
L-Lysine	0.18	0.17	0.14	0.73	0.26
Stachyose	0.19	0.18	0.14	0.65	0.19
L-Serine	0.17	0.17	0.13	0.96	0.01
Mono Methyl Succinate	0.16	0.17	0.13	0.39	0.01
Laminarin	0.17	0.18	0.14	0.92	0.15
Glycyl-L-Aspartic Acid	0.18	0.17	0.13	0.56	0.14
D-Aspartic Acid	0.15	0.16	0.13	0.61	0.17
Lactulose	0.17	0.21	0.13	0.42	0.15
L-Glutamic Acid	0.17	0.18	0.13	0.74	0.06
Tricarballylic Acid	0.15	0.17	0.13	0.31	0.09
Citraconic Acid	0.18	0.18	0.14	0.95	0.27
1,2-Propanediol	0.16	0.17	0.13	0.81	0.25
L-Valine	0.17	0.17	0.14	1.00	0.27
Formic Acid	0.15	0.17	0.13	0.35	0.10
Phenylethylamine	0.15	0.16	0.13	0.39	0.30
N-Acetyl-L-Glutamic Acid	0.18	0.17	0.14	0.87	0.22
Fumaric Acid	0.15	0.17	0.13	0.30	0.08
Citric Acid	0.14	0.16	0.13	0.29	0.19
Succinamic Acid	0.18	0.16	0.14	0.55	0.17
N-Acetyl-D-Galactosamine	0.16	0.16	0.14	0.96	0.38
Glycyl-L-Glutamic Acid	0.17	0.17	0.13	0.75	0.03
L-Homoserine	0.17	0.16	0.14	0.71	0.16
Tween 20	0.15	0.14	0.12	0.91	0.44
L-Glutamine	0.15	0.16	0.12	0.18	0.07
L-Isoleucine	0.17	0.16	0.14	0.92	0.31
myo-Inositol	0.15	0.17	0.12	0.15	0.08
L-Ornithine	0.17	0.17	0.14	0.94	0.10
2,3-Butanediol	0.19	0.17	0.14	0.58	0.12
Glycolic Acid	0.17	0.17	0.14	0.93	0.18
D-Serine	0.15	0.14	0.12	0.90	0.13
Itaconic Acid	0.16	0.14	0.14	0.47	0.36
L-Asparagine	0.16	0.17	0.12	0.79	0.12
Hydroxy-L Prline	0.18	0.17	0.14	0.56	0.10

Quinic Acid	0.18	0.17	0.13	0.65	0.03
Melibionic Acid	0.23	0.20	0.13	0.82	0.32
gamma-Amino Butyric Acid	0.17	0.17	0.13	0.97	0.24
D,L-Malic Acid	0.16	0.17	0.12	0.58	0.06
D-Glucosaminic Acid	0.15	0.17	0.12	0.21	0.10
L-Malic Acid	0.15	0.15	0.12	0.39	<0.01
L-Arginine	0.17	0.16	0.13	0.48	0.11
D,L-Carnitine	0.17	0.17	0.13	0.88	0.10
Acetamide	0.18	0.17	0.13	0.71	0.10
D-Tartaric Acid	0.17	0.17	0.13	0.94	0.14
Citramalic Acid	0.17	0.17	0.13	0.95	0.17
L-Phenylalanine	0.17	0.16	0.13	0.85	0.11
D-Lactic Acid Methyl Ester	0.16	0.16	0.13	0.97	0.07
L-Tartaric Acid	0.17	0.17	0.13	0.88	0.02
Malonic Acide	0.17	0.16	0.12	0.52	0.10

REFERENCES:

1. Goetz M, Bubert A, Wang G, Chico-Calero I, Vazquez-Boland JA, Beck M, et al. Microinjection and growth of bacteria in the cytosol of mammalian host cells. Proc Natl Acad Sci USA. 2001 Oct 9;98(21):12221–6.

2. Creasey EA, Isberg RR. The protein SdhA maintains the integrity of the *Legionella* -containing vacuole. Proc Natl Acad Sci USA. 2012 Feb 28;109(9):3481–6.

3. Zhao W, Moest T, Zhao Y, Guilhon AA, Buffat C, Gorvel JP, et al. The Salmonella effector protein SifA plays a dual role in virulence. Sci Rep. 2015 Aug 13;5(1):12979.

4. Lamason RL, Bastounis E, Kafai NM, Serrano R, Del Álamo JC, Theriot JA, et al. Rickettsia Sca4 Reduces Vinculin-Mediated Intercellular Tension to Promote Spread. Cell. 2016 Oct;167(3):670-683.e10.

5. Gehre L, Gorgette O, Perrinet S, Prevost MC, Ducatez M, Giebel AM, et al. Sequestration of host metabolism by an intracellular pathogen. eLife. 2016 Mar 16;5:e12552.

6. Murdoch CC, Skaar EP. Nutritional immunity: the battle for nutrient metals at the host–pathogen interface. Nat Rev Microbiol. 2022 Nov;20(11):657–70.

7. Olive AJ, Sassetti CM. Metabolic crosstalk between host and pathogen: sensing, adapting and competing. Nat Rev Microbiol. 2016 Apr;14(4):221–34.

8. Keeney KM, Stuckey JA, O'Riordan MXD. LplA1-dependent utilization of host lipoyl peptides enables *Listeria* cytosolic growth and virulence. Molecular Microbiology. 2007 Nov;66(3):758–70.

9. Marquis H, Bouwer HG, Hinrichs DJ, Portnoy DA. Intracytoplasmic growth and virulence of Listeria monocytogenes auxotrophic mutants. Infect Immun. 1993 Sep;61(9):3756–60.

10. Flannagan RS, Farrell TJ, Trothen SM, Dikeakos JD, Heinrichs DE. Rapid removal of phagosomal ferroportin in macrophages contributes to nutritional immunity. Blood Advances. 2021 Jan 26;5(2):459–74.

11. Luan HH, Medzhitov R. Food Fight: Role of Itaconate and Other Metabolites in Antimicrobial Defense. Cell Metabolism. 2016 Sep;24(3):379–87.

12. Benoit M, Desnues B, Mege JL. Macrophage Polarization in Bacterial Infections. The Journal of Immunology. 2008 Sep 15;181(6):3733–9.

13. Portnoy DA, Auerbuch V, Glomski IJ. The cell biology of *Listeria monocytogenes* infection. The Journal of Cell Biology. 2002 Aug 5;158(3):409–14.

14. Scobie A, Kanagarajah S, Harris RJ, Byrne L, Amar C, Grant K, et al. Mortality risk factors for listeriosis - A 10 year review of non-pregnancy associated cases in England 2006-2015. J Infect. 2019 Mar;78(3):208–14.

15. Swaminathan B, Gerner-Smidt P. The epidemiology of human listeriosis. Microbes and Infection. 2007 Aug 1;9(10):1236–43.

16. Todd ECD. Surveillance of listeriosis and its causative pathogen, Listeria monocytogenes. Food Control. 2011;7.

17. Eisenreich W, Dandekar T, Heesemann J, Goebel W. Carbon metabolism of intracellular bacterial pathogens and possible links to virulence. Nat Rev Microbiol. 2010 Jun;8(6):401–12.

18. Rohmer L, Hocquet D, Miller SI. Are pathogenic bacteria just looking for food? Metabolism and microbial pathogenesis. Trends in Microbiology. 2011 Jul;19(7):341–8.

19. Stokes JM, Lopatkin AJ, Lobritz MA, Collins JJ. Bacterial Metabolism and Antibiotic Efficacy. Cell Metabolism. 2019 Aug;30(2):251–9.

20. Milenbachs AA, Brown DP, Moors M, Youngman P. Carbon-source regulation of virulence gene expression in *Listeria monocytogenes*. Molecular Microbiology. 1997 Mar;23(5):1075–85.

21. Hamon M, Bierne H, Cossart P. Listeria monocytogenes: a multifaceted model. Nat Rev Microbiol. 2006 Jun 1;4(6):423–34.

22. Tilney LG, Portnoy DA. Actin filaments and the growth, movement, and spread of the intracellular bacterial parasite, Listeria monocytogenes. Journal of Cell Biology. 1989 Oct 1;109(4):1597–608.

23. Bruno JC, Freitag NE. Constitutive Activation of PrfA Tilts the Balance of Listeria monocytogenes Fitness Towards Life within the Host versus Environmental Survival. Ii RMR, editor. PLoS ONE. 2010 Dec 7;5(12):e15138.

24. Vega Y, Rauch M, Banfield MJ, Ermolaeva S, Scortti M, Goebel W, et al. New *Listeria monocytogenes prfA* * mutants, transcriptional properties of PrfA* proteins and structure–function of the virulence regulator PrfA. Molecular Microbiology. 2004 Jun;52(6):1553–65.

25. Miner MD, Port GC, Freitag NE. Functional impact of mutational activation on the Listeria monocytogenes central virulence regulator PrfA. Microbiology. 2008 Nov 1;154(11):3579–89.

26. Cossart P. Illuminating the landscape of host–pathogen interactions with the bacterium *Listeria monocytogenes*. Proc Natl Acad Sci USA. 2011 Dec 6;108(49):19484–91.

27. Drevets DA. Dissemination of *Listeria monocytogenes* by Infected Phagocytes. Tuomanen EI, editor. Infect Immun. 1999 Jul;67(7):3512–7.

28. Melton-Witt JA, Rafelski SM, Portnoy DA, Bakardjiev AI. Oral Infection with Signature-Tagged Listeria monocytogenes Reveals Organ-Specific Growth and Dissemination Routes in Guinea Pigs. Camilli A, editor. Infect Immun. 2012 Feb;80(2):720–32.

29. Chico-Calero I, Suárez M, González-Zorn B, Scortti M, Slaghuis J, Goebel W, et al. Hpt, a bacterial homolog of the microsomal glucose- 6-phosphate translocase, mediates rapid intracellular proliferation in Listeria. Proc Natl Acad Sci USA. 2002 Jan 8;99(1):431–6.

30. Eylert E, Schär J, Mertins S, Stoll R, Bacher A, Goebel W, et al. Carbon metabolism of *Listeria monocytogenes* growing inside macrophages. Molecular Microbiology. 2008 Aug;69(4):1008–17.

31. Grubmueller S, Schauer K, Goebel W, Fuchs TM, Eisenreich W. Analysis of carbon substrates used by Listeria monocytogenes during growth in J774A.1 macrophages suggests a bipartite intracellular metabolism. Front Cell Infect Microbiol; 4. Available from: http://journal.frontiersin.org/article/10.3389/fcimb.2014.00156/abstract

32. Joseph B, Mertins S, Stoll R, Schär J, Umesha KR, Luo Q, et al. Glycerol Metabolism and PrfA Activity in *Listeria monocytogenes*. J Bacteriol. 2008 Aug;190(15):5412–30.

33. Slaghuis J, Goetz M, Engelbrecht F, Goebel W. Inefficient Replication of *Listeria innocua* in the Cytosol of Mammalian Cells. J INFECT DIS. 2004 Feb;189(3):393–401.

34. Best A, Kwaik YA. Nutrition and bi-partite metabolism of intracellular pathogens. 2020;19.

35. Cantor JR, Abu-Remaileh M, Kanarek N, Freinkman E, Gao X, Louissaint A, et al. Physiologic Medium Rewires Cellular Metabolism and Reveals Uric Acid as an Endogenous Inhibitor of UMP Synthase. Cell. 2017 Apr;169(2):258-272.e17.

36. Rossiter NJ, Huggler KS, Adelmann CH, Keys HR, Soens RW, Sabatini DM, et al. CRISPR screens in physiologic medium reveal conditionally essential genes in human cells. Cell Metabolism. 2021 Jun;33(6):1248-1263.e9.

37. Leney-Greene MA, Boddapati AK, Su HC, Cantor JR, Lenardo MJ. Human Plasma-like Medium Improves T Lymphocyte Activation. iScience. 2020 Jan;23(1):100759.

38. Crespo Tapia N, den Besten HMW, Abee T. Glycerol metabolism induces Listeria monocytogenes biofilm formation at the air-liquid interface. International Journal of Food Microbiology. 2018 May 20;273:20–7.

39. Chen GY, Pensinger DA, Sauer JD. *Listeria monocytogenes* cytosolic metabolism promotes replication, survival, and evasion of innate immunity. Cellular Microbiology. 2017 Oct;19(10):e12762.

40. Wang S, Orsi RH, Tang S, Zhang W, Wiedmann M, Boor KJ. Phosphotransferase System-Dependent Extracellular Growth of Listeria monocytogenes Is Regulated by Alternative Sigma Factors σ^{L} and σ^{H}. Appl Environ Microbiol. 2014 Dec 15;80(24):7673–82.

41. Muchaamba F, Eshwar AK, Stevens MJA, von Ah U, Tasara T. Variable Carbon Source Utilization, Stress Resistance, and Virulence Profiles Among Listeria monocytogenes Strains Responsible for Listeriosis Outbreaks in Switzerland. Front Microbiol. 2019 May 3;10:957.

42. Liu Y, Ceruso M, Jiang Y, Datta AR, Carter L, Strain E, et al. Construction of *Listeria monocytogenes* Mutants with In-Frame Deletions in the Phosphotransferase Transport System (PTS) and Analysis of Their Growth under Stress Conditions. Journal of Food Science;78(9). Available from: https://ift.onlinelibrary.wiley.com/doi/10.1111/1750-3841.12181

43. Barabote RD, Saier MH. Comparative Genomic Analyses of the Bacterial Phosphotransferase System. Microbiol Mol Biol Rev. 2005 Dec;69(4):608–34.

44. Stoll R, Goebel W. The major PEP-phosphotransferase systems (PTSs) for glucose, mannose and cellobiose of Listeria monocytogenes, and their significance for extra- and intracellular growth. Microbiology. 2010 Apr 1;156(4):1069–83.

45. Sauer JD, Herskovits AA, O'Riordan MXD. Metabolism of the Gram-Positive Bacterial Pathogen *Listeria monocytogenes*. Fischetti VA, Novick RP, Ferretti JJ, Portnoy DA, Braunstein M, Rood JI, editors. Microbiol Spectr. 2019 Jul 19;7(4):7.4.26.

46. Abdelhamed H, Ramachandran R, Narayanan L, Islam S, Ozan O, Freitag N, et al. Role of FruR transcriptional regulator in virulence of Listeria monocytogenes and identification of its regulon. Wen ZT, editor. PLoS ONE. 2022 Sep 2;17(9):e0274005.

47. Buchrieser C, Rusniok C, The Listeria Consortium, Kunst F, Cossart P, Glaser P. Comparison of the genome sequences of *Listeria monocytogenes* and *Listeria innocua* : clues for

evolution and pathogenicity. FEMS Immunology & Medical Microbiology. 2003 Apr;35(3):207–13.

48. Hain T, Steinweg C, Kuenne CT, Billion A, Ghai R, Chatterjee SS, et al. Whole-Genome Sequence of *Listeria welshimeri* Reveals Common Steps in Genome Reduction with *Listeria innocua* as Compared to *Listeria monocytogenes*. J Bacteriol. 2006 Nov;188(21):7405–15.

49. Vu-Khac H, Miller KW. Regulation of Mannose Phosphotransferase System Permease and Virulence Gene Expression in *Listeria monocytogenes* by the EII $_{t}^{Man}$ Transporter. Appl Environ Microbiol. 2009 Nov;75(21):6671–8.

50. Maury MM, Tsai YH, Charlier C, Touchon M, Chenal-Francisque V, Leclercq A, et al. Uncovering Listeria monocytogenes hypervirulence by harnessing its biodiversity. Nat Genet. 2016 Mar;48(3):308–13.

51. Saier Jr. MH. The Bacterial Phosphotransferase System: New Frontiers 50 Years after Its Discovery. Microb Physiol. 2015;25(2–3):73–8.

52. Postma PW. Phosphoenolpyruvate:Carbohydrate Phosphotransferase Systems of Bacteria. MICROBIOL REV. 1993;57.

53. Brehm K, Ripio MT, Kreft JR. The bvr Locus of Listeria monocytogenes Mediates Virulence Gene Repression by ᴺʟ-Glucosides. 1999;181.

54. Mertins S, Joseph B, Goetz M, Ecke R, Seidel G, Sprehe M, et al. Interference of Components of the Phosphoenolpyruvate Phosphotransferase System with the Central Virulence Gene Regulator PrfA of *Listeria monocytogenes*. J Bacteriol. 2007 Jan 15;189(2):473–90.

55. Aké FMD, Joyet P, Deutscher J, Milohanic E. Mutational analysis of glucose transport regulation and glucose-mediated virulence gene repression in *Listeria monocytogenes*. Molecular Microbiology. 2011 Jul;81(1):274–93.

56. Freitag NE, Port GC, Miner MD. Listeria monocytogenes — from saprophyte to intracellular pathogen. Nat Rev Microbiol. 2009 Sep;7(9):623–8.

57. Görke B, Stülke J. Carbon catabolite repression in bacteria: many ways to make the most out of nutrients. Nat Rev Microbiol. 2008 Aug;6(8):613–24.

58. Portman JL, Dubensky SB, Peterson BN, Whiteley AT, Portnoy DA. Activation of the *Listeria monocytogenes* Virulence Program by a Reducing Environment. Miller JF, editor. mBio. 2017 Nov 8;8(5):e01595-17.

59. Camilli A, Tilney LG, Portnoy DA. Dual roles of plcA in Listeria monocytogenes pathogenesis. Mol Microbiol. 1993 Apr;8(1):143–57.

60. Sun AN, Camilli A, Portnoy DA. Isolation of Listeria monocytogenes small-plaque mutants defective for intracellular growth and cell-to-cell spread. Infect Immun. 1990 Nov;58(11):3770–8.

61. Chen GY, McDougal CE, D'Antonio MA, Portman JL, Sauer JD. A Genetic Screen Reveals that Synthesis of 1,4-Dihydroxy-2-Naphthoate (DHNA), but Not Full-Length Menaquinone, Is Required for *Listeria monocytogenes* Cytosolic Survival. Swanson MS, editor. mBio; 8(2). Available from: https://journals.asm.org/doi/10.1128/mBio.00119-17

62. Fox EM, Bierne H, Stessl B, editors. Listeria Monocytogenes: Methods and Protocols [Internet]. New York, NY: Springer US; 2021. (Methods in Molecular Biology; vol. 2220). Available from: http://link.springer.com/10.1007/978-1-0716-0982-8

63. Luque-Sastre L, Jordan K, Fanning S, Fox EM. High-Throughput Characterization of Listeria monocytogenes Using the OmniLog Phenotypic Microarray. In: Fox EM, Bierne H, Stessl B, editors. Listeria Monocytogenes: Methods and Protocols. New York, NY: Springer US; 2021. p. 107–13. Available from: https://doi.org/10.1007/978-1-0716-0982-8_8

64. Wishart DS, Tzur D, Knox C, Eisner R, Guo AC, Young N, et al. HMDB: the Human Metabolome Database. Nucleic Acids Research. 2007 Jan 3;35(Database):D521–6.

65. Zemansky J, Kline BC, Woodward JJ, Leber JH, Marquis H, Portnoy DA. Development of a *mariner* -Based Transposon and Identification of *Listeria monocytogenes* Determinants, Including the Peptidyl-Prolyl Isomerase PrsA2, That Contribute to Its Hemolytic Phenotype. J Bacteriol. 2009 Jun 15;191(12):3950–64.

66. Johansson J, Mandin P, Renzoni A, Chiaruttini C, Springer M, Cossart P. An RNA Thermosensor Controls Expression of Virulence Genes in Listeria monocytogenes. Cell. 2002 Sep;110(5):551–61.

67. Dozot M, Poncet S, Nicolas C, Copin R, Bouraoui H, Mazé A, et al. Functional Characterization of the Incomplete Phosphotransferase System (PTS) of the Intracellular Pathogen Brucella melitensis. Moreno E, editor. PLoS ONE. 2010 Sep 10;5(9):e12679.

68. Deutscher J, Francke C, Postma PW. How Phosphotransferase System-Related Protein Phosphorylation Regulates Carbohydrate Metabolism in Bacteria. Microbiol Mol Biol Rev. 2006 Dec;70(4):939–1031.

69. Gera K, Le T, Jamin R, Eichenbaum Z, McIver KS. The Phosphoenolpyruvate Phosphotransferase System in Group A Streptococcus Acts To Reduce Streptolysin S

Activity and Lesion Severity during Soft Tissue Infection. Camilli A, editor. Infect Immun. 2014 Mar;82(3):1192–204.

70. Boulanger EF, Sabag-Daigle A, Baniasad M, Kokkinias K, Schwieters A, Wrighton KC, et al. Sugar-Phosphate Toxicities Attenuate Salmonella Fitness in the Gut. O'Toole G, editor. J Bacteriol. 2022 Dec 20;204(12):e00344-22.

71. Behari J, Youngman P. A Homolog of CcpA Mediates Catabolite Control in Listeria monocytogenes but Not Carbon Source Regulation of Virulence Genes. J BACTERIOL. 1998;180.

72. Thomasen RSS, Jespersen MG, Jørgensen K, Dos Santos PT, Sternkopf Lillebæk EM, Skov MN, et al. The Global Regulator CcpA of Listeria monocytogenes Confers Sensitivity to Antimicrobial Fatty Acids. Front Microbiol. 2022 May 3;13:895942.

73. Fuchs TM, Eisenreich W, Kern T, Dandekar T. Toward a Systemic Understanding of Listeria monocytogenes Metabolism during Infection. Front Microbio;3. Available from: http://journal.frontiersin.org/article/10.3389/fmicb.2012.00023/abstract

74. Han HS, Kang G, Kim JS, Choi BH, Koo SH. Regulation of glucose metabolism from a liver-centric perspective. Exp Mol Med. 2016 Mar 11;48(3):e218–e218.

75. Leong DSZ, Tan JGL, Chin CL, Mak SY, Ho YS, Ng SK. Evaluation and use of disaccharides as energy source in protein-free mammalian cell cultures. Sci Rep. 2017 Mar 30;7(1):45216.

76. Naftalin RJ, Smith PM. A model for accelerated uptake and accumulation of sugars arising from phosphorylation at the inner surface of the cell membrane. Biochimica et Biophysica Acta (BBA) - Biomembranes. 1987 Feb;897(1):93–111.

77. Wilton M, Halverson TWR, Charron-Mazenod L, Parkins MD, Lewenza S. Secreted Phosphatase and Deoxyribonuclease Are Required by Pseudomonas aeruginosa To Defend against Neutrophil Extracellular Traps. Whiteley M, editor. Infect Immun. 2018 Sep;86(9):e00403-18.

78. Demiroz D, Platanitis E, Bryant M, Fischer P, Prchal-Murphy M, Lercher A, et al. Listeria monocytogenes infection rewires host metabolism with regulatory input from type I interferons. O'Riordan M, editor. PLoS Pathog. 2021 Jul 8;17(7):e1009697.

79. Halsey CR, Glover RC, Thomason MK, Reniere ML. The redox-responsive transcriptional regulator Rex represses fermentative metabolism and is required for Listeria monocytogenes pathogenesis. O'Riordan M, editor. PLoS Pathog. 2021 Aug 16;17(8):e1009379.

80. Lauer P, Chow MYN, Loessner MJ, Portnoy DA, Calendar R. Construction, Characterization, and Use of Two Listeria monocytogenes Site-Specific Phage Integration Vectors. J BACTERIOL. 2002;184.

81. Argov T, Rabinovich L, Sigal N, Herskovits AA. An Effective Counterselection System for Listeria monocytogenes and Its Use To Characterize the Monocin Genomic Region of Strain 10403S. Nojiri H, editor. Appl Environ Microbiol. 2017 Mar 15;83(6):e02927-16.

82. Sauer JD, Pereyre S, Archer KA, Burke TP, Hanson B, Lauer P, et al. *Listeria monocytogenes* engineered to activate the Nlrc4 inflammasome are severely attenuated and are poor inducers of protective immunity. Proc Natl Acad Sci USA. 2011 Jul 26;108(30):12419–24.

83. Smith HB, Li TL. Listeria monocytogenes MenI Encodes a DHNA-CoA Thioesterase Necessary for Menaquinone Biosynthesis, Cytosolic Survival, and Virulence. Infection and Immunity. 2021;89(5):12.

84. Vehkala M, Shubin M, Connor TR, Thomson NR, Corander J. Novel R Pipeline for Analyzing Biolog Phenotypic Microarray Data. Aziz RK, editor. PLoS ONE. 2015 Mar 18;10(3):e0118392.

85. Fernandez NF, Gundersen GW, Rahman A, Grimes ML, Rikova K, Hornbeck P, et al. Clustergrammer, a web-based heatmap visualization and analysis tool for high-dimensional biological data. Sci Data. 2017 Oct 10;4(1):170151.

86. Bécavin C, Bouchier C, Lechat P, Archambaud C, Creno S, Gouin E, et al. Comparison of Widely Used Listeria monocytogenes Strains EGD, 10403S, and EGD-e Highlights Genomic Differences Underlying Variations in Pathogenicity. Casadevall A, editor. mBio. 2014 May;5(2):e00969-14.

CHAPTER 3: Understanding the Role of Pyruvate Dehydrogenase in *Listeria monocytogenes* Virulence

Authors and their contributions:

Matthew J. Freeman**: Planned and conducted experiments, wrote, and edited this manuscript.

- Experiments independently conducted include Figures 1C-D, 6, 7, 8, and 9B; Tabel 2; and Supplemental Figure 1. Figures assisted in data generation and analysis include Figures 2, 4, and 9A.

Noah Eral**: Planned and conducted experiments, wrote, and edited this manuscript.

- Experiments independently conducted include Figures 1A-B, 3, and 5. Figures assisted in data generation and analysis include Figures 2, 4, and 9A.

Abigail M. Debrine: Planned and conducted experiments, wrote, and edited this manuscript

David M. Stevenson: Ran LC/MS and HPLC

Daniel Amador-Noguez: Provided equipment and resources for experiments

John-Demian Sauer: Supervised all research and contributed to the design of experiments, edited this manuscript.

*ChatGPT-4o was used for copy editing of my original ideas and writings using the prompt: “Can you copy edit part of my thesis to use correct scientific nomenclature and formatting while improving flow?”

**Denotes Co-First Authorship from substantial contributions of both parties to all aspects of the preparation of the manuscript.

ABSTRACT

To survive within the host, bacterial pathogens must possess finely tuned physiological adaptations to withstand the unique pressures of the restrictive intracellular environment. One such niche inhabited by *Listeria monocytogenes* (*L. monocytogenes*) is the host cell cytosol—a compartment characterized by significant barriers to entry, metabolic limitation, and immune surveillance. Our lab has previously identified multiple *L. monocytogenes* transposon mutants defective for intracellular survival due to disruptions in key metabolic pathways, including cell wall biosynthesis, menaquinone production and pyruvate metabolism including one mutant mapped to a central component of the pyruvate dehydrogenase (PDH) complex, *pdhC*::Tn. Notably, this mutant exhibited pronounced survival defects in both the macrophage cytosol and in murine infection models, despite retaining robust growth and survival in nutrient-rich media. These findings suggest that *pdhC*::Tn is not broadly impaired in core physiology but is instead uniquely susceptible to host-specific environmental stressors. We found that disruption of *pdhA*::Tn and *pdhD*::Tn similarly led to virulence attenuation during intra-macrophage growth, plaquing assays, and murine infections. To define the mechanism underlying PDH mutant attenuation we demonstrated that *pdhC*::Tn mutants displayed altered respiro-fermentative with more prominent secretion of lactate while unbiased metabolomic profiling revealed a global starvation phenotype with lower levels of upper glycolytic intermediates and TCA cycle intermediates coupled with elevated intra-bacterial levels of pyruvate and lactate. We then demonstrated that PDH mutants are unable to efficiently utilize PTS-dependent carbon sources and that their growth can be rescued using non-PTS-mediated carbon sources through an unbiased metabolic screen and directed experimentation. To identify genetic suppressors of PDH deficiency, we performed an EMS mutagenesis screen using fructose—a PTS-transported carbon source—as

the sole carbon source. Five independent suppressors each contained a single independent mutation in the redox sensing regulator *rex* and loss of Rex restored *pdhC*::Tn mutant intracellular growth, but not virulence *in vivo*. Together, these findings indicate that a key defect in PDH mutants is the inability to import and metabolize PTS-dependent carbon sources in the host cytosol. We posit this impairment leads to disruptions in redox balance and a shift in respiro-fermentative metabolism, ultimately contributing to the loss of intracellular fitness and virulence.

INTRODUCTION

Listeria monocytogenes (*L.* monocytogenes) is a Gram-positive, cytosolic bacterial pathogen capable of causing severe morbidity and mortality through the disease listeriosis (1–3). It is well established that for *L. monocytogenes* to successfully infect and cause disease, it must invade host cells, and survive in the restrictive host cytosol (4–8). To access the cytosol, *L. monocytogenes* employs a well-characterized arsenal of virulence factors under the control of its master regulator, PrfA (9,10). Key among these is listeriolysin O (LLO), a pore-forming toxin that targets cholesterol-containing membranes and enables escape from the acidified, toxified phagolysosome (11–13). Once in the cytosol, *L. monocytogenes* induces expression of its hexose phosphate transporter, UhpT, and hijacks host actin polymerization machinery via ActA to facilitate intracellular movement and spread to neighboring cells (14–16). While the canonical virulence factors supporting the intracellular lifecycle of *L. monocytogenes* are well defined, much less is known about the metabolic genes and pathways that support survival in this unique niche (17). *L. monocytogenes* is a professionally adapted cytosolic pathogen capable of surviving in this environment, unlike many other bacteria that are not adapted to cytosolic life (4,18,19) however a comprehensive understanding of the metabolic factors that allow *L. monocytogenes* to use this niche remains elusive.

To investigate how *L. monocytogenes* hijacks the host cell cytosol, our lab previously executed a forward genetic screen to identify genes essential for *L. monocytogenes* survival in the macrophage cytosol (20). We identified mutants with defects in cell wall biosynthesis, menaquinone synthesis, and pyruvate metabolism (20). Interestingly, these mutants showed no growth defects in rich media, suggesting that their attenuation results from specific vulnerabilities to host cytosolic conditions rather than general physiological impairment. Why

pyruvate metabolism, specifically the pyruvate dehydrogenase (PDH) complex, is required for cytosolic survival but not *in vitro* viability, remains unresolved (21–23).

In *L. monocytogenes*, the PDH complex consists of four subunits encoded in a single operon that form a large multiprotein complexe that converts pyruvate into acetyl CoA. (24). The E1 subunit is composed of two proteins encoded by *pdhA* (LMRG_00514) and *pdhB* (LMRG_00515), which decarboxylate pyruvate to form an active acetaldehyde intermediate bound to thiamine pyrophosphate (TPP). The E2 subunit, encoded by *pdhC* (LMRG_00516), then catalyzes transacetylation to CoA and reduces lipoic acid. The E3 subunit, encoded by *pdhD* (LMRG_00517), reoxidizes lipoic acid and transfers electrons to NAD^+, generating NADH. In sum, PDH irreversibly converts pyruvate to acetyl-CoA during aerobic metabolism through tightly coordinated steps that minimize dilution of intermediates and off-target reactions (25). PDH enzymatic activity is allosteric regulated; it is stimulated by phosphoenolpyruvate (PEP) and AMP, and inhibited by NADH and acetyl-CoA, presumably to define when energy sources are low, but resources are high (25,26). Because PDH sits at the metabolic junction between glycolysis and the tricarboxylic acid (TCA) cycle, its disruption is likely to result in broad, pleiotropic effects. For example, PDH mutants are deficient in acetyl-CoA production, a precursor essential for fatty acid biosynthesis (27). In addition, reduced TCA cycle flux may impair NADH generation necessary for electron transport chain function and the synthesis of TCA-derived amino acids (14,28). Thus, analysis of PDH-deficient mutants and their virulence phenotypes must consider this range of interconnected metabolic disruptions.

In evaluating these pleiotropic defects, it is also critical to assess the carbon sources being acquired and funneled into the PDH complex, as well as its broader impact on cellular redox and

energy states. Our lab recently demonstrated that intracellular *L. monocytogenes* is only modestly reliant on glycerol and hexose phosphates, and instead depends heavily on phosphotransferase systems (PTS) to acquire host-derived carbon sources (29). PTS function is tightly linked to pyruvate metabolism, as it terminally relies on the conversion of PEP to pyruvate to transfer phosphate groups via PtsI and HPr to substrate-specific EII complexes (25,30–32). These transporters phosphorylate incoming sugars, which then enter upper glycolysis (25). Interestingly, PTS encoding genes are enriched in bacteria that are facultative or strict anaerobes and PTS appear to be less common among strict aerobes (33,34). It has been hypothesized this evolutionary selection is because for PTS to import and phosphorylate a new carbohydrate a molecule of PEP is used; thus, leaving only one PEP from glycolysis for biosynthetic pathways (33,35). In aerobic organisms, this PEP will be rapidly used, while anaerobic organism can more readily retain PEP for essential biosynthetic purposes (33,34). Some evidence in the field suggest the *L. monocytogenes* splits its carbon use of different metabolites for either anabolic or catabolic processes (36,37). However, recent evidence suggests these previously described carbon sources are not essential for infection and therefore the relevance of this model remains undetermined (29). Thus, for simplicity, from initial phosphorylation, carbon is funneled through glycolysis and into the TCA cycle, generating ATP, NADH, and $FADH_2$ (25). Under aerobic conditions, these reduced cofactors support oxidative phosphorylation and ATP synthesis. Importantly, cells have evolved highly sophisticated methods of detecting the successful balance of NADH and NAD+ (23,38), a process particularly important for bacteria that have both the ability to ferment and respire as they must be able to modulate between these states to promote the most efficient use of carbon and deal with unique environmental stressors (23,39,40).

Bacterial pathogens employ metabolic strategies that allow them to utilize carbon while evading host cell pressures and immune detection (41–43). One example of host defenses targeting bacterial metabolism is the use of reactive nitrogen species (RNS) by macrophages, which inhibit bacterial aerobic respiration (44,45). From the pathogen side, some bacterial species—including *Salmonella enterica* and *Staphylococcus aureus*—require aerobic respiration for full virulence (46–50). *L. monocytogenes*, on the other hand, is known to dynamically modulate its metabolism between fermentation and respiration, often using both simultaneously in what is referred to as respiro-fermentative metabolism (23). During respiration, *L. monocytogenes* regenerates NAD^+ from NADH by transferring electrons through the electron transport chain (ETC) (23) employing two respiratory chains: one utilizing oxygen as the terminal electron acceptor, and another using extracytosolic ferric iron and fumarate (22,23,51,52). Under aerobic conditions, *L. monocytogenes* shifts its fermentative output from lactate to acetate in order to maximize ATP production, albeit at the expense of NADH regeneration (53). To balance this redox requirement, a portion of carbon cannot be fully oxidated and continues to be fermented to lactate, which supports NADH regeneration but yields less ATP. This metabolic modulation results in markedly different carbon consumption profiles and distinct metabolic by-products, which can be used to infer the bacterium's metabolic state: elevated lactate levels indicate purely fermentative metabolism, while acetate production is associated more with respiro-fermentative state (23,53).

To solve the challenge of balancing metabolic demand, bacterial pathogens have acquired sophisticated muli-layered method of sensing cellular metabolic and redox homeostasis (38). Some of this sensing occurs by enzymes that require these cofactors such as dehydrogenase complexes (25,26). One advantage of this model is it allows enzyme to be at the ready for their

respective functions while detecting the metabolic state of the cell. One downside is that it is highly costly for bacteria to produce and retain these enzymes if they are not functional. To overcome this limitation bacteria also utilize regulators and metabolic sensors to control the production of the enzymes and thus control metabolism. *L. monocytogenes* and other pathogens encode Rex, a redox-sensing transcriptional regulator that responds to intracellular NAD^+/NADH ratios (38,54,55). When NAD^+ levels are low, Rex derepresses genes involved in fermentation (54). Conversely, high NAD^+/NADH ratios lead to repression of key fermentation genes. While the full significance of Rex-mediated regulation remains unclear, preliminary data suggest that *rex* mutants of *L. monocytogenes* are modestly attenuated during oral infection in murine models but retain normal *ex vivo* growth within macrophages (38).

In this study, we evaluated the contribution of pyruvate dehydrogenase (PDH) deficiency to *L. monocytogenes* virulence. We found that mutants lacking any individual PDH component (*pdhA*, *pdhC*, or *pdhD*) exhibited equivalent defects in virulence, indicating that loss of any one component completely ablates the function of the complex. *pdhC::Tn* mutants also showed an altered respiro-fermentative metabolism with a shift from acetate production toward that of lactate. Metabolomic profiling of a *pdhC::Tn* mutant revealed global depletion of upper glycolytic and TCA cycle intermediates, accompanied by an accumulation of pyruvate and lactate when grown in rich media. We further demonstrated that PDH mutants are defective in utilizing phosphotransferase system (PTS)-transported carbon sources. However, their growth could be restored in defined media supplemented with hexose phosphates (+glutathione). A suppressor screen identified five independent suppressor mutations in the gene encoding the redox-sensing transcriptional regulator, Rex that restored *pdhC::Tn* mutant growth on PTS-dependent carbon sources. One suppressor, which introduced a premature stop codon in *rex*,

restored growth of *pdhC::Tn* mutants *ex vivo* in macrophages, though it did not rescue virulence *in vivo*. Collectively, our findings demonstrate that *L. monocytogenes* requires rapid conversion of pyruvate to acetyl-CoA via PDH to sustain both redox homeostasis and PTS-dependent carbon acquisition—two processes essential for intracellular growth and pathogenesis. At least part of the virulence defect in macrophages for PDH mutants is attributable to an inability to utilize PTS-transported carbon sources, likely due to Rex-mediated repression of fermentation under redox-imbalanced conditions.

RESULTS

Pyruvate dehydrogenase mutants are significantly attenuated for intracellular growth and virulence, while maintain WT levels of growth in rich media

The *pdhC::Tn* mutant identified in our previous work exhibits significant virulence defects across multiple assays (20). Notably, this mutant was completely unable to grow within the cytosol of bone marrow-derived macrophages and was actively cleared, as indicated by decreasing bacterial burdens over time and bacteriolysis in the macrophage cytosol (20). During acute murine infection, the *pdhC::Tn* mutant was fully attenuated, with bacterial burdens falling to the limit of detection by 48 hours post-infection (20). In contrast, L2 fibroblast plaquing assays—which assess both intracellular growth and cell-to-cell spread—revealed that the *pdhC::Tn* mutant retained partial function, forming plaques approximately 50–70% the size of those formed by wild-type *L. monocytogenes* (20). These findings suggest that the pyruvate dehydrogenase complex (PDH) is critical for intracellular survival and full virulence of *L. monocytogenes*, however, it remained unclear whether these phenotypes were specific to the E2 subunit (PdhC) or were generalizable to other subunits of the PDH complex.

First, we hypothesized that loss of any individual component of the PDH complex would result in similar virulence defects, but like *pdhC*::Tn would retain the ability to grow in rich media. To test this, we obtained unpublished transposon mutants in *pdhA* and *pdhD* from Dr. Daniel Portnoy (University of California, Berkeley) and conducted a series of standard *in vitro* growth curves and virulence assays to determine the contributions of individual PDH subunits.. Notably, a *pdhB* mutant has never been isolated from bacterial forward genetic screens, perhaps due to functional redundancy with the E1β subunit of the branched chain keto-acid dehydrogenase complex which shares 62% identity and ~75-80% similarity with the PDH E1β subunit (56,57). *in vitro* growth curves of PDH mutants in rich media demonstrated that *pdhA*::Tn, *pdhC*::Tn and *pdhD*::Tn mutants readily grow in rich media (**Figure 1A**), again highlighting that PDH mutant defects during virulence are specific to *L. monocytogenes* physiology during infection. Next, we performed intracellular growth curves in bone marrow-derived macrophages (BMDMs) to assess cytosolic invasion and replication over an 8-hour period in the cytosol of cells that *L. monocytogenes* uses as it primary *in vivo* niche (58,59). All available PDH subunit mutants were unable to grow and were cleared from the host cytosol, mirroring the phenotype of the original *pdhC::Tn* mutant (**Figure 1B**). This supported that loss of any one component of the PDH complex would result in the inability to survive and replicate in the cytosol.

Next, we evaluated the requirement for PDH in *L. monocytogenes* L2 fibroblast plaquing assays, predicting—based on our prior results with *pdhC*—that *pdhA* and *pdhD* mutants would retain some ability to grow and spread. While intramacrophage growth curves measure invasion, single cycle infection and growth, plaque assays offer insight into bacterial virulence across prolonged periods of growth and the ability to spread to neighboring cells. While all mutants of

the PDH complex were attenuated relative to WT *L. monocytogenes,* there was no statistically significant difference between individual subunit mutants (**Figure 1C**). Together this data shows that PDH mutants share virulence phenotypes across assays, but do perhaps have minorly different virulence capabilities during more prolong multi-cycle infections versus single cycle infections in macrophages.

Ultimately, to assess virulence *in vivo* under physiologically relevant metabolic and immune pressures, we performed acute murine infection and organ burden assays. In short, C57BL/6 mice were infected intravenously with 1×10^5 CFU of each strain, and spleens and livers were harvested 48 hours post-infection to quantify bacterial burdens. All PDH complex mutants displayed severe attenuation, with bacterial counts near or below the assay's detection limit in the spleens. Notably, each of the PDH complex mutants displayed occasional very low levels of bacterial burdens in the livers, displaying an organ specific sensitivity (**Figure 1D**).

In summary, our results demonstrate that loss of any PDH complex subunit leads to comparable virulence defects, suggesting a shared physiological basis (**Figure 1A-D**). Further, all defects of *pdhC*::Tn could be rescued to near WT levels with heterologous overexpression of *pdhC* (**Figure 1A-D**). Moving forward we sought to investigate the mechanism of *L. monocytogenes'* virulence attenuation from PDH complex deficiency using *pdhC*::Tn as a representative mutant.

PdhC*::Tn mutants show altered respiro-fermentative metabolic byproduct secretion relative to that of WT *L. monocytogenes

Due to an incomplete tricarboxylic acid (TCA) cycle, *L. monocytogenes* relies on a respiro-fermentative metabolism in which pyruvate is predominantly directed toward fermentative acetate production (53). Previously, our lab identified that *Listeria monocytogenes* mutants deficient in menaquinone biosynthesis—and therefore lacking functional respiratory chains—exhibit substantial alterations in their respiro-fermentative metabolism marked by increased lactate production relative to acetate, indicating a shift toward fermentative metabolism over oxidative metabolism (20–23,60). Further this fermentative byproduct shift has also been observed in *aro* mutants similarly defective for respiration (60). We hypothesized that PDH complex mutants may display similar metabolic alterations due to their impaired ability to efficiently channel carbon from glycolysis into the tricarboxylic acid (TCA) cycle resulting in insufficient levels of NADH for the electron transport chain. To test whether the inability to funnel carbon into the TCA resulted in an altered respiro-fermentative metabolism, we grew each strain overnight in rich media (brain, heart infusion) and analyzed the bacterial supernatants and standards via high-performance liquid chromatography (HPLC) to quantify the relative and absolute abundance of acetate and lactate, fermentative byproducts with standards for quantification.

As expected, WT *L. monocytogenes* showed a strong predominance toward the production of acetate versus lactate (**Figure 2**). HPLC of *pdhC*::Tn supernatants revealed that, like other respiration-deficient strains, PDH mutants produce significantly altered respiro-fermentative profiles (**Figure 2 and Supplemental Figure 1B**) (21–23,60). Specifically, PDH mutants exhibited a marked increase in lactate production with a corresponding decrease in acetate, suggesting a shift away from oxidative metabolism with acetate fermentative byproduct production (**Figure 2**). This phenotype could be restored to that of WT *L. monocytogenes*

through the heterologous overexpression of *pdhC* (**Figure 2**). Taken together this data demonstrates that loss of PDH results in a disruption in the respirofermentative metabolism of *L. monocytogenes* in vitro marked by a shift to lactate production.

Pyruvate dehydrogenase mutants are not rescued by restoration of NAD+ production using NOX

We previously demonstrated that one of the primary defects in *L. monocytogenes* menaquinone mutants that contributes to a loss of virulence is an impaired ability to regenerate NAD+ (23). This deficiency is largely attributed to their inability to oxidize NADH via electron transfer through the respiratory chain resulting in a shift in fermentative metabolism toward lactate. In menaquinone-deficient strains, this redox imbalance can be rescued through overexpression of the water-forming NADH oxidase (NOX), which facilitates NADH oxidation independently of the respiratory chain (23). Importantly, NOX overexpression restores virulence in menaquinone mutants across multiple assays, including intracellular growth curves, fibroblast plaquing, and murine infection models (23).

Based on these prior findings and the observation that *pdhC*::Tn mutants show a respiro-fermenatative metabolism shifted toward lactate, we hypothesized that *pdhC*::Tn mutants suffer from NAD^+ depletion due to impaired flux through the tricarboxylic acid (TCA) cycle and therefore impaired respiration. To test this hypothesis, we tested whether overexpression of NOX might similarly rescue virulence defects in *pdhC*::Tn mutants. To test this, we conjugated a NOX overexpression plasmid into the *pdhC::Tn* background and evaluated virulence using the L2 fibroblast plaquing assay, which had previously shown the greatest residual growth in *pdhC::Tn* and provided the least stringent defects for rescue. In contrast to our hypothesis,

the *pdhC::Tn* + NOX strain showed no improvement in plaque formation relative to the isogenic *pdhC::Tn* mutant, and remained significantly attenuated compared to WT *L. monocytogenes* (**Supplemental Figure 1A**). This was further confirmed by analysis of fermentative byproducts produced. We found that the *pdhC*::Tn-NOX strain show modest rescue of acetate production, but not nearly to the extent of menaquinone deficient strains (**Supplemental Figure 1A**). These results suggest that, unlike menaquinone mutants, the virulence defects in *pdhC* mutants cannot be rescued by redox rebalancing through NOX overexpression alone. In sum, we found that rapid regeneration of NAD+ via NOX is insufficient to rescue *pdhC::*Tn virulence in plaquing assays and that the defect must not be driven purely by an inability to regenerate NAD+ via oxidative metabolism.

Unbiased metabolomics reveals elevated pyruvate and lactate levels in *pdhC*::Tn, but otherwise globally decreased metabolites

Given that the *pdhC::Tn* mutant could not be rescued by NOX overexpression—despite exhibiting an altered respiro-fermentative metabolic profile—we sought to gain a more global view of metabolic dysregulation in this strain. We hypothesized that PDH-deficient strains would accumulate upstream glycolytic intermediates due to impaired flux through pyruvate, while tricarboxylic acid (TCA) cycle intermediates would be depleted owing to inefficient conversion of pyruvate to acetyl-CoA. To test this hypothesis, we performed untargeted metabolomics on WT *L. monocytogenes* and *pdhC*::Tn mutants grown in defined medium supplemented with 110 mM of glucose. The use of defined medium was essential, as complex media, such as BHI, contains abundant background metabolites that interfere with LC/MS metabolite detection and analysis. Additionally, excess glucose supplementation (110 mM versus 55 mM) was required

because our lab had observed that PDH mutants show impaired growth in defined medium containing standard glucose concentrations (55mM) (Data not shown). We focused our analysis on glycolytic and TCA cycle intermediates, with supplemental analysis of intracellular levels of the fermentative byproduct lactate. Consistent with our hypothesis, relative to WT *L. monocytogenes*, *pdhC::Tn* mutants exhibited elevated concentrations of pyruvate and lactate, and a marked depletion of TCA cycle metabolites (**Figure 3**). In contrast to our hypothesis however, we observed significantly reduced levels of upper glycolytic intermediates in the *pdhC::Tn* mutants relative to WT (**Figure 3**). Taken together this data suggested three different facets of *pdhC*::Tn mutant metabolism: 1. *pdhC*::Tn was fermenting what sugars it was able to acquire more toward lactate compared to WT. 2. *pdhC*::Tn mutants are reduced in their capacity to funnel metabolites into the TCA cycle compared to WT. 3. *pdhC*::Tn mutants are defective for the acquisition of carbon as represented by lower levels of upper glycolytic metabolites compared to WT.

pdhC:Tn shows reduced utilization of multiple PTS mediated carbon sources on BioLog Phenotypic MicroArrays

The unexpected finding that *pdhC::Tn L. monocytogenes* mutants have reduced levels of upper glycolytic intermediates, despite a block downstream in the conversion of pyruvate to acetyl-CoA, led us to hypothesize that *pdhC::Tn* mutants may be defective in acquiring carbon sources, some of which might be available within the host cytosol. This hypothesis was supported by prior observations from our lab showing that *pdhC::Tn* mutants are unable to grow in defined media supplemented with standard concentrations of glucose (55 mM) (Data not shown). Glucose uptake in *L. monocytogenes* occurs primarily through the phosphotransferase

system (PTS), in addition to PTS independent GLUC transporters (30,61). This phenotype, coupled with the buildup of pyruvate in *pdhC::Tn* mutants, which would inhibit the PTS dependent phosphorelay initiated by the conversion of phospoenolpyruvate to pyruvate by PtsI, led to the hypothesis that *pdhC::Tn* mutants would show impaired respiration of PTS-mediated carbon sources relative to WT *L. monocytogenes* (32). To identify carbon sources that *pdhC::Tn* is unable to utilize effectively, we performed phenotypic screening using BioLog phenotypic carbon microarrays (PM1 and PM2) (62). Assays were performed in biological triplicate, with plates inoculated and incubated under stationary conditions at 37°C for 48 hours. Following incubation, respiration was quantified by measuring tetrazolium dye reduction at OD_{490} using a plate reader. To account for strain-specific differences in overall metabolic activity, OD_{490} values were normalized to glucose for each strain. In total, 190 distinct carbon sources were assessed for differential utilization between WT and *pdhC::Tn* strains (**Figure 4**). Of these, 11 carbon sources were used at significantly lower levels—at least twofold less—by the *pdhC::Tn* mutant compared to WT (**Figure 4 and Table 1**). Two of these carbon sources are not PTS-mediated, L-alynyl-glycine and L-alanine. Supporting our hypothesis, 9 of these underutilized substrates are canonically classified as PTS-dependent carbon sources (**Figure 4 and Table 1**). However, *pdhC::Tn* exhibited broadly similar usage of many other carbon sources, including many that are also PTS-mediated. This partial overlap complicates interpretation, as the BioLog assay does not disclose the exact concentrations of individual metabolites—a critical variable based on our prior observations that PDH complex mutants fail to grow under suboptimal carbon concentrations in defined media. Another import caveat to understanding these phenotypes is that this was a terminal assay and does not display kinetics of carbon source utilization. Nevertheless, the impaired utilization of a subset of PTS-dependent

carbon sources is consistent with our internal data and aligns with previous findings that PTS systems are essential for cytosolic growth of *L. monocytogenes* (29). These data provide incremental support for the model in which defective carbon acquisition, specifically PTS-mediated carbon sources, contributes to the virulence defects observed in PDH complex mutants.

***pdhC*:Tn shows an impaired ability to grow in LSM supplied with PTS-mediated carbon sources and can be rescued for growth on PTS-independent hexose phosphates**

To test the hypothesis that *pdhC::Tn* is impaired in its ability to consume PTS-mediated carbon sources we assessed growth in *Listeria* synthetic media (LSM) with glucose, fructose, mannose, and glucoe-6-phosphate (+glutathione) as the sole carbon source (110 mM). LSM containing defined sole carbon sources was inoculated with WT *L. monocytogenes* or the indicated mutants, and growth was monitored by measuring OD_{600} every 15 minutes for 24 hours. Notably, LSM supplemented with hexose phosphates required the addition of 10 mM reduced glutathione to induce *prfA*—and consequently *uhpT*—expression. As expected, WT *L. monocytogenes* was able to grow readily on all of these carbon sources (**Figure 5A-D**). Of note, we found that *pdhC::Tn* was significantly impaired for growth on PTS-mediated carbon sources of glucose, fructose, and mannose (**Figure 5A-C**). This was characterized by slow growth that did not reach the OD 600 of WT until nearly 24 hours after inoculation. Importantly, each of these growth defects could be rescued to WT levels with heterologous overexpression of *pdhC*. Interestingly, *pdhC::Tn* showed WT levels of growth in LSM supplied with hexose phosphates (+glutathione), consistent with a specific defect in the acquisition of PTS dependent carbon sources (**Figure 5D**). Taken together, these data demonstrate the *pdhC::Tn* is able to grow on PTS mediated carbon sources but that growth is significantly slowed relative to WT *L.*

monocytogenes. Further, *pdhC::Tn* can be rescued for growth in LSM on PTS-independent carbon sources such as hexose phosphates (**Figure 5A-D**).

PdhC::Tn Suppressor screen reveals strains with restored growth on PTS-mediated carbon sources

L. monocytogenes uses host-derived PTS-mediated carbon sources to be able to survive and replicate in the host cytosol (29). As PDH mutants are unable to grow in defined media supplemented with phosphotransferase system (PTS)-mediated carbon sources we hypothesized that a key contributor to the attenuated virulence of PDH mutants is their inability to utilize PTS-dependent carbon substrates (29). To test this hypothesis, we conducted a *pdhC::Tn* mutant suppressor screen on LSM supplemented with 55 mM fructose as the carbon source to identify suppressor mutations that would allow growth of PDH deficient mutants on PTS substrates. Fructose was chosen because it is acquired exclusively via the PTS and, as a hexose sugar, provides a carbon input comparable to glucose or glucose-6-phosphate. Additionally, WT *L. monocytogenes* grows robustly in LSM + 55 mM fructose, whereas *pdhC::Tn* mutants require at least 110 mM fructose to support even limited growth (**Figure 5B**). To efficiently induce suppressor mutations, exponentially growing *pdhC::Tn* cultures were mutagenized with ethyl methanesulfonate (EMS) for five minutes, washed to remove residual mutagen, and stored in 40% glycerol at –80 °C. To avoid false-positive suppressors arising from growth on carryover metabolites in frozen stocks, the mutagenized library was thawed, washed with phosphate-buffered saline (PBS), centrifuged, and resuspended in PBS prior to screening. Approximately 10^7 EMS-mutagenized *pdhC::Tn* mutants were plated per dish across ten LSM + 55 mM fructose plates and incubated at 37 °C for two days. Resulting suppressor colonies were restreaked on selective media to confirm retention of the transposon. Five suppressor colonies that retained the

transposon and exhibited restored growth on LSM + 55 mM fructose plates were selected for analysis by whole-genome sequencing. Strikingly, all five suppressor mutants contained mutations in only one gene and all contained mutations in the same gene, *LMRG_01223* (annotated as *rex*), which encodes a redox-sensing transcriptional repressor (**Table 2**). Of the five identified mutations in *rex*, three were missense mutations, one was a premature stop codon, and one was a large C-terminal deletion extending beyond the native stop codon (**Table 2**). Taken together, these results suggest that inactivation of *rex* is a highly reproducible mechanism of restoring growth of *pdhC::Tn* mutants on PTS-dependent fructose.

pdhC::Tn suppressor mutations for growth on PTS-mediated carbon sources are primarily in the DNA binding domain of Rex

To better understand how the identified mutations may impact Rex function, we sought to map their locations onto a model of the *L. monocytogenes* Rex structure. Previous studies in other organisms have shown that Rex forms homodimers capable of binding NAD^+ or NADH, adopting open or closed conformations, respectively (54). In the open conformation, Rex bound to NAD^+ associates with Rex-specific operator sequences in the bacterial genome to repress genes involved in fermentative metabolism (38,54). This NAD^+-dependent binding is thought to signal active oxidative metabolism, indicating sufficient NAD^+ regeneration relative to NADH (54). Consequently, when possible, the bacterium prioritizes respiration over fermentation to maximize ATP production and biosynthetic efficiency (25). To model this interaction, we used AlphaFold3 to predict the structure of the *L. monocytogenes* Rex homodimer in complex with NAD^+ and target DNA (63). The resulting model was visualized using Jmol (Jmol: an open-source Java viewer for chemical structures in 3D. http://www.jmol.org/), where residue coloring

and mutation annotations were added for clarity. Structural modeling revealed that all three missense mutations reside within the predicted DNA-binding domain (alpha helices 1-4) of Rex in its NAD^+-bound, open conformation (**Figure 6**). This suggests that the mutations likely impair DNA binding and thus prevent Rex from properly regulating gene expression. Notably, none of the mutations are located within the NAD^+/NADH binding pocket, further supporting the interpretation that impaired DNA binding, rather than cofactor recognition, underlies the observed regulatory defects (**Figure 6**).

pdhC::Tn suppressor mutants show restored growth in LSM with fructose

Suppressor mutations enabling *pdhC::Tn* growth on LSM supplemented with fructose were initially identified on solid media but not in liquid cultures. To confirm that these mutations would similarly support growth on PTS-mediated carbon sources in liquid media, we assessed growth in liquid LSM containing fructose. As expected, wild-type (WT) *L. monocytogenes* exhibited robust growth in LSM+fructose, while the *pdhC::Tn* mutant displayed severely impaired growth, requiring approximately 24 hours to begin approaching the terminal OD_{600} achieved by WT (**Figure 7**). Notably, all five suppressor mutants demonstrated rescued growth in LSM with fructose, reaching OD_{600} values comparable to WT with similar kinetics, confirming their restored ability to utilize this PTS-mediated carbon source (**Figure 7**). These results validate that the identified suppressor mutations permit *pdhC::Tn* to grow efficiently on fructose in both solid and liquid media, supporting the conclusion that loss of *rex*-mediated repression facilitates PTS-dependent carbon source utilization.

pdhC::Tn mutants cannot grow on PTS-mediated carbon sources in oxygenated defined media, but can when grown anaerobically or on PTS-independent carbon sources

Previous work by Halsey et al. (2021) demonstrated that *L. monocytogenes* Rex functions as a transcriptional repressor of fermentative metabolism when respiration is available, a state sensed through elevated NAD^+ levels (38). Building upon this finding—and considering that all five identified *rex* mutations in our suppressor screen either disrupt the predicted DNA-binding domain or result in presumed loss-of-function alleles (e.g., premature stop codons or large C-terminal deletions)—we hypothesized that loss of Rex activity in the *pdhC::Tn* background relieves fermentative repression (**Table 2 and Figure 7**). If true, *pdhC::Tn* mutant growth should be rescued on fructose under anaerobic conditions and should phenocopy the *pdhC::Tn-rex* suppressor mutants grown under aerobic conditions. To test this hypothesis, we compared the growth of WT, *pdhC::Tn*, *pdhC::Tn* complemented with *pdhC* (*pdhC::Tn* + *pdhC-C*), and *pdhC::Tn* Suppressor #4 (Rex – Arg51-STOP) under both aerobic and anaerobic conditions. Cultures were inoculated into LSM containing 110 mM fructose and incubated at 30 °C for 48 hours, either aerobically (stationary incubation) or anaerobically in a GasPak chamber. After incubation, cultures were mixed and transferred to a 96-well plate for optical density measurement at 600 nm (OD_{600}). Under aerobic conditions, WT, *pdhC::Tn* + *pdhC-C*, and *pdhC::Tn* Suppressor #4 (Rex – Arg51-STOP) all achieved comparable levels of growth (**Figure 8A**). In contrast, *pdhC::Tn* exhibited markedly impaired growth, supporting the interpretation that functional Rex represses growth on fructose when aerobic respiration is possible (**Figure 8A**). Under anaerobic conditions, however, all strains—including *pdhC::Tn*—grew to similar levels, consistent with the loss of Rex-mediated repression in the absence of respiration (**Figure 8B**). Taken together, these findings support the conclusion that *pdhC::Tn* is capable of growing on PTS-mediated fructose in defined media either by

genetic disruption of *rex* or by shifting to anaerobic culture conditions that naturally relieve fermentative repression.

pdhC::Tn supressor #4 (Rex – Arg51-STOP) rescues intramacrophage growth, but not *in vivo* virulence

Our lab has previously demonstrated that *Listeria monocytogenes* requires a functional phosphotransferase system (PTS) for growth within the macrophage cytosol and for full virulence *in vivo* (29). We hypothesized that *rex* suppressor mutants of *pdhC::Tn* that rescue PTS mediated growth would partially restore virulence. To test this hypothesis, we measured intracellular growth in BMDM to assess the ability of *pdhC::Tn* Suppressor #4 (Rex – Arg51-STOP) to replicate within the host cytosol. As expected, WT *L. monocytogenes* grew robustly in the macrophage cytosol, expanding by approximately 1.5 logs over an 8-hour infection (**Figure 9A**). In contrast, *pdhC::Tn* mutants failed to grow and were progressively cleared, consistent with prior observations (**Figure 9A and Figure 1B**). Remarkably, *pdhC::Tn* Suppressor #4 (Rex – Arg51-STOP) mutants exhibited intracellular replication comparable to WT, indicating that loss of Rex-mediated fermentative repression not only restored growth on PTS carbon sources *in vitro* but also enabled survival and replication in the macrophage cytosol (**Figure 9A**). These data suggest that inability to acquire PTS dependent carbon sources restricts survival and replication of PDH deficient mutants in the macrophage cytosol.

To evaluate whether this rescue extended to *in vivo* infection, we performed an acute murine virulence assay. C57BL/6 mice were intravenously infected with 10^5 CFU of each strain suspended in 200 μL of PBS. After 48 hours, mice were euthanized and bacterial burdens in the spleen and liver were enumerated. WT *L. monocytogenes* successfully colonized both organs

with bacterial burdens of ~10^7 CFU/organ, while *pdhC::Tn* was completely attenuated, with burdens falling below the assay's limit of detection (**Figure 9B**). In contrast to the rescue of intracellular growth observed in BMDMs, *pdhC::Tn* Suppressor #4 (Rex – Arg51-STOP) did not rescue virulence *in vivo* and exhibited organ burdens indistinguishable from the parental *pdhC::Tn* mutant (**Figure 9B**). These results suggest that, although Rex inactivation permits cytosolic replication in cultured macrophages, additional host-specific pressures *in vivo* prevent the suppressor strain from establishing systemic infection. This implies that the murine host imposes metabolic or immunological constraints more stringent than those encountered in *ex vivo* macrophage models—constraints that remain restrictive for both *pdhC::Tn* and its *rex* suppressor derivative.

DISCUSSION

Mechanisms of carbon acquisition, catabolism, and anabolism are critical virulence determinants that support the pathogenesis of intracellular bacterial pathogens (29,36,41,42). However, these mechanisms remain incompletely defined. In particular, how bacterial pathogens acquire nutrients and efficiently metabolize these nutrients while evading host defenses within the nutrient-limited and hostile environment of the cytosol is not fully understood (17). Elucidating how pathogens regulate metabolism during infection is essential to identifying key metabolic determinants of virulence and potential targets for antimicrobial therapies (64). *Listeria monocytogenes* is both an important human pathogen and a well-characterized model organism (3,65). Despite extensive study, our understanding of the metabolic factors that contribute to its virulence remain limited. In this work, we expand upon findings from Chen et

al. (2018), which demonstrated that a *pdhC::Tn* mutant of *L. monocytogenes* exhibits a severe defect in cytosolic growth within macrophages and near-complete attenuation of virulence (20). To further investigate the role of the pyruvate dehydrogenase (PDH) complex during infection, we characterized additional transposon mutants in two other components of this complex: *pdhA::Tn* and *pdhD::Tn*. *pdhA::Tn* and *pdhD::Tn* mutants phenocopy *pdhC::Tn*—exhibiting wild-type (WT) growth in rich media but defective intracellular replication and virulence in both L2 fibroblast plaquing assays and acute murine infection models. We then focused on dissecting the virulence defect of *pdhC::Tn* and found that it alters respiro-fermentative metabolism, producing elevated levels of lactate and reduced levels of acetate compared to WT *L. monocytogenes*. This secreted metabolic profile resembles that of previously described *L. monocytogenes* mutants impaired in respiration (21–23). However, unlike those mutants, the virulence defect of *pdhC::Tn* was not rescued by heterologous expression of NADH oxidase (NOX). Unbiased metabolomic analysis further revealed that *pdhC::Tn* accumulates pyruvate and lactate while being depleted in upper glycolytic and tricarboxylic acid (TCA) cycle intermediates. Using BioLog Phenotypic Microarrays (PM1 and PM2A) alongside targeted growth experiments, we discovered that *pdhC::Tn* is significantly impaired in its ability to utilize phosphotransferase system (PTS)-mediated carbon sources. Based on this observation, we performed a suppressor screen to select for mutants capable of growing on minimal medium containing fructose as the sole PTS-dependent carbon source. Whole-genome sequencing and SNP analysis of five independent suppressor strains revealed mutations in a single gene, *rex* (*LMRG_01223*), a redox-sensing transcriptional repressor. These mutations included missense mutations in the DNA-binding domain, premature stop codons, and truncations likely resulting in loss of function. Functional assays demonstrated that *rex* acts as a fermentative

repressor in *pdhC::Tn* mutants grown on PTS-dependent carbon sources and that loss of *rex* in a *pdhC::Tn* background restored intracellular growth in macrophages ex vivo but failed to rescue virulence in murine infection models. These findings further support that *L. monocytogenes* requires the ability to acquire and use PTS-mediated carbon sources to grow in the host cytosol, but also unveil that other pleiotropic defects of PDH complex mutants must be critical for full virulence *in vivo.* Furthermore, they indicate that Rex likely promotes respiratory metabolism in the host cytosol through fermentative repression, which is essential for full virulence (23).

Although central glycolytic and TCA cycle enzymes have been extensively studied for their roles in carbon metabolism, their contributions to bacterial pathogenesis remain underexplored across many species (25,66). While the necessity of the PDH complex during *L. monocytogenes* infection is loosely established, the specific physiological mechanisms leading to the avirulent phenotype of PDH mutants—despite their robust growth in rich media—has not been elucidated (18). Interestingly, all PDH subunit mutants (*pdhA::Tn*, *pdhC::Tn*, and *pdhD::Tn*) retain the capacity to form plaques in L2 fibroblast monolayers, albeit significantly smaller than WT, suggesting that while the PDH complex is important across multiple host environments, it is not universally essential. This phenotypic discrepancy points to differences in the pressures imposed by distinct host cell types, experimental timelines, or experimental conditions. One hypothesis is that plaque formation may occur independently of robust intracellular replication. Preliminary evidence suggests that *L. monocytogenes* can spread cell-to-cell when host cells reach their carrying capacity, even under metabolically limiting conditions (67). Thus, PDH mutants might form plaques despite failing to survive within macrophages or establish infection *in vivo* due to the ability to bypass metabolic depletion.

Differences in the ability of PDH complex mutants to grow in L2 fibroblast, but not macrophages, may also reflect variation in host cell detection and response to altered bacterial metabolism, possibly driven by differential nutrient availability or immune signaling thresholds. It has been shown that intracellular levels of lactate and acetate can act as signal of infection and host cell response (68–71). Although not addressed in this study, we hypothesize that individual PDH subunit mutants altered fermentative byproducts in their metabolic may be impacting interaction with L2 fibroblast and macrophages, divergently. One way to further identify how production of these organic acids impact host response would be to limit the ability of PDH complex mutants to produce them through deletion of acetate kinase and/or lactate dehydrogenase and assess virulence capabilities and host cell responses.

One key unanswered question in the field is the relative contribution of fermentative versus respiratory metabolism during infection. *L. monocytogenes* appears to balance these states, potentially as an evolutionary adaptation to evade host detection of metabolic byproducts. Rex, previously characterized by Halsey et al. 2021, is largely dispensable for virulence in WT strains (38). However, its role in repressing fermentation during infection may be context-dependent. For instance, *aro* mutants and menaquinone-deficient mutants lacking respiratory capacity are highly attenuated, but both have only been assessed in the presence of Rex (21–23,60). Our findings suggest that Rex enforces respiratory metabolism in macrophages, and loss of Rex may permit survival via fermentation and restoration of PTS-mediate carbon source use. To dissect the respective roles of fermentation and respiration, strains lacking essential respiratory components should be tested in both *rex*-positive and *rex*-negative contexts. Conversely, strains deficient in fermentation could be constructed with Rex overexpression to assess reliance on respiratory metabolism. An example of this would be to delete *ackA* and *ldh*,

enzymes essential for *L. monocytogenes'* production of fermentative byproducts with Rex hyperexpression. This mutant would in theory be completely dependent on respiration for growth and could isolate one side of the respiro-fermentative metabolism. These experiments will clarify how host cells detect and respond to distinct bacterial metabolic states and what is whether respiration or fermentation is the predominant need of cytosolic pathogens.

Unexpectedly in *pdhC::Tn*, acetate is still predominantly produced despite the absence of a functional PDH complex. The suggests that *pdhC*::Tn can still funnel substantial amounts of carbon into acetyl-CoA and the TCA cycle, supporting a minimal respiratory capacity. We hypothesize that some of this metabolic flux in mediated by alternative pathways of pyruvate metabolism include pyruvate oxidase and pyruvate carboxylase (25). It would seem unlikely this is mediate via enzymes such as pyruvate formate lyase, which are intoxicated in the presence of oxygen due to a glycyl free-radical (73). Nevertheless, the conversion of pyruvate to acetyl-CoA, and therefore acetate, seems to be critical for full virulence of *L.* monocytogenes. This is supported by the fact that neither loss of *rex* or addition of NOX was sufficient to rescue *pdhC*::Tn. Understanding what pathways are active for this conversion may be critical to understanding *L. monocytogenes* virulence in the cytosol.

Another question raised by this work is the role of *rex* in *L. monocytogenes'* metabolic regulation and its role during *L. monocytogenes* pathogenesis. Preliminary work to identify how *rex* impacts virulence has been previously characterized by Halsey *et al*. 2021 (38). In which, they showed that *rex* mutants replicate readily in the macrophage cytosol, form larger plaques than WT *L. monocytogenes*, and are only modestly attenuated for *in vivo* virulence of the liver and spleen via an oral infection model (38). Importantly, to date nobody has assessed a *rex*

mutant during intravenous infections, which we hypothesize may show less attenuation via this method of delivery due lack of metabolic transition from the gut to intracellular environment. However, it is also possible that this strain could be more attenuated due to *rex* mutants lacking the ability to repress their fermentation and therefore having a metabolism not well-adjusted for the *in vivo* cytosolic environment. In either case, it is difficult to assess what the metabolism of a *rex* mutant is during cytosolic growth. This is obfuscated by the fact that *rex* mutants don't lack any metabolic capabilities, rather they have access to metabolic pathways likely repressed during infection. Therefore, it is important to ask why certain metabolic pathways are in fact repressed by *rex* during infection and does relying on these pathways for energy generation impact virulence. Initial work done by the Reniere lab has evaluated genes known to be regulated by *rex* and they have shown a wide variety of genes repressed including many PTS, core fermentative enzyme like lactate dehydrogenase and pyruvate format lyase, and some virulence genes including internalins (38). One important question raised by these findings is how over expression of some of these enzymes may independently impact PDH mutants' virulence with *rex* intact, such as lactate dehydrogenase. While restoration of some PTS expression likely explains the phenotypes identified in this work, it is possible that use of PTS could be independently impacting virulence due to the intertwined nature of metabolism and virulence gene regulation. While it is clear that *rex* participates in the repression of internalins, it is possible that *rex*-mediated repression of PTS may be further impacting *prfA* and other virulence gene expression. For that reason, it would be important to assess whether PrfA* addition can further rescue virulence phenotypes of *rex* and PDH mutants. Together, this work could further define how *pdhC*::Tn is rescued by loss of *rex* and further how metabolic shifts *in vivo* may be connected to virulence gene expression.

Pinpointing the exact cause of virulence defects in PDH mutants is challenging due to the centrality of this complex to metabolism. While we show that carbon acquisition via PTS is impaired in PDH-deficient strains, additional physiological perturbations likely contribute to attenuation. Notably, cell-type-specific phenotypes suggest that individual host environments present distinct metabolic challenges or immune barriers. The restoration of intramacrophage growth in *rex*-deficient *pdhC::Tn* mutants, coupled with persistent *in vivo* attenuation, implies that host tissues may be more metabolically stringent or better equipped to detect altered bacterial metabolism. It is possible that PDH complex mutants with loss of function Rex may be producing excess lactate and this is being detected by host cells *in vivo,* but not *ex vivo*. Potential reasons for lack of *ex vivo* detection could be the supraphysiologic conditions as well as pH buffering of the media. A deeper understanding of how host cells detect bacterial fermentation versus respiration will yield insight into both immune surveillance mechanisms and pathogen evasion strategies. Similarly, understanding how *pdhC::Tn* retains the ability to bypass PDH complex mediated conversion of pyruvate into acetyl-CoA may unveil pathways essential for virulence.

MATERIALS AND METHODS

Ethics Statement

All animal-based experiments were performed using the protocol (M005916-R01-A01) approved by the Animal Use and Care Committee of the University of Wisconsin—Madison and consistent with the standards of the National Institutes of Health.

Bacterial strains and culture

All *Listeria monocytogenes* strains used for experiments in this study were in a 10403s background. All *L. monocytogenes* strains were grown overnight in BHI and at 30°C stationary for all experiments, except as described. *Escherichia coli* strains were grown in Luria broth (LB) at 37°C shaking. Antibiotics used on *E. coli* were at a concentration of 100 μg/ml carbenicillin or 30 μg/ml kanamycin when appropriate. Antibiotics used on *L. monocytogenes* were at a concentration of 200 μg/mL streptomycin and/or 10 μg/mL chloramphenicol and/or 2 μg/mL erythromycin, when appropriate. Plasmids were transformed into chemically competent *E. coli* and further conjugated in *L. monocytogenes* using S17 *E.coli*.

Construction of strains

The pPL2 integrative vector pIMK2 was used for constitutive expression of *L. monocytogenes* genes (74). pIMK2 complement constructs were cloned in XL1-Blue *E. coli* with 30μg/mL Kanamycin and grown for plasmid harvest using Promega MiniPrep Kit. Harvested plasmid sequences were confirmed using was performed by Plasmidsaurus using Oxford Nanopore Technology with custom analysis and annotation. Plasmid were then shuttled into *L. monocytogenes* through conjugation with S17 (pIMK2) *E. coli*. All mutants were confirmed via PCR, plasmid sequencing, and whole-genome sequencing using Oxford Nanopore technology from Plasmidsaurus with custom analysis and annotation.

***In vitro* Growth Assays**

Bacteria were grown overnight in BHI at 30°C stationary. Overnight cultures were used to generate inoculums with ~$3.7x10^8$ CFU in PBS. 100 μLs per well of a flat bottom clear 96-well plate of *Listeria* synthetic media (LSM) with carbons source (supplied with amounts noted in text and figures) was inoculated with 2 μL of inoculums. Plates were parafilmed on the edge to

prevent evaporation and evaluated for OD_{600} in plate reader at 37°C shaking (250 r.p.m.) and reads every 15 minutes for times displayed.

Terminal Optical Density Aerobic and Anaerobic Growth Assays

Bacteria were grown overnight in BHI at 30°C stationary. Overnight cultures were used to generate inoculums with ~$3.7x10^8$ CFU in PBS. 14 mL tubes were setup with 3 mL of *Listeria* synthetic media (LSM) with carbon sources (supplied with amounts noted in text and figures) and inoculated with 20 µL of inoculums. Tubes were loosely capped and placed, slanted, in 30°C incubator either exposed to air (aerobic) or placed in GasPak (anaerobic) chambers with 2 GasPaks for oxygen depletion (Fischer: 11-816-2). Samples were left for 48 hours and then 100 µL was harvested from each and plated into 96-well plate for OD600 to be taken in a plate reader. Optical density values were normalized to WT and averaged for display and statistical analysis.

Intra-macrophage growth curves

Bone marrow-derived macrophages were isolated from CL57/BL6 mice and cultured as previously described in Roswell Park Memorial Institute Medium (RPMI) based media (Invitrogen: 11875093) (75). BMDMs were plated into 60 mm dishes contain 13 degassed coverslips. BMDMs cells were infected with *L. monocytogenes* strains at a multiplicity of infection [MOI] of 0.2. Inoculums of *L. monocytogenes* were grown in 3mL of BHI at 30°C stationary until all strains had reach stationary phase. Colony forming units to OD_{600} ratios were determined for each strain and adjusted to ensure infection results in a comparable MOI across strains. After 30 minutes BMDM media was exchanged for media containing 50 µg/ml Gentamycin. Coverslips were harvested, cells lysed in pure water, bacteria rescued isotonically,

and plated to quantify CFU at displayed time points. All strains were assayed in biological triplicate and data displayed is one representative biologic replicate.

Plaque Assay

Plaque assays were conducted using a L2 fibroblast cell line grown in Dulbecco's Minimal Essential Media (DMEM) based media (Thermo Fischer: 11965092) as previously described with minor modifications for visualization and quantification of plaques (21). L2 fibroblasts were seeded at 1.2×10^6 per well of a 6-well plate, then infected at an MOI of 0.5 to obtain approximately 10-30 PFU per dish. Inoculums of *L. monocytogenes* were grown in 3mL of BHI at 30°C stationary until all strains had reached stationary phase. Colony forming units to OD_{600} ratios were determined for each strain and adjusted to ensure infection results in a comparable MOI across strains. At 4 days postinfection, cells were stained with 0.3% crystal violet for 10 min and washed twice with deionized water. Stained wells were scanned, uploaded, and areas of plaque formation were measured on ImageJ analysis software. All strains were assayed in biological triplicate and the average plaque areas of each strain (one-well per strain were normalized to wild-type plaque size within each replicate.

Murine Infection and Organ Burdens

Infections were performed as previously described (21). Briefly, 6 to 12-week-old female and male C57BL/6 mice were infected IV with 1×10^5 CFU logarithmically growing *L. monocytogenes* (optical density at 600 nm [OD600] = 0.5) in 200 μL of PBS. Colony forming units to OD600 ratios were determined for each strain and adjusted to ensure infection results in a comparable MOI across strains. 48 hours post-infection, mice were euthanized, and livers and

spleens were harvested, homogenized in water with 0.1% NP-40, and plated for CFU. Two independent replicates of each experiment with 5 mice per group were performed.

Fermentation Byproduct Measurement

Indicated strains of *L. monocytogenes* were grown in BHI at 37°C, shaking overnight. Cultures were centrifuged to pellet bacteria, and 1 mL of the supernatant was filtered using a 0.2µm-pore-size syringe filter (09-740-113; Fisher Scientific). Supernatants were then treated with 2µL of H_2SO_4 to precipitate running buffer incompatible bacterial components. The samples were then centrifuged at >16000 r.c.f. for 10 min. Subsequently, 200µL of each supernatant was transferred to an HPLC vial. HPLC analysis was performed using a ThermoFisher (Waltham, MA) Ultimate 3000 UHPLC system equipped with a UV detector (210 nm). Compounds were separated on a 250 × 4.6 mm Rezex© ROA-Organic acid LC column (Phenomenex Torrance, CA) run with a flow rate of 0.2 mL min^{-1} and at a column temperature of 50 °C. Prior to injection samples were kept at 4 °C. Separation was isocratic with a mobile phase of HPLC grade water acidified with 0.015 N H_2SO_4 (415 µL L^{-1}). Byproduct standards were 100, 20, 4, and 0.8mM concentrations of lactate or acetate. HPLC peaks were analyzed and quantified using the Thermofisher Chromeleon 7 software package.

Metabolic Profiling using HPLC

Overnight cultures of wild-type (WT) and *pdhC::Tn L. monocytogenes* were grown in brain heart infusion (BHI) broth at 30°C. The following day, 1 mL of each culture was washed with phosphate-buffered saline (PBS) and used to inoculate 50 mL of Listeria Synthetic Medium (LSM) supplemented with 110 mM glucose in baffled flasks. Cultures were incubated at 37°C

with shaking until mid-log phase ($OD_{600} \approx 0.4$) was reached. At this point, 5 mL of each culture was filtered through a 0.2 μm nylon membrane filter. Filters were then transferred to sterile petri dishes containing 1.5 mL of cold extraction solvent (acetonitrile:methanol:water, 2:2:1). The solvent was gently swirled and pipetted across the filter surface to extract intracellular metabolites, after which the filter was flipped and the process repeated to maximize extraction efficiency. The pooled extract was transferred to centrifuge tubes, vortex vigorously for 2 minutes, and centrifuged at maximum speed (≥13,000 × *g*) for 5 minutes to pellet insoluble material. A 200 μL aliquot of the clarified supernatant was collected, dried under a stream of nitrogen gas, and resuspended in 70 μL of HPLC-grade water prior to analysis. All cultures were grown in biological triplicate and processed in technical duplicate.

Metabolite quantification and analysis was performed as previously described. In short, samples were run through an ACQUITY UPLC BEH C18 column in an 18-min gradient with Solvent A consisting of 97% water, 3% methanol, 10 mM tributylamine (TBA), 9.8 mM acetic acid, pH 8.2, and Solvent B being 100% methanol. Gradient was 5% Solvent B for 2.5 min, gradually increased to 95% Solvent B at 18 min, held at 95% Solvent B until 20.5 min, returned to 5% Solvent B over 0.5 min, and held at 5% Solvent B for the remaining 4 min. Ions were generated by heated electrospray ionization (HESI; negative mode) and quantified by a hybridquadrupole high-resolution mass spectrometer (Q Exactive Orbitrap, Thermo Scientific). MS scans consisted of full MS scanning for 70 to 1,000 m/z from time zero to18 min, except that MOPS m/z of 208 to 210 was excluded from 1.5 to 3 min. Metabolite peaks were identified from Kegg Known Compound list and quantified in Metabolomics Analysis and Visualization Engine (MAVEN).

In vitro Suppressor Screen

The Δ*pdhC*::Tn mutant was mutagenized by a 5-minute exposure to ethyl methanesulfonate (EMS) as previously described (76,77). One ml of the library was thawed, washed in 10 mL PBS and resuspended in PBS to a concentration of $7x10^8$ CFU/mL, and plated across 10 *Listeria* synthetic media (LSM) agar plates with 55 mM fructose. Plates were incubated for 48 hours post-inoculation, at which time single colonies were picked and selected for on BHI plates with erythromycin and streptomycin to confirm resistance. Successful growth of colonies were grown overnight at 37°C with shaking, pelleted by centrifugation, resuspended in 100 µl BHI + 40% glycerol, and stored at -80°C. All five isolates from the LSM with fructose plates was subsequently grown overnight in BHI broth, and subjected to whole genome sequencing and SNP analysis as described below.

Whole genome sequencing and SNP identification

PdhC::Tn *L. monocytogenes* suppressor isolates were grown overnight in 3 mL culture of BHI. Genomic DNA was purified using the MasterPure Gram-positive DNA purification kit (Epicentre) per the manufacturer's instructions, except that 5 U/µl mutanolysin was used instead of lysozyme. DNA was submitted Plasmidsaurus for whole-genome sequencing using Oxford Nanopore technology. Fastq reads were uploaded to Galaxy and mapped onto the *L. monocytogenes* 10403S reference sequence (GCA_000168695.2_ASM16869v2) using Snippy (version 4.6.0). Single nucleotide polymorphisms (SNPs) were assessed for impact on *L. monocytogenes* coding sequences and genes manually utilizing Jbrowse (Version 1.16.11).

Cell Culture

L2 cells were all kind gifts from Daniel Portnoy (UC Berkeley). Bone marrow-derived macrophages (BMDM) were prepared from 6-to-8-week-old mice as previously described (78).

Phenotypic Microarrays

Phenotype Microarrays 1 (Cat. #12111) and 2A (Cat. #12112) were obtained from BioLog (BioLog). Plates were prepared and inoculated as previously described (62,79). OmniLog incubation was substituted with incubation at 37°C stationary. OD490 was collected for each plate at 24 and 48 hours. Data was then normalized to consumption of α-D-glucose for each strain and replicate, and averaged across triplicate. Value were clustered based on similarity using clustergrammer and plotted as a heat-map in Prism 6 (80). Data normalized to glucose was used for statistical analysis and displayed in tables. Statistics are representative of a student's T-test between two strains.

Statistical Analysis

Prism 6 (GraphPad Software) was used for statistical analysis of data. Means from two groups of BioLog plates were compared with unpaired two-tailed Student's T-test. Means from more than two groups for all other assays were analyzed by one-way ANOVA test. Independently, Mann-Whitney Test was used to analyze two group comparison of non-normal data from animal experiments. * $p < 0.05$, ** $p < 0.01$, *** $p < 0.001$ for all statistical tests displayed.

FIGURES

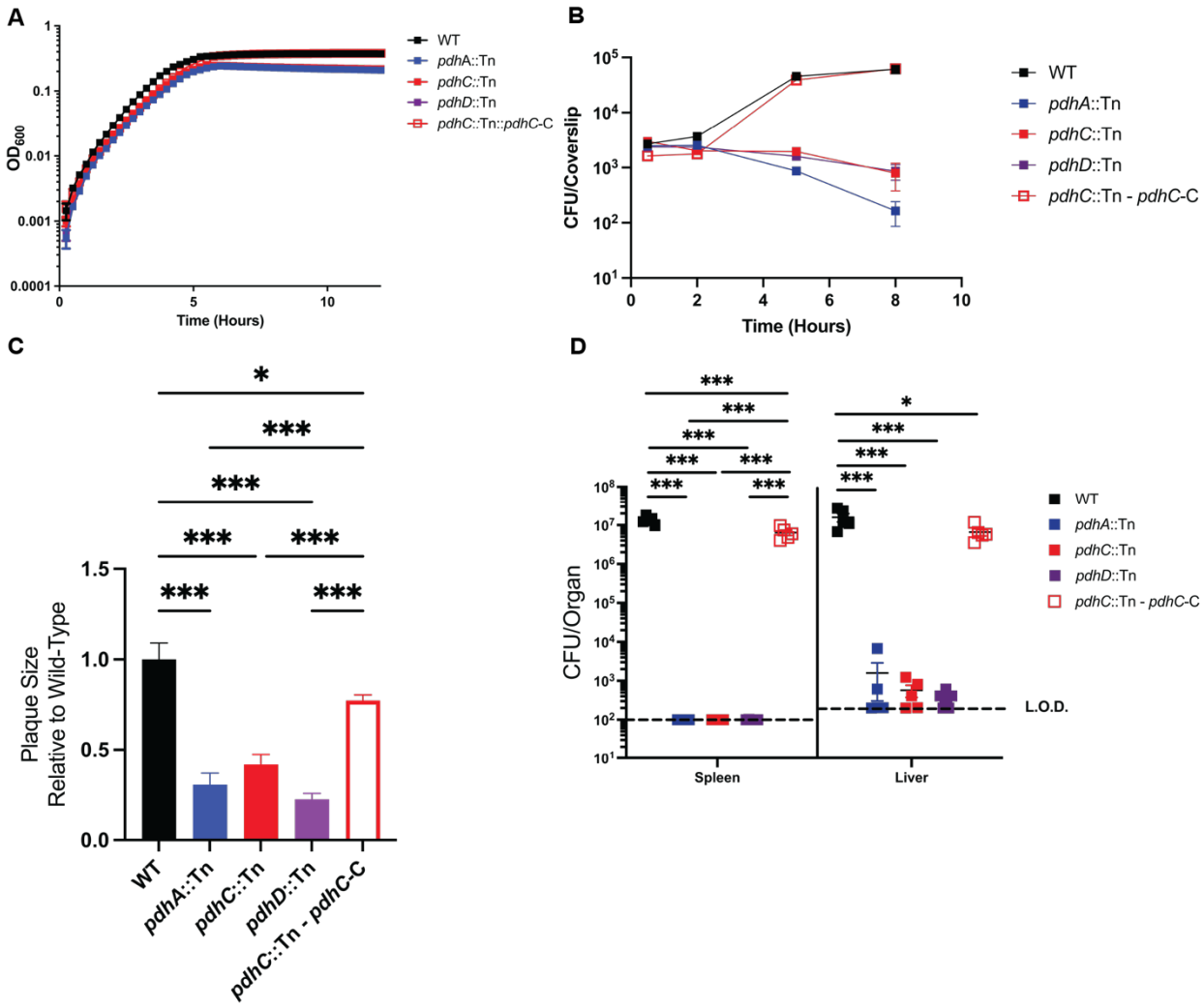

Figure 1. PDH complex mutants retain wild-type growth in rich media and have phenotypically similar virulence defects. (A) Indicated strains were grown in Brain, Heart Infusion (BHI) at 37°C, shaking at 250 r.p.m. and had OD600 measured every 15 minutes for 12 hours in a plate reader. (B) Intracellular growth of indicated strains was determined in BMDMs following infection at an MOI of 0.2. Growth curves are representative of one experiment. Error bars represent the standard error of the means of technical triplicates within the representative experiment. (C) L2 fibroblasts were infected with indicated *L. monocytogenes* strains at an MOI of 0.5 and were examined for plaque formation 4 days post infection. Assays were performed in

biological triplicate and data displayed is the Mean and SEM of a strain's plaque size relative to WT in one of three representative biological replicates. (D) Bacterial burdens from the spleen and liver were enumerated at 48 hours post-intravenous infection with $1x10^5$ bacteria. Data are representative of results from one experiments. Horizontal dashed lines represent the limits of detection, and the bars associated with the individual strains represents the mean and SEM of the group.

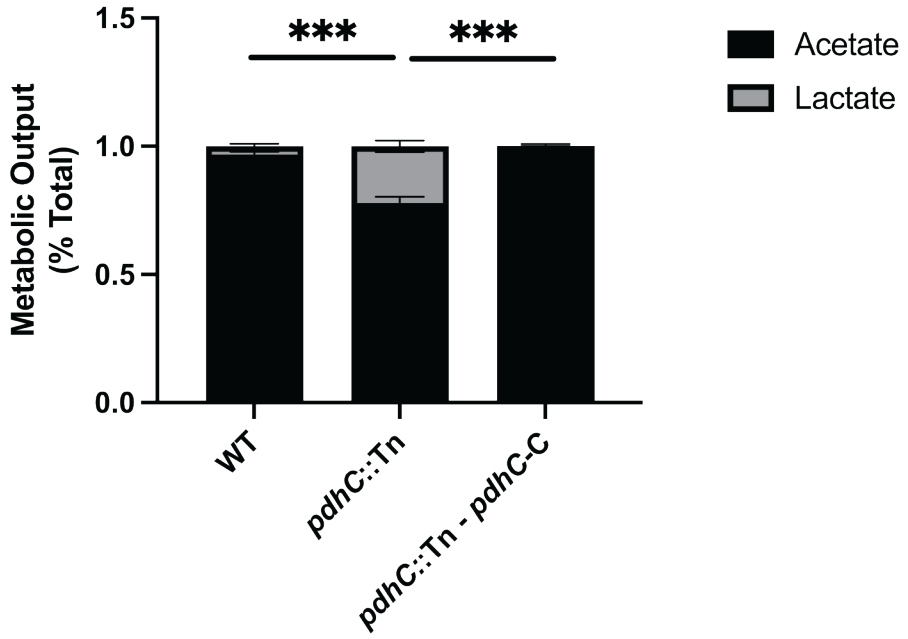

Figure 2. *PdhC*::Tn mutants show altered respiro-fermentative metabolite byproducts relative to WT *L. monocytogenes*. High-performance liquid chromatography (HPLC) was used to quantify fermentation products (acetate and lactate) produced and secreted by the indicated *L. monocytogenes* strains grown aerobically in BHI medium at 37°C to stationary phase. The mean percentage of acetate and lactate production by each strain was compared to that of the wild-type *L. monocytogenes*.

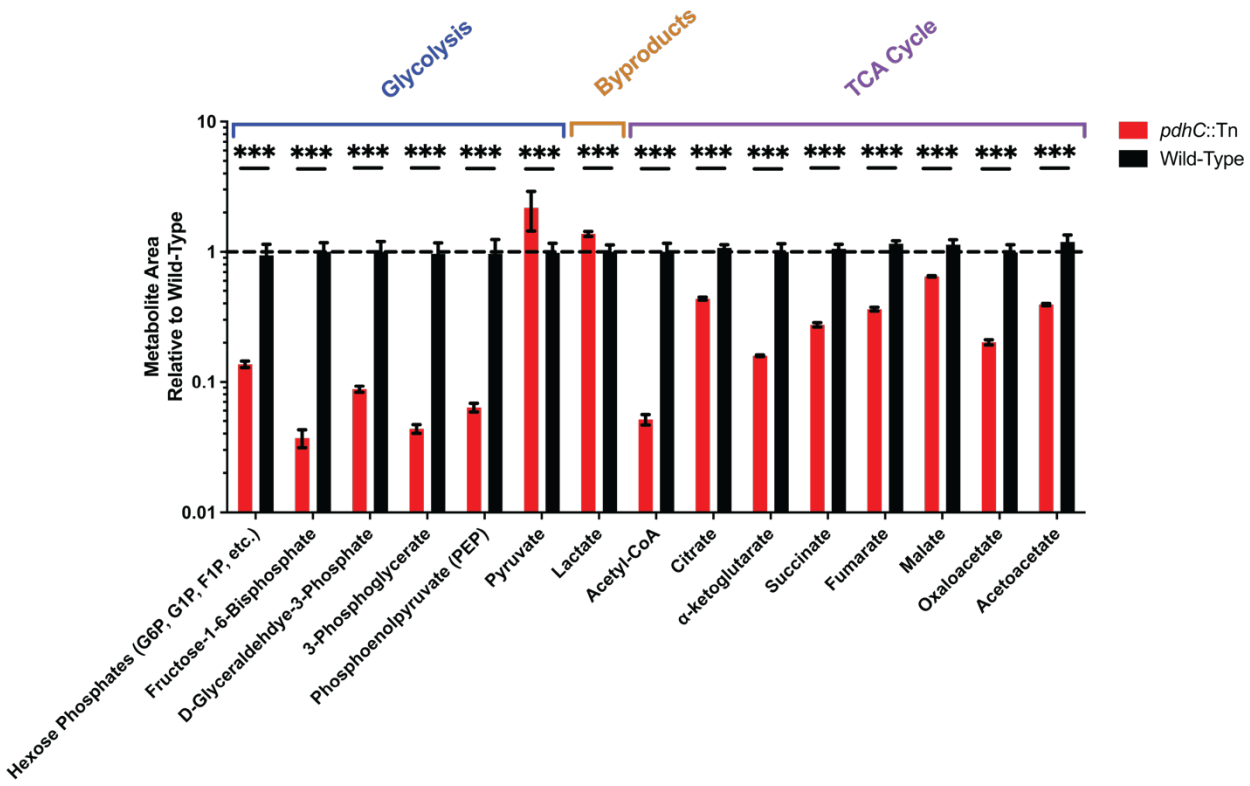

Figure 3. Metabolomic profiling of *pdhC*::Tn and WT *L. monocytogenes* glycolytic, fermentative byproduct, and TCA cycles metabolites. Indicated *L. monocytogenes* strains were grown to mid-log phase ($OD_{600} \approx 0.4$) in Listeria Synthetic Medium (LSM) supplemented with 110 mM glucose. Intracellular metabolites were extracted and analyzed via HPLC-MS. Tricarboxylic acid (TCA) cycle intermediates, upper glycolytic metabolites, and lactate were identified based on accurate mass-to-charge (m/z) ratios and retention times using reference values from the KEGG Compound Database, as implemented in MAVEN software. Peak areas were quantified and normalized to wild-type (WT) levels for each metabolite. Data represent three biological replicates, each with two technical replicates. Statistical comparisons were performed using unpaired two-tailed Student's *t*-tests for each metabolite within a strain.

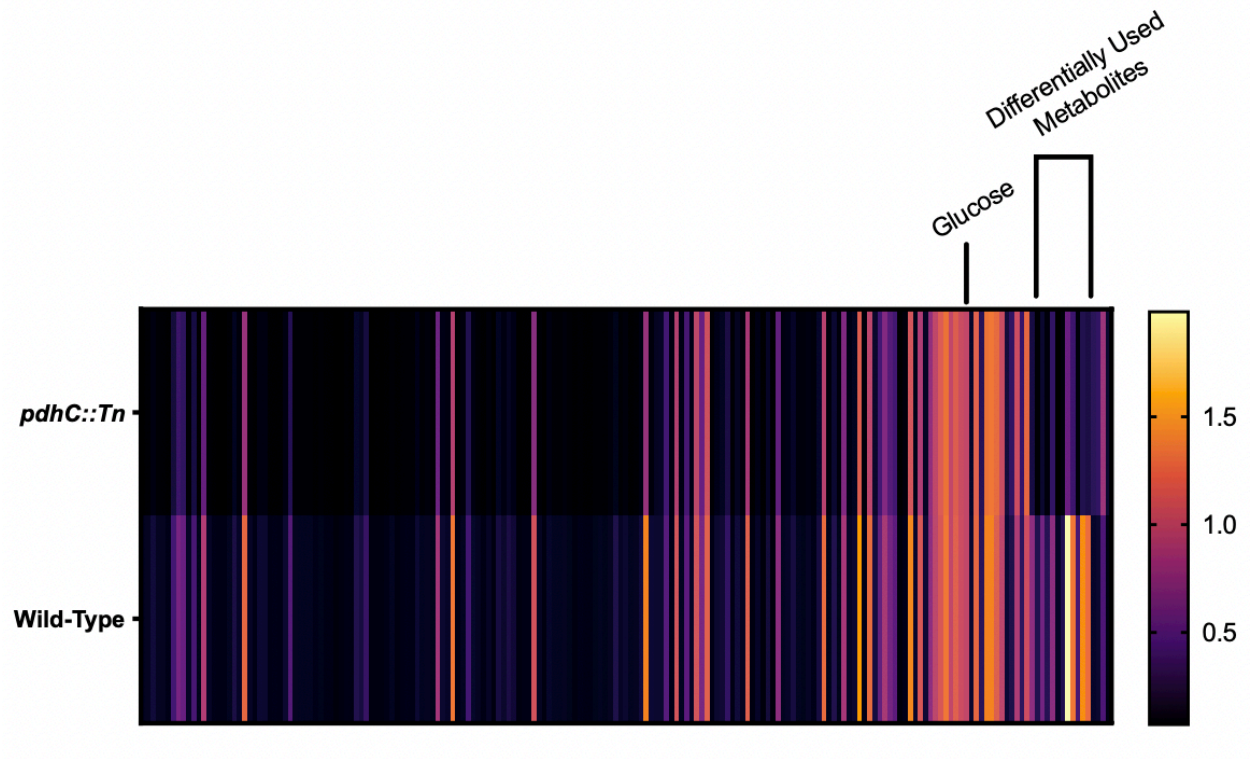

Figure 4. Carbon metabolite respiration of WT and *pdhC*::Tn *L. monocytogenes* show differential use of PTS mediated carbon source. Clustered heatmaps indicating level of tetrazolium dye color change as measured by OD_{490} at 48 hours in response to *pdhC*::Tn (Top) and WT (Bottom) respiration of carbon metabolites (PM1 & PM2A) at 37°C stationary. Each bar indicates the average of 3 biologic replicates. Samples were normalized to readings of a α-D-glucose control (~1 on scale and labeled) and sorted based on cluster analysis. Select differentially used metabolites clusters are labeled above for full list see **Table 1**.

Table 1. Statistically significant and greater than 2-fold differentially used metabolites between WT and *pdhC*::Tn *L. monocytogenes*

Metabolite	**Fold Usage (WT/*pdhC*::Tn)**	***P-value***
D-Psicose	5.10	<0.001
Glycerol	3.55	<0.001
alpha-keto-Butyric Acid	3.96	<0.001
L-Alanyl-Glycine	2.38	<0.001
alpha-D-Lactose	5.19	<0.001
D-Melezitose	2.94	<0.001
alpha-Methyl-D-Glucoside	3.59	0.001
L-Alanine	2.25	0.001
Pyruvic Acid	2.87	0.005
Turanose	2.13	0.005
Sedoheptulosan	3.13	0.006

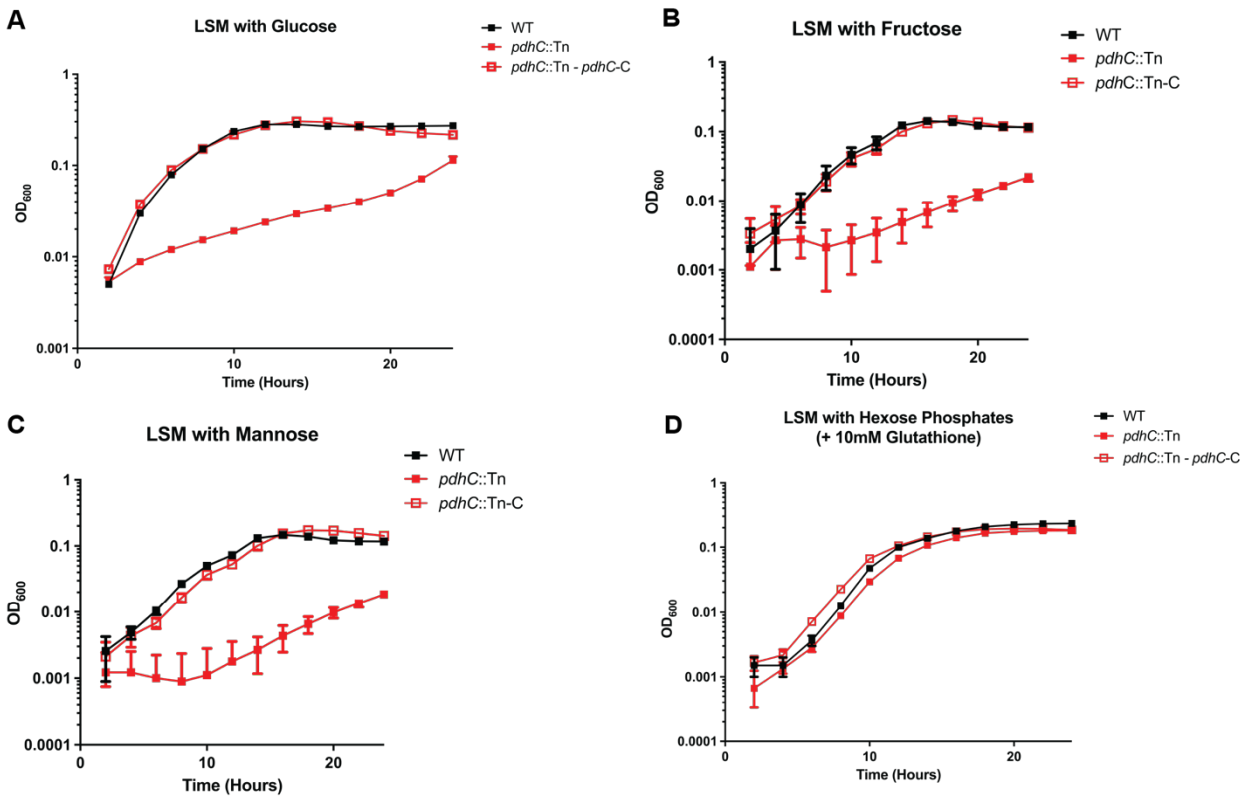

Figure 5. *PdhC*::Tn mutants are defective for growth on PTS-mediated carbon Source of glucose, fructose, and mannose, but retain growth on non-PTS-mediated hexose phosphates. Indicated strains were grown in LSM at 37°C, shaking at 250 r.p.m. with the addition of 110mM glucose (A) or molar equivalent amounts of fructose (B), mannose (C), or hexose phosphates (+10mM glutathione) (D). OD600 was monitored every 15 minutes for 24 hours is a plate reader. Data represents average of three technical replicates from one representative of three biological replicates.

Table 2. Suppressors mutations in *rex* (LMRG_01223) of *pdhC*::Tn *L. monocytogenes* growth on LSM with fructose plates.

Suppressor Name	Genomic Location	Basepair Change	Mutation Classification	Amino Acid Change	Color in Figure 5
pdhC::Tn Supp 1	LMRG_01223 b.p 2107837	G to A	Missense	Serine-36-Phenylalanine	Red
pdhC::Tn Supp 2	LMRG_01223 b.p. 2107901	G to A	Missense	Arginine-14-Methionine	Red
pdhC::Tn Supp 3	LMRG_01223 b.p. 2107763	C to A	Missense	Glycine-60-Cysteine	Red
pdhC::Tn Supp 4	LMRG_01223 b.p. 2107790	G to A	Premature Stop	Argine-51-STOP	Red
pdhC::Tn Supp 5	LMRG_01223 b.p. 2107239	TAAAAGGCGTAAAAAAACCTGTAGAAAGTAAGTTTAGCTTACCTTCTACAGGTTTTTTTATTCTGTTTTCGCTGGATAATTTTCCAGGAAATAGATTAACGTTTGTAATTCCGTTGTAAGGTCGATATGGTGCACACGAACTTGTTTTGGAACACTG to T	Deletion of ~100 BP from C-terminus	Loss of RISVPKQVRVHHIDLTTELQTLIYFLENYPAKTE-C'	Orange

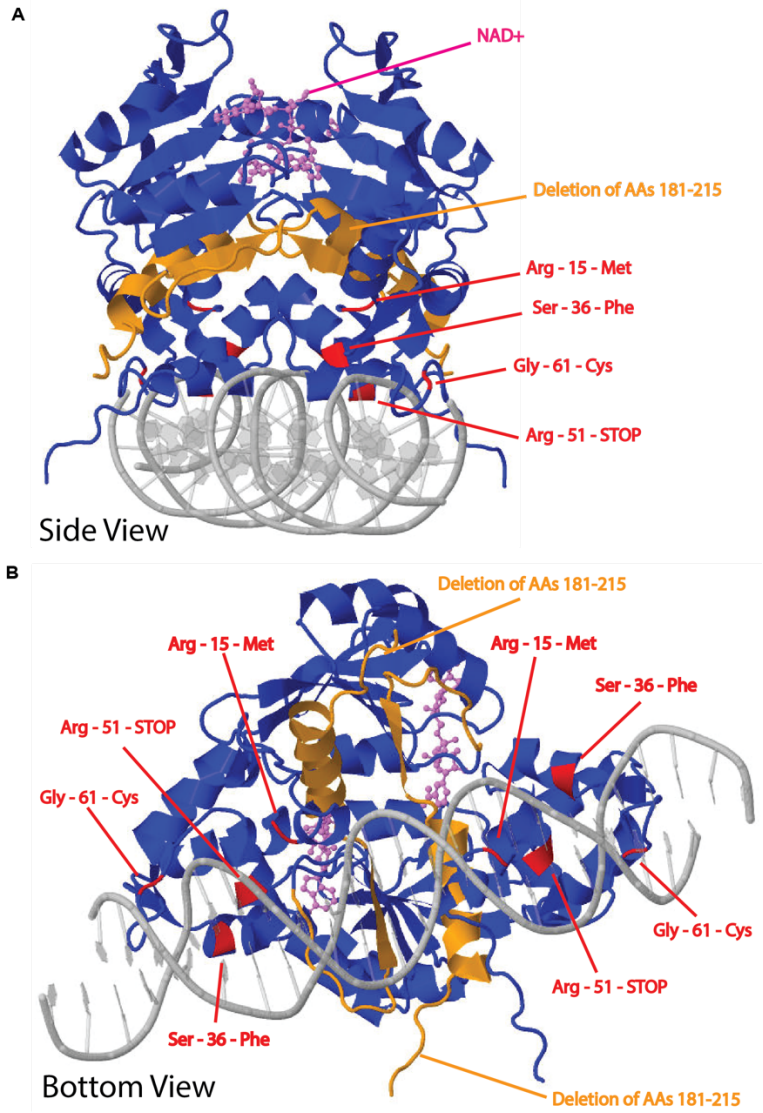

Figure 6. Suppressors of *pdhC*::Tn growth on PTS mediated carbon sources mapped onto *L. monocytogenes*' Rex (LMRG_01223) homodimer bound to NAD+ and DNA. *L. monocytogenes (10403s)* protein sequence for Rex (LMRG_01223) was obtained from NCBI (GCA_000168695.2_ASM16869v2) and was input into AlphaFold as a homodimer with the ligands of NAD+ (pink) and Rex-specific DNA-binding sequences (grey DNA helix). Predicted output was further processed in Jmol to represent amino acids modified (red) or lost (orange) due to suppressor mutations. Complete molecular structure is pictured from two angles: side-side (A) and bottom-up (B).

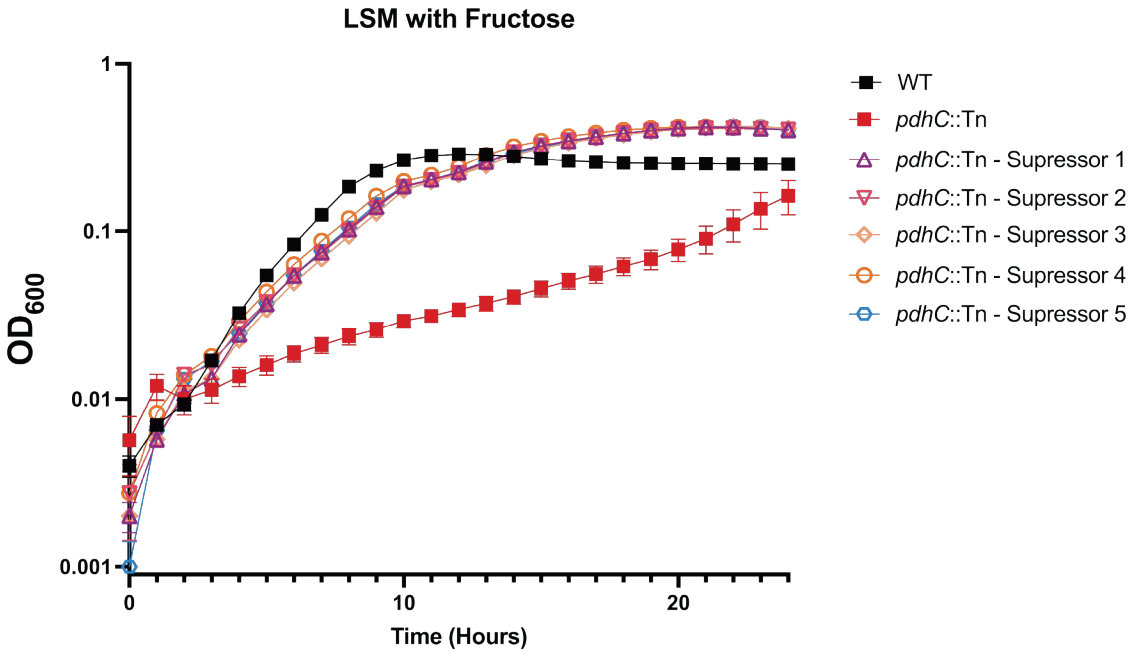

Figure 7. *PdhC*::Tn suppressor mutants restore growth in define media with fructose as the sole carbon source. Indicated strains were grown in LSM at 37°C, shaking at 250 r.p.m. with the addition of 110mM Fructose. OD600 was monitored every 15 minutes for 24 hours is a plate reader. Data represents average of three technical replicates from one biological replicate.

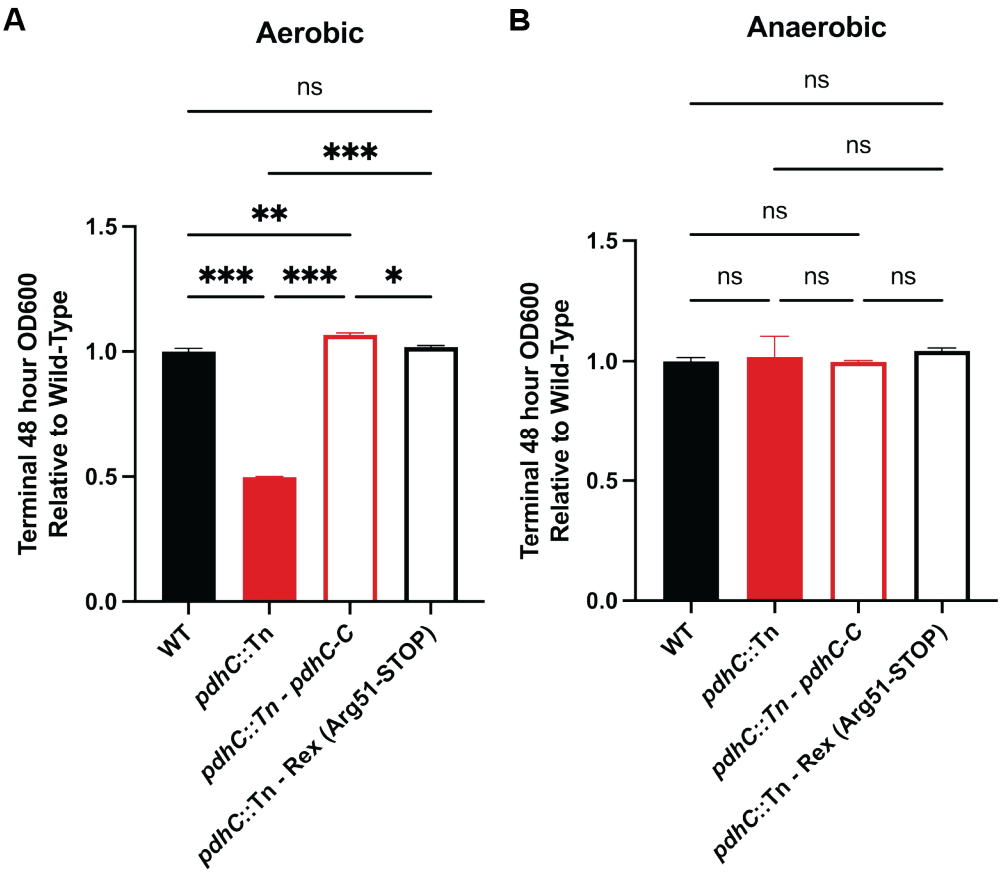

Figure 8. Loss of rex permits *pdhC*::Tn growth on PTS-mediated carbon sources aerobically similar to that of anaerobic growth. Indicated strains were grown in LSM at 30°C, stationary for 48 hours with the addition of 110mM Fructose. OD600 was taken at 48 hours and normalized to WT. Data represents average of three biological replicates and statistical analysis was performed comparing all strains using one-way ANOVA with Tukey correction.

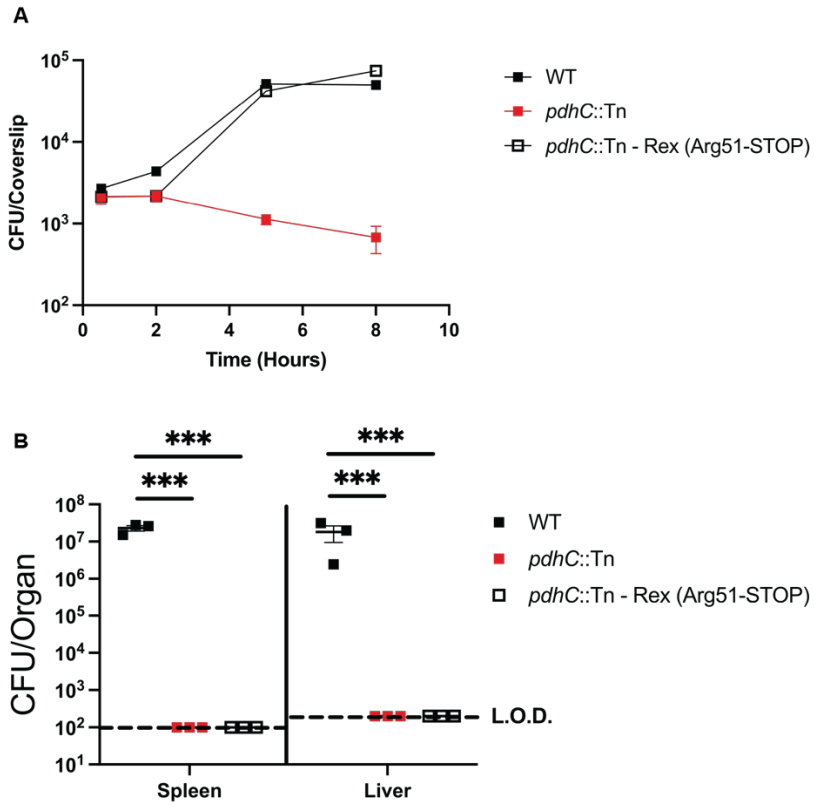

Figure 9. *PdhC*::Tn rex suppressor mutations rescue intramacrophage growth but fail to rescue in vivo. (A) Intracellular growth of indicated strains was determined in BMDMs following infection at an MOI of 0.2. Growth curves are representative of one experiment. Error bars represent the standard error of the means of technical triplicates within the representative experiment. (D) Bacterial burdens from the spleen and liver were enumerated at 48 hours post-intravenous infection with 1x105 bacteria. Data are representative of results from one experiments. Horizontal dashed lines represent the limits of detection, and the bars associated with the individual strains represents the mean and SEM of the group.

SUPPLEMENTARY INFORMATION

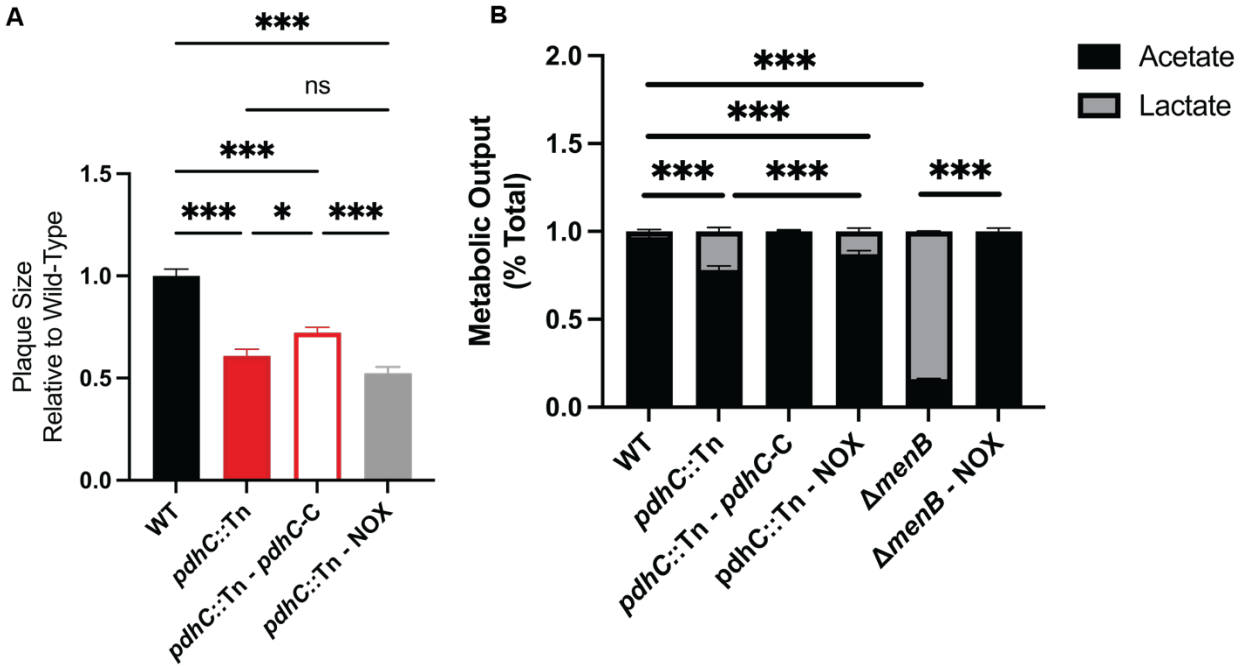

Supplemental Figure 1. Overexpression of NADH Oxidase, NOX, fails to rescue *pdhC*::Tn virulence as measured by plaquing assay and fermentative byproducts. (A) L2 fibroblasts were infected with indicated *L. monocytogenes* strains at an MOI of 0.5 and were examined for plaque formation 4 days post infection. Assays were performed in biological triplicate and data displayed is the Mean and SEM of a strain's plaque size relative to WT in one of three representative biological replicates. (B) Note data for WT, *pdhC*::Tn, and *pdhC*::Tn-*pdhC*-C is recapitulation of data presented in **Figure 2**. High-performance liquid chromatography (HPLC) was used to quantify fermentation products (acetate and lactate) produced and secreted by the indicated *L. monocytogenes* strains grown aerobically in BHI medium at 37°C to stationary phase. The mean percentage of acetate and lactate production by each strain was compared to that of the wild-type *L. monocytogenes*.

Supplemental Table 1. Bacterial strains used in this study.

Strain	Description	Reference
XL1-Blue	competent *E. coli* strain	(80)
S17	*E. coli* strain for conjugations into *L. monocytogenes;* Sp^R	(77)
10403S [JDS 1]	Background *L. monocytogenes* 10403s strain	(84)
JDS 875	*pdhA*::Tn	This Work
JDS 1203	*pdhC*::Tn	(20)
JDS 876	*pdhD*::Tn	This Work
JDS 1064	*pdhC*::Tn – *pdhC*-C	This Work
MJF 363	*pdhC*::Tn - NOX	This Work
MJF 368	*pdhC*::Tn Supp 1	This Work
MJF 370	*pdhC*::Tn Supp 2	This Work
MJF 372	*pdhC*::Tn Supp 3	This Work
MJF 374	*pdhC*::Tn Supp 4	This Work
MJF 376	*pdhC*::Tn Supp 5	This Work

Supplemental Table 2. Results of BioLog PM1 and PM2A at 48 hours for WT and *pdhC*::Tn

	Fold Usage Normalized to α-D-Glucose		P-value (Student's T-Test)
Metabolite	**WT**	***pdhC*::Tn**	**WT v.s. *pdhC*::Tn**
alpha-Methyl-D-Glucoside	1.99	0.55	<0.001
Amygdalin	1.52	1.17	<0.001
alpha-D-Lactose	1.44	0.28	<0.001
Xylitol	1.40	1.11	0.006
Beta-Cyclodextrin	1.39	1.31	0.451
Alpha-Methyl-D-Mannoside	1.39	0.76	<0.001
Arbutin	1.39	1.30	0.259
Uridine	1.32	0.93	0.001
Glycerol	1.31	0.37	0.000
alpha-Cyclodextrin	1.31	1.30	0.823
D-Psicose	1.27	0.25	0.000
L-Rhamnose	1.26	0.94	<0.001
D-Arabitol	1.25	0.97	0.007
Beta-Methyl-D-Glucoside	1.24	1.18	0.330
Maltose	1.24	0.76	0.008
Gentiobiose	1.19	1.07	0.062
L-Lyxose	1.18	0.85	<0.001
Beta-D-Allose	1.18	1.17	0.890
Gamma-Cyclodextrin	1.18	1.24	0.357
D-Mannose	1.12	1.15	0.476
Dihydroxy Acetone	1.12	0.89	0.006
D-Glucosamine	1.11	0.98	0.084
Sailcin	1.10	0.91	0.010
Dextrin	1.10	0.70	<0.001
D-Trehalose	1.06	1.24	0.066
N-Acetyl-D-Glucosamine	1.05	1.04	0.855
Maltotriose	1.01	1.00	0.902
alpha-D-Glucose	1.00	1.00	1.000
D-Cellobiose	0.97	0.98	0.827
D-Fructose	0.97	1.03	0.108
Capric Acid	0.90	0.53	0.054

N-Acetyl-Beta-D-Mannosamine	0.88	1.06	0.001
Acetic Acid	0.86	0.66	0.082
D-Ribose	0.84	0.65	0.001
Acetoacetic Acid	0.84	0.57	<0.001
Inosine	0.73	0.74	0.933
D-Melezitose	0.72	0.24	<0.001
2-Deoxy-D-Ribose	0.71	0.52	<0.001
Turanose	0.71	0.33	0.005
D-Xylose	0.63	0.55	0.020
D-Fucose	0.62	0.36	0.201
5-Keto-D-Gluconic Acid	0.60	0.46	0.001
Sedoheptulosan	0.60	0.19	0.006
N-Acetyl-D-Glucosaminitol	0.55	0.32	0.002
D-Arabinose	0.52	0.40	0.004
Butyric Acid	0.51	0.39	0.060
Sorbic Acid	0.50	0.41	0.090
L-Arabinose	0.47	0.40	0.002
Caproic Acid	0.46	0.29	0.013
Adenosine	0.42	0.79	0.002
Mucic Acid	0.42	0.24	0.075
alpha-keto-Butyric Acid	0.41	0.10	<0.001
Palatinose	0.40	0.27	0.022
3-0-Beta-D-Galactopyranosyl-D-Arabinose	0.39	0.23	<0.001
Propionic Acid	0.35	0.23	0.043
Sec-Butylamine	0.34	0.25	0.079
D-Tagatose	0.31	0.36	0.394
Oxalic Acid	0.31	0.30	0.750
Gelatin	0.30	0.11	0.099
Pyruvic Acid	0.27	0.10	0.005
Mannan	0.27	0.18	0.002
L-Alanyl-Glycine	0.27	0.11	<0.001
2,3-Butanedione	0.27	0.20	0.018
L-Methionine	0.27	0.14	0.015
Chondroitin Sulfate C	0.27	0.33	0.576
Inulin	0.25	0.15	0.034
Glycogen	0.25	0.16	0.002

Glucuronamide	0.24	0.19	<0.001
Negative Control	0.24	0.18	0.188
3-Hydroxy-2-Butanone	0.24	0.15	0.106
Pectin	0.24	0.18	<0.001
L-Sorbose	0.23	0.16	0.035
D-Raffinose	0.23	0.17	0.117
Glycyl-L-Aspartic Acid	0.22	0.12	0.005
Stachyose	0.22	0.13	0.005
Oxalomalic Acid	0.22	0.16	0.067
Tween 20	0.21	0.14	<0.001
N-Acetyl-D-Galactosamine	0.21	0.15	0.005
Glyoxylic Acid	0.21	0.17	0.011
Beta-Methyl-D-Galactoside	0.21	0.11	0.004
3-Methyl Glucose	0.21	0.23	0.417
Tween 40	0.20	0.14	0.005
L-Isoleucine	0.20	0.12	0.025
L-Fucose	0.20	0.17	0.008
Acetamide	0.20	0.12	0.028
D,L-Octopamine	0.20	0.13	0.032
D-Saccharic Acid	0.19	0.14	0.028
Maltitol	0.19	0.15	0.205
D-Fructose-6-Phosphate	0.19	0.16	0.035
L-Lactic Acid	0.19	0.10	<0.001
Beta-Methyl-D-Xyloside	0.19	0.12	0.149
2-Deoxy-Adenosine	0.19	0.34	<0.001
Melibionic Acid	0.19	0.18	0.927
L-Leucine	0.19	0.12	0.010
N-Acetyl-Neuaminic Acid	0.19	0.15	0.012
L-Valine	0.19	0.12	0.007
L-Glucose	0.18	0.12	0.029
Thymidine	0.18	0.31	0.001
alpah-Keto-Valeric Acid	0.18	0.12	0.026
D-Glucuronic Acid	0.18	0.13	0.001
L-Proline	0.18	0.13	0.013
Glycyl-L-Proline	0.18	0.11	0.002
2,3-Butanediol	0.17	0.10	0.016

Succinic Acid	0.17	0.11	<0.001
D-Sorbitol	0.17	0.14	0.016
Lactulose	0.17	0.09	0.002
Methyl Pyruvate	0.17	0.10	<0.001
Adonitol	0.17	0.10	0.001
L-Galactonic Acide-gamma-lactone	0.17	0.12	0.015
L-Alanine	0.16	0.07	<0.001
Negative Control	0.16	0.11	<0.001
D-Galactonic Acid-gamma-Lactone	0.16	0.13	<0.001
L-Aspartic Acid	0.16	0.11	0.008
Beta-Methyl-D-Glucuronic Acid	0.16	0.11	<0.001
Sebacic Acid	0.16	0.09	<0.001
D-Glucose-6-Phosphate	0.16	0.10	0.005
alpha-Methyl-D-Galactoside	0.16	0.10	0.006
L-Lysine	0.16	0.09	0.004
Lactitol	0.16	0.09	0.004
Tween 80	0.16	0.10	0.002
L-Asparagine	0.16	0.09	<0.001
D,L-alpha-glycerol-phosphate	0.16	0.11	<0.001
Dulcitol	0.16	0.11	<0.001
D-Glucosaminic Acid	0.16	0.10	<0.001
D-Galactose	0.16	0.13	0.017
p-Hydroxy Phenyl Acetic Acid	0.15	0.10	0.002
L-Ornithine	0.15	0.12	0.166
L-Arabitol	0.15	0.10	0.004
L-Alaninamide	0.15	0.09	0.015
Putrescine	0.15	0.09	0.010
myo-Inositol	0.15	0.09	<0.001
D-Melibiose	0.15	0.10	<0.001
Phenylethylamine	0.15	0.10	0.002
Glycyl-L-Glutamic Acid	0.15	0.10	0.002
L-Threonine	0.15	0.08	0.003
2-Aminoethanol	0.15	0.10	<0.001
L-Serine	0.15	0.09	0.003
D-Galacturonic Acid	0.15	0.11	0.006
4-Hydroxy Benzoic Acid	0.15	0.10	0.004

1,2-Propanediol	0.15	0.10	<0.001
Sucrose	0.15	0.10	0.022
m-Hydroxy Phenyl Acetic Acid	0.14	0.10	0.002
D-Alanine	0.14	0.11	0.004
L-Pyroglutamic Acid	0.14	0.11	0.027
D-Gluconic Acid	0.14	0.11	0.007
L-Histidine	0.14	0.08	<0.001
D-Aspartic Acid	0.14	0.09	<0.001
alpha-Hydroxy Butyric Acid	0.14	0.08	<0.001
D-Lactic Acid Methyl Ester	0.14	0.09	0.005
L-Arginine	0.14	0.09	0.012
Laminarin	0.14	0.12	0.013
i-Erythritol	0.14	0.11	0.225
Alpha-Keto-Glutaric Acid	0.14	0.09	<0.001
L-Glutamic Acid	0.14	0.10	0.002
D-Serine	0.14	0.10	<0.001
D-Threonine	0.14	0.08	0.006
Glycine	0.14	0.11	0.015
Formic Acid	0.13	0.09	<0.001
Mono Methyl Succinate	0.13	0.08	0.001
Hydroxy-L Prline	0.13	0.08	<0.001
D-Mannitol	0.13	0.09	0.001
L-Phenylalanine	0.13	0.09	0.007
D-Glucose-1-Phosphate	0.13	0.09	0.003
Beta-Hydroxy Butyric Acid	0.13	0.08	0.011
D,L-Carnitine	0.13	0.09	0.012
Itaconic Acid	0.13	0.09	0.050
Citraconic Acid	0.13	0.08	<0.001
Apha-Hydroxy Glutaric Acid-gamma-lactone	0.13	0.08	<0.001
L-Homoserine	0.13	0.08	<0.001
2-Hydroxy Benzoic Acid	0.13	0.08	0.010
Fumaric Acid	0.13	0.08	0.001
Citric Acid	0.13	0.09	0.007
Succinamic Acid	0.13	0.08	0.002
L-Glutamine	0.13	0.09	0.002
N-Acetyl-L-Glutamic Acid	0.13	0.08	<0.001

Tricarballylic Acid	0.13	0.08	<0.001
Tyramine	0.13	0.19	0.552
Delta-Amino Valeric Acid	0.13	0.09	0.011
Bromo Succinic Acid	0.13	0.08	0.001
Quinic Acid	0.12	0.08	0.004
D-Tartaric Acid	0.12	0.08	0.010
L-Tartaric Acid	0.12	0.08	0.001
D-Malic Acid	0.12	0.08	0.005
gamma-Amino Butyric Acid	0.12	0.08	0.004
L-Malic Acid	0.12	0.08	0.001
D,L-Malic Acid	0.12	0.09	0.001
Glycolic Acid	0.12	0.08	<0.001
Glycolic Acid	0.12	0.08	0.015
Citramalic Acid	0.11	0.08	0.003
Malonic Acide	0.11	0.08	0.003
m-Tartaric Acid	0.11	0.08	0.004
D-Ribono-1,4-Lactone	0.11	0.08	0.015

REFERENCES

1. Huang C, Lu TL, Yang Y. Mortality risk factors related to listeriosis — A meta-analysis. Journal of Infection and Public Health. 2023 May 1;16(5):771–83.

2. McCollum JT, Cronquist AB, Silk BJ, Jackson KA, O'Connor KA, Cosgrove S, et al. Multistate Outbreak of Listeriosis Associated with Cantaloupe. N Engl J Med. 2013 Sep 5;369(10):944–53.

3. Hamon M, Bierne H, Cossart P. Listeria monocytogenes: a multifaceted model. Nat Rev Microbiol. 2006 Jun 1;4(6):423–34.

4. Goetz M, Bubert A, Wang G, Chico-Calero I, Vazquez-Boland JA, Beck M, et al. Microinjection and growth of bacteria in the cytosol of mammalian host cells. Proc Natl Acad Sci USA. 2001 Oct 9;98(21):12221–6.

5. Creasey EA, Isberg RR. The protein SdhA maintains the integrity of the *Legionella* -containing vacuole. Proc Natl Acad Sci USA. 2012 Feb 28;109(9):3481–6.

6. Zhao Q, Hu P, Li Q, Zhang S, Li H, Chang J, et al. Prevalence and transmission characteristics of *Listeria* species from ruminants in farm and slaughtering environments in China. Emerging Microbes & Infections. 2021 Jan 1;10(1):356–64.

7. Lamason RL, Bastounis E, Kafai NM, Serrano R, Del Álamo JC, Theriot JA, et al. Rickettsia Sca4 Reduces Vinculin-Mediated Intercellular Tension to Promote Spread. Cell. 2016 Oct;167(3):670-683.e10.

8. Gehre L, Gorgette O, Perrinet S, Prevost MC, Ducatez M, Giebel AM, et al. Sequestration of host metabolism by an intracellular pathogen. eLife. 2016 Mar 16;5:e12552.

9. Bruno JC, Freitag NE. Constitutive Activation of PrfA Tilts the Balance of Listeria monocytogenes Fitness Towards Life within the Host versus Environmental Survival. Ii RMR, editor. PLoS ONE. 2010 Dec 7;5(12):e15138.

10. Scortti M, Monzó HJ, Lacharme-Lora L, Lewis DA, Vázquez-Boland JA. The PrfA virulence regulon. Microbes and Infection. 2007 Aug;9(10):1196–207.

11. Beauregard KE, Lee KD, Collier RJ, Swanson JA. pH-dependent Perforation of Macrophage Phagosomes by Listeriolysin O from *Listeria monocytogenes*. The Journal of Experimental Medicine. 1997 Oct 6;186(7):1159–63.

12. Mengaud J, Chenevert J, Geoffroy C, Gaillard JL. Identification of the Structural Gene Encoding the SH-Activated Hemolysin of Listeria monocytogenes: Listeriolysin 0 Is Homologous to Streptolysin 0 and Pneumolysin.

13. Seveau S. Multifaceted Activity of Listeriolysin O, the Cholesterol-Dependent Cytolysin of Listeria monocytogenes. In: Anderluh G, Gilbert R, editors. MACPF/CDC Proteins - Agents of Defence, Attack and Invasion [Internet]. Dordrecht: Springer Netherlands; 2014 [cited 2025 Apr 5]. p. 161–95. (Subcellular Biochemistry; vol. 80). Available from: https://link.springer.com/10.1007/978-94-017-8881-6_9

14. Chico-Calero I, Suárez M, González-Zorn B, Scortti M, Slaghuis J, Goebel W, et al. Hpt, a bacterial homolog of the microsomal glucose- 6-phosphate translocase, mediates rapid intracellular proliferation in Listeria. Proc Natl Acad Sci USA. 2002 Jan 8;99(1):431–6.

15. Kocks C, Gouin E, Tabouret M, Berche P, Ohayon H, Cossart P. L. monocytogenes-induced actin assembly requires the actA gene product, a surface protein. Cell. 1992 Feb;68(3):521–31.

16. Mitchell G, Ge L, Huang Q, Chen C, Kianian S, Roberts MF, et al. Avoidance of Autophagy Mediated by PlcA or ActA Is Required for Listeria monocytogenes Growth in Macrophages. Roy CR, editor. Infect Immun. 2015 May;83(5):2175–84.

17. Chen GY, Pensinger DA, Sauer JD. *Listeria monocytogenes* cytosolic metabolism promotes replication, survival, and evasion of innate immunity. Cellular Microbiology. 2017 Oct;19(10):e12762.

18. Mitchell G, Cheng MI, Chen C, Nguyen BN, Whiteley AT, Kianian S, et al. *Listeria monocytogenes* triggers noncanonical autophagy upon phagocytosis, but avoids subsequent growth-restricting xenophagy. Proc Natl Acad Sci USA [Internet]. 2018 Jan 9 [cited 2022 Jun 2];115(2). Available from: https://pnas.org/doi/full/10.1073/pnas.1716055115

19. Bielecki J, Youngman P, Connelly P, Portnoy DA. Bacillus subtilis expressing a haemolysin gene from Listeria monocytogenes can grow in mammalian cells. Nature. 1990 May;345(6271):175–6.

20. Chen GY, McDougal CE, D'Antonio MA, Portman JL, Sauer JD. A Genetic Screen Reveals that Synthesis of 1,4-Dihydroxy-2-Naphthoate (DHNA), but Not Full-Length Menaquinone, Is Required for *Listeria monocytogenes* Cytosolic Survival. Swanson MS, editor. mBio [Internet]. 2017 May 3 [cited 2021 Dec 14];8(2). Available from: https://journals.asm.org/doi/10.1128/mBio.00119-17

21. Smith HB, Li TL. Listeria monocytogenes MenI Encodes a DHNA-CoA Thioesterase Necessary for Menaquinone Biosynthesis, Cytosolic Survival, and Virulence. Infection and Immunity. 2021;89(5):12.

22. Smith HB, Lee K, Freeman MJ, Stevenson DM, Amador-Noguez D, Sauer JD. Listeria monocytogenes requires DHNA-dependent intracellular redox homeostasis facilitated by Ndh2 for survival and virulence. Infection and Immunity. 2023;91(10):e00022-23.

23. Rivera-Lugo R, Deng D, Anaya-Sanchez A, Tejedor-Sanz S, Tang E, Reyes Ruiz VM, et al. Listeria monocytogenes requires cellular respiration for NAD+ regeneration and pathogenesis. eLife. 2022 Apr 5;11:e75424.

24. Patel MS, Nemeria NS, Furey W, Jordan F. The Pyruvate Dehydrogenase Complexes: Structure-based Function and Regulation. Journal of Biological Chemistry. 2014 Jun;289(24):16615–23.

25. White D, Drummond JT, Fuqua C. The Physiology and Biochemistry of Prokaryotes [Internet]. Oxford University Press; 2012. Available from: https://books.google.com/books?id=ToF6pwAACAAJ

26. Kim Y, Ingram LO, Shanmugam KT. Dihydrolipoamide Dehydrogenase Mutation Alters the NADH Sensitivity of Pyruvate Dehydrogenase Complex of *Escherichia coli* K-12. J Bacteriol. 2008 Jun;190(11):3851–8.

27. Soares Da Costa TP, Nanson JD, Forwood JK. Structural characterisation of the fatty acid biosynthesis enzyme FabF from the pathogen Listeria monocytogenes. Sci Rep. 2017 Jan 3;7(1):39277.

28. Whiteley AT, Garelis NE, Peterson BN, Choi PH, Tong L, Woodward JJ, et al. c -di- AMP modulates *L isteria monocytogenes* central metabolism to regulate growth, antibiotic resistance and osmoregulation. Molecular Microbiology. 2017 Apr;104(2):212–33.

29. Freeman MJ, Sauer JD. Listeria monocytogenes Requires Phosphotransferase Systems to Facilitate Intracellular Growth and Virulence. bioRxiv. 2024 Jan 1;2024.08.12.607557.

30. Choe M, Park YH, Lee CR, Kim YR, Seok YJ. The general PTS component HPr determines the preference for glucose over mannitol. Sci Rep. 2017 Feb 22;7(1):43431.

31. McCoy JG, Levin EJ, Zhou M. Structural insight into the PTS sugar transporter EIIC. Biochimica et Biophysica Acta (BBA) - General Subjects. 2015 Mar;1850(3):577–85.

32. Stoll R, Goebel W. The major PEP-phosphotransferase systems (PTSs) for glucose, mannose and cellobiose of Listeria monocytogenes, and their significance for extra- and intracellular growth. Microbiology. 2010 Apr 1;156(4):1069–83.

33. Barabote RD, Saier MH. Comparative Genomic Analyses of the Bacterial Phosphotransferase System. Microbiol Mol Biol Rev. 2005 Dec;69(4):608–34.

34. Roseman S, Meadow ND, Kukuruzinska MA. [69] General description and assay principles. In: Wood WA, editor. Methods in Enzymology [Internet]. Academic Press; 1982. p. 417–23. Available from: https://www.sciencedirect.com/science/article/pii/S0076687982901653

35. Kim HJ, Jeong H, Lee SJ. Short-Term Adaptation Modulates Anaerobic Metabolic Flux to Succinate by Activating ExuT, a Novel D-Glucose Transporter in Escherichia coli. Front Microbiol. 2020 Jan 23;11:27.

36. Best A, Abu Kwaik Y. Nutrition and Bipartite Metabolism of Intracellular Pathogens. Trends in Microbiology. 2019 Jun 1;27(6):550–61.

37. Grubmuller S, Schauer K, Goebel W, Fuchs TM, Eisenreich W. Analysis of carbon substrates used by Listeria monocytogenes during growth in J774A.1 macrophages suggests a bipartite intracellular metabolism. Front Cell Infect Microbiol [Internet]. 2014 Nov 3 [cited 2022 Jun 2];4. Available from: http://journal.frontiersin.org/article/10.3389/fcimb.2014.00156/abstract

38. Halsey CR, Glover RC, Thomason MK, Reniere ML. The redox-responsive transcriptional regulator Rex represses fermentative metabolism and is required for Listeria monocytogenes pathogenesis. O'Riordan M, editor. PLoS Pathog. 2021 Aug 16;17(8):e1009379.

39. Trojan D, García-Robledo E, Hausmann B, Revsbech NP, Woebken D, Eichorst SA. A respiro-fermentative strategy to survive nanoxia in *Acidobacterium capsulatum*. FEMS Microbiology Ecology. 2024 Nov 23;100(12):fiae152.

40. Fuentes DAF, Manfredi P, Jenal U, Zampieri M. Pareto optimality between growth-rate and lag-time couples metabolic noise to phenotypic heterogeneity in Escherichia coli. Nat Commun. 2021 May 28;12(1):3204.

41. Sanman LE, Qian Y, Eisele NA, Ng TM, van der Linden WA, Monack DM, et al. Disruption of glycolytic flux is a signal for inflammasome signaling and pyroptotic cell death. eLife. 2016 Mar 24;5:e13663.

42. Wynosky-Dolfi MA, Snyder AG, Philip NH, Doonan PJ, Poffenberger MC, Avizonis D, et al. Oxidative metabolism enables Salmonella evasion of the NLRP3 inflammasome. Journal of Experimental Medicine. 2014 Apr 7;211(4):653–68.

43. Tucey TM, Verma J, Harrison PF, Snelgrove SL, Lo TL, Scherer AK, et al. Glucose Homeostasis Is Important for Immune Cell Viability during Candida Challenge and Host Survival of Systemic Fungal Infection. Cell Metabolism. 2018 May;27(5):988-1006.e7.

44. Borisov VB, Forte E. Bioenergetics and Reactive Nitrogen Species in Bacteria. IJMS. 2022 Jun 30;23(13):7321.

45. Fang FC, Vázquez-Torres A. Reactive nitrogen species in host–bacterial interactions. Current Opinion in Immunology. 2019 Oct;60:96–102.

46. Craig M, Sadik AY, Golubeva YA, Tidhar A, Slauch JM. Twin-arginine translocation system (*TAT*) mutants of *S almonella* are attenuated due to envelope defects, not respiratory defects. Molecular Microbiology. 2013 Sep;89(5):887–902.

47. Srivastav S, Biswas A, Anand A. Interplay of niche and respiratory network in shaping bacterial colonization. Journal of Biological Chemistry. 2025 Jan 1;301(1):108052.

48. Hammer ND, Reniere ML, Cassat JE, Zhang Y, Hirsch AO, Indriati Hood M, et al. Two Heme-Dependent Terminal Oxidases Power Staphylococcus aureus Organ-Specific Colonization of the Vertebrate Host. Gilmore MS, editor. mBio. 2013 Aug 30;4(4):e00241-13.

49. Proctor R. Respiration and Small Colony Variants of *Staphylococcus aureus*. Fischetti VA, Novick RP, Ferretti JJ, Portnoy DA, Braunstein M, Rood JI, editors. Microbiol Spectr. 2019 May 31;7(3):7.3.22.

50. Jones-Carson J, Husain M, Liu L, Orlicky DJ, Vázquez-Torres A. Cytochrome *bd* -Dependent Bioenergetics and Antinitrosative Defenses in *Salmonella* Pathogenesis. Freitag NE, editor. mBio. 2016 Dec 30;7(6):e02052-16.

51. Light SH, Méheust R, Ferrell JL, Cho J, Deng D, Agostoni M, et al. Extracellular electron transfer powers flavinylated extracellular reductases in Gram-positive bacteria. Proc Natl Acad Sci USA. 2019 Dec 26;116(52):26892–9.

52. Corbett D, Goldrick M, Fernandes VE, Davidge K, Poole RK, Andrew PW, et al. Listeria monocytogenes Has Both Cytochrome *bd* -Type and Cytochrome aa_3 -Type Terminal Oxidases, Which Allow Growth at Different Oxygen Levels, and Both Are Important in Infection. Freitag NE, editor. Infect Immun. 2017 Nov;85(11):e00354-17.

53. Trivett TL, Meyer EA. Citrate Cycle and Related Metabolism of *Listeria monocytogenes*. J Bacteriol. 1971 Sep;107(3):770–9.

54. Zheng Y, Ko TP, Sun H, Huang CH, Pei J, Qiu R, et al. Distinct structural features of Rex-family repressors to sense redox levels in anaerobes and aerobes. Journal of Structural Biology. 2014 Dec 1;188(3):195–204.

55. Bitoun JP, Wen ZT. Transcription factor R ex in regulation of pathophysiology in oral pathogens. Molecular Oral Microbiology. 2016 Apr;31(2):115–24.

56. Kader Chowdhury QMM, Islam S, Narayanan L, Ogunleye SC, Wang S, Thu D, et al. An insight into the role of branched-chain α-keto acid dehydrogenase (BKD) complex in branched-chain fatty acid biosynthesis and virulence of *Listeria monocytogenes*. Federle MJ, editor. J Bacteriol. 2024 Jul 25;206(7):e00033-24.

57. Sun Y, O'Riordan MXD. Branched-Chain Fatty Acids Promote *Listeria monocytogenes* Intracellular Infection and Virulence. Infect Immun. 2010 Nov;78(11):4667–73.

58. Fischer M, Engelgeh T, Rothe P, Fuchs S, Thürmer A, Halbedel S. Listeria monocytogenes gene essentiality under laboratory conditions and during macrophage infection. bioRxiv. 2022 Jan 1;2022.03.04.482958.

59. Price JV, Vance RE. The Macrophage Paradox. Immunity. 2014 Nov;41(5):685–93.

60. Stritzker J, Janda J, Schoen C, Taupp M, Pilgrim S, Gentschev I, et al. Growth, Virulence, and Immunogenicity of *Listeria monocytogenes aro* Mutants. Infect Immun. 2004 Oct;72(10):5622–9.

61. Aké FMD, Joyet P, Deutscher J, Milohanic E. Mutational analysis of glucose transport regulation and glucose-mediated virulence gene repression in *Listeria monocytogenes*. Molecular Microbiology. 2011 Jul;81(1):274–93.

62. Vehkala M, Shubin M, Connor TR, Thomson NR, Corander J. Novel R Pipeline for Analyzing Biolog Phenotypic Microarray Data. Aziz RK, editor. PLoS ONE. 2015 Mar 18;10(3):e0118392.

63. Jumper J, Evans R, Pritzel A, Green T, Figurnov M, Ronneberger O, et al. Highly accurate protein structure prediction with AlphaFold. Nature. 2021 Aug 26;596(7873):583–9.

64. Stokes JM, Lopatkin AJ, Lobritz MA, Collins JJ. Bacterial Metabolism and Antibiotic Efficacy. Cell Metabolism. 2019 Aug;30(2):251–9.

65. Cossart P. Illuminating the landscape of host–pathogen interactions with the bacterium *Listeria monocytogenes*. Proc Natl Acad Sci USA. 2011 Dec 6;108(49):19484–91.

66. Bhagwat A, Haldar T, Kanojiya P, Saroj SD. Bacterial metabolism in the host and its association with virulence. Virulence. 2025 Dec 31;16(1):2459336.

67. Radhakrishnan P, Theriot JA. *Listeria monocytogenes* cell-to-cell spread bypasses nutrient limitation for replicating intracellular bacteria [Internet]. 2025 [cited 2025 Apr 5]. Available from: http://biorxiv.org/lookup/doi/10.1101/2025.01.31.635960

68. Shi W, Cassmann TJ, Bhagwate AV, Hitosugi T, Ip WKE. Lactic acid induces transcriptional repression of macrophage inflammatory response via histone acetylation. Cell Reports. 2024 Feb 27;43(2):113746.

69. Wang X, Yang B, Ma S, Yan X, Ma S, Sun H, et al. Lactate promotes *Salmonella* intracellular replication and systemic infection via driving macrophage M2 polarization. Gao B, editor. Microbiol Spectr. 2023 Dec 12;11(6):e02253-23.

70. Machado MG, Patente TA, Rouillé Y, Heumel S, Melo EM, Deruyter L, et al. Acetate Improves the Killing of Streptococcus pneumoniae by Alveolar Macrophages via NLRP3 Inflammasome and Glycolysis-HIF-1α Axis. Front Immunol. 2022 Jan 20;13:773261.

71. Li N, Gong Y, Zhu Y, Li B, Wang C, Wang Z, et al. Exogenous acetate attenuates inflammatory responses through HIF-1α-dependent glycolysis regulation in macrophage. Cell Mol Life Sci. 2024 Dec 27;82(1):21.

72. Sauer JD, Herskovits AA, O'Riordan MXD. Metabolism of the Gram-Positive Bacterial Pathogen *Listeria monocytogenes*. Fischetti VA, Novick RP, Ferretti JJ, Portnoy DA, Braunstein M, Rood JI, editors. Microbiol Spectr. 2019 Jul 19;7(4):7.4.26.

73. Lauer P, Chow MYN, Loessner MJ, Portnoy DA, Calendar R. Construction, Characterization, and Use of Two Listeria monocytogenes Site-Specific Phage Integration Vectors. J BACTERIOL. 2002;184.

74. Sauer JD, Sotelo-Troha K, Von Moltke J, Monroe KM, Rae CS, Brubaker SW, et al. The *N* -Ethyl- *N* -Nitrosourea-Induced *Goldenticket* Mouse Mutant Reveals an Essential Function of *Sting* in the *In Vivo* Interferon Response to *Listeria monocytogenes* and Cyclic Dinucleotides. Flynn JL, editor. Infect Immun. 2011 Feb;79(2):688–94.

75. Shetron-Rama LM, Mueller K, Bravo JM, Bouwer HGA, Way SS, Freitag NE. Isolation of *Listeria monocytogenes* mutants with high-level *in vitro* expression of host cytosol-induced gene products. Molecular Microbiology. 2003 Jun;48(6):1537–51.

76. Chen GY, Kao CY, Smith HB, Rust DP, Powers ZM, Li AY, et al. Mutation of the Transcriptional Regulator YtoI Rescues Listeria monocytogenes Mutants Deficient in the

Essential Shared Metabolite 1,4-Dihydroxy-2-Naphthoate (DHNA). Freitag NE, editor. Infect Immun. 2019 Dec 17;88(1):e00366-19.

77. Sun AN, Camilli A, Portnoy DA. Isolation of Listeria monocytogenes small-plaque mutants defective for intracellular growth and cell-to-cell spread. Infect Immun. 1990 Nov;58(11):3770–8.

78. Luque-Sastre L, Jordan K, Fanning S, Fox EM. High-Throughput Characterization of Listeria monocytogenes Using the OmniLog Phenotypic Microarray. In: Fox EM, Bierne H, Stessl B, editors. Listeria Monocytogenes: Methods and Protocols [Internet]. New York, NY: Springer US; 2021. p. 107–13. Available from: https://doi.org/10.1007/978-1-0716-0982-8_8

79. Fernandez NF, Gundersen GW, Rahman A, Grimes ML, Rikova K, Hornbeck P, et al. Clustergrammer, a web-based heatmap visualization and analysis tool for high-dimensional biological data. Sci Data. 2017 Oct 10;4(1):170151.

80. Bécavin C, Bouchier C, Lechat P, Archambaud C, Creno S, Gouin E, et al. Comparison of Widely Used Listeria monocytogenes Strains EGD, 10403S, and EGD-e Highlights Genomic Differences Underlying Variations in Pathogenicity. Casadevall A, editor. mBio. 2014 May;5(2):e00969-14.

CHAPTER 4: Conclusions and future directions.

Authors and their contributions:

Matthew J. Freeman: Planned, organized, and wrote this manuscript

John-Demian Sauer: Supervised writing and editing of this manuscript

*ChatGPT-4o was used for copy editing of my original ideas and writings using the prompt: “Can you copy edit part of my thesis to use correct scientific nomenclature and formatting while improving flow?”

OVERVIEW

Intracellular pathogens are specifically and exquisitely adapted to survive and replicate within distinct host cell niches (1–3). Among this broad class of bacterial pathogens, a smaller subset has evolved to utilize the host cell cytosol as a primary replicative niche (2,4,5). However, the cytosol is a restrictive environment that imposes unique pressures, requiring specialized bacterial adaptations for survival and replication (2,4). *Listeria monocytogenes* is one such pathogen capable of entering the cytosol and withstanding the defense mechanisms and metabolic constraints imposed by host cells (3,6–8). This capacity has established *L. monocytogenes* as both a clinically significant pathogen and a valuable model organism for studying cytosolic bacterial pathogenesis (9).

Understanding the strategies employed by *L. monocytogenes* to persist and proliferate within the cytosol is critical, as these insights can inform the development of novel antimicrobial therapies targeting *L. monocytogenes* and other intracellular pathogens (9). While numerous factors contribute to cytosolic pathogenesis, components of central metabolism—particularly those governing carbon acquisition and utilization—are increasingly recognized as key virulence determinants (1,8,10–12). This growing appreciation has led to the broader conclusion that bacterial metabolism not only reveals vulnerabilities for therapeutic intervention but also offers a lens through which to interrogate host defenses and responses (13,14).

The research presented in this thesis aims to define the metabolic strategies employed by *L. monocytogenes* to support cytosolic survival and replication. In Chapter 2, I characterize the genetic determinants of what have long been considered the primary cytosolic carbon sources for *L. monocytogenes (1,15,16)*. Through a comprehensive genetic analysis, we demonstrate that

previous assumptions regarding the central role of hexose phosphates and glycerol during infection were overstated (11,12,16–18). While these carbon sources do contribute to *in vivo* pathogenesis, mutants deficient in their acquisition and utilization retain substantial intracellular growth and virulence (16).

Instead, we identify phosphotransferase systems (PTS) as primary drivers of carbon acquisition and virulence during cytosolic infection (16). Notably, our data reveal that *L. monocytogenes* employs a previously underappreciated diversity of carbon transport systems within the host cytosol. These systems not only contribute to metabolic flexibility but also significantly influence virulence gene expression—though in ways that differ from prior models (12,16,19). Taken together, our findings establish PTS transporters as essential virulence factors supporting cytosolic carbon acquisition by *L. monocytogenes (16)*. This work offers a foundational framework for understanding cytosolic carbon metabolism, though many questions remain about which systems are indispensable for virulence: what host-derived carbon sources are being utilized, and how host cells respond to metabolic perturbation by bacterial mutants?

In Chapter 3, we investigate the role of the pyruvate dehydrogenase (PDH) complex in *L. monocytogenes* virulence. Consistent with previous work from our laboratory, we confirm that disruption of any single PDH complex component results in significant attenuation of virulence and an inability to replicate in the host cytosol (8). Using unbiased metabolite screening and metabolomic profiling, we find that PDH complex mutants are markedly deficient in upper glycolytic and tricarboxylic acid (TCA) cycle intermediates. Additionally, these mutants exhibit altered respiro-fermentative metabolism, marked by a shift in fermentation end products from acetate to lactate.

These findings led us to hypothesize—and subsequently demonstrate—that PDH complex mutants are impaired in their ability to utilize PTS-transported carbon sources. Leveraging this insight, we employed an unbiased genetic screen to isolate suppressor mutations that restore the growth of PDH-deficient strains on fructose, a PTS-dependent carbon source, in defined media. All suppressor mutations were identified as deleterious alleles in *rex*, which encodes a redox-sensing transcriptional repressor. We show that Rex normally represses fermentative pathways, and that its loss relieves this repression in PDH mutants, thereby enabling fermentation of PTS-transported sugars.

Remarkably, these *rex* suppressor mutants not only restored growth on fructose *in vitro*, but also rescued intracellular replication during macrophage infection. However, these suppressors did not restore full *in vivo* virulence, indicating that additional factors contribute to the attenuation observed in PDH complex mutants during infection. These findings suggest the need for further investigation into the metabolic and regulatory mechanisms underpinning *L. monocytogenes* virulence in host tissues.

Defining macrophage responses to carbon utilization by *L. monocytogenes*

An emerging concept in the study of host–pathogen interactions is that shared metabolic interdependencies may serve as a mechanism by which host cells detect bacterial invaders (8,13,14,20). Conversely, bacterial pathogens may sense host cell metabolism as an environmental cue to regulate distinct stages of infection (18,21,22). Even in the absence of direct host cell sensing of bacterial metabolism, increasing evidence suggests that during physiological infections, pathogens and host cells compete for nutrient sources to support their

respective metabolic demands (20). Therefore, the area of shared host-pathogen metabolism deserves further study to characterize these previously underappreciated interactions.

It is well established that pathogenic bacteria must possess highly evolved and adaptable metabolic strategies to survive and replicate within specific host niches (1,23). In Chapter 2 of this thesis, we advance the current understanding of cytosolic metabolism in *Listeria monocytogenes*. We demonstrate that hexose phosphates and glycerol contribute only marginally to the intracellular metabolic needs of *L. monocytogenes*, whereas phosphotransferase (PTS)-mediated carbon sources constitute a major component of its cytosolic metabolism (16). The identification of these preferred metabolic inputs, along with the development of corresponding mutant strains, now enables deeper exploration into the shared metabolic landscape between macrophages and *L. monocytogenes*.

With this foundation, we can begin to address a central question: Why do *L. monocytogenes* and many other intracellular bacterial pathogens engage in multipronged metabolic strategies during infection (1)? We hypothesize that this approach enables intracellular pathogens to evade host detection by diversifying their carbon source consumption, thereby minimizing perturbations to any single host metabolic pathway. If this is correct, it raises the question of how host cells detect and respond to bacterial carbon acquisition. Using *L. monocytogenes* and the metabolic mutant strains developed in Chapter 2, we can begin to investigate this phenomenon experimentally.

One way to conceptualize the potential for host detection is through metabolic burden estimates. For example, it has been calculated that producing a single daughter cell of *Escherichia coli* requires approximately 8×10^9 ATP molecules (24). If we assume *L.*

monocytogenes requires a similar energetic investment, then generating 50–100 daughter cells per infected macrophage would necessitate ~4×10^{11} ATP (25). To meet this demand solely through glucose metabolism, *L. monocytogenes* would need to consume a volume of glucose that, in theory, could fill the entire cytosolic space of a macrophage—assuming no concurrent glucose consumption by the host cell itself (26). This rudimentary calculation alone highlights the considerable metabolic burden imposed by cytosolic bacterial replication. Coupled with published data showing that macrophages can detect and respond to nutrient deprivation induced by cytosolic pathogens, these observations underscore the importance of understanding how macrophages respond to metabolically disruptive infections by *L. monocytogenes (13)*. To fully elucidate how macrophages *ex vivo* may respond to bacterial metabolism, it is essential to employ models that are more physiologically relevant than those currently used in this thesis and more broadly in the literature. Unfortunately, evaluating host cell responses *in vivo* remains challenging due to difficulties in harvesting infected cells and conducting analyses like metabolomics and RNA-seq on the appropriate timescale.

A major advancement toward physiologic modeling in recent years has been the development of Human Plasma-Like Medium (HPLM) (27–29). Culturing immune cells in HPLM has been shown to significantly alter cellular metabolism, immune responsiveness, and intracellular bacterial metabolism (28,30). Thus, to evaluate macrophage responses to metabolically perturbed *Listeria monocytogenes*, one could isolate bone marrow-derived macrophages (BMDMs) from C57BL/6 mice and differentiate them in HPLM. This approach would maintain macrophages under more physiological conditions during their differentiation and subsequent exposure to *L. monocytogenes*.

Under such conditions, the metabolic burden imposed by *L. monocytogenes*' cytosolic replication may become sufficient to elicit detectable host responses. For these experiments, macrophages could be infected with various metabolic mutants: strains deficient in hexose phosphate acquisition (Δ*uhpT*), glycerol utilization (Δ*glpD*/Δ*golD*), or both (Δ*glpD*/Δ*golD*/Δ*uhpT*), as well as mutants impaired in phosphoenolpyruvate-dependent phosphotransferase system (PTS)-mediated carbon uptake (Δ*ptsI*). A wild-type *L. monocytogenes* strain would serve as a baseline control to determine whether host responses are specifically triggered by metabolic perturbation or WT carbon acquisition. Notably, a mutant defective in PTS-mediated carbon uptake has been shown to be effectively metabolically inert as evidence by lack of cytosolic growth, and such a strain would serve as a valuable control to assess host responses to non-replicating bacteria (16).

Given that the specific PTS-imported carbon sources of *L. monocytogenes* remain incompletely defined, one could prevent cytosolic bacterial metabolism by treating WT *L. monocytogenes* with irreversible glycolytic inhibitors, such as 3-bromopyruvate (31). This compound targets multiple glycolytic enzymes—including hexokinase, glycerol-3-phosphate dehydrogenase, and lactate dehydrogenase—and may effectively suppress bacterial central metabolism (31). Alternatively, a phosphofructokinase (PFK) knockout strain could be constructed; however, transposon mutagenesis screens have identified housekeeping PFK as essential in *L. monocytogenes* (32). Therefore, such a mutant may require an inducible expression system to support bacterial growth *in vitro* prior to infection, followed by withdrawal of the inducer (e.g., IPTG) to abrogate PFK expression within the host cytosol (33).

A key assumption underlying this strategy is that glycolytic flux is not maintained through alternative pathways such as through 1-phosphofructokinases, which can convert fructose-1-phosphate to fructose-1,6-bisphosphate after fructose uptake via PTS (25). Each of these proposed metabolic mutants would rely on distinct categories of carbon sources, thereby enabling us to directly test the hypothesis that *L. monocytogenes* employs metabolic diversity to avoid host cell detection.

However, even under more physiological conditions afforded by HPLM, host cells may still not experience the same degree of starvation stress as they would *in vivo*. To further sensitize macrophages, one could replace HPLM post-infection with glucose-deficient media or treat cells with upper glycolytic inhibitors such as 2-deoxy-D-glucose (2-DG), which inhibits hexokinase (34). Importantly, 2-DG should selectively inhibit host glycolysis, as *L. monocytogenes* can utilize glycerol (downstream of hexokinase), glucose-6-phosphate (bypassing hexokinase), or PTS-imported sugars (phosphorylated independently of hexokinase) (11,15,25,35). Literature evidence supports this approach, showing that 2-DG-induced metabolic stress enhances host resistance to *L. monocytogenes* infection in mice (36).

To evaluate how macrophages respond to cytosolic *L. monocytogenes* under these metabolic stress conditions, several assays should be employed. First, unbiased approaches such as transcriptomic profiling (RNA-seq) could reveal global gene expression changes in infected macrophages. Additionally, cytokine production in culture supernatants could be assessed using multiplex cytokine bead arrays. These analyses may uncover host defense or cell death pathways activated in response to metabolically perturbed *L. monocytogenes*.

Given previous studies from the Bogyo and Brodsky labs, which demonstrate that metabolic stress from cytosolic bacterial replication can induce inflammasome-dependent cell death, it is reasonable to suspect pyroptotic death in the context of infection with metabolically perturbed *L. monocytogenes (13,14)*. To test this, infected cells could be assayed for lactate dehydrogenase (LDH) release and propidium iodide uptake over time (37,38). If inflammasome-mediated death is implicated, macrophages from CASPASE-1-deficient mice could be used to determine whether cell death is rescued in the absence of canonical pyroptosis (38).

Bacterial viability could also be measured using bacteriolysis assays previously established in our lab, alongside intracellular growth curves to track pathogen clearance over time (39). Should these experiments demonstrate that metabolic perturbation renders *L. monocytogenes* detectable and eliminable by host macrophages, the findings could be extended *in vivo*. Mice could be infected with the engineered metabolic mutants, with or without 2-DG pre-treatment, and evaluated for IL-1β production (via cytokine bead analysis) and bacterial burden in CASPASE-1-deficient mice.

Taken together, the experiments proposed here—using metabolically perturbed *L. monocytogenes* strains developed in Chapter 2—may illuminate whether host cells can detect and respond to bacterial metabolism under metabolically stressful conditions. Moreover, these studies directly test the hypothesis that *L. monocytogenes* utilizes a diversified carbon acquisition strategy to evade immune detection. Long-term implications of these findings may include new insights into host cell death pathways triggered by metabolic disruption and potential applications for optimizing *L. monocytogenes* as an anti-cancer immunotherapeutic through modulation of host immune memory and response (40).

Defining the role of macrophage polarization in *L. monocytogenes* intracellular growth and pathogenesis

This thesis has primarily focused on how *Listeria monocytogenes* acquires and utilizes carbon within the host cytosol. However, one natural extension of this work—yet still unexplored here—is how host cell metabolic states may influence *L. monocytogenes* intracellular growth and pathogenesis. Within the field of innate immune metabolism, it is well established that macrophages exist along a continuum of polarization, classically described as M1 versus M2 (41). M1 macrophages are typically characterized by heightened glycolytic activity, whereas M2 macrophages rely more heavily on oxidative phosphorylation and mitochondrial metabolism via the tricarboxylic acid (TCA) cycle (42,43).

This polarization is largely governed by cytokine and pathogen-associated molecular pattern (PAMP) signaling (41). M1 polarization is generally induced by stimuli such as lipopolysaccharide (LPS), interferon-γ (IFN-γ), granulocyte-macrophage colony-stimulating factor (GM-CSF), and tumor necrosis factor-α (TNF-α), whereas M2 polarization arises in response to anti-inflammatory cytokines like interleukin-4 (IL-4) and interleukin-13 (IL-13) (42,43). These metabolic states can be hijacked by bacterial pathogens to their advantage, or alternatively, represent a form of host defense against infection (41,44).

Despite the importance of macrophage polarization, it remains unclear whether *L. monocytogenes* preferentially drives or thrives within a particular polarization state, and how this may influence its cytosolic survival. Conflicting evidence exists. For example, in murine models of *L. monocytogenes* infection, macrophages have been reported to polarize predominantly toward an M1 phenotype (45,46). In contrast, work from the Huttenlocher lab at the University

of Wisconsin–Madison has demonstrated that, in zebrafish wound models infected with *L. monocytogenes*, macrophages tend to adopt an M2-like state (47). These results suggest that *L. monocytogenes* can induce both M1 and M2 phenotypes depending on host species, tissue context, bacterial strain, and the surrounding immunological milieu.

Understanding how *L. monocytogenes* interacts with polarized macrophages—and whether it preferentially induces or benefits from one polarization state over another—is essential, particularly given the tissues this pathogen targets. For example, tissue-resident macrophages in the liver (Kupffer cells) and brain (microglia) often exhibit M2-like characteristics under homeostatic conditions (48,49). *L. monocytogenes* is well known to establish necrotic foci within the liver, and these lesions contain both M1- and M2-like macrophages, with M2 macrophages playing a dominant role in tissue repair and resolution of inflammation (3,50). Moreover, some studies suggest that M2-like macrophages may restrict *L. monocytogenes* growth more effectively. This has been observed in Hofbauer cells—placental macrophages with M2-like traits—in which *L. monocytogenes* is significantly impaired in its ability to replicate (51).

Together, these findings raise two unresolved questions relevant to host–pathogen metabolic interplay: (1) What is the dominant polarization state of macrophages *in vivo* during *L. monocytogenes* infection? (2) Does macrophage polarization influence the ability of *L. monocytogenes* to grow and survive?

While defining the dominant *in vivo* macrophage polarization induced by *L. monocytogenes* lies outside the scope of this thesis, it remains an important question for the field (50). However, within the scope of this work is the investigation of how macrophage polarization

influences bacterial intracellular growth and virulence. Chapter 2 of this thesis identifies PTS-mediated carbon sources as critical for *L. monocytogenes* cytosolic growth and full virulence (16). While hexose phosphates and glycerol are minor contributors to virulence, they still play meaningful roles (16). Importantly, M1 and M2 macrophages exhibit distinct profiles of these carbon metabolites (52). M1 macrophages—defined by elevated glycolytic flux—harbor increased levels of free sugars and hexose phosphates, whereas M2 macrophages, driven by mitochondrial and TCA cycle activity, contain relatively fewer upper glycolytic intermediates (52). It is possible, then, that *L. monocytogenes* does not employ a multi-partite metabolism primarily to evade host detection, but instead to enable growth across a range of cell types, including macrophages with distinct metabolic profiles.

Based on this, I hypothesize that M1 macrophages will be more permissive to *L. monocytogenes* mutants deficient in the acquisition and utilization of hexose phosphates and glycerol (Δ*glpD*/Δ*golD*/Δ*uhpT*), as these mutants should still retain access to PTS-derived carbon sources that are enriched in M1-polarized cells (50). Conversely, I expect that these same mutants will be significantly restricted in M2-polarized macrophages, due to limited availability of their preferred carbon substrates. This hypothesis can be directly tested using the metabolic mutants developed in Chapter 2 by infecting M1- or M2-polarized macrophages and assessing bacterial replication, cytosolic lysis, and host cell death (e.g., via LDH release assays). However, this represents only a targeted view of the broader question: what are the genetic determinants that govern *L. monocytogenes* survival in macrophages of different polarization states?

To address this on a larger scale, I propose using transposon insertion sequencing (TIS) to identify genes that are differentially essential in M1 versus M2 macrophages (53). Our lab can

employ established protocols to generate a high-density transposon mutant library using the *Himar1* mariner system (39). This complex library would be used to infect macrophages polarized toward either an M1 or M2 phenotype, at a multiplicity of infection (MOI) ≤1 to avoid phenotypic complementation among mutants within a single cell. After approximately 6 hours of infection, macrophages would be lysed using sterile water to recover viable intracellular bacteria. Recovered mutants would be briefly outgrown in rich medium, followed by genomic DNA isolation, fragmentation, and PCR amplification of transposon-adjacent sequences. Sequencing would be performed using high-throughput platforms such as the NovaSeq 6000 at the UW–Madison Biotechnology Center. TIS outputs from M1- and M2-polarized macrophages would then be compared to the input library and to one another. If the above hypothesis is correct, genes such as *uhpT* (required for hexose phosphate transport) would remain prevalent after passage through M1 macrophages but would be depleted following passage through M2 macrophages. Conversely, genes universally required for cytosolic survival, such as *prfA* (PrfA) and *hly* (LLO), should be depleted in both polarization states but not in the rich medium control. Candidate genes uniquely essential in either M1 or M2 macrophages could be validated via targeted knockouts and functional assays both *ex vivo* and *in vivo*.

Together, the experiments outlined here aim to clarify why *L. monocytogenes* relies on a multi-partite metabolism during cytosolic growth and how macrophage polarization affects its survival. More broadly, they illuminate how host–pathogen metabolic interactions shape intracellular infection outcomes. These findings contribute to the central conceptual aim of this thesis: to understand how hosts and pathogens share metabolic resources, and how perturbation of this shared metabolism alters the landscape of their interactions.

Generation of macrophage cytosol-like media and identification of carbon source and respective PTS used by *L. monocytogenes* in the macrophage cytosol

One of the most challenging yet critical questions that emerges from Chapter 2 of this thesis is: which specific PTS systems are utilized by *Listeria monocytogenes* to support growth in the host cytosol, and what carbon sources are these systems extracting from the host? Early in this work (data not shown), we attempted to address this question using a dual host–pathogen metabolomics approach (54). Macrophages cultured *ex vivo* were infected with *L. monocytogenes*, and after six hours of intracellular replication, the shared host–pathogen metabolome was extracted and analyzed via HPLC–MS. However, these efforts yielded little detectable differential carbon utilization. We suspect this was primarily due to the supraphysiologic conditions of *ex vivo* macrophage culture systems, which allow for near-constant replenishment of depleted metabolites. Furthermore, untargeted metabolomics is intrinsically limited in its ability to distinguish among carbon sources of similar mass and charge (55). As a result, new methods and models are needed to disentangle these complex questions.

Seminal work by the Whiteley lab has demonstrated that *in vivo* models do not always faithfully recapitulate bacterial physiology during infection (56,57). To address this, they developed a method using detailed and iterative omics analyses to characterize bacterial niches and then recreate them *in vitro* using media formulations that mimic the *in vivo* transcriptome of pathogens (56–58). Building upon this approach, Dr. Marvin Whiteley founded a company called Synthbiome (https://www.synthbiome.com), which seeks to commercially develop defined *in vitro* media that simulate host environments.

I propose leveraging this technology to generate a macrophage cytosol-like medium, which could then be used to more precisely identify the carbon sources and transport systems

that *L. monocytogenes* depends on during intracellular growth. Fortunately, the transcriptomic profile of wild-type *L. monocytogenes* during cytosolic growth in macrophages is well defined (59,60). Therefore, using this known bacterial transcriptome as a reference, Synthbiome could perform detailed metabolomic analysis of the macrophage cytosol to inform *in vitro* media design, followed by iterative optimization to mimic the cytosolic environment as closely as possible.

One major advantage of using macrophage cytosol-like media is that it would be fully defined and compositionally static. This enables precise monitoring of metabolite consumption and depletion over time. Once developed, wild-type and metabolically perturbed *L. monocytogenes* strains (characterized in Chapter 2) could be grown in this medium. At mid-log phase, cultures would be centrifuged and filtered to remove bacteria, and the resulting supernatants subjected to HPLC–MS. Because the media composition is defined and stable, both unbiased and targeted metabolomics (using known standards) could be applied to identify carbon sources utilized by wild-type and mutant strains (61).

If successful, a natural extension of this work would be to identify which PTS systems specifically support growth on the relevant carbon sources in this macrophage cytosol-like environment (16). As previously described, one powerful method for this would be transposon insertion sequencing (TIS). A high-density transposon mutant library of wild-type *L. monocytogenes* could be screened for defects in growth in macrophage cytosol-like media—either in its full formulation or in modified versions containing only the most depleted carbon sources identified above (53). From this screen, a set (or sets) of PTS systems essential for growth could be identified. Clean, defined gene deletions in these systems could then be

constructed and evaluated using our lab's well-established *in vitro*, *ex vivo*, and *in vivo* infection models.

In sum, these proposed experiments offer a powerful and unbiased way to define both the carbon sources utilized by *L. monocytogenes* in the macrophage cytosol and the PTS systems responsible for their acquisition**.** Beyond directly answering the questions raised by Chapter 2, the development of macrophage cytosol-like media could revolutionize our broader understanding of *L. monocytogenes* physiology during intracellular infection. These efforts should also be viewed in the context of adjacent sections of this thesis, which explore host cell responses to bacterial metabolism, genetic determinants of survival in polarized macrophages, conditionally essential mutations in metabolic pathways, and potential non-metabolic roles of PTS systems. Many of these features are likely to be interdependent on understanding which carbon sources and transport systems *L. monocytogenes* relies on during infection.

Identification of function of *uhpT* in *L. monocytogenes* pathogenesis

Another challenging but important question arising from Chapter 2 of this thesis concerns the nonessentiality of *uhpT* during *Listeria monocytogenes* growth in the macrophage cytosol—and its only modest role in *in vivo* virulence (11,16,62). Generally, bacterial pathogens are highly evolved to survive and replicate within their host niches, and, in line with the Black Queen Hypothesis, tend toward genome reduction in pursuit of this goal (63). It is therefore striking that *L. monocytogenes* encodes *uhpT*, a gene tightly regulated by PrfA—the master virulence regulator of *Listeria*—yet appears largely dispensable for intracellular growth under the conditions tested (11,16). Further supporting the importance of *uhpT* is its presence in pathogenic *L. monocytogenes* strains, but not in nonpathogenic relatives such as *Listeria innocua*

(64,65). Taken together with our findings that *uhpT* is largely dispensable for cytosolic growth and only modestly impacts *in vivo* infection, this raises a compelling question: why does this finely tuned pathogen maintain a transporter that appears to have limited importance under standard experimental conditions?

I hypothesize that *uhpT* does not contribute meaningfully to steady-state intracellular metabolism but instead serves as a virulence-regulated metabolic "kickstarter"—priming *L. monocytogenes* for subsequent PTS-dependent carbon acquisition. Many bacterial pathogens are known to use different carbon sources at various infection stages (18,66,67). Our data in Chapter 2 illustrate that PTS-mediated carbon uptake is critical for *L. monocytogenes* intracellular replication (16). However, data in Chapter 3 suggest that PTS function depends on the availability of upper glycolytic intermediates, particularly phosphoenolpyruvate (PEP), as a phosphate donor. Therefore, it is possible that *L. monocytogenes* being starved requires carbon uptake to initiate the use of PTS for sustained intracellular growth, possible through *uhpT*.

Notably, most of the models used in this thesis involve infections initiated with *L. monocytogenes* grown in rich, non-physiological conditions—either in nutrient-rich media or in macrophages cultured in supra-physiologic environments. These conditions likely mask the true nutrient limitations encountered during natural infections (68,69). I propose that *uhpT* allows *L. monocytogenes* to import host-derived hexose phosphates early during infection—helping restore glycolytic intermediates (including PEP)—and thereby enabling activation of PTS-mediated carbon uptake. This would explain the gene's conservation, virulence regulation, and context-specific importance, and could resolve the differential phenotypes observed between *ex vivo* and *in vivo* models described in Chapter 2.

To test this hypothesis, I propose an *in vitro* model followed by *in vivo* validation. First, *L. monocytogenes* inocula should be pre-starved of carbon sources to simulate the early metabolic constraints of infection. This can be accomplished by growing strains overnight in defined minimal media containing limiting glucose as the sole carbon source. The ideal glucose concentration can be empirically determined by titrating glucose levels and identifying a threshold where further reduction diminishes growth. After overnight culture to stationary phase under glucose-limited conditions, bacteria should be washed and resuspended in PBS to minimize metabolite carryover. These metabolically deprived cultures can then be used for both *in vitro* growth curves and infection-based assays. To test whether *uhpT* functions as a metabolic kickstarter, metabolically starved *L. monocytogenes* strains constitutively expressing *uhpT* (to bypass PrfA or glutathione regulation) could be inoculated into defined media containing:

- 55 mM fructose (PTS-dependent carbon source)
- 50 mM fructose + 5 mM hexose phosphates (PTS substrate + UhpT substrate)

If *uhpT*-mediated hexose phosphate uptake accelerates the restoration of PEP and glycolytic flux, we would expect a shorter lag phase in the presence of hexose phosphates. Metabolomic profiling could complement these assays by measuring intracellular metabolite restoration over time.

To extend this into a physiologically relevant context, these metabolically starved strains could be used for intravenous or oral infections in wild-type, *uhpT* knockout, and *uhpT*-overexpressing strains. However, intravenous models may not fully recapitulate the metabolic stress encountered during natural infection. Therefore, oral infection models—in which *L.*

monocytogenes must traverse nutrient-limited environments such as the gastrointestinal tract and compete with commensals—may be more appropriate (70).

If *uhpT* serves as a metabolic kickstarter, we would expect a greater attenuation of *uhpT*-deficient strains under these metabolically stressful oral infection conditions, compared to intravenous infection. Finally, this hypothesis could be tested more directly via *in vivo* competition assays, comparing wild-type, *uhpT*-deficient, and *uhpT*-overexpressing strains during oral infection (71). Together, these experiments test one of several hypotheses for why *L. monocytogenes* encodes a transporter for hexose phosphates—despite its apparent dispensability under standard laboratory conditions. These studies may also help explain why *L. monocytogenes* employs a multipartite carbon acquisition strategy: not merely to evade host cell detection, but to maintain metabolic flexibility and readiness during complex, physiologically relevant stages of infection that are not fully recapitulated in the models used throughout this thesis.

Defining *L. monocytogenes'* broken TCA cycle as a metabolic determinant of virulence

One of the key deficits in the pyruvate dehydrogenase complex (PDH) mutants characterized in Chapter 3 of this thesis is their impaired ability to direct carbon from pyruvate into acetyl-CoA and subsequently into the tricarboxylic acid (TCA) cycle. Despite this impairment, it is apparent from our data that some carbon flux into the TCA cycle still occurs. This is evidenced by metabolomic profiling, which detects TCA cycle intermediates—albeit at reduced levels. Additionally, analysis of fermentative byproduct production indicates that *pdhC::Tn* mutants still readily produce acetate, which is derived from the TCA cycle intermediate acetyl-CoA.

Taken together, these findings suggest that although the TCA cycle is still being supplied in PDH mutants, it is relatively starved compared to WT *L. monocytogenes*. This raises the question: what is the actual contribution of the TCA cycle to *L. monocytogenes* virulence? We hypothesize that impaired TCA cycle flux may partially account for the virulence defects observed in PDH mutants. One way to test this hypothesis would be to mutate genes encoding enzymes immediately downstream of PDH in the TCA cycle, such as citrate synthase (*citZ*, LMRG_01400), aconitase (*citB*, LMRG_01325), and isocitrate dehydrogenase kinase/phosphatase (*citC*, LMRG_01401). Deleting these genes in both WT and PDH mutant backgrounds, followed by assessment using our lab's standard virulence assays—including intracellular growth curves, plaque formation, and acute murine infections—would allow us to evaluate how much of the PDH mutant-associated virulence defect is attributable to impaired TCA cycle flux, as opposed to altered fermentation or an inability to utilize PTS-mediated carbon sources.

On a broader scale, the contribution of broken or incomplete TCA cycles to bacterial virulence remains poorly understood. Intriguingly, *L. monocytogenes*—like many other intracellular pathogens—encodes a fragmented TCA cycle (7,8,72–74). We hypothesize that this is an evolutionary adaptation to evade host cell detection (14). Supporting this idea, the Brodsky lab has demonstrated that *Salmonella* tightly regulates its TCA cycle to avoid immune recognition (14). Interestingly, our own data may suggest a similar phenomenon in *L. monocytogenes*: complementation of *pdhC::Tn* with an overexpression construct for *pdhC* does not fully rescue the virulence defect and surprisingly remains attenuated (Chapter 3). This could be due to inappropriate or excessive carbon flux into the TCA cycle—a flux pattern that would not naturally occur in wild-type *L. monocytogenes*.

To test this, I propose two complementary genetic approaches:

1. Overexpression of TCA cycle components in *L. monocytogenes* to assess whether increased flux results in further attenuation due to heightened host immune detection.
2. Reconstitution of a complete TCA cycle in *L. monocytogenes* by expressing the missing enzymes—α-ketoglutarate dehydrogenase, succinyl-CoA synthetase, and malate dehydrogenase—using codon-optimized sequences from the closely related *Bacillus subtilis*. These constructs could be stably expressed under constitutive or inducible promoters.

If the fragmented TCA cycle is indeed an evolutionary adaptation, we would expect that *L. monocytogenes* strains expressing a completed TCA cycle would be broadly attenuated across multiple virulence assays, including intracellular replication, plaque formation, and *in vivo* infection models.

Together, the experiments proposed here could clarify the relative contribution of the TCA cycle to *L. monocytogenes* pathogenesis, as well as the evolutionary rationale behind its incomplete architecture. These studies would also help define the extent to which impaired TCA flux accounts for the virulence defects of PDH complex mutants. Ultimately, understanding this metabolic feature may explain why many other intracellular pathogens also harbor broken TCA cycles—and how such adaptations contribute to their success within host environments.

Characterization the HPr role as a regulator of *L. monocytogenes* pathogenesis

As explored in Appendix 3 of this thesis, HPr functions not only as a component of the phosphotransferase system (PTS) for sugar import, but also as a regulatory factor influencing

multiple aspects of *Listeria monocytogenes* biology and virulence (19,75,76). This regulatory function is distributed across HPr's two phosphorylation sites. The conserved histidine residue is responsible for phosphor-relay activity necessary for sugar uptake and phosphorylation, whereas the serine residue plays a more direct role in gene regulation (25).

Evidence for HPr's regulatory importance comes from the observation that overexpression of HPr is detrimental to plaque formation in both Δ*ptsH* and WT *L. monocytogenes* strains. This toxicity manifests as stationary-phase lysis on agar plates (data not shown), impaired intracellular growth, and reduced plaque-forming ability. The underlying mechanism remains unclear, but it is likely related to disruptions n relative prevelance of phosphorylated and unphosphorylated HPr-Ser. Overexpression may increase both phosphorylated and unphosphorylated HPr-Ser; however, given the limiting availability of phosphate, it is more plausible that the primary effect is an accumulation of unphosphorylated HPr, which may be physiologically disruptive (75,77,78).

This hypothesis is further supported by genetic evidence: attempts to generate a phosphorylation-incompetent HPr mutant through deletion of its respective kinase (Δ*hprK; LMRG_01765*) in a wild-type background were unsuccessful, yet the same mutation could be readily introduced in a Δ*ptsH* background. This suggests that expression of unphosphorylated HPr-Ser in the presence is toxic, possibly due to dominant-negative effects or interference with regulatory networks. To further test this model, we propose generating phosphoablative and phosphomimetic mutants at the regulatory serine residue (Ser46) of HPr. Substitution of Ser46 with alanine (S46A) would prevent phosphorylation and model a constitutively

unphosphorylated state, while substitution with aspartic acid (S46D) would mimic constitutive phosphorylation (33).

While HPr's regulatory effects are thought to occur via phospho-dependent interactions with other proteins, there is evidence that phosphorylated HPr binds to the transcriptional regulator CcpA, enabling CcpA to bind DNA and modulate gene expression (79). To investigate both dimensions of HPr regulation—phosphorylation-mediated signaling and DNA-associated transcriptional control—we propose performing phosphoproteomic analysis of wild-type, HPr S46A, and HPr S46D strains of *L. monocytogenes*. These experiments should be performed *in vitro* using defined media that include or exclude PTS sugars as the sole carbon source (e.g. fructose versus hexose phosphates), to determine how HPr-mediated regulation shifts in response to nutrient availability. This approach could uncover PTS-dependent and independent regulatory pathways and may help identify genes involved in virulence that are misregulated in these mutants.

In parallel, bacterial RNA-seq should be conducted during *ex vivo* macrophage infection to assess transcriptional responses of the phosphoablative and phosphomimetic *ptsH* mutants in the cytosolic environment. This would help reveal how HPr phosphorylation status affects virulence gene regulation, stress adaptation, and metabolic response during infection.

Although Δ*ptsH* strains exhibit significant attenuation *in vivo*, it remains unclear what proportion of this defect is due to the loss of carbon source acquisition versus disruption of HPr-mediated regulatory functions. The similar virulence phenotypes observed between Δ*ptsH* and Δ*ptsI* (EI) mutants suggest that the majority of the defect stems from

impaired carbon import. However, some portion may result from misregulated gene expression or metabolic imbalance (Chapter 2) (16).

Importantly, a Δ*ptsH* mutant eliminates all HPr function, but it does not replicate the physiological effects of unphosphorylated HPr accumulation, which may occur in overexpression or phosphoablative contexts. Thus, understanding the distinct phenotypes of HPr mutants with altered phosphorylation states is essential for dissecting its dual role as both a metabolic and regulatory hub in *L. monocytogenes* pathogenesis.

Together, this work highlights the dual role of HPr, encoded by *ptsH*, in *L. monocytogenes* as both a central player in phosphotransferase system (PTS)-mediated carbon acquisition and as a regulatory protein that influences virulence. Evidence from overexpression toxicity and mutant analysis suggests that imbalances in HPr phosphorylation—particularly accumulation of unphosphorylated HPr—may disrupt cellular physiology. To dissect these roles, we propose generating phosphoablative and phosphomimetic HPr mutants and analyzing their phosphoproteomes and transcriptional profiles under defined metabolic conditions and during *ex vivo* macrophage infection. These approaches aim to clarify how HPr integrates metabolic and regulatory functions and to determine whether HPr-mediated signaling contributes to the virulence defects observed in Δ*ptsH* mutants beyond impaired carbon source uptake.

CONCLUSION

Overall, this thesis investigates the role of carbon acquisition and utilization by *Listeria monocytogenes* during its intracellular life cycle. In Chapter 2, we examined the importance of the phosphotransferase system (PTS) in *L. monocytogenes* virulence and moved one step closer

to defining the specific carbon sources utilized during infection. We demonstrate that functional PTS components are essential for *L. monocytogenes* replication in the host cytosol and for full virulence (16). In Chapter 3, we explored the mechanistic consequences of *L. monocytogenes* lacking a functional pyruvate dehydrogenase complex (PDH). Our findings reveal that the ability to metabolize PTS-derived carbon sources is a key determinant of intracellular virulence, though it is less critical during *in vivo* infection. We further show that PDH mutants can be rescued for growth on PTS sugars when repression by the redox-sensitive regulator Rex is alleviated, highlighting the interplay between carbon metabolism and redox regulation in supporting cytosolic survival. Finally, in the Discussion and Conclusion, we outline several ongoing and emergent questions stemming from this work, including how *L. monocytogenes* interacts with the host through shared metabolic pathways, the evolutionary rationale behind certain metabolic adaptations, and the potential non-metabolic roles of carbon acquisition systems in pathogenesis. Together, this thesis represents an incremental but meaningful step toward elucidating how *L. monocytogenes* engages with the host cell environment. These insights contribute not only to *Listeria* biology but also to a broader understanding of host–pathogen metabolic interactions and the fundamental principles underlying bacterial pathogenesis.

REFERENCES

1. Best A, Abu Kwaik Y. Nutrition and Bipartite Metabolism of Intracellular Pathogens. Trends in Microbiology. 2019 Jun 1;27(6):550–61.

2. Goetz M, Bubert A, Wang G, Chico-Calero I, Vazquez-Boland JA, Beck M, et al. Microinjection and growth of bacteria in the cytosol of mammalian host cells. Proc Natl Acad Sci USA. 2001 Oct 9;98(21):12221–6.

3. Vazquez-Boland JAV, Kuhn M, Berche P, Chakraborty T, Dominguez-Bernal G, Goebel W, et al. Listeria Pathogenesis and Molecular Virulence Determinants. CLIN MICROBIOL REV. 2001;14:57.

4. O'Riordan M, Portnoy DA. The host cytosol: front-line or home front? Trends in Microbiology. 2002 Aug 1;10(8):361–4.

5. Price JV, Vance RE. The Macrophage Paradox. Immunity. 2014 Nov;41(5):685–93.

6. Scortti M, Monzó HJ, Lacharme-Lora L, Lewis DA, Vázquez-Boland JA. The PrfA virulence regulon. Microbes and Infection. 2007 Aug;9(10):1196–207.

7. Sauer JD, Herskovits AA, O'Riordan MXD. Metabolism of the Gram-Positive Bacterial Pathogen *Listeria monocytogenes*. Fischetti VA, Novick RP, Ferretti JJ, Portnoy DA, Braunstein M, Rood JI, editors. Microbiol Spectr. 2019 Jul 19;7(4):7.4.26.

8. Chen GY, Pensinger DA, Sauer JD. *Listeria monocytogenes* cytosolic metabolism promotes replication, survival, and evasion of innate immunity. Cellular Microbiology. 2017 Oct;19(10):e12762.

9. Cossart P. Illuminating the landscape of host–pathogen interactions with the bacterium *Listeria monocytogenes*. Proc Natl Acad Sci USA. 2011 Dec 6;108(49):19484–91.

10. Freeman MJ, Sauer JD. Listeria monocytogenes Requires Phosphotransferase Systems to Facilitate Intracellular Growth and Virulence. bioRxiv. 2024 Jan 1;2024.08.12.607557.

11. Chico-Calero I, Suárez M, González-Zorn B, Scortti M, Slaghuis J, Goebel W, et al. Hpt, a bacterial homolog of the microsomal glucose- 6-phosphate translocase, mediates rapid intracellular proliferation in Listeria. Proc Natl Acad Sci USA. 2002 Jan 8;99(1):431–6.

12. Joseph B, Mertins S, Stoll R, Schär J, Umesha KR, Luo Q, et al. Glycerol Metabolism and PrfA Activity in *Listeria monocytogenes*. J Bacteriol. 2008 Aug;190(15):5412–30.

13. Sanman LE, Qian Y, Eisele NA, Ng TM, van der Linden WA, Monack DM, et al. Disruption of glycolytic flux is a signal for inflammasome signaling and pyroptotic cell death. eLife. 2016 Mar 24;5:e13663.

14. Wynosky-Dolfi MA, Snyder AG, Philip NH, Doonan PJ, Poffenberger MC, Avizonis D, et al. Oxidative metabolism enables Salmonella evasion of the NLRP3 inflammasome. Journal of Experimental Medicine. 2014 Apr 7;211(4):653–68.

15. GrubmÃ¼ller S, Schauer K, Goebel W, Fuchs TM, Eisenreich W. Analysis of carbon substrates used by Listeria monocytogenes during growth in J774A.1 macrophages suggests a bipartite intracellular metabolism. Front Cell Infect Microbiol [Internet]. 2014 Nov 3 [cited 2021 Dec 14];4. Available from: http://journal.frontiersin.org/article/10.3389/fcimb.2014.00156/abstract

16. Freeman MJ, Eral NJ, Sauer JD. Listeria monocytogenes requires phosphotransferase systems to facilitate intracellular growth and virulence. O'Riordan MX, editor. PLoS Pathog. 2025 Apr 15;21(4):e1012492.

17. Crespo Tapia N, den Besten HMW, Abee T. Glycerol metabolism induces Listeria monocytogenes biofilm formation at the air-liquid interface. International Journal of Food Microbiology. 2018 May 20;273:20–7.

18. Häuslein I, Manske C, Goebel W, Eisenreich W, Hilbi H. Pathway analysis using^{13} C-glycerol and other carbon tracers reveals a bipartite metabolism of *Legionella pneumophila*. Molecular Microbiology. 2016 Apr;100(2):229–46.

19. Mertins S, Joseph B, Goetz M, Ecke R, Seidel G, Sprehe M, et al. Interference of Components of the Phosphoenolpyruvate Phosphotransferase System with the Central Virulence Gene Regulator PrfA of *Listeria monocytogenes*. J Bacteriol. 2007 Jan 15;189(2):473–90.

20. Tucey TM, Verma J, Harrison PF, Snelgrove SL, Lo TL, Scherer AK, et al. Glucose Homeostasis Is Important for Immune Cell Viability during Candida Challenge and Host Survival of Systemic Fungal Infection. Cell Metabolism. 2018 May;27(5):988-1006.e7.

21. Ortega FE, Koslover EF, Theriot JA. Listeria monocytogenes cell-to-cell spread in epithelia is heterogeneous and dominated by rare pioneer bacteria. eLife. 2019 Feb 5;8:e40032.

22. Radhakrishnan P, Theriot JA. *Listeria monocytogenes* cell-to-cell spread bypasses nutrient limitation for replicating intracellular bacteria [Internet]. 2025 [cited 2025 Apr 5]. Available from: http://biorxiv.org/lookup/doi/10.1101/2025.01.31.635960

23. Srivastav S, Biswas A, Anand A. Interplay of niche and respiratory network in shaping bacterial colonization. Journal of Biological Chemistry. 2025 Jan 1;301(1):108052.

24. Orth JD, Conrad TM, Na J, Lerman JA, Nam H, Feist AM, et al. A comprehensive genome-scale reconstruction of *Escherichia coli* metabolism—2011. Molecular Systems Biology. 2011 Jan;7(1):535.

25. White D, Drummond JT, Fuqua C. The Physiology and Biochemistry of Prokaryotes [Internet]. Oxford University Press; 2012. Available from: https://books.google.com/books?id=ToF6pwAACAAJ

26. Krombach F, Allmeling AM, Gerlach JT, Behr J, Dbrgerl M. Cell size of alveolar macrophages: an interspecies comparison. Environmental Health Perspectives. 1997;105.

27. Cantor JR, Abu-Remaileh M, Kanarek N, Freinkman E, Gao X, Louissaint A, et al. Physiologic Medium Rewires Cellular Metabolism and Reveals Uric Acid as an Endogenous Inhibitor of UMP Synthase. Cell. 2017 Apr;169(2):258-272.e17.

28. Leney-Greene MA, Boddapati AK, Su HC, Cantor JR, Lenardo MJ. Human Plasma-like Medium Improves T Lymphocyte Activation. iScience. 2020 Jan;23(1):100759.

29. Rossiter NJ, Huggler KS, Adelmann CH, Keys HR, Soens RW, Sabatini DM, et al. CRISPR screens in physiologic medium reveal conditionally essential genes in human cells. Cell Metabolism. 2021 Jun;33(6):1248-1263.e9.

30. Bussi C, Lai R, Athanasiadi N, Gutierrez MG. Physiologic medium renders human iPSC-derived macrophages permissive for *M. tuberculosis* by rewiring organelle function and metabolism. Hube B, Schaible UE, editors. mBio. 2024 Aug 14;15(8):e00353-24.

31. Visca P, Pisa F, Imperi F. The antimetabolite 3-bromopyruvate selectively inhibits Staphylococcus aureus. International Journal of Antimicrobial Agents. 2019 Apr 1;53(4):449–55.

32. Fischer M, Engelgeh T, Rothe P, Fuchs S, Thürmer A, Halbedel S. Listeria monocytogenes gene essentiality under laboratory conditions and during macrophage infection. bioRxiv. 2022 Jan 1;2022.03.04.482958.

33. Kelliher JL, Grunenwald CM, Abrahams RR, Daanen ME, Lew CI, Rose WE, et al. PASTA kinase-dependent control of peptidoglycan synthesis via ReoM is required for cell wall stress responses, cytosolic survival, and virulence in Listeria monocytogenes. Sassetti CM, editor. PLoS Pathog. 2021 Oct 8;17(10):e1009881.

34. Aft RL, Zhang FW, Gius D. Evaluation of 2-deoxy-D-glucose as a chemotherapeutic agent: mechanism of cell death. Br J Cancer. 2002 Sep;87(7):805–12.

35. Stoll R, Goebel W. The major PEP-phosphotransferase systems (PTSs) for glucose, mannose and cellobiose of Listeria monocytogenes, and their significance for extra- and intracellular growth. Microbiology. 2010 Apr 1;156(4):1069–83.

36. Miller ES, Bates RA, Koebel DA, Fuchs BB, Sonnenfeld G. 2-Deoxy-d-Glucose–Induced Metabolic Stress Enhances Resistance to Listeria monocytogenes Infection in Mice. Physiology & Behavior. 1998 Oct 1;65(3):535–43.

37. Manna S, Howitz WJ, Oldenhuis NJ, Eldredge AC, Shen J, Nihesh FN, et al. Immunomodulation of the NLRP3 Inflammasome through Structure-Based Activator Design and Functional Regulation via Lysosomal Rupture. ACS Cent Sci. 2018 Aug 22;4(8):982–95.

38. Theisen E, Sauer JD. Listeria monocytogenes-Induced Cell Death Inhibits the Generation of Cell-Mediated Immunity. Freitag NE, editor. Infect Immun. 2017 Jan;85(1):e00733-16.

39. Chen GY, McDougal CE, D'Antonio MA, Portman JL, Sauer JD. A Genetic Screen Reveals that Synthesis of 1,4-Dihydroxy-2-Naphthoate (DHNA), but Not Full-Length Menaquinone, Is Required for *Listeria monocytogenes* Cytosolic Survival. Swanson MS, editor. mBio [Internet]. 2017 May 3 [cited 2021 Dec 14];8(2). Available from: https://journals.asm.org/doi/10.1128/mBio.00119-17

40. Lauer P, Hanson B, Lemmens EE, Liu W, Luckett WS, Leong ML, et al. Constitutive Activation of the PrfA Regulon Enhances the Potency of Vaccines Based on Live-Attenuated and Killed but Metabolically Active *Listeria monocytogenes* Strains. Infect Immun. 2008 Aug;76(8):3742–53.

41. Benoit M, Desnues B, Mege JL. Macrophage Polarization in Bacterial Infections. The Journal of Immunology. 2008 Sep 15;181(6):3733–9.

42. Chen S, Saeed AFUH, Liu Q, Jiang Q, Xu H, Xiao GG, et al. Macrophages in immunoregulation and therapeutics. Sig Transduct Target Ther. 2023 May 22;8(1):207.

43. Strizova Z, Benesova I, Bartolini R, Novysedlak R, Cecrdlova E, Foley LK, et al. M1/M2 macrophages and their overlaps – myth or reality? Clinical Science. 2023 Aug 14;137(15):1067–93.

44. Wang X, Yang B, Ma S, Yan X, Ma S, Sun H, et al. Lactate promotes *Salmonella* intracellular replication and systemic infection via driving macrophage M2 polarization. Gao B, editor. Microbiol Spectr. 2023 Dec 12;11(6):e02253-23.

45. Kuhn M, Goebel W. Responses by murine macrophages infected with Listeria monocytogenes crucial for the development of immunity to this pathogen. Immunological Reviews. 1997 Aug;158(1):57–93.

46. Chalenko YM, Slonova DA, Kechko OI, Kalinin EV, Mitkevich VA, Ermolaeva SA. Natural Isoforms of Listeria monocytogenes Virulence Factor Inlb Differ in c-Met Binding Efficiency and Differently Affect Uptake and Survival Listeria in Macrophage. IJMS. 2023 Apr 14;24(8):7256.

47. Miskolci V, Tweed KE, Lasarev MR, Britt EC, Walsh AJ, Zimmerman LJ, et al. In vivo fluorescence lifetime imaging of macrophage intracellular metabolism during wound responses in zebrafish. eLife. 2022 Feb 24;11:e66080.

48. Wan J, Benkdane M, Teixeira-Clerc F, Bonnafous S, Louvet A, Lafdil F, et al. M2 Kupffer cells promote M1 Kupffer cell apoptosis: A protective mechanism against alcoholic and nonalcoholic fatty liver disease. Hepatology. 2014 Jan;59(1):130–42.

49. Ransohoff RM. A polarizing question: do M1 and M2 microglia exist? Nat Neurosci. 2016 Aug;19(8):987–91.

50. Thiriot JD, Martinez-Martinez YB, Endsley JJ, Torres AG. Hacking the host: exploitation of macrophage polarization by intracellular bacterial pathogens. Pathogens and Disease. 2020 Feb 1;78(1):ftaa009.

51. Azari S, Johnson LJ, Webb A, Kozlowski SM, Zhang X, Rood K, et al. Hofbauer Cells Spread Listeria monocytogenes among Placental Cells and Undergo Pro-Inflammatory Reprogramming while Retaining Production of Tolerogenic Factors. Vazquez-Boland JA, editor. mBio. 2021 Aug 31;12(4):e01849-21.

52. Kelly B, O'Neill LA. Metabolic reprogramming in macrophages and dendritic cells in innate immunity. Cell Res. 2015 Jul;25(7):771–84.

53. Fischer MA, Engelgeh T, Rothe P, Fuchs S, Thürmer A, Halbedel S. *Listeria monocytogenes* genes supporting growth under standard laboratory cultivation conditions and during macrophage infection. Genome Res. 2022 Sep;32(9):1711–26.

54. Olson WJ, Martorelli Di Genova B, Gallego-Lopez G, Dawson AR, Stevenson D, Amador-Noguez D, et al. Dual metabolomic profiling uncovers Toxoplasma manipulation of the host metabolome and the discovery of a novel parasite metabolic capability. Soldati-Favre D, editor. PLoS Pathog. 2020 Apr 7;16(4):e1008432.

55. Caesar LK, Kellogg JJ, Kvalheim OM, Cech NB. Opportunities and Limitations for Untargeted Mass Spectrometry Metabolomics to Identify Biologically Active Constituents in Complex Natural Product Mixtures. J Nat Prod. 2019 Mar 22;82(3):469–84.

56. Fung C, Naughton S, Turnbull L, Tingpej P, Rose B, Arthur J, et al. Gene expression of Pseudomonas aeruginosa in a mucin-containing synthetic growth medium mimicking cystic fibrosis lung sputum. Journal of Medical Microbiology. 2010 Sep 1;59(9):1089–100.

57. Palmer KL, Aye LM, Whiteley M. Nutritional Cues Control *Pseudomonas aeruginosa* Multicellular Behavior in Cystic Fibrosis Sputum. J Bacteriol. 2007 Nov 15;189(22):8079–87.

58. Turner KH, Wessel AK, Palmer GC, Murray JL, Whiteley M. Essential genome of *Pseudomonas aeruginosa* in cystic fibrosis sputum. Proc Natl Acad Sci USA. 2015 Mar 31;112(13):4110–5.

59. Chatterjee SS, Hossain H, Otten S, Kuenne C, Kuchmina K, Machata S, et al. Intracellular Gene Expression Profile of *Listeria monocytogenes*. Infect Immun. 2006 Feb;74(2):1323–38.

60. Severino P, Dussurget O, Vêncio RZN, Dumas E, Garrido P, Padilla G, et al. Comparative Transcriptome Analysis of *Listeria monocytogenes* Strains of the Two Major Lineages Reveals Differences in Virulence, Cell Wall, and Stress Response. Appl Environ Microbiol. 2007 Oct;73(19):6078–88.

61. Zhou J, Wang P, Liang L, Guo J, Chen Y. Application of metabolomics analysis to aid in understanding the pathogenicity of different lineages and different serotypes of Listeria monocytogenes. International Journal of Food Microbiology. 2022 Jul 16;373:109694.

62. Grubmuller S, Schauer K, Goebel W, Fuchs TM, Eisenreich W. Analysis of carbon substrates used by Listeria monocytogenes during growth in J774A.1 macrophages suggests a bipartite intracellular metabolism. Front Cell Infect Microbiol [Internet]. 2014 Nov 3 [cited 2022 Jun 2];4. Available from: http://journal.frontiersin.org/article/10.3389/fcimb.2014.00156/abstract

63. Morris JJ, Lenski RE, Zinser ER. The Black Queen Hypothesis: Evolution of Dependencies through Adaptive Gene Loss. mBio. 2012 May 2;3(2):e00036-12.

64. Buchrieser C, Rusniok C, The Listeria Consortium, Kunst F, Cossart P, Glaser P. Comparison of the genome sequences of *Listeria monocytogenes* and *Listeria innocua* : clues for evolution and pathogenicity. FEMS Immunology & Medical Microbiology. 2003 Apr;35(3):207–13.

65. Bécavin C, Bouchier C, Lechat P, Archambaud C, Creno S, Gouin E, et al. Comparison of Widely Used Listeria monocytogenes Strains EGD, 10403S, and EGD-e Highlights Genomic

Differences Underlying Variations in Pathogenicity. Casadevall A, editor. mBio. 2014 May;5(2):e00969-14.

66. Schunder E, Gillmaier N, Kutzner E, Herrmann V, Lautner M, Heuner K, et al. Amino Acid Uptake and Metabolism of Legionella pneumophila Hosted by Acanthamoeba castellanii. Journal of Biological Chemistry. 2014 Jul;289(30):21040–54.

67. Mashabela GT, De Wet TJ, Warner DF. *Mycobacterium tuberculosis* Metabolism. Fischetti VA, Novick RP, Ferretti JJ, Portnoy DA, Braunstein M, Rood JI, editors. Microbiol Spectr. 2019 Jul 19;7(4):7.4.18.

68. Maury MM, Bracq-Dieye H, Huang L, Vales G, Lavina M, Thouvenot P, et al. Hypervirulent Listeria monocytogenes clones' adaption to mammalian gut accounts for their association with dairy products. Nat Commun. 2019 Jun 6;10(1):2488.

69. Lecuit M. Understanding how Listeria monocytogenes targets and crosses host barriers. Clinical Microbiology and Infection. 2005 Jun;11(6):430–6.

70. Pitts M, D'Orazio S. A Comparison of Oral and Intravenous Mouse Models of Listeriosis. Pathogens. 2018 Jan 20;7(1):13.

71. Auerbuch V, Lenz LL, Portnoy DA. Development of a Competitive Index Assay To Evaluate the Virulence of *Listeria monocytogenes actA* Mutants during Primary and Secondary Infection of Mice. DiRita VJ, editor. Infect Immun. 2001 Sep;69(9):5953–7.

72. Milenbachs AA, Brown DP, Moors M, Youngman P. Carbon-source regulation of virulence gene expression in *Listeria monocytogenes*. Molecular Microbiology. 1997 Mar;23(5):1075–85.

73. Whiteley AT, Garelis NE, Peterson BN, Choi PH, Tong L, Woodward JJ, et al. c -di- AMP modulates *L isteria monocytogenes* central metabolism to regulate growth, antibiotic resistance and osmoregulation. Molecular Microbiology. 2017 Apr;104(2):212–33.

74. Tian J, Bryk R, Itoh M, Suematsu M, Nathan C. Variant tricarboxylic acid cycle in *Mycobacterium tuberculosis* : Identification of α-ketoglutarate decarboxylase. Proc Natl Acad Sci USA. 2005 Jul 26;102(30):10670–5.

75. Choe M, Park YH, Lee CR, Kim YR, Seok YJ. The general PTS component HPr determines the preference for glucose over mannitol. Sci Rep. 2017 Feb 22;7(1):43431.

76. Woo JKK, Zimnicka AM, Federle MJ, Freitag NE. Novel motif associated with carbon catabolite repression in two major Gram-positive pathogen virulence regulatory proteins. Kolodkin-Gal I, editor. Microbiol Spectr. 2024 Nov 5;12(11):e00485-24.

77. Nessler S, Fieulaine S, Poncet S, Galinier A, Deutscher J, Janin J. HPr Kinase/Phosphorylase, the Sensor Enzyme of Catabolite Repression in Gram-Positive Bacteria: Structural Aspects of the Enzyme and the Complex with Its Protein Substrate. J Bacteriol. 2003 Jul 15;185(14):4003–10.

78. Cochu A, Roy D, Vaillancourt K, LeMay JD, Casabon I, Frenette M, et al. The Doubly Phosphorylated Form of HPr, HPr(Ser-P)(His~P), Is Abundant in Exponentially Growing Cells of *Streptococcus thermophilus* and Phosphorylates the Lactose Transporter LacS as Efficiently as HPr(His~P). Appl Environ Microbiol. 2005 Mar;71(3):1364–72.

79. Behari J, Youngman P. A Homolog of CcpA Mediates Catabolite Control in Listeria monocytogenes but Not Carbon Source Regulation of Virulence Genes. J BACTERIOL. 1998;180.

APPENDIX 1 – *Listeria monocytogenes* requires DHNA-dependent intracellular redox homeostasis facilitated by Ndh2 for survival and virulence

Authors and their contributions:

Hans B. Smith: Planned, organized, design and conducted experiments, and wrote and edited this manuscript

Kijeong Lee: Planned, organized, design and conducted experiments, and wrote and edited this manuscript

Matthew J. Freeman: Planned, organized, design and conducted experiments, and wrote and edited this manuscript

- Experiments planned and conducted include Figures 1B, 2B, 3B & 3D, and 5A-B.

David M. Stevenson: Planned and conducted experiments, and wrote and edited this manuscript

Daniel Amador-Noguez: Provided super staff and resource for experiments, supervised writing and editing of this manuscript

John-Demian Sauer: Supervised writing and editing of this manuscript

As published from Smith *et. al.*, *Infection and Immunity*, October 2023

ABSTRACT

Listeria monocytogenes is a remarkably well-adapted facultative intracellular pathogen that can thrive in a wide range of ecological niches. *L. monocytogenes* maximizes its ability to generate energy from diverse carbon sources using a respiro-fermentative metabolism that can function under both aerobic and anaerobic conditions. Cellular respiration maintains redox homeostasis by regenerating NAD^+ while also generating a proton motive force (PMF). The end products of the menaquinone (MK) biosynthesis pathway are essential to drive both aerobic and anaerobic cellular respiration. We previously demonstrated that intermediates in the MK biosynthesis pathway, notably 1,4-dihydroxy-2-naphthoate (DHNA), are required for the survival and virulence of *L. monocytogenes* independent of their role in respiration. Furthermore, we found that restoration of NAD^+/NADH ratio through expression of water-forming NADH oxidase (NOX) could rescue phenotypes associated with DHNA deficiency. Here we extend these findings to demonstrate that endogenous production or direct supplementation of DHNA restored both the cellular redox homeostasis and metabolic output of fermentation in *L. monocytogenes*. Further, exogenous supplementation of DHNA rescues the *in vitro* growth and *ex vivo* virulence of *L. monocytogenes* DHNA-deficient mutants. Finally, we demonstrate that exogenous DHNA restores redox balance in *L. monocytogenes* specifically through the recently annotated NADH dehydrogenase Ndh2, independent of the extracellular electron transport (EET) pathway. These data suggest that the production of DHNA may represent an additional layer of metabolic adaptability by *L. monocytogenes* to drive energy metabolism in the absence of respiration-favorable conditions.

INTRODUCTION

Listeria monocytogenes is a Gram-positive, facultative intracellular pathogen that is exceptionally well-adapted to survive and replicate in the restrictive mammalian host cytosol (1–3). Bacteria that lack the specific adaptations required to survive or replicate in the host niche are effectively cleared (4–7), often by triggering host defense mechanisms comprised of innate immune pathways (8–13). *L. monocytogenes* utilizes its internalin proteins to facilitate invasion into the host cell where it becomes captured in a phagosome (14, 15). The pore-forming cytolysin listeriolysin O (LLO) then facilitates escape from the phagosome into the cytosol (14, 16), where *L. monocytogenes* can utilize ActA to mediate actin-based motility by hijacking the host's actin machinery (17–20). Using this motility, *L. monocytogenes* moves into adjacent cells where they again invade the cytosol by expressing LLO and two phospholipase Cs, PlcA and PlcB, enabling it to restart its life cycle (14, 21).

L. monocytogenes can also thrive in a diverse range of ecological niches that contain highly variable pools of fermentable and non-fermentable carbon sources (2, 22) *L. monocytogenes* employs both fermentative and respiratory metabolic mechanisms to maximize its energy output from scavenged nutrients (22, 23). In contrast to canonical respiratory organisms however, *L. monocytogenes* contains an incomplete tricarboxylic acid (TCA) cycle and is therefore unable to fully oxidize its carbon substrates (24). Accordingly, *L. monocytogenes* utilizes a respiro-fermentative metabolism characterized by glycolysis-derived pyruvate that is funneled into the fermentative production of acetate, generating ATP through substrate-level phosphorylation (SLP) via the activity of acetate kinase (24, 25). During the respiro-fermentative process, the activity of *L. monocytogenes*' respiratory electron transport chain (ETC) enables it to regenerate NAD^+, without having to rely upon lactate dehydrogenase, while also producing a

functional proton motive force (PMF) (22, 24, 25). Further lending to its diverse metabolic adaptability, *L. monocytogenes* possesses two distinct respiratory ETCs that allow it to respire both aerobically and anaerobically (26). The aerobic ETC in *L. monocytogenes* mediates electron transfer from a type II NADH dehydrogenase, Ndh1, to a membrane-bound menaquinone (MK) and subsequently to terminal cytochrome oxidases QoxAB (aa3) or CydAB (bd) for final transfer to O_2 (27, 28). In contrast, the recently annotated anaerobic respiratory pathway in *L. monocytogenes* uses a flavin-based ETC to drive extracellular electron transfer (EET) to extracytosolic acceptors such as fumarate or ferric ion using a novel NADH dehydrogenase (Ndh2) and an alternative demethylmenaquinone (DMK) intermediate (26, 29). Both of the respiratory ETC in *L. monocytogenes* rely upon the MK biosynthesis pathway to generate their respective quinone electron acceptors, with the biosynthetic intermediate 1,4-dihydroxy-2-naphthoate (DHNA) functioning as a mutual branching point (**Fig. S1**) (26).

The requirement for *L. monocytogenes* to perform cellular respiration during infection has been well documented (30–33). However, understanding the specific contributions of maintaining cellular redox homeostasis via NAD^+ regeneration versus the production of a functional PMF to achieve virulence has remained elusive. Further complicating our ability to dissect the specific contributions that cellular respiration may have during infection, the MK intermediates DHNA-CoA and DHNA have recently been reported to be required for the survival and virulence of *L. monocytogenes* independent of MK synthesis and aerobic respiration (30, 32, 33). Importantly, although it was observed that the supplementation of exogenous DHNA could rescue the *in vitro* growth of a DHNA-deficient *L. monocytogenes* mutant, this rescue did not coincide with the restoration of its PMF (32). Therefore, although DHNA-deficient strains of *L. monocytogenes* possess the downstream enzymes to produce MK or DMK,

these data suggest that exogenous DHNA is not utilized to promote either aerobic or anaerobic cellular respiration. Recent work from Rivera-Lugo *et al.* sought to dissect the relative importance of maintaining redox homeostasis versus PMF generation for the pathogenesis of *L. monocytogenes* using a water-forming NADH oxidase (NOX) that specifically regenerates NAD^+ independent of respiration and PMF function (25). Through the heterologous expression of NOX in respiration-deficient strains of *L. monocytogenes*, it was concluded that the regeneration of NAD^+ represents a major role for cellular respiration during pathogenesis.

The studies presented here sought to define the respiration-independent mechanisms of DHNA utilization to promote the survival and virulence of *L. monocytogenes*. Consistent with observations from Rivera-Lugo *et. al*, in the absence of respiration, the *ex vivo* and *in vivo* virulence defects associated with DHNA-deficiency were a result of impaired redox homeostasis which could be rescued upon ectopic NOX expression. Similarly, exogenous DHNA supplementation rescues the *in vitro* and *ex vivo* growth and cytosolic survival of DHNA-deficient mutants. Indeed, DHNA-dependent rescue by direct supplementation resulted in a restored cellular redox homeostasis with a concurrent shift of fermentative flux from lactate production to acetate in *L. monocytogenes*, independent of respiration. We further go on to show that the recently annotated anaerobic-specific Ndh2 is essential for DHNA-deficient *L. monocytogenes* mutants to utilize exogenous DHNA for growth in defined medium, independent of its canonical role in EET, suggesting that Ndh2 is the NADH dehydrogenase specifically required for the restoration of redox homeostasis via DHNA. Taken together, these data suggest that the endogenous production of DHNA can be utilized by *L. monocytogenes* to restore both its intracellular redox homeostasis and fermentative metabolic flux through an undefined mechanism requiring Ndh2.

RESULTS

Redox homeostasis via NOX shifts fermentative output and rescues *in vitro* growth of DHNA-deficient *L. monocytogenes*.

Two main outcomes of cellular respiration include 1) maintaining intracellular redox homeostasis by regenerating NAD^+ from NADH and 2) the generation of a PMF to drive oxidative phosphorylation and various other aspects of bacterial physiology. A recent study employed a water-forming NADH oxidase (NOX) expression system in *L. monocytogenes* to dissect the relative importance of cellular respiration in maintaining redox homeostasis versus PMF generation (25). We had previously demonstrated that *L. monocytogenes* mutants lacking the key MK biosynthetic intermediate DHNA were attenuated, in part, independent of loss of respiration (30, 32, 33). We hypothesized that restoration of NAD^+ pools might rescue these virulence defects similar to the rescue observed for mutants lacking components of the respiratory chains (25). To test this hypothesis, we assessed NAD^+/NADH levels in Δ*menB*, Δ*menI* and Δ*menA* mutants +/- expression of NOX *in trans*. The inability to generate endogenous DHNA by the Δ*menB* mutant results in a severely diminished redox homeostasis as measured by the ratio of oxidized NAD^+ to reduced NADH. This imbalance was significantly restored by ectopic expression of NOX to a level similar to the Δ*menA* mutant (**Fig. 1A**). The Δ*menI* mutant, which can generate DHNA-CoA, displays an intermediate phenotype between Δ*menB* and Δ*menA* levels, which is similarly rescued upon NOX expression (**Fig. 1A**), consistent with possible respiration independent roles for DHNA in NAD^+/NADH redox balancing.

L. monocytogenes employs a respiro-fermentative metabolism due to an incomplete TCA cycle, characterized by the funneling of pyruvate towards the fermentative production of acetate

(23, 24). Respiration-deficient mutants of *L. monocytogenes* are impaired in their ability to maintain cellular redox homeostasis and as a result nearly exclusively produce lactate rather than acetate as a metabolic byproduct (25). To test whether impaired redox homeostasis due to DHNA-deficiency would similarly result in the predominant production of lactate, we analyzed fermentation byproducts in bacterial supernatants using high-performance liquid chromatography (HPLC). As expected, wild-type *L. monocytogenes* predominantly generated acetate whereas DHNA-deficient Δ*menB* had a drastic shift to lactate production (**Fig. 1B**). Heterologous NOX expression rescued Δ*menB* acetate production back to wild-type levels, consistent with restored redox homeostasis driving acetate production to generate ATP (**Fig. 1B**). Consistent with the results seen in our NAD^+/NADH experiments, the Δ*menI* mutant displayed an intermediate phenotype by producing similar levels of acetate and lactate, which was also fully restored to wild-type upon NOX expression (**Fig. 1B**). The Δ*menA* mutant produced slightly more lactate and less acetate when compared to wild-type, likely attributed to the difference in redox homeostasis observed previously (**Fig. 1A, B**).

Finally, we have previously shown that the production of DHNA is critical for *L. monocytogenes in vitro* growth in chemically defined medium (30, 32, 33). To test whether restoration of redox homeostasis can rescue this growth defect, we've assayed for *in vitro* growth of the above mutants complemented with NOX in defined medium. As expected, Δ*menB* showed the largest growth defect followed by Δ*menI*, and both mutants showed wild-type level growth upon NOX complementation (**Fig. 1C**). Together, these data suggest that metabolic defects associated with DHNA deficiency in *L. monocytogenes* are due to NAD^+/NADH redox imbalances and that restoration of this balance can rescue Δ*menB* mutant growth and carbon metabolism in *L. monocytogenes*.

Restoration of redox homeostasis rescues virulence defects associated with DHNA-deficiency.

Based on the restoration of *in vitro* growth of Δ*menB* mutants via expression of NOX, we hypothesized that restoration of NAD^+ pools would similarly rescue virulence defects of DHNA-deficient mutants. DHNA-deficient mutants are susceptible to cytosolic killing in the macrophage cytosol, therefore we assessed cytosolic survival of Δ*menB*, Δ*menI*, and Δ*menA* with or without expression of NOX *in trans* (30, 34). As hypothesized, Δ*menB* and Δ*menI* displayed increased cytosolic killing and NOX expression rescued their survival in the macrophage cytosol (**Fig. 2A**). Rescue by NOX expression was specific to mutants with disrupted NAD^+/NADH redox homeostasis as NOX expression was unable to rescue cytosolic survival of a Δ*glmR* mutant susceptible to cytosolic killing due to cell wall defects (**Fig 2A**) (34–36). Consistent with NAD^+ pool restoration supporting cytosolic survival, Δ*menB* mutant replication in the macrophage cytosol was also rescued upon expression of NOX *in trans* (**Fig. 2B**).

Finally, we had previously demonstrated that DHNA-deficient mutants are more attenuated *in vivo* than respiration-deficient mutants, suggesting that DHNA contributes to virulence in a respiration independent manner (30, 32, 33). To determine if the respiration independent function of DHNA during *in vivo* infection is due to NAD^+/NADH homeostasis defects, we assessed virulence of Δ*menB*, Δ*menI*, and Δ*menA* mutant *L. monocytogenes* with and without expression of NOX *in trans*. Ectopic NOX expression rescued the *in vivo* burden of Δ*menB* mutants by ~100-fold in the spleen and liver (**Fig. 2C**) and an even greater rescue for Δ*menI* mutants in the liver following NOX expression was also observed (**Fig. 2C**). However, unlike our *in vitro* data, NOX expression did not rescue *in vivo* virulence back to wild-type

levels. Interestingly, there was little to no change in the *in vivo* virulence of Δ*menA* upon the introduction of NOX (**Fig 2C**). This is in agreement with our previous results that showed both redox homeostasis and acetate production of the Δ*menA* mutant was also not significantly altered upon NOX expression (**Fig 1A, B**). Taken together, these data suggest that in *L. monocytogenes* maintaining cellular redox homeostasis in the absence of DHNA is sufficient to promote survival and virulence both *ex vivo* and *in vivo*.

DHNA production or supplementation promotes similar effects to NOX complementation in *L. monocytogenes*.

We have previously demonstrated that exogenous addition of either purified DHNA or culture supernatant from DHNA sufficient strains of *L. monocytogenes* could rescue the *in vitro* growth of DHNA-deficient *L. monocytogenes* in defined media (32), suggesting that *L. monocytogenes*, like other bacteria including *Propionibacterium* spp. and *Lactobacillus* spp., may secrete DHNA (37, 38). To test the hypothesis that *L. monocytogenes* secretes DHNA, we assayed culture supernatants for DHNA via mass spectrometry. As hypothesized, wild-type *L. monocytogenes* contained abundant levels of DHNA, while Δ*menB* mutants contained no detectable extracellular DHNA **(Fig. S2)**. Given that exogenous DHNA could rescue the *in vitro* growth of DHNA-deficient *L. monocytogenes* mutants and that DHNA-deficient mutants could similarly be rescued by NAD^+ regeneration through NOX expression, we hypothesized that exogenous DHNA could act to restore NAD^+ levels in Δ*menB* mutants. To test this hypothesis, we measured cellular NAD^+/NADH with or without DHNA supplementation. Consistent with the results observed with NOX expression, the exogenous supplementation of DHNA rescued redox homeostasis of Δ*menB* mutants to levels similar to those seen with Δ*menA* mutants, suggesting that exogenous DHNA might be utilized in a similar fashion to DHNA produced

endogenously (**Fig. 3A**). Consistent with DHNA supplementation of Δ*menB* rescuing cellular redox homeostasis, exogenous DHNA also shifted the metabolic flux of Δ*menB* back towards acetate production, similar to Δ*menA* levels (**Fig. 3B**). Importantly, we had previously demonstrated that exogenous DHNA does not restore respiration and membrane potential (32). Taken together, these data suggest that DHNA, independent of its role in respiration, restores cellular redox homeostasis, subsequently shifting the fermentative output from lactate back towards acetate that likely drives ATP production through acetate kinase (24, 25).

Having previously observed that DHNA can restore NAD^+ redox homeostasis and that NOX-dependent NAD^+ restoration could restore virulence defects of Δ*menB* mutants, we hypothesized that exogenous DHNA supplementation during infection may similarly rescue the cytosolic survival and intracellular growth of DHNA-deficient *L. monocytogenes*. Indeed, the addition of exogenous DHNA during macrophage infection with Δ*menB* or Δ*menI* mutants restored their cytosolic survival back to wild-type and Δ*menA* levels (**Fig. 3C**). Importantly, as observed with NOX expression, DHNA supplementation did not rescue the cytosolic survival of Δ*glmR* mutants whose virulence phenotypes are due to cell wall stress response defects (**Fig. 3C**) (35, 36), demonstrating that the rescue of cytosolic survival by DHNA is specific to DHNA-deficient *L. monocytogenes*. Accordingly, supplementing DHNA during macrophage infection also rescued the ability of Δ*menB* mutants to replicate intracellularly to levels similar of that during Δ*menA* infection (**Fig. 3D**). Taken together, these results demonstrate that exogenously provided DHNA can balance NAD^+/NADH redox homeostasis thereby potentiating *L. monocytogenes* virulence.

Ndh2 is conditionally essential for DHNA utilization *in vitro*.

Although DHNA can drive regeneration of NAD^+ in *L. monocytogenes* upon exogenous supplementation, it does not restore membrane potential suggesting that it is not simply imported and used to synthesize MK as described in Streptococci (39, 40). We hypothesized that the two annotated *L. monocytogenes'* NADH dehydrogenases encoded by *ndh1* (*LMRG_02734*) and *ndh2* (*LMRG_02183*), respectively, may utilize DHNA independent of the respiratory pathways to facilitate NAD^+/NADH homeostasis (23, 26). To test this hypothesis, we generated Δ*ndh1*/*menB*::Tn and Δ*menB*/*ndh2*::Tn mutants and assayed for growth with or without 5μM exogenous DHNA in defined medium. As expected, both double mutants were unable to grow without exogenous DHNA due them being a Δ*menB* mutant (**Fig. 4A**). DHNA supplementation rescued growth of the Δ*ndh1*/*menB*::Tn mutant suggesting that Ndh1 is not required for DHNA-dependent NAD^+/NADH redox homeostasis. In contrast, the Δ*menB*/*ndh2*::Tn mutant was unable to grow in the presence of exogenous DHNA (**Fig. 4B**). *ndh2* is required for the function of the recently described EET pathway in *L. monocytogenes* (26), therefore we hypothesized that EET may be necessary to utilize DHNA for NAD^+/NADH redox homeostasis. To test this hypothesis, we transduced *pplA*::Tn, *dmkA*::Tn, *eetA*::Tn, and *fmnA*::Tn mutations into a Δ*menB* background. The growth of all four of these double mutants were rescued upon DHNA supplementation in defined medium (**Fig. S3**). Finally, exogenous MK supplementation can restore not only growth of DHNA deficient mutants but also their membrane potential (32, 33), likely through direct insertion of MK in the membrane and subsequent restoration of the aerobic respiratory chain. To ensure that Δ*menB*/*ndh2*::Tn mutants are not more generally incapable of growing in defined media, we supplemented Δ*menB*/*ndh2*::Tn mutants with either DHNA or MK directly. Supplementation of MK rescued growth of Δ*menB*/*ndh2*::Tn in defined medium unlike

DHNA, showing that this mutant is specifically dysfunctional in the use of DHNA as a redox homeostasis substrate (**Fig. 4C**). Taken together, these data suggest that Ndh2 facilitates DHNA-dependent NAD^+/NADH redox homeostasis in the absence of respiration in *L. monocytogenes*.

Ndh2 is required for DHNA-dependent rescue of intra-macrophage replication *ex vivo*.

Given that DHNA supplementation *in vitro* cannot rescue growth of the Δ*menB*/*ndh2*::Tn mutant, we asked whether this growth defect would impact *ex vivo* virulence. To test the hypothesis that Δ*menB*/*ndh2*::Tn mutant has *ex vivo* virulence defects that cannot be rescued by DHNA, we assessed intracellular growth in both DHNA-treated and non-treated macrophages. As expected, DHNA-deficient Δ*menB* mutants failed to grow to wild-type levels in macrophages without exogenous DHNA (**Fig. 5A**). Interestingly, the double mutants (Δ*menB*/*pplA*::Tn and Δ*menB*/*ndh2*::Tn) displayed further growth defects compared to Δ*menB* suggesting a potential DHNA-independent role of EET in regard to intra-macrophage replication. The Δ*menB*/*ndh2*::Tn mutant was not rescued to wild-type level replication with exogenous DHNA (**Fig. 5B**), consistent with our *in vitro* observation (**Fig. 4B**). Importantly, exogenous DHNA was sufficient to rescue intra-macrophage replication defects of the Δ*menB*/*pplA*::Tn mutant, suggesting that disruption of EET, in general, does not hinder DHNA utilization (**Fig. 5B**). Taken together, these data further reinforce that Ndh2, independent of its role in EET, is required for DHNA utilization and virulence.

DISCUSSION

Cytosolic pathogens require specific adaptations to survive and replicate within the host. In *L. monocytogenes*, MK biosynthetic intermediate DHNA is among those factors necessary for cytosolic survival, independent of its known role in MK synthesis and cellular respiration (30,

32). In the present study, we sought to address the respiration-independent mechanism by which DHNA is required for the survival and virulence of *L. monocytogenes*. Utilizing a heterologous NOX expression system, we demonstrated that virulence defects associated with loss of DHNA could be rescued by restoration of NAD^+/NADH homeostasis (**Fig. 1, 2**). However, NOX expression did not fully rescue *in vivo* virulence defects back to wild-type levels in DHNA-deficient strains (**Fig. 2C**), possibly due to combined effects of the general lack of *in vivo* fitness of these mutants and the incomplete restoration of NAD^+/NADH levels compared to wild-type (**Fig. 1A**).

We then found that exogenous DHNA supplementation restores NAD^+/NADH balance, cytosolic survival, and intracellular replication of the DHNA-deficient mutant Δ*menB* (**Fig.3**). Balancing of redox homeostasis also coincided with a marked shift in fermentative flux from lactate to acetate upon DHNA production or supplementation (**Fig. 3B**) to maximize ATP production via SLP through the activity of acetate kinase (25, 41). Importantly, we provide evidence that Ndh2 is the NADH dehydrogenase responsible for restoring redox homeostasis during exogenous DHNA utilization (**Fig. 4)**, independent of its role in EET. *In vivo* supplementation of DHNA was unsuccessful due to toxicity of DMSO, the solvent used to deliver DHNA, when injected in mice intravenously. Additionally, DHNA is a known agonist of aryl hydrocarbon receptors, a ligand-activated transcriptional regulator of cellular metabolism and inflammatory responses ((42, 43)), which could lead to unexpected immunomodulatory effects that may prevent accurate *in vivo* virulence assessment. Due to such technical challenges and potential complications, we've determined virulence of the Δ*menB*/*ndh2*::Tn mutant *ex vivo* by assessing intra-macrophage replication. In agreement with our *in vitro* data, the

Δ*menB*/*ndh2*::Tn mutant was not rescued upon DHNA supplementation, suggesting that Ndh2 is required for DHNA-dependent virulence.

Although we've demonstrated that Ndh2 is conditionally essential for DHNA utilization in *L. monocytogenes*, it is still unclear how Ndh2 utilizes DHNA to maintain intracellular redox homeostasis. One possibility is that DHNA, or one of its derivatives, may be used as an alternative quinone to directly accept electrons from Ndh2, regenerating NAD^+ similar to the system recently described in *Shewanella oneidensis* MR-1. Mevers *et al*. recently demonstrated that a derivative of DHNA, 2-amino-3-carboxy-1,4-naphthoquinone (ACNQ), could serve as a novel electron shuttle that functioned to promote redox balance and energy metabolism (44). The authors went on to show that ACNQ is produced non-enzymatically from extracellular DHNA under oxidizing conditions in the presence of a nitrogen donor (i.e. ammonium or amino acids)(44). We have confirmed that indeed, DHNA is secreted by wild-type *L. monocytogenes* (**Fig. S2**) and extracellular DHNA is readily converted to ACNQ in our defined medium based on mass spectrometry analysis (data not shown). Based on this model, it is possible that DHNA produced by *L. monocytogenes* is secreted outside of the cell to shuttle electrons away where it is then freely oxidized non-enzymatically in the local environment to form ACNQ. Newly formed ACNQ would then be imported back into *L. monocytogenes* to be reduced again through the activity of Ndh2. The repeated oxidation and reduction of DHNA and/or ACNQ is the hallmark of an "electron shuttle" and is one of the proposed mechanisms of EET in *S. oneidensis* (44, 45). A strikingly similar model has been described in *Pseudomonas aeruginosa* in which endogenous production of phenazine is cyclically reduced intracellularly, shuttled outside of the cell, and oxidized by a terminal electron acceptor where it is then imported again by the cell (46). Studies to determine whether DHNA/ACNQ fuels an Ndh2-dependent electron shuttle to maintain

intracellular redox homeostasis or whether DHNA works via an alternative mechanism are currently ongoing.

It has been proposed that in addition to serving as an electron shuttle by *P. aeruginosa,* secreted phenazine may be used as a shared resource by the surrounding microbial community to fuel their own redox shuttling (47). The function of phenazine as a shared metabolite is also similar to what has been previously documented with the secretion of DHNA being used as a shared resource to fuel metabolic processes of other localized microbes (32, 37–39). Furthermore, a recent study by Tejedor-Sanz *et al.* reported that the homofermentative lactic acid bacteria *Lactiplantibacillus plantarum* contains the EET gene locus previously annotated in *L. monocytogenes*, however it is missing the upstream genes necessary for quinone biosynthesis (48). Upon addition of exogenous DHNA, *L. plantarum* was observed to employ an Ndh2-dependent form of EET that functioned to increase intracellular redox homeostasis by enhancing metabolic flux through fermentative pathways, generating additional lactate, while increasing ATP generation through SLP (48). Importantly, the capacity of DHNA supplementation to induce EET in *L. plantarum* did not coincide with the generation of a PMF to drive oxidative phosphorylation, similar to the phenotypes observed in *L. monocytogenes*. Whether there are functions of *L. monocytogenes* secreted DHNA as a shared metabolite in complex microbial communities such as those found in the intestine during the early stages of infection will require additional future studies.

Overall, we've shown that *L. monocytogenes* can utilize DHNA to maintain redox homeostasis through the anaerobic-specific NADH dehydrogenase Ndh2, independent of other EET proteins. Utilization of extracellular DHNA can aid DHNA-deficient *L. monocytogenes* mutants to restore their ability to grow and replicate within the cytosol by potentially driving a

yet unclear method of energy metabolism. Pathways involved in unique energy metabolism by various pathogens are increasingly viewed as attractive drug targets and as such future studies utilizing the important model pathogen *L. monocytogenes* to understand the mechanisms of DHNA-dependent redox homeostasis could provide novel insights into the generation of new antimicrobials.

MATERIALS AND METHODS

Bacterial strains, plasmid construction, and growth conditions in vitro

L. monocytogenes strain 10403S is referred to as the wild-type strain, and all other strains used in this study are isogenic derivatives of this parental strain. Vectors were conjugated into *L. monocytogenes* by *Escherichia coli* strain S17 or SM10 (51). The integrative vector pIMK2 was used for constitutive expression of *L. monocytogenes* genes for complementation (52).

L. monocytogenes strains were grown at 37°C or 30°C in brain heart infusion (BHI) medium (237500; VWR) or defined medium supplemented with glucose as the sole carbon source. Defined medium is identical to the formulation described by Smith *et al.* (33). *Escherichia coli* strains were grown in Luria-Bertani (LB) broth at 37°C. Antibiotics were used at concentrations of 100 μg/ml carbenicillin (IB02020; IBI Scientific), 10 μg/ml chloramphenicol (190321; MP Biomedicals), 2 μg/ml erythromycin (227330050; Acros Organics), or 30 μg/ml kanamycin (BP906-5; Fisher Scientific) when appropriate. Medium, where indicated, was supplemented with 5 μM 1,4-dihydroxy-2-naphthoate (DHNA) (281255; Sigma) or 5 μM menaquinone (MK) (V9378; Sigma), both of which were dissolved in DMSO.

Phage Transduction

Phage transductions were performed as previously described (53). Briefly, MACK *L. monocytogenes* was grown overnight in 3mL LB at 30°C stationary to propagate U153 phage stocks. MACK cultures were pelleted and resuspended in LB + 10mM $CaSO_4$ + 10mM $MgCl_2$ and added into LB + 0.7% agar + 10mM $CaSO_4$ + 10mM $MgCl_2$ at 42°C. This mixture was immediately poured on BHI plates and incubated overnight at 30°C. U153 phage plaques were collected and soaked out with 10mM Tris (pH7.5) + 10mM $CaSO_4$ + 10mM $MgCl_2$. Donor plaque soak-outs were propagated the same way and were filter-sterilized using a 0.2µm syringe filter (09-740-113; Fisher Scientific) and additionally kept sterile by adding 500µL chloroform. Recipient Δ*menB* strain was infected with these donor soak-outs for 30 minutes at room temperature and subsequently plated on BHI agar with erythromycin for selection at 37°C.

Intracellular bacteriolysis assay

Standard intracellular bacteriolysis assays were performed as previously described (30). Briefly, primary or immortalized bone marrow-derived *IFNAR* $^{-/-}$ macrophages (5×10^5 per well of 24-well plates) were grown in a monolayer overnight in 500 µL volume. *L. monocytogenes* strains carrying the bacteriolysis reporter pBHE573 (34) were grown at 30°C without shaking overnight. Cultures were then diluted to a final concentration of 5×10^8 CFU/mL in PBS and used to infect macrophages at a MOI of 10. At 1 hr postinfection, media were removed and replaced with media containing 50 µg/ml gentamicin. At 6 hr post infection, media from the wells were aspirated and macrophages were lysed using TNT lysis buffer (20 mM Tris, 200 mM NaCl, 1% Triton [pH 8.0]). Cell lysates were transferred to opaque 96-well plates, and luciferin reagent was added and assayed for luciferase activity (Synergy HT, BioTek; Winooski, VT).

Intracellular growth assay

Bone marrow-derived macrophages (BMDMs) were prepared from C57BL/6 mice as previously described (54). BMDMs were plated on coverslips at 5×10^6 cells per 60mm dish and allowed to adhere overnight. For assays including DHNA treatment, BMDMs were pretreated prior to infection for 30 minutes with media containing 5μM DHNA. BMDMs were then infected at an MOI of 0.2 with their respective strain and infection proceeded for 8 hr. At 30 min postinfection, media were removed and replaced with media containing 50 μg/ml gentamicin. Total CFU were quantified at various time points as previously described (55).

NAD+ and NADH measurements

L. monocytogenes strains were grown in defined medium at 37°C with shaking to mid-logarithmic phase (OD_{600} 0.4-0.6). Cultures were centrifuged and then resuspended in PBS. Resuspended bacteria were then lysed (2×10^8 total CFU) by a 1:1 addition of 1% dodecyltrimethylammonium bromide (DTAB) (AC409310250; Fisher Scientific) for 5 min with agitation. Lysates were then processed to measure NAD^+ and NADH levels using the NAD/NADH-Glo assay (Promega, G9071) per the manufacturer's protocol.

Fermentation byproduct measurements

Cultures of *L. monocytogenes* were grown in BHI at 37°C with shaking overnight. Bacteria were then centrifuged and 1 mL of the resulting supernatant was filtered through a 0.2μm-pore-size syringe filter (09-740-113; Fisher Scientific). Supernatant samples were next treated with 2μL of H_2SO_4 to precipitate any components that might be incompatible with the running buffer. The samples were then centrifuged at 16000 × g for 10 min and then 200μL of each sample transferred to an HPLC vial. HPLC analysis was performed using a ThermoFisher (Waltham, MA) Ultimate 3000 UHPLC system equipped with a UV detector (210 nm).

Compounds were separated on a 250 × 4.6 mm Rezex© ROA-Organic acid LC column (Phenomenex Torrance, CA) run with a flow rate of 0.2 mL min^{-1} and at a column temperature of 50 °C. The samples were held at 4 °C prior to injection. Separation was isocratic with a mobile phase of HPLC grade water acidified with 0.015 N H_2SO_4 (415 μL L^{-1}). At least two standard sets were run along with each sample set. Standards were 100, 20, 4, and 0.8mM concentrations of lactate or acetate. The resultant data was analyzed using the Thermofisher Chromeleon 7 software package.

Acute virulence assay

All techniques were reviewed and approved by the University of Wisconsin — Madison Institutional Animal Care and Use Committee (IACUC) under the protocol M02501. Female C57BL/6 mice (6 to 8 weeks of age; purchased from Charles River) were used for the purposes of this study. *L. monocytogenes* strains were grown in BHI medium at 30°C without shaking overnight. These cultures were then back-diluted the following day 1:5 into fresh BHI medium and grown at 37°C with shaking until mid-exponential phase (OD_{600} 0.4-0.6). Bacteria were diluted in PBS to a concentration of 5×10^5 CFU/mL and mice were injected intravenously with 1×10^5 total CFU. At 48 hr postinfection, spleens and livers were harvested and homogenized in 0.1% Nonidet P-40 in PBS. Homogenates were then plated on LB plates to enumerate CFU and quantify bacterial burdens.

Statistical analysis

Statistical significance analysis (GraphPad Prism, version 6.0h) was determined by one-way analysis of variance (ANOVA) with a Dunnett's posttest comparing wild-type to all other indicated strains or by one-way ANOVA with Tukey's multiple comparisons test unless otherwise stated (*, $P \leq 0.05$; **, $P \leq 0.01$; ***, $P \leq 0.001$; ****, $P \leq 0.0001$).

ACKNOWLEDGEMENTS

We would like to thank Dr. Samuel Light for providing the vector pPL2-NOX, expressing the water-forming NADH oxidase for integration into *Listeria monocytogenes*.

FUNDING INFORMATION

This work was funded by the National Institutes of Health (T32007215 [HBS] and R01AI137070 [J-D S]). The funders had no role in study design, data collection and interpretation, or the decision to submit the work for publication.

FIGURES

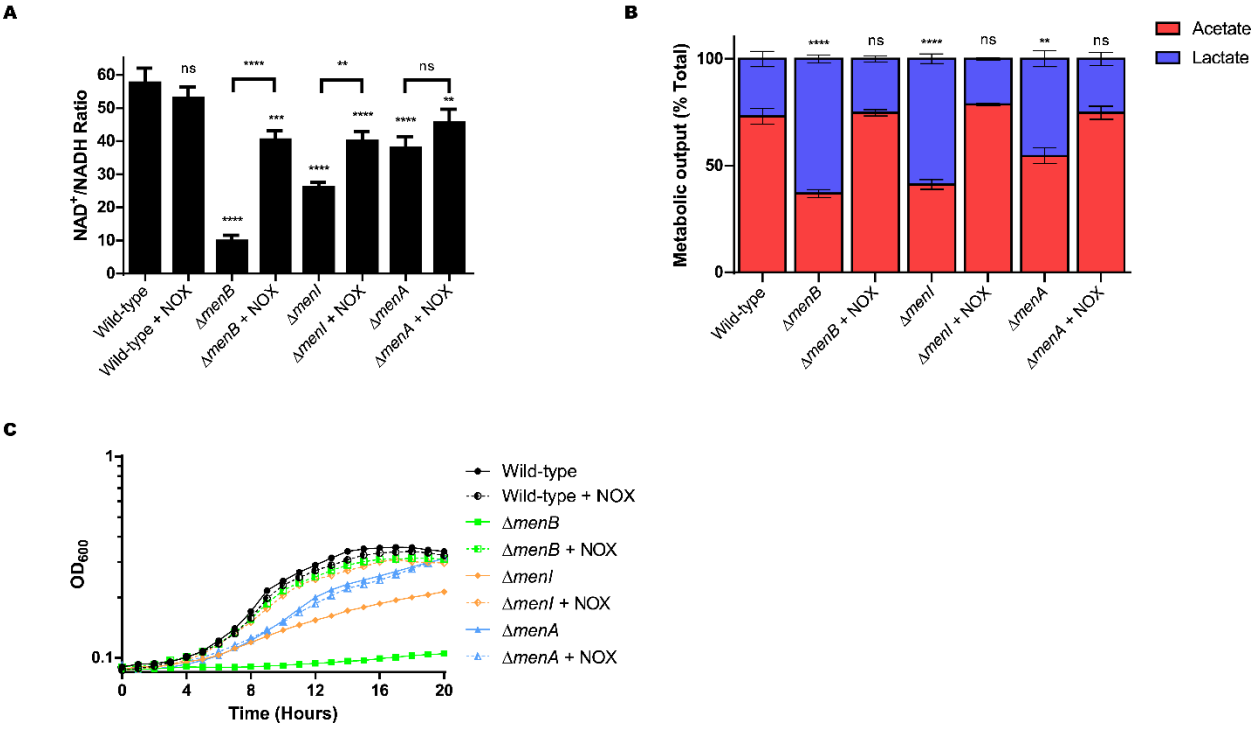

Figure 1. Redox homeostasis via NOX shifts fermentative output and rescues in vitro growth of DHNA-deficient *L. monocytogenes*. (A) NAD^+/NADH ratios of indicated *L. monocytogenes* strains +/- NOX plasmid complementation grown aerobically at 37°C in defined medium to mid-logarithmic phase (OD_{600} 0.4-0.6). Δ*menB* mutant fails to grow in defined medium, thus these culture samples were spiked with 2×10^8 total CFU from an overnight BHI culture during experimental setup. (B) HPLC quantification of fermentation products (Lactate and Acetate) produced and secreted by indicated *L. monocytogenes* strains +/- NOX plasmid complementation grown in BHI media aerobically at 37°C to stationary phase. (C) *L. monocytogenes* strains +/- NOX plasmid complementation were grown in defined medium at 37°C. OD_{600} was monitored for 20 hours. Data are representative of three (A, C) or two (B) independent experiments. ns, not significant; WT, wild-type

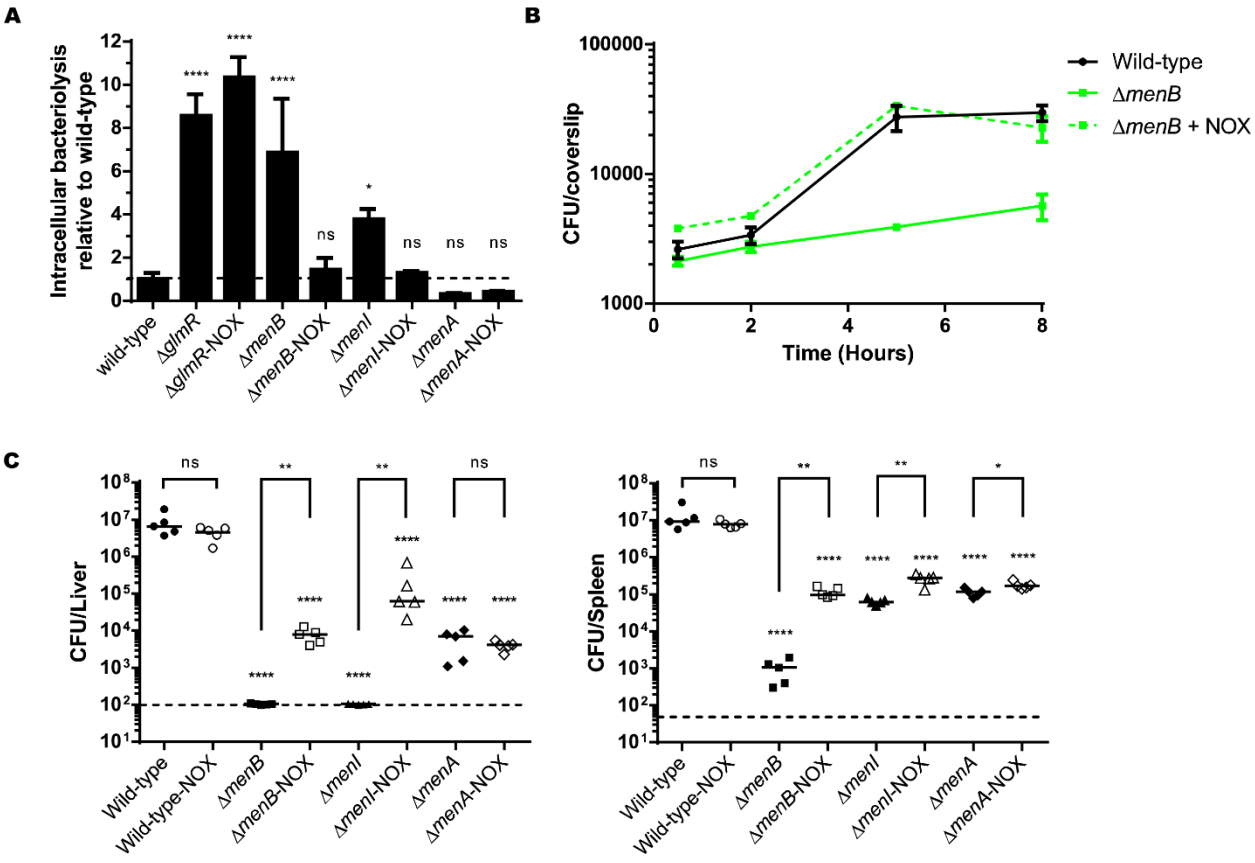

Figure 2. Restoration of redox homeostasis rescues virulence defects associated with DHNA-deficiency. (A) Indicated *L. monocytogenes* strains (MOI of 10) +/- NOX plasmid complementation were tested for cytosolic survival in immortalized IFNAR$^{-/-}$ bone marrow-derived macrophages (BMDM) over a 6 hr infection. Data are normalized to wild-type levels of bacteriolysis and presented as the standard deviation of the means from three independent experiments. (B) Intracellular growth of wild-type, Δ*menB*, or Δ*menB*-NOX was determined in BMDMs following infection at an MOI of 0.2. Growth curves are representative of at least three independent experiments. Error bars represent the standard deviation of the means of technical triplicates within the representative experiment. (C) Bacterial burdens from the spleen and liver were enumerated at 48 hr post-intravenous infection with 1×10^5 total CFU of indicated *L. monocytogenes* strains +/- NOX plasmid complementation. Data are representative of results

from two independent experiments. Horizontal bars represent the limits of detection and the bars associated with the individual strains represents the mean of the group. ns, not significant.

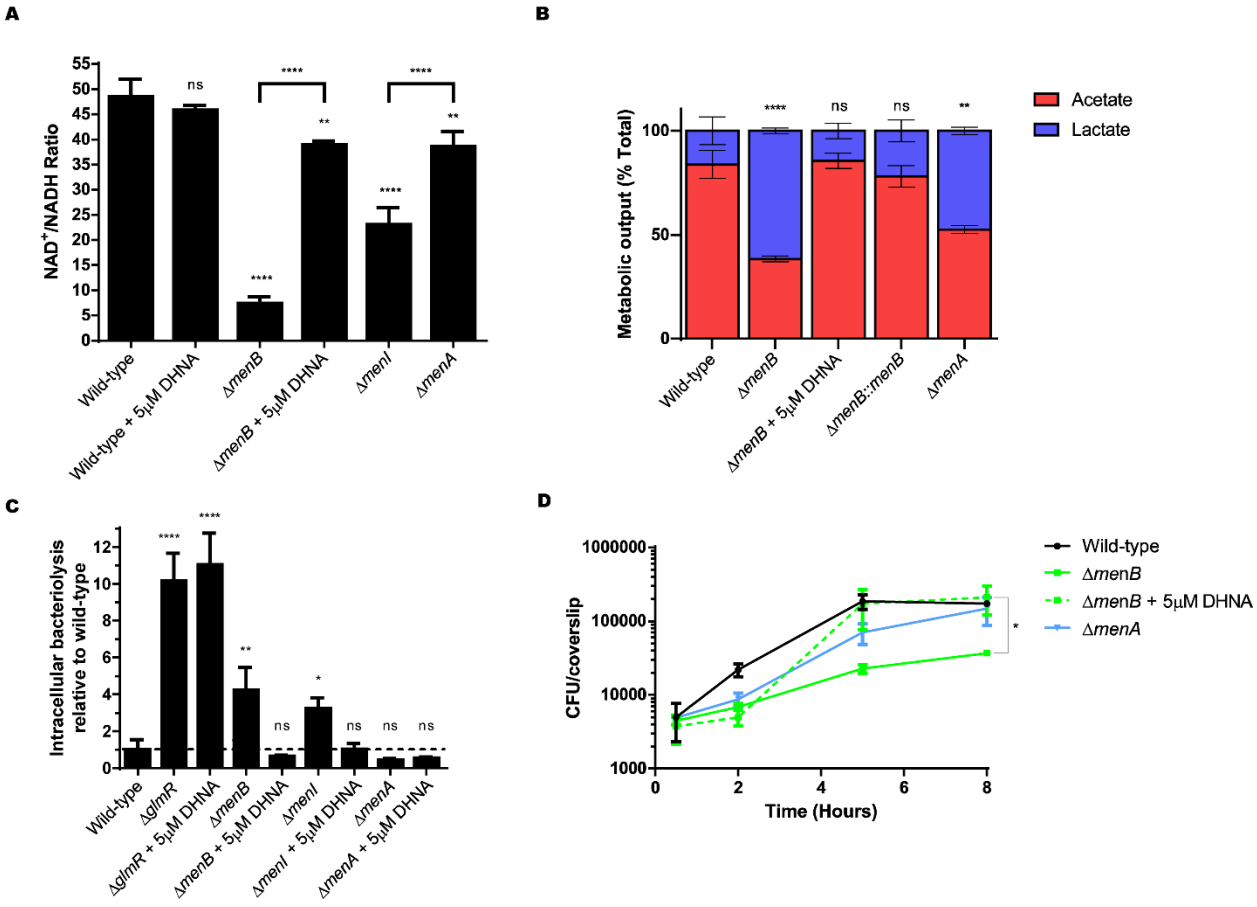

Figure 3. DHNA production or supplementation promotes similar effects to NOX complementation in *L. monocytogenes*. (A) NAD^+/NADH ratios of indicated *L. monocytogenes* strains +/- 5μM exogenous DHNA supplementation grown aerobically at 37°C in defined medium to mid-logarithmic phase. Again, Δ*menB* were spiked with 2×10^8 total CFU from an overnight BHI culture during experimental setup. Data are presented as the standard deviation of the means from three independent experiments. (B) HPLC quantification of fermentation products (Lactate and Acetate) produced and secreted by indicated *L. monocytogenes* strains +/- exogenous DHNA supplementation grown in BHI media aerobically at 37°C to stationary phase. Data are representative of two independent experiments. (C) Indicated *L. monocytogenes* strains (MOI of 10) +/- DHNA supplementation were tested for cytosolic survival in primary IFNAR -/-

BMDMs over a 6 hr infection. Data are normalized to wild-type levels of bacteriolysis and presented as the standard deviation of the means from three independent experiments. (D) Intracellular growth of wild-type, Δ*menB*, or Δ*menA* was determined in BMDMs following infection at an MOI of 0.2. Growth curves are representative of at least three independent experiments. Error bars represent the standard deviation of the means of technical triplicates within the representative experiment. ns, not significant.

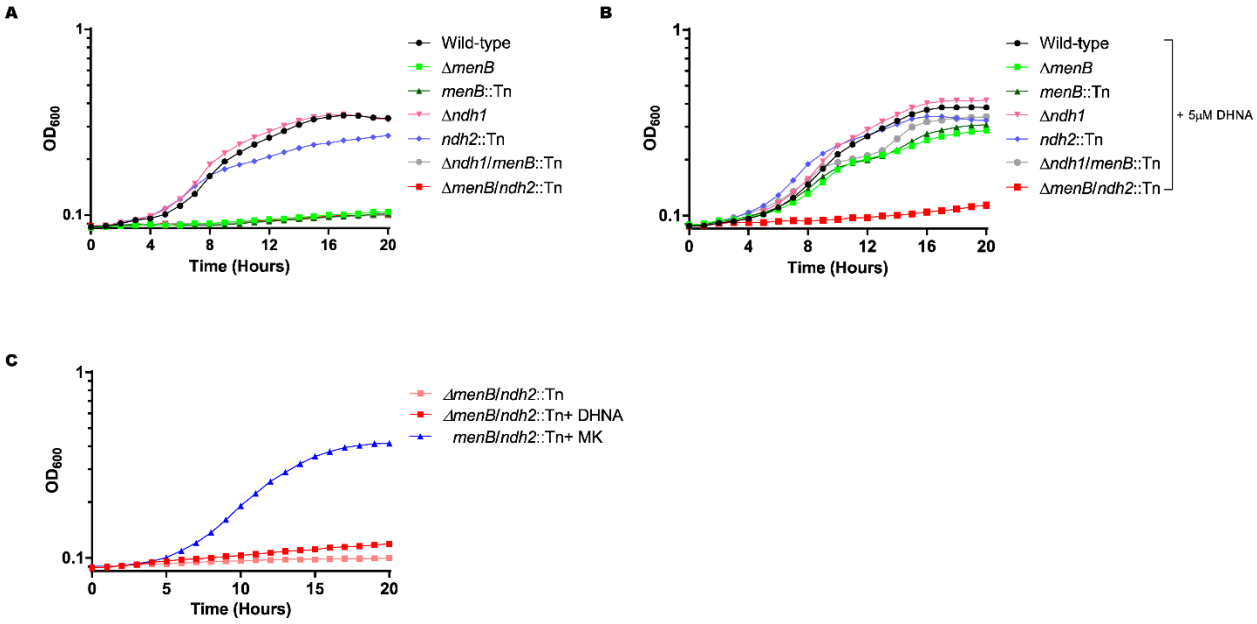

Figure 4. Ndh2 is conditionally essential for DHNA utilization *in vitro*. Indicated strains of *L. monocytogenes* were grown in defined medium without (A) or with (B) 5μM DHNA supplementation aerobically at 37°C and monitored for OD_{600} over 20 hr. (C) Δ*menB*/*ndh2*::Tn *L. monocytogenes* was grown aerobically in defined medium with either 5μM DHNA or 5μM MK and monitored for growth (OD_{600}) over 20 hr. All data represent one representative out of three biological replicates.

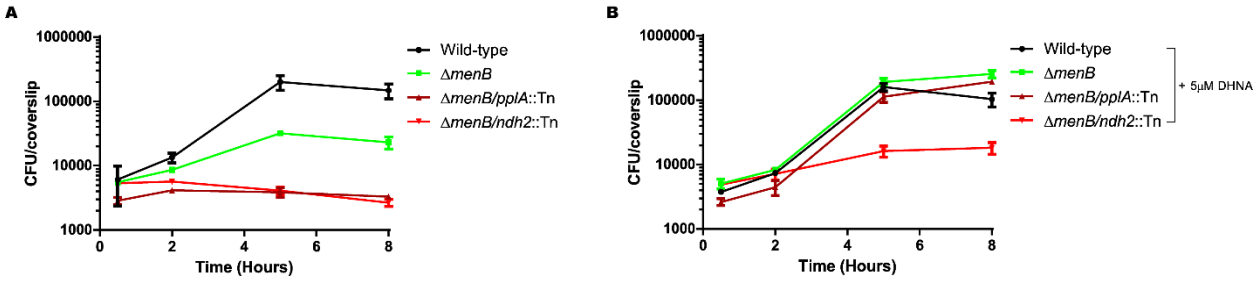

Figure 5. Ndh2 is necessary for DHNA utilization in macrophages *ex vivo*. Intracellular growth of indicated strains of *L. monocytogenes* was assayed in both untreated and DHNA-treated BMDMs at an MOI of 0.2. BMDMs were treated with media containing 5μM DHNA for 30 minutes prior to infection. Growth curves are representative of two independent experiments. Error bars represent the standard deviation of the means of technical triplicates within the representative experiment.

SUPPLEMENTAL INFORMATION

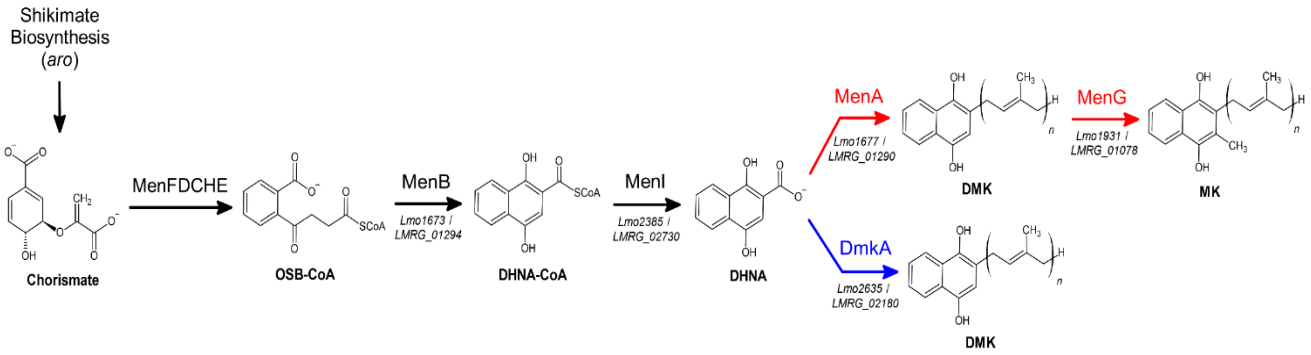

Figure S1. Menaquinone biosynthetic pathway in *Listeria monocytogenes*. Chorismate is generated by the upstream shikimate biosynthesis pathway and is converted to DHNA by the series of listed enzymes (MenFDCHEBI). Red arrows indicate DHNA branching point towards aerobic respiration. Blue arrow indicates DHNA branching point towards anaerobic respiration. Corresponding gene locus numbers for *L. monocytogenes* strains EGD-e (*Lmo*) and 10403S (*LMRG*; parental strain used in this study) are listed underneath reaction arrows. OSB, *o*-succinylbenzoate; DMK, demethylmenaquinone.

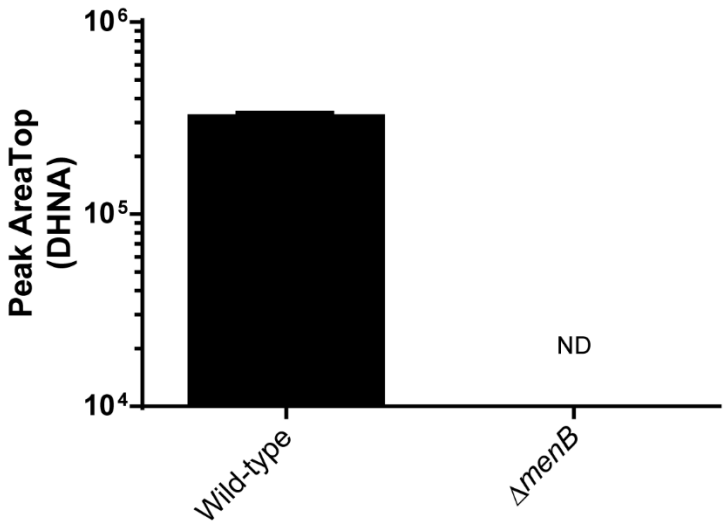

Figure S2. Detection of secreted DHNA by mass spectrometry. Detection of DHNA from the cell-free supernatants of overnight aerobic cultures of wildtype or Δ*menB* strains by mass spectrometry. Data were analyzed via Metabolomics Analysis and Visualization Engine (MAVEN) (49, 50) and plotted for Peak AreaTop, the mean signal intensity of the three top points in the peak identified as DHNA. Error bars represent the standard deviation of the means from two independent experiments. ND, not detected.

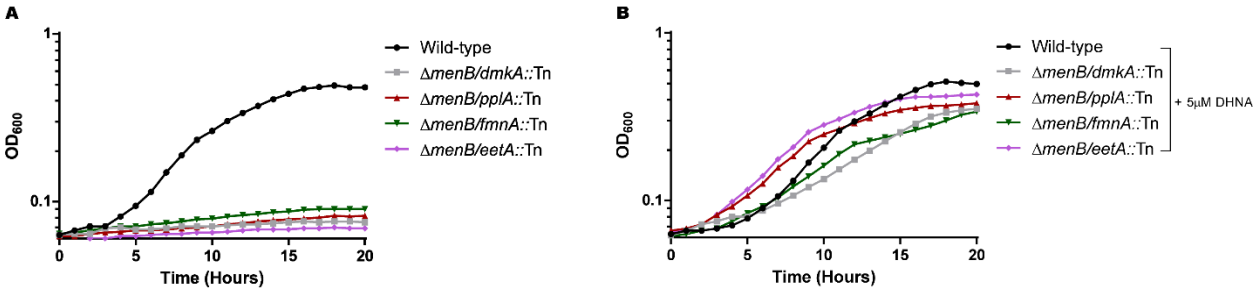

Figure S3. Other EET mutants in a Δ*menB* background were rescued upon DHNA supplementation *in vitro*. Indicated strains were grown in defined medium at 37°C with the addition of 5μM DHNA. OD_{600} was monitored for 20 hours. Data represents one representative out of three biological replicates.

Table S3.1 Strains used in this study.

Strain	Description	Reference
XL1-Blue	Competent *E. coli* strain	-
SM10	*E. coli* strain for conjugations into *Lm;* Km^R	(51)
10403S	Parental *L. monocytogenes* (*Lm*) 10403s strain [Wild-type]	-
JDS18	*Lm* with pBHE573	(34)
HS28	*Lm* with pPL2-NOX	(25)
JDS2328	*Lm* with pBHE573 and pPL2-NOX	(25)
JDS25	*Lm* Δ*glmR*	(34)
JDS21	*Lm* Δ*glmR* with pBHE573	(34)
JDS2327	*Lm* Δ*glmR* with pPL2-NOX	This work
JDS2329	*Lm* Δ*glmR* with pBHE573 and pPL2-NOX	(25)
JDS1161	*Lm* Δ*menB*	(30)
JDS1175	*Lm* Δ*menB* with pYL116	(33)
JDS1958	*Lm* Δ*menB* with pPL2-NOX	(25)
JDS1191	*Lm* Δ*menB* with pBHE573	(30)
JDS2333	*Lm* Δ*menB* with pBHE573 and pPL2-NOX	(25)
JDS2240	*Lm* Δ*menI*	(33)
JDS2155	*Lm* Δ*menI* with pBHE573	(33)
JDS2325	*Lm* Δ*menI* with pPL2-NOX	This work
JDS2326	*Lm* Δ*menI* with pBHE573 and pPL2-NOX	This work
JDS1047	*Lm* Δ*menA*	(30)
JDS813	*Lm* Δ*menA* with pBHE573	(30)
HS30	*Lm* Δ*menA* with pPL2-NOX	This work
JDS2330	*Lm* Δ*menA* with pBHE573 and pPL2-NOX	This work
JDS1213	*Lm* Δ*menD*	(56)
JDS17	SM10 *E. coli* with pBHE537	(34)
JDS1957	SM10 *E. coli* with pPL2-NOX	(25)
KL1	*Lm* Δ*ndh1*/*menB*::Tn	This work
KL4	*Lm* Δ*menB*/*ndh2*::Tn	This work
KL9	*Lm* Δ*menB*/*dmkA*::Tn	This work
KL10	*Lm* Δ*menB*/*pplA*::Tn	This work
KL11	*Lm* Δ*menB*/*fmnA*::Tn	This work
KL12	*Lm* Δ*menB*/*eetA*::Tn	This work

Table S3.2 Plasmids used in this study.

Plasmids	Description	Reference
pBHE573	Bacteriolysis reporter; Cam^R	(34)
pIMK2	Constitutive expression vector for complementation, P_{help}; Kan^R	(52)
pYL116	*menB* cloned into pIMK2	(33)
pPL2-NOX	NADH oxidase (NOX) cloned into the backbone of pPL2	(25)

REFERENCES

1. Goetz M, Bubert A, Wang G, Chico-Calero I, Vazquez-Boland JA, Beck M, Slaghuis J, Szalay AA, Goebel W. 2001. Microinjection and growth of bacteria in the cytosol of mammalian host cells. Proc Natl Acad Sci U S A 98:12221–12226.

2. Freitag NE, Port GC, Miner MD. 2009. Listeria monocytogenes — from saprophyte to intracellular pathogen. Nature Reviews Microbiology 2009 7:9 7:623–628.

3. Ray K, Marteyn B, Sansonetti PJ, Tang CM. 2009. Life on the inside: the intracellular lifestyle of cytosolic bacteria. Nature Reviews Microbiology 2009 7:5 7:333–340.

4. Beuzón CR, Salcedo SP, Holden DW. 2002. Growth and killing of a Salmonella enterica serovar Typhimurium sifA mutant strain in the cytosol of different host cell lines. Microbiology (N Y) 148:2705–2715.

5. Brumell JH, Rosenberger CM, Gotto GT, Marcus SL, Finlay BB. 2001. SifA permits survival and replication of Salmonella typhimurium in murine macrophages. Cell Microbiol 3:75–84.

6. Laguna RK, Creasey EA, Li Z, Valtz N, Isberg RR. 2006. A Legionella pneumophila-translocated substrate that is required for growth within macrophages and protection from host cell death. Proc Natl Acad Sci U S A 103:18745–18750.

7. Slaghuis J, Goetz M, Engelbrecht F, Goebel W. 2004. Inefficient Replication of Listeria innocua in the Cytosol of Mammalian Cells. Journal of Infectious Diseases 189:393–401.

8. Zhang Y, Yeruva V, Marinov A, Wyrick P, Lupashin V, Nagarajan U. 2014. The DNA sensor, cyclic GMP-AMP synthase (cGAS) is essential for induction of IFN beta during Chlamydia trachoma tis infection (INM6P.407). The Journal of Immunology 192:122.4-122.4.

9. Ge J, Gong YN, Xu Y, Shao F. 2012. Preventing bacterial DNA release and absent in melanoma 2 inflammasome activation by a Legionella effector functioning in membrane trafficking. Proc Natl Acad Sci U S A 109:6193–6198.

10. Collins AC, Cai H, Li T, Franco LH, Li XD, Nair VR, Scharn CR, Stamm CE, Levine B, Chen ZJ, Shiloh MU. 2015. Cyclic GMP-AMP Synthase Is an Innate Immune DNA Sensor for Mycobacterium tuberculosis. Cell Host Microbe 17:820–828.

11. Watson RO, Bell SL, MacDuff DA, Kimmey JM, Diner EJ, Olivas J, Vance RE, Stallings CL, Virgin HW, Cox JS. 2015. The Cytosolic Sensor cGAS Detects Mycobacterium tuberculosis DNA to Induce Type I Interferons and Activate Autophagy. Cell Host Microbe 17:811–819.

12. Wassermann R, Gulen MF, Sala C, Perin SG, Lou Y, Rybniker J, Schmid-Burgk JL, Schmidt T, Hornung V, Cole ST, Ablasser A. 2015. Mycobacterium tuberculosis Differentially Activates cGAS- and Inflammasome-Dependent Intracellular Immune Responses through ESX-1. Cell Host Microbe 17:799–810.

13. McNab F, Mayer-Barber K, Sher A, Wack A, O'Garra A. 2015. Type I interferons in infectious disease. Nature Reviews Immunology 2015 15:2 15:87–103.

14. Portnoy DA, Auerbuch V, Glomski IJ. 2002. The cell biology of Listeria monocytogenes infection the intersection of bacterial pathogenesis and cell-mediated immunity. Journal of Cell Biology 158:409–414.

15. Vázquez-Boland JA, Kuhn M, Berche P, Chakraborty T, Domínguez-Bernal G, Goebel W, González-Zorn B, Wehland J, Kreft J. 2001. Listeria Pathogenesis and Molecular Virulence Determinants. Clin Microbiol Rev 14:584.

16. Portnoy DA, Suzanne Jacks P, Hinrichs DJ. 1988. Role of hemolysin for the intracellular growth of Listeria monocytogenes. Journal of Experimental Medicine 167:1459–1471.

17. Tilney LG, Portnoy DA. 1989. Actin filaments and the growth, movement, and spread of the intracellular bacterial parasite, Listeria monocytogenes. Journal of Cell Biology 109:1597–1608.

18. Brundage RA, Smith GA, Camilli A, Theriot JA, Portnoy DA. 1993. Expression and phosphorylation of the Listeria monocytogenes ActA protein in mammalian cells. Proc Natl Acad Sci U S A 90:11890–4.

19. Moors MA, Levitt B, Youngman P, Portnoy DA. 1999. Expression of listeriolysin O and ActA by intracellular and extracellular Listeria monocytogenes. Infect Immun 67:131–9.

20. Shetron-Rama LM, Marquis H, Bouwer HGA, Freitag NE. 2002. Intracellular induction of Listeria monocytogenes actA expression. Infect Immun 70:1087–96.

21. Smith GA, Marquis H, Jones S, Johnston NC, Portnoy DA, Goldfine H. 1995. The two distinct phospholipases C of Listeria monocytogenes have overlapping roles in escape from a vacuole and cell-to-cell spread. Infect Immun 63:4231–7.

22. Sauer J-D, Herskovits AA, O'Riordan MXD. 2019. Metabolism of the Gram-Positive Bacterial Pathogen Listeria monocytogenes. Microbiol Spectr 7.

23. Glaser P, Frangeul L, Buchrieser C, Rusniok C, Amend A, Baquero F, Berche P, Bloecker H, Brandt P, Chakraborty T, Charbit A, Chetouani F, Couvé E, de Daruvar A, Dehoux P, Domann E, Domínguez-Bernal G, Duchaud E, Durant L, Dussurget O, Entian KD, Fsihi H, García-del Portillo F, Garrido P, Gautier L, Goebel W, Gómez-López N, Hain T, Hauf J, Jackson D, Jones LM, Kaerst U, Kreft J, Kuhn M, Kunst F, Kurapkat G, Madueno E, Maitournam A, Vicente JM, Ng E, Nedjari H, Nordsiek G, Novella S, de Pablos B, Pérez-Diaz JC, Purcell R, Remmel B, Rose M, Schlueter T, Simoes N, Tierrez A, Vázquez-Boland JA, Voss H, Wehland J, Cossart P. 2001. Comparative genomics of Listeria species. Science 294:849–52.

24. Romick TL, Fleming HP, McFeeters RF. 1996. Aerobic and anaerobic metabolism of Listeria monocytogenes in defined glucose medium. Appl Environ Microbiol 62:304–7.

25. Rivera-Lugo R, Deng D, Anaya-Sanchez A, Tejedor-Sanz S, Tang E, Reyes Ruiz VM, Smith HB, Titov D V, Sauer J-D, Skaar EP, Ajo-Franklin CM, Portnoy DA, Light SH. 2022. Listeria monocytogenes requires cellular respiration for NAD+ regeneration and pathogenesis. Elife 11.
26. Light SH, Su L, Rivera-Lugo R, Cornejo JA, Louie A, Iavarone AT, Ajo-Franklin CM, Portnoy DA. 2018. A flavin-based extracellular electron transfer mechanism in diverse Gram-positive bacteria. Nature 562:140–144.

27. Meganathan R. 2001. Biosynthesis of menaquinone (vitamin K2) and ubiquinone (coenzyme Q): a perspective on enzymatic mechanisms. Vitam Horm 61:173–218.

28. Corbett D, Goldrick M, Fernandes VE, Davidge K, Poole RK, Andrew PW, Cavet J, Roberts IS. 2017. Listeria monocytogenes Has Both Cytochrome bd-Type and Cytochrome aa 3-Type Terminal Oxidases, Which Allow Growth at Different Oxygen Levels, and Both Are Important in Infection. Infect Immun 85.

29. Light SH, Méheust R, Ferrell JL, Cho J, Deng D, Agostoni M, Iavarone AT, Banfield JF, D'Orazio SEF, Portnoy DA. 2019. Extracellular electron transfer powers flavinylated extracellular reductases in Gram-positive bacteria. Proc Natl Acad Sci U S A 116:26892–26899.

30. Chen GY, McDougal CE, D'Antonio MA, Portman JL, Sauer J-D. 2017. A Genetic Screen Reveals that Synthesis of 1,4-Dihydroxy-2-Naphthoate (DHNA), but Not Full-Length Menaquinone, Is Required for Listeria monocytogenes Cytosolic Survival. mBio 8.

31. Stritzker J, Janda J, Schoen C, Taupp M, Pilgrim S, Gentschev I, Schreier P, Geginat G, Goebel W. 2004. Growth, virulence, and immunogenicity of Listeria monocytogenes aro mutants. Infect Immun 72:5622–9.

32. Chen GY, Kao C-Y, Smith HB, Rust DP, Powers ZM, Li AY, Sauer J-D. 2019. Mutation of the Transcriptional Regulator YtoI Rescues Listeria monocytogenes Mutants Deficient in the Essential Shared Metabolite 1,4-Dihydroxy-2-Naphthoate (DHNA). Infect Immun 88.

33. Smith HB, Li TL, Liao MK, Chen GY, Guo Z, Sauer J-D. 2021. Listeria monocytogenes MenI Encodes a DHNA-CoA Thioesterase Necessary for Menaquinone Biosynthesis, Cytosolic Survival, and Virulence. Infect Immun 89.

34. Sauer J-D, Witte CE, Zemansky J, Hanson B, Lauer P, Portnoy DA. 2010. Listeria monocytogenes triggers AIM2-mediated pyroptosis upon infrequent bacteriolysis in the macrophage cytosol. Cell Host Microbe 7:412–9.

35. Pensinger DA, Gutierrez K V., Smith HB, Vincent WJB, Stevenson DS, Black KA, Perez-Medina KM, Dillard JP, Rhee KY, Amador-Noguez D, Huynh TN, Sauer J-D. 2021. Listeria monocytogenes GlmR is an accessory uridyltransferase essential for cytosolic survival and virulence. bioRxiv 2021.10.27.466214.

36. Pensinger DA, Boldon KM, Chen GY, Vincent WJB, Sherman K, Xiong M, Schaenzer AJ, Forster ER, Coers J, Striker R, Sauer J-D. 2016. The Listeria monocytogenes PASTA Kinase PrkA and Its

Substrate YvcK Are Required for Cell Wall Homeostasis, Metabolism, and Virulence. PLoS Pathog 12:e1006001.

37. Isawa K, Hojo K, Yoda N, Kamiyama T, Makino S, Saito M, Sugano H, Mizoguchi C, Kurama S, Shibasaki M, Endo N, Sato Y. 2002. Isolation and identification of a new bifidogenic growth stimulator produced by Propionibacterium freudenreichii ET-3. Biosci Biotechnol Biochem 66:679–81.
38. Kang J-E, Kim T-J, Moon G-S. 2015. A Novel Lactobacillus casei LP1 Producing 1,4-Dihydroxy-2-Naphthoic Acid, a Bifidogenic Growth Stimulator. Prev Nutr Food Sci 20:78–81.

39. Franza T, Delavenne E, Derré-Bobillot A, Juillard V, Boulay M, Demey E, Vinh J, Lamberet G, Gaudu P. 2016. A partial metabolic pathway enables group b streptococcus to overcome quinone deficiency in a host bacterial community. Mol Microbiol 102:81–91.

40. Lencina AM, Franza T, Sullivan MJ, Ulett GC, Ipe DS, Gaudu P, Gennis RB, Schurig-Briccio LA. 2018. Type 2 NADH Dehydrogenase Is the Only Point of Entry for Electrons into the Streptococcus agalactiae Respiratory Chain and Is a Potential Drug Target. mBio 9.

41. Hunt KA, Flynn JM, Naranjo B, Shikhare ID, Gralnick JA. 2010. Substrate-level phosphorylation is the primary source of energy conservation during anaerobic respiration of Shewanella oneidensis strain MR-1. J Bacteriol 192:3345–51.

42. Cheng Y, Jin U-H, Davidson LA, Chapkin RS, Jayaraman A, Tamamis P, Orr A, Allred C, Denison MS, Soshilov A, Weaver E, Safe S. 2017. Microbial-Derived 1,4-Dihydroxy-2-naphthoic Acid and Related Compounds as Aryl Hydrocarbon Receptor Agonists/Antagonists: Structure-Activity Relationships and Receptor Modeling. Toxicol Sci 155:458–473.

43. Fukumoto S, Toshimitsu T, Matsuoka S, Maruyama A, Oh-Oka K, Takamura T, Nakamura Y, Ishimaru K, Fujii-Kuriyama Y, Ikegami S, Itou H, Nakao A. 2014. Identification of a probiotic bacteria-derived activator of the aryl hydrocarbon receptor that inhibits colitis. Immunol Cell Biol 92:460–5.

44. Mevers E, Su L, Pishchany G, Baruch M, Cornejo J, Hobert E, Dimise E, Ajo-Franklin CM, Clardy J. 2019. An elusive electron shuttle from a facultative anaerobe. Elife 8.

45. Brutinel ED, Gralnick JA. 2012. Shuttling happens: soluble flavin mediators of extracellular electron transfer in Shewanella. Appl Microbiol Biotechnol 93:41–8.

46. Wang Y, Kern SE, Newman DK. 2010. Endogenous phenazine antibiotics promote anaerobic survival of Pseudomonas aeruginosa via extracellular electron transfer. J Bacteriol 192:365–9.

47. Rabaey K, Boon N, Höfte M, Verstraete W. 2005. Microbial phenazine production enhances electron transfer in biofuel cells. Environ Sci Technol 39:3401–8.

48. Tejedor-Sanz S, Stevens ET, Li S, Finnegan P, Nelson J, Knoesen A, Light SH, Ajo-Franklin CM, Marco ML. 2022. Extracellular electron transfer increases fermentation in lactic acid bacteria via a hybrid metabolism. Elife 11.

49. Melamud E, Vastag L, Rabinowitz JD. 2010. Metabolomic analysis and visualization engine for LC-MS data. Anal Chem 82:9818–26.

50. Clasquin MF, Melamud E, Rabinowitz JD. 2012. LC-MS data processing with MAVEN: a metabolomic analysis and visualization engine. Curr Protoc Bioinformatics Chapter 14:Unit14.11.

51. Simon R, Priefer U, Pühler A. 1983. A Broad Host Range Mobilization System for In Vivo Genetic Engineering: Transposon Mutagenesis in Gram Negative Bacteria. Bio/Technology 784–791.

52. Monk IR, Gahan CGM, Hill C. 2008. Tools for functional postgenomic analysis of listeria monocytogenes. Appl Environ Microbiol 74:3921–34.

53. Hodgson DA. 2000. Generalized transduction of serotype 1/2 and serotype 4b strains of Listeria monocytogenes. Mol Microbiol 35:312–23.

54. Jones S, Portnoy DA. 1994. Characterization of Listeria monocytogenes pathogenesis in a strain expressing perfringolysin O in place of listeriolysin O. Infect Immun 62:5608–13.

55. Rohmer L, Hocquet D, Miller SI. 2011. Are pathogenic bacteria just looking for food? Metabolism and microbial pathogenesis. Trends Microbiol 19:341–8.

56. Perry KJ, Higgins DE. 2013. A differential fluorescence-based genetic screen identifies Listeria monocytogenes determinants required for intracellular replication. J Bacteriol 195:3331–40.

Appendix 2 – C-di-AMP accumulation disrupts glutathione metabolism in *Listeria monocytogenes*

Authors and their contributions:

Cheta Siletti: Planned, organized, design and conducted experiments, and wrote and edited this manuscript
Matthew Freeman: Planned, organized, design and conducted experiments, and wrote and edited this manuscript

- Experiments planned and conducted include Figures 6.

Justin Dang: Planned, organized, design and conducted experiments, and wrote and edited this manuscript
Zepeng Tu: Planned, organized, design and conducted experiments, and wrote and edited this manuscript
David M. Stevenson: Planned, organized, design and conducted experiments, and wrote and edited this manuscript
Daniel Amador-Noguez: Supervised writing and editing of this manuscript
John-Demian Sauer: Supervised writing and editing of this manuscript
Tu-Anh N. Huynh: Supervised writing and editing of this manuscript

As published from Siletti *et. al*., *Infection and Immunity*, December 2024

ABSTRACT

C-di-AMP is an essential second messenger that regulates many cellular processes in bacterial cells. Unregulated c-di-AMP accumulation confers several phenotypes related to stress response, cell wall integrity, and virulence. Except for osmotic stress response, the molecular mechanisms underlying these phenotypes are not well defined. A *Listeria monocytogenes* mutant lacking both c-di-AMP phosphodiesterases, denoted as the ΔPDE mutant, accumulates a high c-di-AMP level and is significantly attenuated in the mouse model of systemic infection. We therefore utilized the ΔPDE mutant to define the molecular functions of c-di-AMP. Our transcriptomic analysis revealed that the ΔPDE mutant is significantly impaired for the expression of virulence genes regulated by the master transcription factor PrfA, which is activated by reduced glutathione (GSH) during infection. Subsequent quantitative gene expression analyses revealed that the ΔPDE strain is defective for PrfA-regulated gene expression both at the basal level and upon activation by GSH. We further found the ΔPDE strain to be significantly depleted for cytoplasmic GSH, and impaired for GSH uptake. The ΔPDE strain was also deficient in GSH under conditions that activate GSH synthesis by the synthase GshF, and upon constitutive expression of *gshF*, suggesting that c-di-AMP accumulation inhibits GSH synthesis activity or promotes GSH catabolism. A constitutively active PrfA* variant, PrfA G145S, which mimics the GSH-bound conformation, restored virulence gene expression in ΔPDE in broth cultures supplemented with GSH, but did not rescue virulence defect in a mouse model of infection. Therefore, virulence attenuation at high c-di-AMP is likely associated with defects outside of the PrfA regulon. For instance, the ΔPDE strain was sensitive to oxidative stress, a phenotype partially attributed to GSH deficiency. Our data highlights the complex role of c-di-AMP in bacterial pathogenesis, and reveals GSH metabolism as another pathway that is regulated by c-di-AMP.

IMPORTANCE

C-di-AMP regulates both bacterial pathogenesis and interactions with the host. Although c-di-AMP is essential in many bacteria, its accumulation also attenuates the virulence of many bacterial pathogens. Therefore, disrupting c-di-AMP homeostasis is a promising antibacterial treatment strategy, and has inspired several studies that screened for chemical inhibitors of c-di-AMP phosphodiesterases. However, the molecular functions of c-di-AMP are still not fully defined, and the underlying mechanisms for attenuated virulence at high c-di-AMP levels are unclear. Our analyses in *L. monocytogenes* indicate that virulence-related defects are likely outside of the virulence gene regulon. We found c-di-AMP accumulation to impair *L. monocytogenes* virulence gene expression and disrupt GSH metabolism. Further studies are necessary to establish the relative contributions of these regulations to virulence and host adaptation.

INTRODUCTION

The Gram-positive bacterial pathogen *Listeria monocytogenes* is a leading cause of mortality and hospitalization among foodborne illnesses. Although acquired orally, *L. monocytogenes* can cross the intestinal barrier to cause systemic infection with mortality rates approaching 16% in clinical cases (1). A hallmark of *L. monocytogenes* pathogenesis is its intracellular life cycle (2). *L. monocytogenes* can invade many mammalian cell types, including non-phagocytic cells, using surface-anchored internalins such as InlA and InlB. Following host-cell entry, *L. monocytogenes* escapes the vacuole using the pore-forming toxin listeriolysin O (LLO, encoded by the *hly* gene), the phospholipases PlcA and PlcB, and the metalloprotease Mpl. In the cell cytosol, *L. monocytogenes* uses ActA to polymerize host actin, required for intracellular motility and cell-to-cell spread. All virulence genes required for the intracellular lifestyle, including those listed above, are transcriptionally regulated by the master transcription factor PrfA (3).

PrfA belongs to the Crp/Fnr family of transcription factors, which function as homodimers with a DNA-binding helix-turn-helix motif in each monomer (3, 4). Unlike other Crp/Fnr proteins that require a co-factor for DNA binding, apo-PrfA can bind to its consensus palindromic DNA operator, called PrfA box, to maintain a basal expression of some virulence genes in the absence of activating signals. During infection, PrfA is allosterically activated by reduced glutathione (GSH), which is derived from the host or synthesized by *L. monocytogenes* (5). GSH binds PrfA at the stoichiometry of one GSH per PrfA monomer, inducing an active DNA-binding conformation of the helix-turn-helix motif (6). A single mutation (G145S) near the GSH binding site renders PrfA constitutively active by mimicking the GSH-bound conformation (6, 7). During broth growth in *Listeria* Synthetic Medium (LSM), PrfA can be activated by supplementation with GSH or reducing reagents such as TCEP (8).

L. monocytogenes makes and secretes c-di-AMP, a nucleotide second messenger that regulates many molecular targets in bacterial cells (9, 10). C-di-AMP-binding proteins within *L. monocytogenes* have different cellular functions, such as potassium and carnitine uptake, central metabolism and ppGpp synthesis, and signal transduction (11–15). During infection, secreted c-di-AMP is recognized by mammalian cytosolic receptors to activate inflammatory and type I interferon responses (9, 16). Type I interferon response promotes *L. monocytogenes* pathogenesis in an intravenous model of infection (17). By contrast, secreted c-di-AMP activates an antibacterial response during foodborne infection, although this response is mediated by STING rather than type I interferon signaling (18).

C-di-AMP homeostasis is critical to *L. monocytogenes* growth and infection. In *L. monocytogenes*, c-di-AMP is synthesized from ATP by a single diadenylate cyclase, DacA, and degraded by the phosphodiesterases PdeA and PgpH into the linear nucleotide pApA (19). In rich media, such as Brain Heart Infusion (BHI) broth, the Δ*dacA* mutant accumulates a toxic level of ppGpp that inhibits bacterial growth (20). By contrast, the Δ*pdeA* Δ*pgpH* mutant (hereafter denoted as the ΔPDE mutant) does not exhibit an appreciable growth defect in BHI, but is greatly attenuated for virulence in the mouse model of intravenous infection, despite hyper-activating type I interferon response (21). These phenotypes indicate that the mechanisms underlying ΔPDE virulence attenuation are related to bacterial defects during infection.

Exploiting the ΔPDE mutant as a genetic tool to study c-di-AMP functions, we found that c-di-AMP accumulation inhibits the expression of the PrfA core regulon in *L. monocytogenes*. We attribute this defect to a depletion of cytoplasmic GSH, required to activate PrfA during infection. A constitutive PrfA* variant, PrfA G145S, rescued the ΔPDE strain for virulence gene expression in vitro but does not rescue virulence in the mouse model of infection, suggesting that c-di-AMP

accumulation impairs host adaptation mechanisms outside of the PrfA regulon, such as oxidative stress sensitivity or diminished cell wall integrity.

RESULTS

The ΔPDE mutant is defective for virulence gene expression in the PrfA core regulon

The ΔPDE mutant does not have an appreciable growth defect in broth media (**Fig. S1**), but is highly attenuated for virulence in a mouse model of infection (21). To identify genes that could contribute to ΔPDE virulence defect, we performed RNAseq to profile the transcriptomes of the wild-type (WT) and ΔPDE strains, grown in LSM to mid-exponential phase (20). The cDNA libraries were sequenced at the depth of 17 – 20 million reads, and had 856x-1042x mapped read coverage of the *L. monocytogenes* genome. Compared to WT, the ΔPDE strain displayed mostly a transcriptional downshift, with 67 genes being down-regulated by ≥4-fold, and 9 genes being up-regulated by ≥4-fold (P value < 0.05) (**Table S1**). Remarkably, the vast majority of down-regulated genes in ΔPDE belong to the 10403S prophage locus (41 genes) or the PrfA core regulon (11 genes) (**Fig. 1A**). In addition to the core regulon, PrfA has been shown to putatively or indirectly regulate the expression of up to 145 other genes (22). We did not observe those genes among the most significantly altered in ΔPDE, except for the upregulation of a cellobiose transporter (*lmo2683*) and two genes of hypothetical function (*lmo0186* and *lmo0019*) **(Table S1)**. Furthermore, *kdpA* expression was also reduced by ~6-fold in the ΔPDE strain, consistent with an inhibitory effect of c-di-AMP on the expression of the *kdp* operon, which encodes a potassium uptake system (**Table S1**) (13, 23).

PrfA is the master transcription factor that upregulates *L. monocytogenes* virulence gene expression required for the intracellular life cycle (4). Our RNAseq analysis revealed that the PrfA

core regulon was significantly down-regulated in the ΔPDE strain (**Fig. 1A-B**). To validate RNAseq results, we employed RT-qPCR to quantify the expression of three genes in the PrfA core regulon: *prfA*, *hly* (an early gene), and *actA* (a late gene). In LSM cultures, the ΔPDE strain was significantly impaired for the expression of all three genes, reflecting a defect in basal PrfA function (**Fig. S2**). To examine gene expression upon PrfA activation, we next performed RT-qPCR for cultures grown in the presence of GSH. Although these genes were up-regulated by GSH in both the WT and ΔPDE strains, their expression levels in ΔPDE remained significantly lower than in WT (**Fig. S2**). Furthermore, of the three genes, we noticed that the ΔPDE strain was most impaired for *actA* expression, which was reduced by 10 – 100-fold compared to the basal and activated levels in WT (**Fig. S2C**). As an independent method to quantify *actA* expression, we used a red fluorescent reporter fused with the *actA* promoter (P_{actA}-RFP) (8). This assay confirmed that the ΔPDE strain was significantly defective for *actA* expression both at the basal level and upon PrfA activation by GSH or TCEP (**Fig. 1C-D**). Finally, immunoblots revealed that PrfA protein level is significantly reduced in ΔPDE compared to WT, both in broth cultures and infected macrophages (**Fig. S3**).

Defective PrfA function contributes to diminished virulence expression at high c-di-AMP levels

Reduced gene expression in the PrfA core regulon suggests that the ΔPDE strain is defective for PrfA function or activation. We tested this idea by replacing the native *prfA* allele with a constitutive PrfA* variant (G145S) that structurally mimics the GSH-bound form (6, 7). In transcriptional reporter assays with P_{actA}-RFP, the *prfA** strain exhibited constitutive *actA* expression, independent of GSH supplementation, as expected (**Fig. 2**). In the ΔPDE background, the *prfA** allele restored *actA* expression to the WT level in LSM + GSH (**Fig. 2**). Interestingly,

actA expression was not constitutive in ΔPDE *prfA**. These data indicate that impaired PrfA activity is responsible for low virulence gene expression in ΔPDE. Furthermore, there appears to be factors that inhibit PrfA activity in the absence of GSH.

The ΔPDE strain is deficient in glutathione

The restorative effect of PrfA* on virulence gene expression suggests that the ΔPDE strain might be impaired for PrfA activation by GSH. We quantified cytoplasmic GSH in *L. monocytogenes* cells using a luminescence-based assay, which couples glutathione-S-transferase activity with firefly luciferase. We found that GSH levels were significantly depleted in the ΔPDE strain compared to WT, in all culture conditions that we quantified PrfA-regulated gene expression (with or without GSH/TCEP treatments) (**Fig. 3A-B)**. GSH deficiency was not due to oxidation, since the total glutathione pool and oxidized glutathione (GSSG) were also reduced in ΔPDE (**Fig. S4A-B)**. Furthermore, a previous study found that methylglyoxalase is important to maintain a sufficient GSH pool in *L. monocytogenes* (24). We found no evidence for an impaired methylglyoxalase activity in the ΔPDE strain, since ΔPDE exhibited a comparable methylglyoxal susceptibility to WT (**Fig. S4C**).

L. monocytogenes synthesizes GSH by the glutathione synthase GshF (25), and also imports GSH via CtaP and OppDF (26). The ΔPDE strain could fully induce *actA* expression to the activated level in WT, but only upon both GSH supplementation and *gshF* over-expression (**Fig. 3C** and **Fig. S5**). These data suggest that GSH deficiency impairs PrfA activity in the ΔPDE strain in broth cultures.

C-di-AMP accumulation inhibits GSH uptake

GSH depletion in the ΔPDE strain could be due to impaired uptake, synthesis, or increased catabolism. We evaluated GSH uptake in the Δ*gshF* and ΔPDE Δ*gshF* strains, which cannot synthesize GSH. These strains were grown in LSM until mid-exponential phase, then supplemented with GSH for ~0.7 doubling times, and quantified for cytoplasmic GSH levels. In these assays, we found that ΔPDE Δ*gshF* accumulated about one third of GSH levels compared to Δ*gshF*, suggesting a GSH uptake defect at high c-di-AMP levels (**Fig. 4A**). We further verified this phenotype in ^{3}H-GSH uptake assays for the Δ*gshF* and ΔPDE Δ*gshF* cultures (**Fig. 4B**).

The intracellular lifecycle of *L. monocytogenes*, including cytosolic replication and cell-to-cell spread, can be assessed by a plaque formation assay upon infection of murine fibroblasts (L2 cells) (27). To evaluate GSH uptake during infection, we performed an L2 plaque formation assay. Consistent with a previous study (5), we found the Δ*gshF* mutant to form significantly smaller plaques than the WT strain (**Fig. 4C**). Compared to Δ*gshF*, the ΔPDE Δ*gshF* strain was much further diminished for plaque formation, indicating that c-di-AMP accumulation impairs GSH uptake during infection (**Fig. 4C**).

The Ctp complex and OppDF ATPases mediate high-affinity GSH/GSSG uptake by *L. monocytogenes* (28). Our RNAseq data indicated that the WT and ΔPDE strains exhibit similar levels of *ctaP* (encoding the substrate-binding component of Ctp) and *oppD* gene expression in LSM, and qPCR revealed comparable expression of these genes in LSM + GSH (**Fig. S6**). These data indicate that GSH uptake defect in ΔPDE is not at the transcriptional level. Of note, the ΔPDE strain does not appear defective for cysteine uptake, since it exhibited a similar cysteine level to WT (**Fig. S5C**). Therefore, the GSH uptake defect is likely caused by an impaired Opp activity.

C-di-AMP also depletes cytoplasmic GSH by inhibiting synthesis or promoting catabolism

The ΔPDE mutant was deficient in intracellular GSH during growth in the absence of GSH supplementation, suggesting a defect in GSH synthesis (**Fig. 3A**). *L. monocytogenes* GshF is a bi-functional GSH synthase that uses glycine, cysteine, and glutamate as substrates, all of which are provided in LSM (29). Our LC-MS did not reliably quantify glutamate, but we found glycine and cysteine levels to be comparable in ΔPDE and WT (**Fig. S5C**). Given that cysteine is the limiting substrate for GshF activity in bacterial cells (30), it is unlikely that the ΔPDE strain is lacking in substrates for GSH synthesis.

The gene expression levels of *gshF* were comparable in the WT and ΔPDE strains, with and without exogenous GSH in the culture medium (**Fig. S5A**). Therefore, we next examined post-transcriptional regulation of GshF by replacing the native *gshF* gene with a constitutively expressed allele (P_{spac}-*gshF*). To evaluate GSH synthesis, we grew cultures in the absence or presence of TCEP, which activates GSH synthesis without adding GSH to the culture medium (8). Even upon constitutive *gshF* expression, the ΔPDE mutant was still significantly depleted for GSH, both under the basal condition and TCEP activation, despite exhibiting a similar level of GshF protein to the WT strain (**Fig. 5A** and **Fig. S5B**). In L2 plaque formation assay, *gshF* over-expression only moderately increased the ΔPDE plaque sizes, suggesting that GshF activity might be impaired (**Fig. 5B**). However, we noticed that the ΔPDE Δ*gshF* strain formed significantly smaller plaques than the ΔPDE strain, indicating that GSH synthesis is not completely inhibited at high c-di-AMP levels during infection (**Fig. 4C**). Therefore, c-di-AMP accumulation might also promote GSH catabolism.

A constitutive PrfA* variant does not rescue ΔPDE for virulence

Given an impaired PrfA activity and virulence gene expression in ΔPDE in broth cultures, we next examined the contribution of PrfA defect to ΔPDE virulence attenuation in a mouse model of

intravenous infection. The *prfA** allele modestly increased median bacterial burdens by ~2-fold in the WT strain, in both the spleen and liver, as expected (**Fig. 6**). Although deemed statistically significant, *prfA** increased bacterial burdens by a similar magnitude in the ΔPDE genetic background. Unexpectedly, immunoblots revealed a reduced PrfA protein level in the ΔPDE *prfA** strain compared to *prfA** (**Fig. S7**). Nevertheless, this reduced PrfA protein level was apparently sufficient to fully induce *actA* expression in the ΔPDE *prfA** strain. Therefore, virulence-related defects conferred by c-di-AMP accumulation are most likely outside of the PrfA regulon.

GshF is important for oxidative stress resistance

GSH is an established anti-oxidant that quenches reactive oxygen species such as superoxide and H_2O_2 (31). Consistent with a previous report that GshF is important for H_2O_2 tolerance in BHI cultures of *L. monocytogenes* (32), we found the Δ*gshF* strain to be also highly sensitive to H_2O_2 in LSM (**Fig. 7**). Although much more resistant than Δ*gshF*, the ΔPDE strain was also H_2O_2 sensitive, and this phenotype was substantially exacerbated in the absence of GshF, highlighting a pronounced role of GshF in oxidative stress resistance upon c-di-AMP accumulation.

DISCUSSION

C-di-AMP homeostasis is critical for bacterial growth and pathogenesis. The attenuated virulence conferred by c-di-AMP accumulation is widely observed in many pathogens, including *Mycobacterium tuberculosis*, which does not require c-di-AMP for growth (33, 34), and *Borrelia burgdorferi*, which produces a very low level of c-di-AMP (35, 36). In the c-di-AMP phosphodiesterase (Δ*dhhP*) mutant of *B. burgdorferi*, the transcription factor BosR is inhibited, causing reduced expression of the major virulence factor OspC (35). However, the *B. burgdorferi*

Δ*dhhP* mutant also has a significant growth defect, and DhhP might degrade other nucleotides in addition to c-di-AMP (37, 38). For *Bacillus anthracis*, the ΔPDE mutant also grows poorly and is diminished for anthrax toxin production, a defect that is partially attributed to the upregulation of the transcriptional repressor AbrB (39). The molecular mechanisms by which c-di-AMP inhibits virulence factor expression in these bacteria are unclear, and the mechanisms by which c-di-AMP impairs the virulence of other pathogens are even less understood.

The *L. monocytogenes* c-di-AMP ΔPDE mutant does not have a significant growth defect in rich media, but is attenuated for virulence, suggesting defects that are pertinent to replication and adaptation in the host. Our findings here reveal GSH metabolism as another pathway that is regulated by c-di-AMP with implications for *L. monocytogenes* pathogenesis. First, we found that c-di-AMP accumulation inhibits GSH uptake. High affinity GSH transport in *L. monocytogenes* was recently shown to require the Ctp complex and the ATPases OppDF, the latter of which are components of the Opp complex that transports oligopeptides (28). Since the ΔPDE strain was not deficient in cysteine, which is provided in LSM, it is unlikely that c-di-AMP inhibits Ctp activity (40). Based on the demonstrated function of c-di-AMP in inhibiting potassium, Mg^{2+}, and carnitine transporters (10), it is conceivable that c-di-AMP might inhibit the OppDF ATPase function particularly. As for how c-di-AMP accumulation depletes cytoplasmic GSH, we found that c-di-AMP does not inhibit *gshF* gene expression or impair GshF stability. Although our ex vivo infection and H_2O_2 susceptibility data suggests that GshF is operational in the ΔPDE strain during infection, its activity might be reduced. Finally, c-di-AMP might also activate GSH catabolism. Future investigations are necessary to distinguish these mechanisms.

Because GSH is an allosteric activator of the master virulence factor PrfA, an expected consequence of GSH depletion is a reduced virulence program expression in vitro. Indeed, we

found virulence gene expression to be impaired at high c-di-AMP levels, but can be restored by a constitutive PrfA* variant, or a combination of increased GSH synthesis and GSH supplementation. However, PrfA* did not rescue ΔPDE virulence in vivo. Interestingly, the ΔPDE *prfA** strain exhibited a reduced PrfA protein level compared to *prfA**, and investigating this phenotype will likely reveal interesting mechanisms of PrfA regulation and c-di-AMP function. Nevertheless, a reduced PrfA level in the ΔPDE *prfA** mutant still appeared sufficient to induce *actA* expression in vitro, suggesting that virulence attenuation upon c-di-AMP accumulation is likely due to defects outside of the PrfA regulon.

As an example of infection-relevant defects, we found the ΔPDE strain to be sensitive to oxidative stress, although this phenotype was rather modest compared to Δ*gshF*. The mechanisms for H_2O_2 sensitivity in the ΔPDE strain are unclear, but an impaired PrfA function can contribute to this phenotype (41). Furthermore, we previously reported that the *L. monocytogenes* ΔPDE strain is sensitive to cell wall-targeting antimicrobials, including lysozyme that is abundant in mammalian cell cytosol (42). Given the requirement of cell wall homeostasis for successful infection by *L. monocytogenes* (43–45), it is conceivable that cell wall defects also contribute to ΔPDE virulence attenuation. Another well-established function of c-di-AMP in *L. monocytogenes* is the inhibition of the carnitine transporter OpuC and multiple potassium uptake channels (12, 13). However, mutants abolished for carnitine transport do not exhibit a systemic infection defect like the ΔPDE strain (46), and the cell cytosol is highly enriched in potassium (47). Therefore, reduced osmolyte uptake may not significantly impact *L. monocytogenes* replication in the cytosol. Among other c-di-AMP-binding proteins that have been studied in *L. monocytogenes*, PstA has a minor role in infection (14); and the ΔPDE mutant does not have a growth defect that would be associated with a significantly reduced pyruvate carboxylase function (11, 48). The roles of other

c-di-AMP molecular targets in *L. monocytogenes* pathogenesis should be investigated in future studies.

In addition to recognizing GSH as a virulence signal, *L. monocytogenes* also metabolizes GSH as a source of essential cysteine and uses GSH as antioxidant in broth cultures (26, 32). Consistent with previous studies, we found GshF to be important for oxidative stress resistance in *L. monocytogenes* (31, 32, 49). The role of GshF appears even more pronounced in the ΔPDE strain, suggesting an increase in reactive oxygen species or impairment in other redox stress resistance mechanisms (50, 51). In addition, if GSH is a relevant cysteine source in the mammalian host, a defect in GSH uptake can confer a nutritional disadvantage and explain why the ΔPDE *prfA** strain was not fully restored for virulence. Furthermore, a reduced function of the GSH importers Ctp and OppDF at high c-di-AMP levels can also deprive *L. monocytogenes* of nutrient oligopeptides, which are also imported through these uptake channels (40, 52).

It is curious that the PrfA* (G145S) variant, which is active independent of GSH binding, did not confer constitutive *actA* expression in ΔPDE in the absence of GSH supplementation. Outside of the allosteric activation site that binds GSH, PrfA has four cysteine residues that can be glutathionylated, although this model is yet to be biochemically validated (5). PrfA glutathionylation, if existed, would modestly contribute to PrfA activation in the WT strain (5), but might have a more significant role at high c-di-AMP levels. Furthermore, the regulatory mechanisms of PrfA activity are complex, and PrfA can be inhibited by several factors such as metals or oligopeptides that do not contain cysteine (4). It is conceivable that the ΔPDE strain accumulates those PrfA inhibitors that can be identified in future metabolomics studies.

Altogether, our studies present an exciting avenue to investigate how c-di-AMP disrupts GSH metabolism in *L. monocytogenes*. Given the importance of GSH as a virulence signal, nutrient,

and antioxidant in different bacteria (53), it will be interesting to examine whether c-di-AMP regulates GSH metabolism in other species, and the consequences of such regulation on bacterial growth and infection.

MATERIALS AND METHODS

Strains and culture conditions

L. monocytogenes strains are listed in **Table S2**. Improved *Listeria* Synthetic Medium (LSM) was prepared based on published recipe (20). Over-expression of genes was accomplished using the integrative plasmid pPL2 (54). Gene allelic exchange was performed using plasmid pKSV7. For all experiments related to broth cultures, *L. monocytogenes* was grown at 37°C with shaking and without antibiotics. For glycerol stocks and maintenance, strains carrying derivatives of the integrative plasmid pPL2 were grown in Brain Heart Infusion broth with 200μg/mL streptomycin and 10μg/mL chloramphenicol. For mouse and L2 cell infection, *L. monocytogenes* was grown static in BHI at 30°C.

RNAseq and data analysis

L. monocytogenes cultures were grown to OD_{600} of ~ 0.5, and harvested by mixing 1:1 with cold methanol and centrifugation. RNA was extracted using acidified phenol:chloroform at pH 5.2 as previously described (55). Contaminated DNA was removed from extracted RNA using Turbo DNase (Thermo Scientific). RNA sequencing and read mapping was performed by MiGS Sequencing Center (Pittsburgh, PA). Reads were mapped to the *L. monocytogenes* 10403S genome (NCBI:txid393133). Differentially expressed gene analysis was performed by EdgeR (56).

RT-qPCR for L. monocytogenes genes in broth

For quantification of PrfA activity upon activation by GSH, *L. monocytogenes* cultures were grown in LSM or LSM + 10mM GSH to OD_{600} ~0.5. For PrfA activation by TCEP, *L. monocytogenes* cultures were grown in LSM to OD ~0.5, then split into two aliquots of identical volumes. One culture aliquot was left untreated and the other was supplemented with 2mM TCEP for 2 hours, and both were shaken at 37°C. RNA was extracted, treated with Turbo DNase and converted to cDNA using iScript cDNA synthesis kit (BioRad). Gene expression was quantified using iTaq Universal SYBR Green (BioRad) with primers specific to each target, with *rplD* as the control housekeeping gene. Primers are listed in **Table S3**.

Quantification of GSH and GSSG

L. monocytogenes cultures were grown to an OD_{600} of ~0.5 and harvested by centrifugation. Cell pellets were washed three times in phosphate-buffered saline, and lysed by sonication. Lysates were centrifuged to remove cell debris. GSH and GSSG were quantified using the luminescence-based GSH/GSSG-Glo assay kit (Promega). The assay system utilizes glutathione-S-transferase to convert GSH and luciferin-NT into luciferin, which serves as the substrate for the coupled luciferase activity to generate a luminescence read out. GSH standards of 0.5 – 20 μM were quantified to determine the linear range of luminescence readings, and bacterial lysates were diluted appropriately such that luminescence values were within the linear range.

L2 plaque assay

Plaque formation upon *L. monocytogenes* infection of L2 cells was quantified as previously described (27, 55). Briefly, $1.2x10^6$ cells were infected with *L. monocytogenes* at multiplicity of infection (MOI) of 0.25. At 1 hour post infection, cells were washed, and fresh cell medium in 0.7% agarose was supplemented with 10μg/mL gentamicin to kill extracellular *L. monocytogenes*.

At 5 days post infection, cells were stained with 0.3% crystal violet to visualize plaques. Plaque sizes were analyzed using ImageJ software.

PactA::RFP assay

A pPL2 plasmid expressing red fluorescent protein from the *actA* promoter was used to quantify transcriptional activity. Fluorescence assays were performed based on published methods (8). Briefly, *L. monocytogenes* strains carrying pPL2-P_{actA}::RFP were grown in overnight at 37°C in LSM. Cultures were diluted 1:10 into fresh LSM, LSM + 10mM GSH, or LSM + 2mM TCEP and grown to OD_{600} of 1.5-2. Cultures were harvested by centrifugation and resuspended in phosphate-buffered saline to achieve a 5X concentration. Fluorescence was quantified in black-bottom 96-well plates (Greiner Bio) for fluorescence measurement (excitation 540nm, emission 650nm) (BioTek Synergy H1 Microplate Reader). Fluorescence values were normalized to OD_{600}.

Mouse infection

All techniques were reviewed and approved by the University of Wisconsin—Madison Institutional Animal Care and Use Committee under the protocol M005916-R01-A01. Five 6-week-old female C57BL/6 mice (Charles River NCI facility) per bacterial strain were infected via tail vein injection with 0.2 cc of PBS with $1x10^5$ of logarithmically growing bacteria. At 48hpi, spleens and livers were harvested, and homogenized in organ lysis buffer. Organ homogenates were diluted, as necessary using PBS, spiral plated on LB agar, and CFU counts were obtained using the Q count. Bacterial CFUs per organ were calculated using known dilution factors.

3H-GSH uptake assay

Cultures were grown in LSM to an OD_{600} of ~0.5, harvested by centrifugation, washed twice in uptake buffer (phosphate-buffered saline + 5mM glucose), and resuspended in an equivalent

volume of LSM lacking cysteine. Cultures were grown an additional 45 minutes, then pelleted and resuspended in 52µL uptake buffer. 2µL of resuspension was reserved for OD_{600} measurement. 0.5µL 1µCi/µL ^{3}H-GSH, and 0.5µL10mM cold GSH was added to remaining 50µL and incubated at room temperature for 30 minutes. Cells were added to a filter membrane fitted on a vacuum filter unit and washed with ~10mL phosphate-buffered saline. Filter membrane containing washed cells was transferred to a scintillation vial containing 3mL scintillation fluid, and counts per minute (CPM) were measured on a liquid scintillation counter and normalized to OD_{600}.

Quantification of amino acids by LC-MS

L. monocytogenes strains were grown overnight in 3mL LSM cultures at 37°C, shaking. Overnight cultures were diluted 1:100 in LSM and grown with aeration to mid logarithmic phase (0.4-0.6 OD_{600}) at 37°C, shaking at 200 rpm. Bacterial metabolite extraction and quantification were performed as previously described (44). Briefly, bacterial cells were filtered and resuspended in extraction solvent (HPLC-grade acetonitrile, methanol, and water at a 2:2:1 ratio), and immediately frozen on in dry ice. Samples were analyzed on a Dionex UHPLC system coupled with a hybrid quadrupole–high-resolution mass spectrometer (Q Exactive Orbitrap; Thermo Scientific), using an Acquity UPLC BEH C18 column (Waters). Solvent A was composed of 97% water, 3% methanol, 10 mM tributylamine, pH 8.1-8.2. Solvent B was 100% methanol. Mobile phase was run on a gradient from 5 – 95% solvent B over 25 minutes. MS data in mzXML format was used for metabolite identification with the MAVEN software (57)

Western Blot for L. monocytogenes proteins in broth and during macrophage growth.

For broth cultures, *L. monocytogenes* overnight cultures were subcultured 1:10 into LSM or LSM + 10mM GSH, and grown to OD_{600} of 1.5-2. Cultures were washed in one in 1x PBS and

pellets were stored at -80C. For macrophage infections, immortalized bone marrow-derived macrophages were infected with *L. monocytogenes* strains at MOI of 10, with washing and supplementation of 10μg/mL gentamicin at 1 hpi. *L. monocytogenes* was harvested at 8 hpi using Tris-buffered saline (TBS) + 0.5% Tween-20. Lysed cells were pelleted, washed in PBS, and resuspended in TBS + 0.05% □-mercaptoethanol + 1mM PMSF, and sonicated until lysates were clear. Saturated trichloroacetic acid was added to a final concentration of 6% and samples were precipitated on ice for one hour and washed 3x with 100% acetone. Pellets were fully dried in a SpeedVac, resuspended in 10% SDS + 0.05% □-mercaptoethanol, and boiled for 5 minutes. Redissolved pellet was mixed with Laemmli sample loading buffer for SDS-PAGE gel with 12.5% acrylamide. Protein transfer onto nitrocellulose membrane was performed at 90V for 60 minutes. Membrane was incubated with primary antibodies overnight in TBS + 0.1% Tween-20. Anti-PrfA antibody (ThermoFisher Scientific, #PA5-144446) was diluted 1:5000, and Anti-RpoA antibody (a gift from Briana Burton) was diluted 1:15,000. Secondary antibody (Anti-Rabbit IgG (H+L), HRP Conjugate, #W4011, Promega) was diluted 1:2500. Membrane was visualized using the Clarity Western ECL Substrate Kit (BioRad) and imaged with a BioRad system using the chemiluminescence setting. Images were quantified using ImageJ software to subtract background and measure band areas.

H2O2 Susceptibility

Strains were grown overnight in LSM, washed once in PBS, and normalized to an OD_{600} of 0.01 in 1mL of LSM or LSM containing indicated concentrations of H_2O_2. Cultures were grown shaking at 37°C for 16 hours, at which point OD_{600} was measured.

ACKNOWLEDGEMENTS

This work was supported by R35 GM147519 (TNH) and R01 AI137070 (JDS). Briana Burton generously provided anti-RpoA antibody.

FIGURES

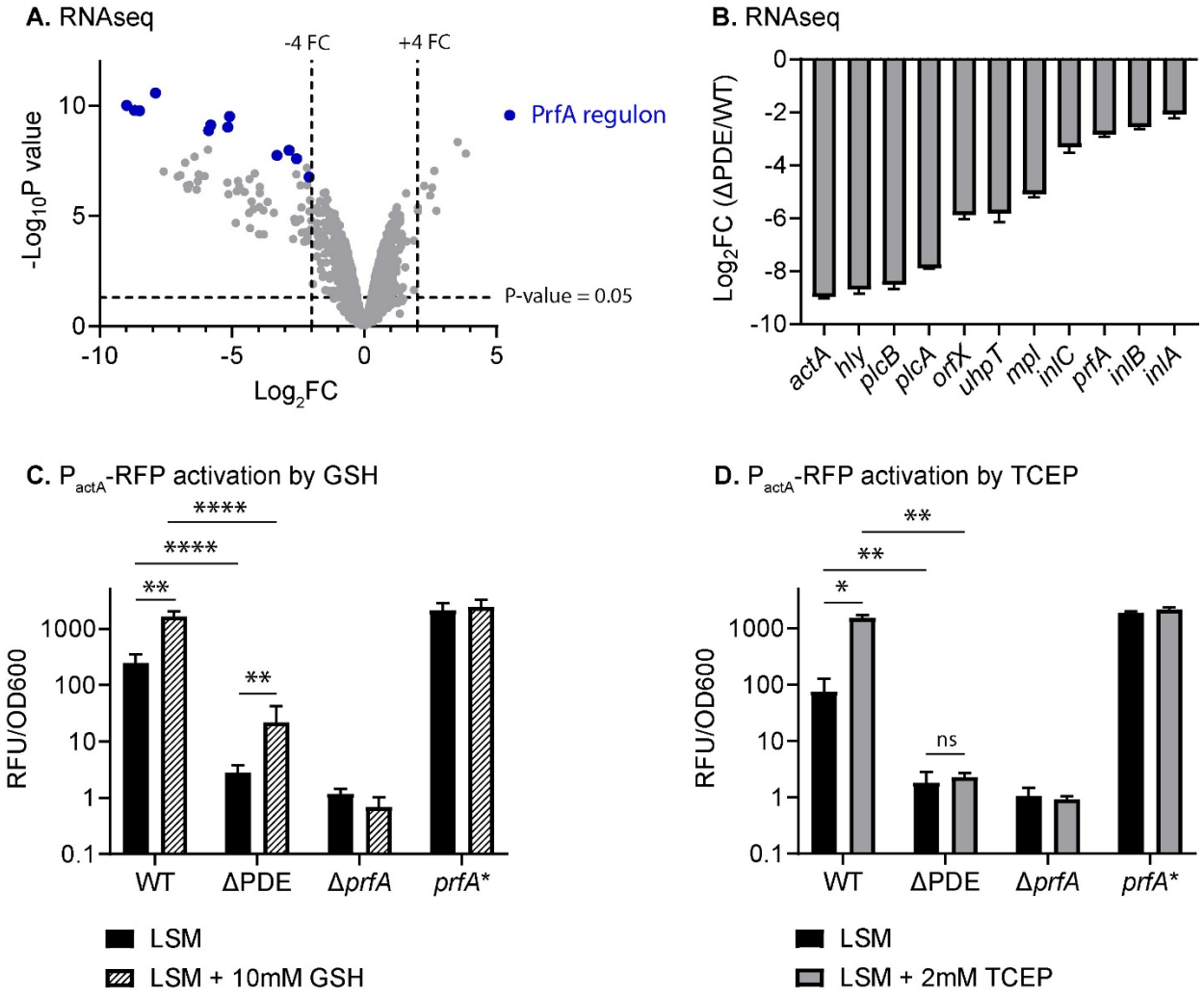

Figure 1: C-di-AMP accumulation impairs virulence gene expression in *L. monocytogenes*. **A.** Volcano plot of differentially expressed genes in the ΔPDE mutant compared to the WT strain. RNAseq was performed on mid-log cultures grown in *Listeria* Synthetic Medium (LSM). Blue dots indicate genes within the PrfA core regulon. **B.** Log_2fold change of PrfA-regulated gene expression was calculated from read counts per million (cpm) of two independent ΔPDE cultures, compared to the average of two independent WT cultures. Data in A and B are from the same RNAseq experiment. **C.** PrfA-regulated gene expression was quantified in *L. monocytogenes* strains carrying P_{actA}::RFP transcriptional reporter. The Δ*prfA* and *prfA** strains were examined as

negative and positive controls, respectively. Cultures were grown to mid-log in LSM or LSM + 10mM GSH. Red fluorescence was normalized to OD600 of each respective culture. **D.** Red fluorescence was quantified as in C. LSM cultures were left untreated or treated with 2mM TCEP for 2 hours. Data in C and D are average of 3-6 independent experiments. Error bars show standard deviations. Statistical analyses were performed by two-way ANOVA with multiple comparisons for the indicated pairs: ns, non-significant; *, $P < 0.05$; **, $P < 0.01$; ****, $P < 0.0001$

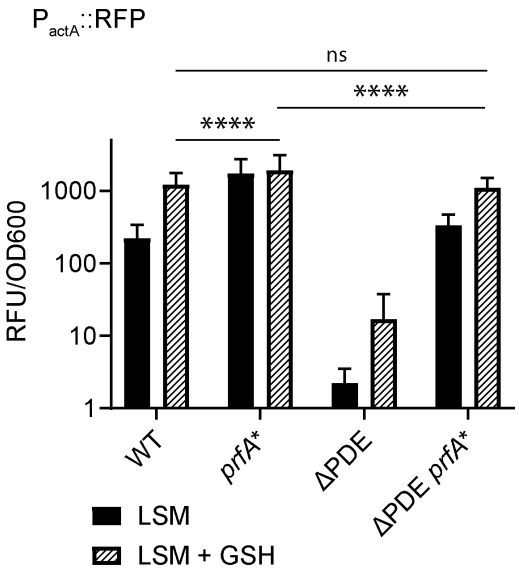

Figure 2: A constitutive PrfA variant (PrfA*) restores virulence gene expression in vitro. A. P_{actA}::RFP transcriptional activity was quantified in WT, ΔPDE, and isogenic strains in which the native *prfA* allele is replaced with *prfA** (G145S). Red fluorescence, normalized to OD600, was measured for mid-log cultures grown in LSM or LSM + 10mM GSH, and normalized to OD600. Error bars show standard deviations. Statistical analyses were performed by two-way ANOVA, with multiple comparisons for the indicated pairs: ns, non-significant; **, $P < 0.01$; ****, $P < 0.0001$.

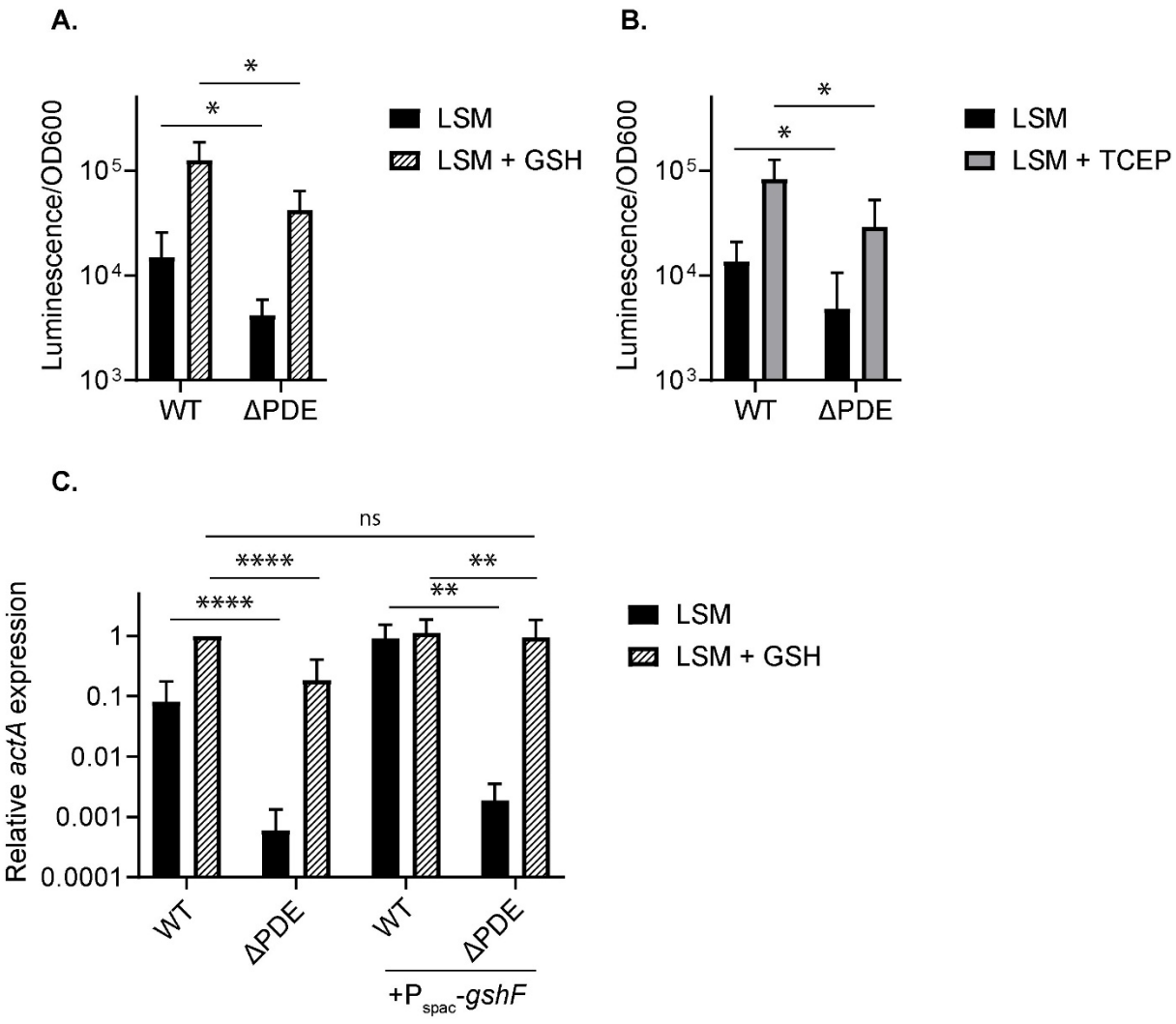

Figure 3: A deficiency in reduced glutathione (GSH) contributes to diminished virulence gene expression at high c-di-AMP levels. A. Reduced glutathione (GSH) levels of mid-log cultures grown in LSM or LSM + 10mM GSH. GSH levels are reported by luminescence and normalized to OD600. Several GSH standards were quantified to determine the linear range of the assay, and all biological samples were quantified at appropriate dilutions to ensure measurements were within the linear range. **B.** Mid-log LSM cultures were left untreated, or treated with 2mM TCEP for 2 hours, and quantified for GSH levels as in A. **C.** *actA* gene expression by RT-qPCR.

Cultures were grown in LSM or LSM + 10mM GSH to mid-log phase. In each culture, the expression level of *actA* was normalized to that of *rplD* as a housekeeping gene. Error bars represent standard deviations. Statistical analyses were performed by two-way ANOVA with multiple comparisons for the indicated pairs: ns, non-significant; *, $P < 0.05$; **, $P < 0.01$; ****, $P < 0.0001$

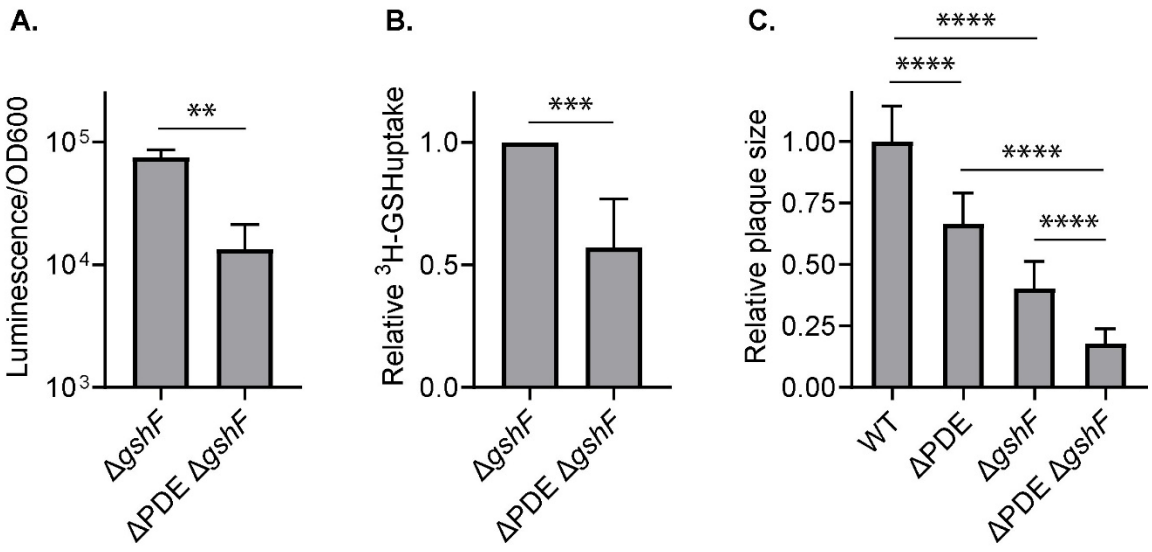

Figure 4: C-di-AMP accumulation inhibits GSH uptake in broth culture and ex-vivo infection. A. The Δ*gshF* and ΔPDE Δ*gshF* strains were grown to mid-log phase in LSM and supplemented with 10mM GSH for one hour (approximately 0.7 doublings in LSM). Cultures were thoroughly washed and quantified for intracellular GSH, reported as luminescence normalized to OD600. **B.** ^{3}H-GSH uptake assay. Cultures were grown to mid-log, then supplemented with ^{3}H-GSH for 30 minutes. Uptake activity was assessed by radioactivity normalized to OD600. **C.** Plaque formation at 4 days post infection of L2 fibroblasts. Plaque sizes were quantified by ImageJ. In each experiment, the average plaque size by each strain was normalized to the average WT plaque size, set at 1. Error bars represent standard deviations. Statistical analyses were performed by Student's t-test in A-B and one-way ANOVA in C, with multiple comparisons for the indicated pairs: **, $P < 0.01$; ***, $P < 0.001$; ****, $P < 0.0001$

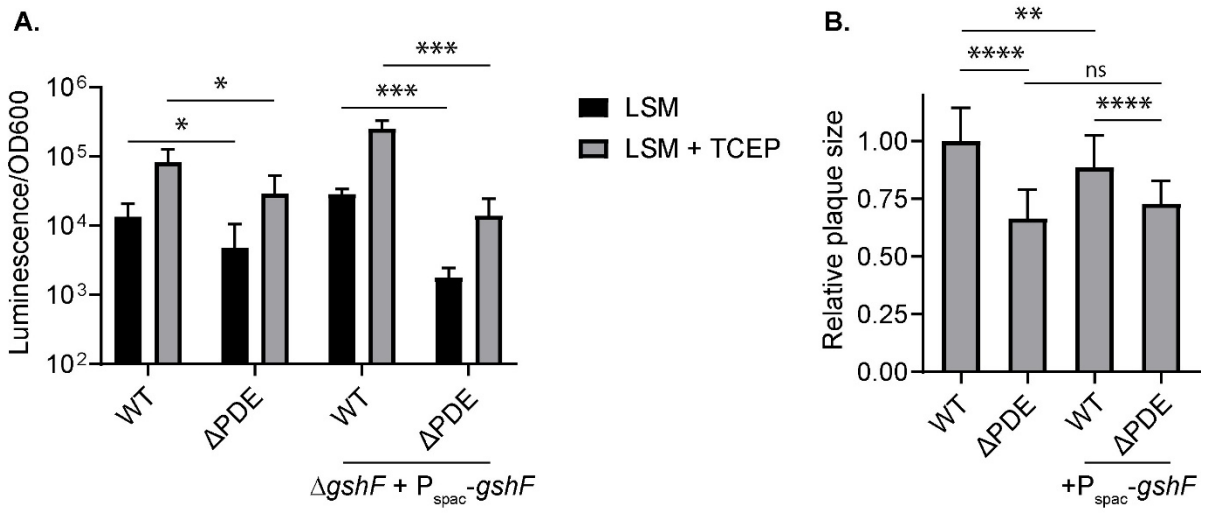

Figure 5: Activation of GSH synthesis activity does not restore GSH levels in the ΔPDE strain. A. Intracellular GSH levels. Cultures were left untreated or treated with 2mM TCEP for 2 hours. GSH levels are reported as luminescence normalized to OD600 of each culture. **B.** Plaque formation at 4 days post infection of L2 fibroblasts. Plaque sizes were quantified by ImageJ. In each experiment, the average plaque size by each strain was normalized to the average WT plaque size, set at 1. Error bars show standard deviations. Statistical analyses were performed by two-way ANOVA in A and one-way ANOVA in B, with multiple comparisons for the indicated pairs: ns, non-significant; *, $P < 0.05$; **, $P < 0.01$; ***, $P < 0.001$; ****, $P < 0.0001$

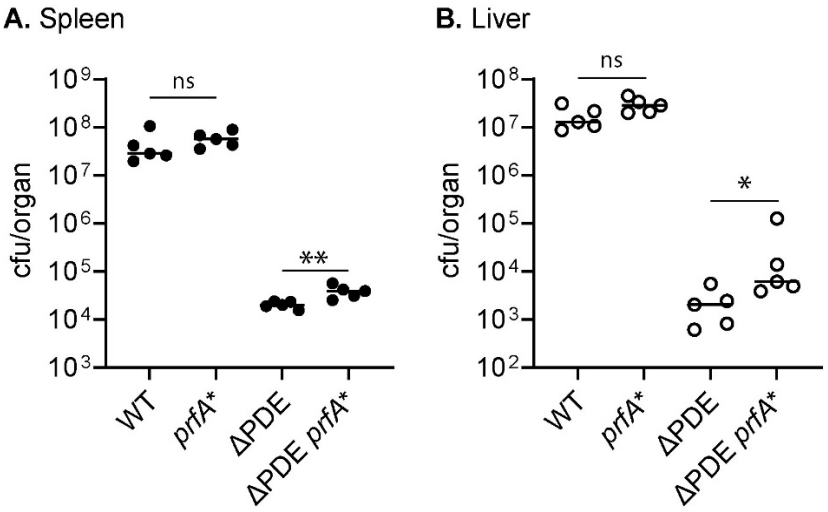

Figure 6: A constitutive PrfA* variant does not rescue DPDE virulence defect. Bacterial burdens in the spleen and liver at 48 hours post-intravenous infection with 1 x 10^5 cfu of *L. monocytogenes*. Each dot represents *L. monocytogenes* burden from one animal. Bars represent medians of the groups. Statistical analyses were performed Mann-Whitney tests: ns, non-significant; *, $P < 0.05$; **, $P < 0.01$.

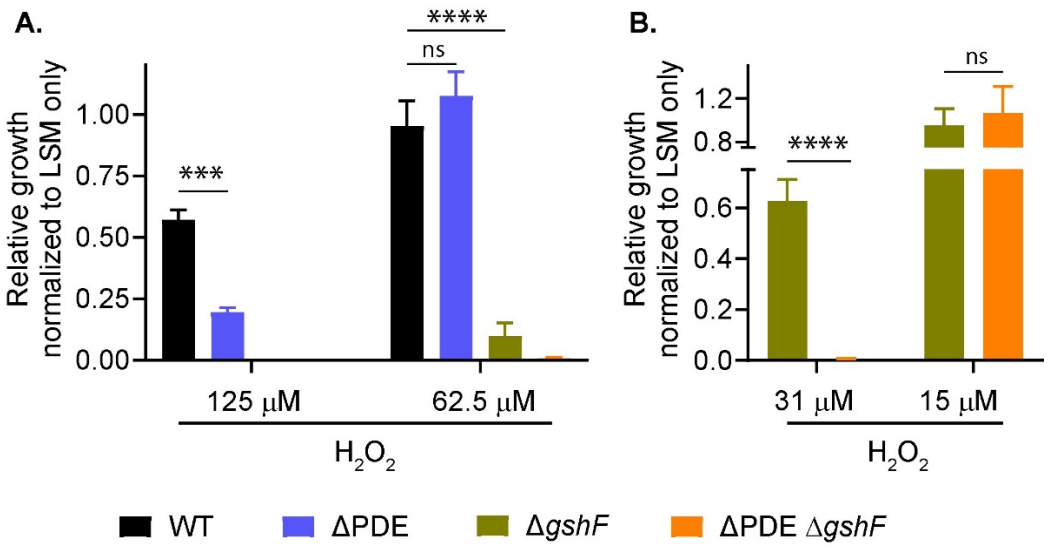

Figure 7: The ΔPDE strain is sensitive to H2O2. *L. monocytogenes* cultures were grown with shaking in LSM with varying H2O2 concentrations for 16 hours. For each strain, OD_{600} of cultures grown in H_2O_2 were normalized to OD_{600} of the same strain grown in LSM only. The Δ*gshF* strains did not grow at 125 □M H_2O_2 in panel A, and were re-examined at lower H_2O_2 concentrations in panel B. Statistical analyses were performed by one-way ANOVA: ***, $P < 0.001$; ****, $P < 0.0001$.

REFERENCES

1. National Center for Emerging and Zoonotic Infectious Diseases. 2018. Estimated Annual Number of Hospitalizations and Deaths Caused by 31 Pathogens.

2. Radoshevich L, Cossart P. 2018. Listeria monocytogenes: towards a complete picture of its physiology and pathogenesis. Nat Rev Microbiol 16:32–46.

3. de las Heras A, Cain RJ, Bielecka MK, Vázquez-Boland JA. 2011. Regulation of Listeria virulence: PrfA master and commander. Curr Opin Microbiol 14:118–127.

4. Johansson J, Freitag NE. 2019. Regulation of *Listeria monocytogenes* Virulence. Microbiol Spectr 7.

5. Reniere ML, Whiteley AT, Hamilton KL, John SM, Lauer P, Brennan RG, Portnoy DA. 2015. Glutathione activates virulence gene expression of an intracellular pathogen. Nature 517:170–173.

6. Hall M, Grundström C, Begum A, Lindberg MJ, Sauer UH, Almqvist F, Johansson J, Sauer-Eriksson AE. 2016. Structural basis for glutathione-mediated activation of the virulence regulatory protein PrfA in *Listeria*. Proceedings of the National Academy of Sciences 113:14733–14738.

7. Eiting M, Hagelüken G, Schubert W, Heinz DW. 2005. The mutation G145S in PrfA, a key virulence regulator of *Listeria monocytogenes* , increases DNA-binding affinity by stabilizing the HTH motif. Mol Microbiol 56:433–446.

8. Portman JL, Dubensky SB, Peterson BN, Whiteley AT, Portnoy DA. 2017. Activation of the Listeria monocytogenes Virulence Program by a Reducing Environment. mBio 8.

9. Woodward JJ, Iavarone AT, Portnoy DA. 2010. c-di-AMP secreted by intracellular Listeria monocytogenes activates a host type I interferon response. Science 328:1703–1705.

10. Stülke J, Krüger L. 2020. Cyclic di-AMP Signaling in Bacteria. Annu Rev Microbiol https://doi.org/10.1146/annurev-micro-020518-115943.

11. Sureka K, Choi PH, Precit M, Delince M, Pensinger DA, Huynh TN, Jurado AR, Goo YA, Sadilek M, Iavarone AT, Sauer J-D, Tong L, Woodward JJ. 2014. The cyclic dinucleotide c-di-AMP is an allosteric regulator of metabolic enzyme function. Cell 158:1389–1401.

12. Huynh TN, Choi PH, Sureka K, Ledvina HE, Campillo J, Tong L, Woodward JJ. 2016. Cyclic di-AMP targets the cystathionine beta-synthase domain of the osmolyte transporter OpuC. Mol Microbiol 102:233–243.

13. Gibhardt J, Hoffmann G, Turdiev A, Wang M, Lee VT, Commichau FM. 2019. c-di-AMP assists osmoadaptation by regulating the Listeria monocytogenes potassium transporters KimA and KtrCD. J Biol Chem 294:16020–16033.

14. Choi PH, Sureka K, Woodward JJ, Tong L. 2015. Molecular basis for the recognition of cyclic-di-AMP by PstA, a PII-like signal transduction protein. Microbiologyopen 4:361–374.
15. Peterson BN, Young MKM, Luo S, Wang J, Whiteley AT, Woodward JJ, Tong L, Wang JD, Portnoy DA. 2020. (p)ppGpp and c-di-AMP Homeostasis Is Controlled by CbpB in Listeria monocytogenes. mBio 11.

16. McFarland AP, Luo S, Ahmed-Qadri F, Zuck M, Thayer EF, Goo YA, Hybiske K, Tong L, Woodward JJ. 2017. Sensing of Bacterial Cyclic Dinucleotides by the Oxidoreductase RECON Promotes NF-κB Activation and Shapes a Proinflammatory Antibacterial State. Immunity 46:433–445.

17. Peignier A, Parker D. 2021. Impact of Type I Interferons on Susceptibility to Bacterial Pathogens. Trends Microbiol 29:823–835.

18. Louie A, Bhandula V, Portnoy DA. 2020. Secretion of c-di-AMP by Listeria monocytogenes Leads to a STING-Dependent Antibacterial Response during Enterocolitis. Infect Immun 88.

19. Schwedt I, Wang M, Gibhardt J, Commichau FM. 2023. Cyclic di-AMP, a multifaceted regulator of central metabolism and osmolyte homeostasis in *Listeria monocytogenes*. microLife 4.

20. Whiteley AT, Pollock AJ, Portnoy DA. 2015. The PAMP c-di-AMP Is Essential for Listeria monocytogenes Growth in Rich but Not Minimal Media due to a Toxic Increase in (p)ppGpp. [corrected]. Cell Host Microbe 17:788–798.

21. Huynh TN, Luo S, Pensinger D, Sauer J-D, Tong L, Woodward JJ. 2015. An HD-domain phosphodiesterase mediates cooperative hydrolysis of c-di-AMP to affect bacterial growth and virulence. Proc Natl Acad Sci U S A 112:E747-56.

22. Milohanic E, Glaser P, Coppée J, Frangeul L, Vega Y, Vázquez-Boland JA, Kunst F, Cossart P, Buchrieser C. 2003. Transcriptome analysis of *Listeria monocytogenes* identifies three groups of genes differently regulated by PrfA. Mol Microbiol 47:1613–1625.

23. Moscoso JA, Schramke H, Zhang Y, Tosi T, Dehbi A, Jung K, Gründling A. 2016. Binding of Cyclic Di-AMP to the Staphylococcus aureus Sensor Kinase KdpD Occurs via the Universal Stress Protein Domain and Downregulates the Expression of the Kdp Potassium Transporter. J Bacteriol 198:98–110.

24. Anaya-Sanchez A, Feng Y, Berude JC, Portnoy DA. 2021. Detoxification of methylglyoxal by the glyoxalase system is required for glutathione availability and virulence activation in Listeria monocytogenes. PLoS Pathog 17:e1009819.

25. Gopal S, Borovok I, Ofer A, Yanku M, Cohen G, Goebel W, Kreft J, Aharonowitz Y. 2005. A Multidomain Fusion Protein in Listeria monocytogenes Catalyzes the Two Primary Activities for Glutathione Biosynthesis. J Bacteriol 187:3839–3847.

26. Berude JC, Kennouche P, Reniere ML, Portnoy DA. 2023. Listeria monocytogenes utilizes glutathione and limited inorganic sulfur compounds as a source of essential L-cysteine. bioRxiv.

27. Reniere ML, Whiteley AT, Portnoy DA. 2016. An In Vivo Selection Identifies Listeria monocytogenes Genes Required to Sense the Intracellular Environment and Activate Virulence Factor Expression. PLoS Pathog 12:e1005741.

28. Berude JC, Kennouche P, Reniere ML, Portnoy DA. 2024. *Listeria monocytogenes* utilizes glutathione and limited inorganic sulfur compounds as sources of essential cysteine. Infect Immun 92.

29. Gopal S, Borovok I, Ofer A, Yanku M, Cohen G, Goebel W, Kreft J, Aharonowitz Y. 2005. A multidomain fusion protein in Listeria monocytogenes catalyzes the two primary activities for glutathione biosynthesis. J Bacteriol 187:3839–3847.

30. Brenner M, Friedman S, Haber A, Livnat-Levanon N, Borovok I, Sigal N, Lewinson O, Herskovits AA. 2022. Listeria monocytogenes TcyKLMN Cystine/Cysteine Transporter Facilitates Glutathione Synthesis and Virulence Gene Expression. mBio 13.

31. Korshunov S, Imlay JA. 2024. Antioxidants are ineffective at quenching reactive oxygen species inside bacteria and sould not be used to diagnose oxidative stress. Mol Microbiol 122:113–128.

32. Chen M, Zhang J, Xia J, Sun J, Zhang X, Xu J, Deng S, Han Y, Jiang L, Song H, Cheng C. 2023. *Listeria monocytogenes* GshF contributes to oxidative stress tolerance via regulation of the phosphoenolpyruvate-carbohydrate phosphotransferase system. Microbiol Spectr 11.

33. Yang J, Bai Y, Zhang Y, Gabrielle VD, Jin L, Bai G. 2014. Deletion of the cyclic di-AMP phosphodiesterase gene (cnpB) in Mycobacterium tuberculosis leads to reduced virulence in a mouse model of infection. Mol Microbiol 93:65–79.

34. Dey B, Dey RJ, Cheung LS, Pokkali S, Guo H, Lee J-H, Bishai WR. 2015. A bacterial cyclic dinucleotide activates the cytosolic surveillance pathway and mediates innate resistance to tuberculosis. Nat Med 21:401–406.

35. Ye M, Zhang J-J, Fang X, Lawlis GB, Troxell B, Zhou Y, Gomelsky M, Lou Y, Yang XF. 2014. DhhP, a cyclic di-AMP phosphodiesterase of Borrelia burgdorferi, is essential for cell growth and virulence. Infect Immun 82:1840–1849.

36. Savage CR, Arnold WK, Gjevre-Nail A, Koestler BJ, Bruger EL, Barker JR, Waters CM, Stevenson B. 2015. Intracellular Concentrations of Borrelia burgdorferi Cyclic Di-AMP Are Not Changed by Altered Expression of the CdaA Synthase. PLoS One 10:e0125440.

37. Commichau FM, Heidemann JL, Ficner R, Stülke J. 2019. Making and Breaking of an Essential Poison: the Cyclases and Phosphodiesterases That Produce and Degrade the Essential Second Messenger Cyclic di-AMP in Bacteria. J Bacteriol 201.

38. Huynh TN, Woodward JJ. 2016. Too much of a good thing: regulated depletion of c-di-AMP in the bacterial cytoplasm. Curr Opin Microbiol 30:22–29.

39. Hu J, Zhang G, Liang L, Lei C, Sun X. 2020. Increased Excess Intracellular Cyclic di-AMP Levels Impair Growth and Virulence of Bacillus anthracis. J Bacteriol 202.

40. Xayarath B, Marquis H, Port GC, Freitag NE. 2009. *Listeria monocytogenes* CtaP is a multifunctional cysteine transport-associated protein required for bacterial pathogenesis. Mol Microbiol 74:956–973.

41. Mains DR, Eallonardo SJ, Freitag NE. 2021. Identification of Listeria monocytogenes Genes Contributing to Oxidative Stress Resistance under Conditions Relevant to Host Infection. Infect Immun 89.

42. Massa SM, Sharma AD, Siletti C, Tu Z, Godfrey JJ, Gutheil WG, Huynh TN. 2020. C-di-AMP accumulation impairs muropeptide synthesis in Listeria monocytogenes. J Bacteriol https://doi.org/10.1128/JB.00307-20.

43. Kelliher JL, Grunenwald CM, Abrahams RR, Daanen ME, Lew CI, Rose WE, Sauer J-D. 2021. PASTA kinase-dependent control of peptidoglycan synthesis via ReoM is required for cell wall stress responses, cytosolic survival, and virulence in Listeria monocytogenes. PLoS Pathog 17:e1009881.

44. Pensinger DA, Gutierrez K V., Smith HB, Vincent WJB, Stevenson DS, Black KA, Perez-Medina KM, Dillard JP, Rhee KY, Amador-Noguez D, Huynh TN, Sauer J-D. 2023. Listeria monocytogenes GlmR Is an Accessory Uridyltransferase Essential for Cytosolic Survival and Virulence. mBio 14.

45. Rismondo J, Möller L, Aldridge C, Gray J, Vollmer W, Halbedel S. 2015. Discrete and overlapping functions of peptidoglycan synthases in growth, cell division and virulence of Listeria monocytogenes. Mol Microbiol 95:332–351.

46. Wemekamp-Kamphuis HH, Wouters JA, Sleator RD, Gahan CGM, Hill C, Abee T. 2002. Multiple deletions of the osmolyte transporters BetL, Gbu, and OpuC of Listeria monocytogenes affect virulence and growth at high osmolarity. Appl Environ Microbiol 68:4710–4716.

47. Do EA, Gries CM. 2021. Beyond Homeostasis: Potassium and Pathogenesis during Bacterial Infections. Infect Immun 89.

48. Schär J, Stoll R, Schauer K, Loeffler DIM, Eylert E, Joseph B, Eisenreich W, Fuchs TM, Goebel W. 2010. Pyruvate Carboxylase Plays a Crucial Role in Carbon Metabolism of Extra- and Intracellularly Replicating *Listeria monocytogenes*. J Bacteriol 192:1774–1784.

49. Zhang Y, Guo Q, Fang X, Yuan M, Hu W, Liang X, Liu J, Yang Y, Fang C. 2023. Destroying glutathione peroxidase improves the oxidative stress resistance and pathogenicity of Listeria monocytogenes. Front Microbiol 14.

50. Imlay JA. 2013. The molecular mechanisms and physiological consequences of oxidative stress: lessons from a model bacterium. Nat Rev Microbiol 11:443–454.

51. Ruhland BR, Reniere ML. 2019. Sense and sensor ability: redox-responsive regulators in Listeria monocytogenes. Curr Opin Microbiol 47:20–25.

52. Borezee E, Pellegrini E, Berche P. 2000. OppA of Listeria monocytogenes, an Oligopeptide-Binding Protein Required for Bacterial Growth at Low Temperature and Involved in Intracellular Survival. Infect Immun 68:7069–7077.

53. Ku JW, Gan Y-H. 2019. Modulation of bacterial virulence and fitness by host glutathione. Curr Opin Microbiol 47:8–13.

54. Lauer P, Chow MYN, Loessner MJ, Portnoy DA, Calendar R. 2002. Construction, characterization, and use of two Listeria monocytogenes site-specific phage integration vectors. J Bacteriol 184:4177–4186.

55. Gall AR, Hsueh BY, Siletti C, Waters CM, Huynh TN. 2022. NrnA Is a Linear Dinucleotide Phosphodiesterase with Limited Function in Cyclic Dinucleotide Metabolism in Listeria monocytogenes. J Bacteriol 204:e0020621.

56. Robinson MD, McCarthy DJ, Smyth GK. 2010. <tt>edgeR</tt> : a Bioconductor package for differential expression analysis of digital gene expression data. Bioinformatics 26:139–140.

57. Clasquin MF, Melamud E, Rabinowitz JD. 2012. LC-MS Data Processing with MAVEN: A Metabolomic Analysis and Visualization Engine. Curr Protoc Bioinformatics 37.

Appendix 3 – Preliminary Work in Further Understanding the Role of PTS During *L. monocytogenes* infection

Authors and their contributions:

Matthew J. Freeman: Planned and conducted experiments, wrote, and edited this manuscript.

Noah Eral: Planned and conducted experiments, wrote, and edited this manuscript.

John-Demian Sauer: Supervised all research and contributed to the design of experiments, edited this manuscript.

*ChatGPT-4o was used for copy editing of my original ideas and writings using the prompt: “Can you copy edit part of my thesis to use correct scientific nomenclature and formatting while improving flow?”

INTRODUCTION

As discussed extensively in Chapter 2 and the Introduction of this thesis, phosphotransferase systems (PTS) are essential for the growth and survival of *Listeria monocytogenes* in the host cytosol (1). However, the data presented thus far primarily implicate PTS in carbon acquisition and do not fully address their roles in transcriptional regulation during pathogenesis. In this appendix, I present preliminary results that begin to explore specific carbon source imported by *L. monocytogenes* PTS, additional regulatory contributions of PTS to *L. monocytogenes* virulence, and I outline experimental approaches to further interrogate these roles.

PTS systems include two core phospho-cycling proteins: HPr and EI, encoded by *ptsH* and *ptsI*, respectively (2). Importantly, EI has not been shown to directly participate in transcriptional regulation. Therefore, the virulence phenotype associated with Δ*ptsI*, as described in Chapter 2, is likely attributable to the inability to import carbon sources via PTS. Δ*ptsH*, on the other hand, was used primarily in Chapter 2 to validate the essential role of PTS in virulence (1). Although Δ*ptsI* and Δ*ptsH* mutants largely phenocopy one another in terms of attenuation, the Δ*ptsH* mutant appears slightly more attenuated and is less readily complemented by overexpression constructs (Chapter 2) (1). These observations suggest an additional role for HPr beyond its canonical function in sugar transport during virulence.

HPr-mediated transcriptional regulation is thought to be governed primarily through phosphorylation at the conserved serine-46 residue (3–5). This phosphorylation is carried out by HPr kinase (HPrK) in response to elevated intracellular levels of ATP and fructose-1,6-bisphosphate, effectively linking HPr activity to cellular energy status and glycolytic flux (2,5).

Once phosphorylated at serine-46, HPr can bind to the transcriptional regulator CcpA and co-regulate specific gene targets, mostly associated with carbon source acquisition (6–8). This mechanism has been studied extensively in the context of carbon catabolite repression and hierarchical carbon source utilization (6,9). Additionally, serine-phosphorylated HPr has been proposed to donate its phosphate group to other regulators, including PrfA, potentially influencing virulence gene expression (3). Despite these insights, the full impact of HPr abundance—and its phosphorylation state—on *L. monocytogenes* virulence remains poorly understood, both in this organism and in related bacterial pathogens (10–12).

Another unresolved question from Chapter 2 is what governs the transcriptional regulation of PTS systems during *L. monocytogenes* pathogenesis. It is broadly recognized that PTS expression is regulated by sigma factors (13–15). Among these, σ^B (encoded by *sigB*) is the most prominently studied in the context of PTS regulation is the setting of bacterial stess responses (14,16). Intriguingly, laboratory-passaged *L. monocytogenes* often accumulates mutations in *sigB*, suggesting a strong selective pressure against σ^B activity under artificial growth conditions (17). A better understanding of which PTS genes are transcriptionally up- or downregulated during infection may help identify which PTS are active during the cytosolic phase of infection, and how their activity contributes to virulence.

In this appendix, I describe preliminary data that support a regulatory role for HPr in virulence. First, we utilized BioLog phenotypic microarrays to compare carbon source utilization between wild-type *L. monocytogenes* and a Δ*ptsH* mutant. Second, we show that HPr abundance influences *L. monocytogenes* fitness: altered levels of HPr impact growth, intracellular replication, and survival. These data provide an initial list of carbon sources that may be lost in

PTS-deficient strains and potentially utilized by *L. monocytogenes* during infection. Finally, we describe a possible suppressor mutation arising in Δ*ptsI*. This mutation appears to confer a growth benefit in the absence of functional PTS but becomes detrimental when PTS systems are reactivated, suggesting compensatory metabolic rewiring. Together, these findings open new avenues for investigating how PTS components function beyond carbon transport and how their regulation influences the pathogenesis of *L. monocytogenes*. They also underscore the importance of considering both metabolic and regulatory dimensions of PTS activity in future studies.

RESULTS & DISCUSSION

Overall, the work presented in Chapter 2 of this thesis demonstrates that *Listeria monocytogenes* requires a functional phosphotransferase system (PTS) to support intracellular growth and virulence (1). However, one outstanding question is which specific carbon sources are imported via PTS and support *L. monocytogenes* replication in the host cytosol. To begin addressing this, we employed BioLog Phenotypic Microarrays (PM1 and PM2A) to screen 190 different carbon sources for differential utilization between WT and Δ*ptsH L. monocytogenes* strains (18,19). We hypothesized that a subset of carbon sources would be differentially metabolized and that some of these may also be available within the host cytosol. Surprisingly, the Δ*ptsH* mutant utilized many of the same carbon sources as WT *L. monocytogenes* (**Figure 1**). However, 20 carbon sources were used at least twofold less and statistically significantly impaird for use by the Δ*ptsH* mutant (**Table 1**). Notably, 19 of these 20 metabolites are found in human samples according to the Human Metabolome Database (**Table 1**) (20). This screen provides an

important list of candidate carbon sources that should be prioritized in future studies investigating PTS-dependent nutrient acquisition in the cytosol.

Given the differential virulence phenotypes observed between Δ*ptsH* and Δ*ptsI* mutants, we next sought to understand why Δ*ptsH* was generally more attenuated. Consistent with data from Chapter 2, *ΔptsH* exhibited significantly reduced virulence in L2 plaque assays, more so than Δ*ptsI* mutants (**Chapter 2 and Figure 2A**). Strikingly, when all known carbon acquisition pathways were deleted (*ΔuhpT/ΔglpD/Δglo/ ΔptsH*), the resulting strain was completely avirulent in the plaque assay. Similarly, *ΔptsH* was unable to replicate in macrophages, and the quadruple mutant was similarly impaired (**Figure 2B**). These results indicate that while Δ*ptsH* and Δ*ptsI* mutants share many phenotypes, Δ*ptsH* exhibits distinct and more pronounced defects. This suggests that the additional attenuation in the Δ*ptsH* mutant may be due to transcriptional dysregulation of genes involved in carbon acquisition or cytosolic stress adaptation—functions in which HPr is known to participate (9,21). To test whether these defects could be complemented, and to assess how HPr overexpression affects virulence, we cloned *ptsH* under constitutive expression using the pIMK2 vector (22). Complementation of *ΔptsH* (*ΔptsH::ptsH-C*) only partially restored virulence in plaque assays and intracellular growth, indicating that HPr function is sensitive to expression level (**Figure 2A&B**). Notably, WT *L. monocytogenes* overexpressing *ptsH* also showed reduced plaque formation, further supporting the idea that precise regulation of HPr is required for optimal virulence (**Figure 2A**). We hypothesize that overexpression leads to accumulation of unphosphorylated HPr, particularly at the regulatory serine residue, which may disrupt transcriptional control and contribute to the observed defects. This hypothesis is further supported by genetic evidence: attempts to generate a phosphorylation-incompetent HPr mutant through deletion of its respective kinase (Δ*hprK;*

LMRG_01765) in a wild-type background were unsuccessful, yet the same mutation could be readily introduced in a Δ*ptsH* background (Data not shown).

During the course of these experiments, we became aware of discrepancies between our Δ*ptsI* mutant phenotypes and those reported by the Reniere lab (1,23). Specifically, the Reniere lab *ΔptsI* strain exhibited restored intracellular growth between 5 and 8 hours post-infection, while our *ΔptsI* remained unable to grow (1,23). Additionally, their strain showed only mildly reduced plaque formation, whereas ours phenocopied WT *L. monocytogenes*. Most intriguingly, their *ΔptsI* strain became more attenuated upon complementation with a native-promoter-driven *ptsI* construct, while our strain showed no such defect when complemented using a hyperexpression construct (1,23).

To investigate whether these differences were due to distinct complementation strategies or genetic background, we obtained both the Reniere lab's *ΔptsI* and *ΔptsI::ptsI-C* strains. When we assessed them using our plaque assay, we confirmed that our and their *ΔptsI* strains, as well as our complemented strain, were all phenotypically similar to WT *L. monocytogenes* (**Figure 3**). However, their *ΔptsI* strain remained attenuated in plaque formation—even when complemented with either their native-promoter construct or our hyperexpression vector (**Figure 3**). These results led us to hypothesize that their *ΔptsI* strain carries an additional mutation that interferes with complementation.

To test this, we performed full-genome sequencing of the Reniere lab *ΔptsI* strain and its isogenic parent using Oxford Nanopore sequencing (Plasmidsaurus). Remarkably, we identified a single-nucleotide polymorphism (SNP) in the *ΔptsI* strain located 49 base pairs upstream of *LMRG_02456*, which encodes a PTS beta-glucoside EIICBA component. While the functional

impact of this mutation remains unknown, its location in a putative promoter region is striking. We hypothesize that this SNP may prevent effective complementation by altering the regulatory environment in a way that compensates for loss of *ptsI* but becomes detrimental when PTS systems are restored.

To evaluate this hypothesis, several experiments are needed. First, engineering this SNP into a WT *L. monocytogenes* background will test whether it alone can confer the observed complementation failure. Second, qPCR of *LMRG_02456* in the presence or absence of this SNP will determine whether the mutation alters expression levels. An if so, to what extent. These simple experiments could ultimately identify a PTS transporter that plays a critical role in *L. monocytogenes* pathogenesis.

In sum, this appendix provides three important insights into the role of PTS systems in *L. monocytogenes* virulence. First, we offer a preliminary, but prioritized, list of carbon sources likely imported by PTS and potentially available in the cytosol. Second, we provide evidence that tight regulation of HPr expression is essential for virulence and that increased levels of unphosphorylated HPr-Ser may be detrimental. Finally, we identify a potential suppressor mutation that appears to restore some *ΔptsI* phenotypes while being deleterious when PTS systems are functional. Understanding the function of this mutation may help uncover a previously unrecognized PTS components critical for cytosolic survival. Together, these findings provide valuable leads for future exploration of PTS regulation and function in *L. monocytogenes* intracellular pathogenesis.

MATERIALS AND METHODS

Bacterial strains and culture

All *Listeria monocytogenes* strains used for experiments in this study were in a 10403s background. All *L. monocytogenes* strains were grown overnight in BHI and at 30°C stationary for all experiments, except as described. *Escherichia coli* strains were grown in Luria broth (LB) at 37°C shaking. Antibiotics used on *E. coli* were at a concentration of 100 μg/ml carbenicillin or 30 μg/ml kanamycin when appropriate. Antibiotics used on *L. monocytogenes* were at a concentration of 200 μg/mL streptomycin and/or 10 μg/mL chloramphenicol, when appropriate. Plasmids were transformed into chemically competent *E. coli* and further conjugated in *L. monocytogenes* using SM10 or S17 *E.coli*.

Construction of strains

pLIM (from Arne Rietsche at Case Western) suicide plasmid or pKSV7 plasmid was used for generation of in frame deletions (24,25). The pPL2 integrative vector pIMK2 was used for constitutive expression of *L. monocytogenes* genes (22). pLIM and pKSV7 knockout constructs were cloned in XL1-Blue *E. coli* with 100 μg/ml carbenicillin (30μg/mL Kanamycin for pIMK2) and grown for plasmid harvest using Promega MiniPrep Kit. Harvested plasmid sequences were confirmed using was performed by Plasmidsaurus using Oxford Nanopore Technology with custom analysis and annotation. Plasmid were then shuttled into *L. monocytogenes* through conjugation with SM10 (pLIM1 and pKSV7) or S17 (pIMK2) *E. coli*. In-frame deletions of genes in *L. monocytogenes* were performed by allelic exchange using suicide plasmid pLIM as previously described with p-chlorophenylalanine as a counter selectable marker (26). Generated strains were frozen in 50:50 (glycerol:overnight culture) solution at -80°C. All mutants were

confirmed via PCR, plasmid sequencing, and whole-genome sequencing using Oxford Nanopore technology from Plasmidsaurus with custom analysis and annotation.

Cell Culture

L2 cells were all kind gifts from Daniel Portnoy (UC Berkeley). Bone marrow-derived macrophages (BMDM) were prepared from 6-to-8-week-old mice as previously described (27).

Phenotypic Microarrays

Phenotype Microarrays 1 (Cat. #12111) and 2A (Cat. #12112) were obtained from BioLog (BioLog). Plates were prepared and inoculated as previously described (18,19). OmniLog incubation was substituted with incubation at 37°C stationary. OD490 was collected for each plate at 48 hours. Data was then normalized to consumption of α-D-glucose for each strain and replicate, and averaged across triplicate. Value were clustered based on similarity using clustergrammer and plotted as a heat-map in Prism 6 (28). Data normalized to glucose was used for statistical analysis and displayed in tables. Statistics are representative of a student's T-test between two strains.

Plaque Assay

Plaque assays were conducted using a L2 fibroblast cell line grown in Dulbecco's Minimal Essential Media (DMEM) based media (Thermo Fischer: 11965092) as previously described with minor modifications for visualization and quantification of plaques (29). L2 fibroblasts were seeded at 1.2×10^6 per well of a 6-well plate, then infected at an MOI of 0.5 to obtain approximately 10-30 PFU per dish. Inoculums of *L. monocytogenes* were grown in 3mL of BHI at 30°C stationary until all strains had reached stationary phase. Colony forming units to OD_{600} ratios were determined for each strain and adjusted to ensure infection results in a comparable

MOI across strains. At 4 days postinfection, cells were stained with 0.3% crystal violet for 10 min and washed twice with deionized water. Stained wells were scanned, uploaded, and areas of plaque formation were measured on ImageJ analysis software. All strains were assayed in biological triplicate and the average plaque areas of each strain (one-well per strain were normalized to wild-type plaque size within each replicate.

Intra-macrophage growth curves

Bone marrow-derived macrophages were isolated from CL57/BL6 mice and cultured as previously described in Roswell Park Memorial Institute Medium (RPMI) based media (Invitrogen: 11875093) (30). BMDMs were plated into 60 mm dishes contain 13 degassed coverslips. BMDMs cells were infected with *L. monocytogenes* strains at a multiplicity of infection [MOI] of 0.2. Inoculums of *L. monocytogenes* were grown in 3mL of BHI at 30°C stationary until all strains had reach stationary phase. Colony forming units to OD_{600} ratios were determined for each strain and adjusted to ensure infection results in a comparable MOI across strains. After 30 minutes BMDM media was exchanged for media containing 50 μg/ml Gentamycin. Coverslips were harvested, cells lysed in pure water, bacteria rescued isotonically, and plated to quantify CFU at displayed time points. All strains were assayed in biological triplicate and data displayed is one representative biologic replicate.

Statistical Analysis

Prism 6 (GraphPad Software) was used for statistical analysis of data. Means from two groups of BioLog plates were compared with unpaired two-tailed Student's T-test. Means from more than two groups for all other assays were analyzed by one-way ANOVA test. Independently, Mann-

Whitney Test was used to analyze two group comparison of non-normal data from animal experiments. * $p < 0.05$, ** $p < 0.01$, *** $p < 0.001$ for all statistical tests displayed.

FIGURES

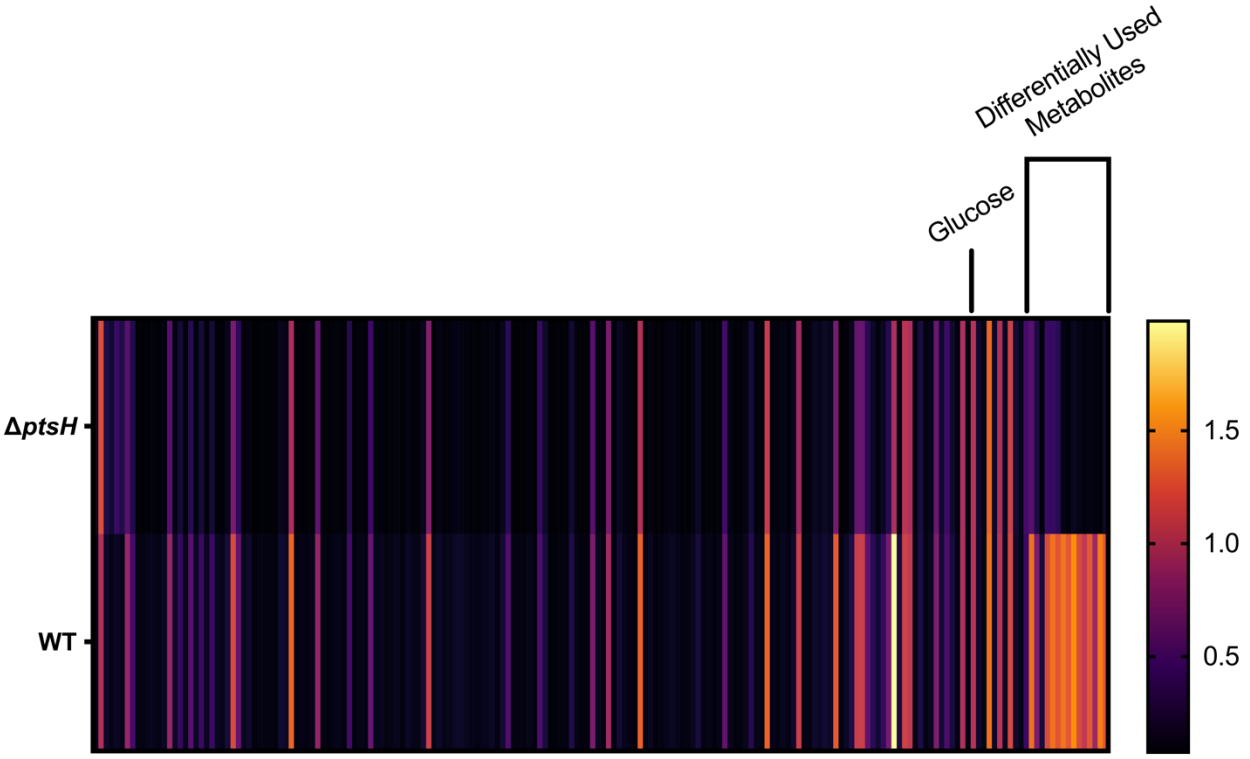

Figure 1. Carbon metabolite respiration of WT and Δ*ptsH L. monocytogenes* show differential use of PTS mediated carbon source. Clustered heatmaps indicating level of tetrazolium dye color change as measured by OD_{490} at 48 hours in response to *ΔptsH* (Top) and WT (Bottom) respiration of carbon metabolites (PM1 & PM2A) at 37°C stationary. Each bar indicates the average of 3 biologic replicates. Samples were normalized to readings of a α-D-glucose control (~1 on scale and labeled) and sorted based on cluster analysis. Select differentially used metabolites clusters are labeled above for full list see **Table 1**.

Table 1. Statistically significant and greater than 2-fold differentially used metabolites between WT and Δ*ptsH L. monocytogenes*

Metabolite	**Fold Usage (WT/*pdhC*::Tn)**	***P-value***	**In Humans?**
D-Psicose	8.91	<0.001	Yes
L-Alanyl-Glycine	2.37	<0.001	Yes
Beta-Methyl-D-Glucoside	3.48	<0.001	Yes
N-Acetyl-Beta-D-Mannosamine	7.26	<0.001	Yes
Pyruvic Acid	2.11	0.012	Yes
alpha-D-Lactose	13.99	<0.001	Yes
D-Trehalose	8.78	<0.001	Yes
Maltose	5.51	<0.001	Yes
Gentiobiose	2.85	<0.001	Yes
Beta-D-Allose	8.15	<0.001	Yes
Melibionic Acid	0.44	0.450	No
Amygdalin	8.35	<0.001	Yes
D-Melezitose	2.49	0.001	Yes
D-Arabitol	10.62	<0.001	Yes
alpha-Methyl-D-Glucoside	2.08	0.001	Yes
Turanose	2.08	0.005	Yes
Arbutin	2.48	<0.001	Yes
Xylitol	9.76	<0.001	Yes
Alpha-Methyl-D-Mannoside	3.48	0.001	Yes
Palatinose	2.08	<0.001	Yes

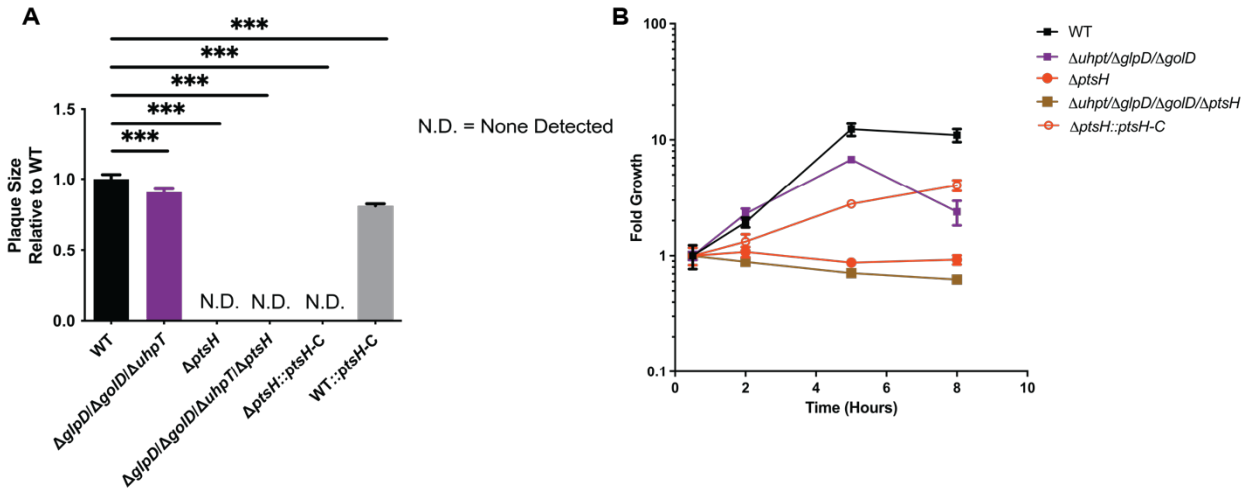

Figure 2. Δ*ptsH* are attenuated for plaquing and intracellular growth and failed complementation with *ptsH* hyperexpression. (A) L2 fibroblasts were infected with indicated *Lm* strains (MOI of 0.5) and were examined for plaque formation 4 days post infection. Data are normalized to wild-type plaque size and represent the standard deviation of the means from a single well's plaques. ND, not detected. (B) Intracellular growth of wild-type, Δ*glpD*/Δ*golD*/Δ*uhpT*, Δ*ptsH*, Δ*glpD*/Δ*golD*/Δ*uhpT*/Δ*ptsH*, and *ΔptsH::ptsH-C* was determined in BMDMs following infection at an MOI of 0.2. Growth curves are representative one independent experiments. Error bars represent the standard deviation of the means of technical triplicates within the representative experiment.

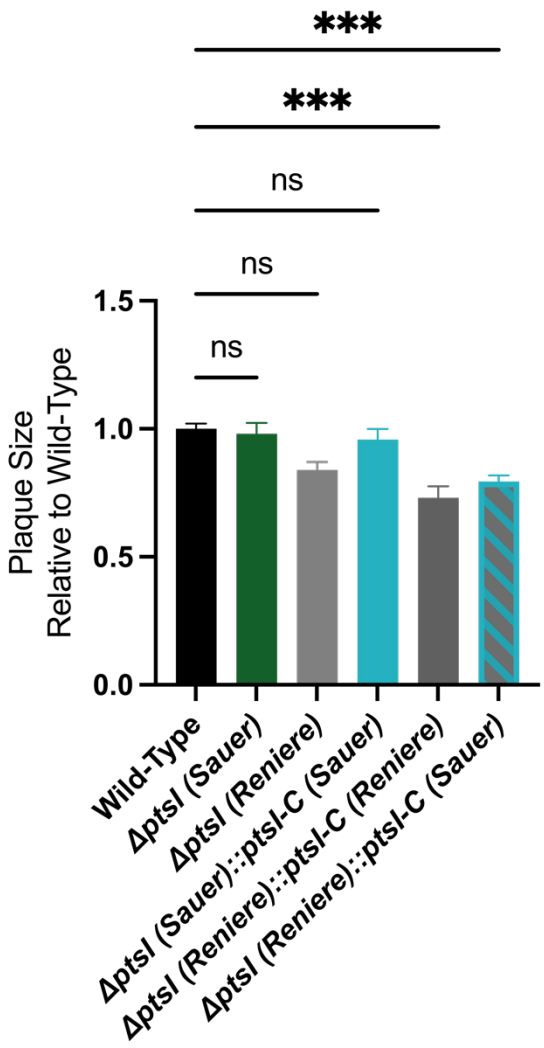

Figure 3. Sauer and Reniere Δ*ptsI* phenocopy and complementation of Reniere Δ*ptsI* via hyper- and native-expression fails to rescue plaquing. L2 fibroblasts were infected with indicated *L. monocytogenes* strains grown in Brain Heart Infusion (BHI) overnight at 30°C stationary (MOI of 0.5) and were examined for plaque formation 4 days post infection. Data from all strains (one-well per strain) are normalized to WT plaque size in each assay and the bars associated with the individual strains represents the median and SEM of the group. Assays were performed in biological replicates and data displayed is of one representative biological replicate.

* $p < 0.05$

REFERENCES

1. Freeman MJ, Eral NJ, Sauer JD. Listeria monocytogenes requires phosphotransferase systems to facilitate intracellular growth and virulence. O'Riordan MX, editor. PLoS Pathog. 2025 Apr 15;21(4):e1012492.

2. White D, Drummond JT, Fuqua C. The Physiology and Biochemistry of Prokaryotes [Internet]. Oxford University Press; 2012. Available from: https://books.google.com/books?id=ToF6pwAACAAJ

3. Woo JKK, Zimnicka AM, Federle MJ, Freitag NE. Novel motif associated with carbon catabolite repression in two major Gram-positive pathogen virulence regulatory proteins. Kolodkin-Gal I, editor. Microbiol Spectr. 2024 Nov 5;12(11):e00485-24.

4. Cochu A, Roy D, Vaillancourt K, LeMay JD, Casabon I, Frenette M, et al. The Doubly Phosphorylated Form of HPr, HPr(Ser-P)(His∼P), Is Abundant in Exponentially Growing Cells of *Streptococcus thermophilus* and Phosphorylates the Lactose Transporter LacS as Efficiently as HPr(His∼P). Appl Environ Microbiol. 2005 Mar;71(3):1364–72.

5. Nessler S, Fieulaine S, Poncet S, Galinier A, Deutscher J, Janin J. HPr Kinase/Phosphorylase, the Sensor Enzyme of Catabolite Repression in Gram-Positive Bacteria: Structural Aspects of the Enzyme and the Complex with Its Protein Substrate. J Bacteriol. 2003 Jul 15;185(14):4003–10.

6. Behari J, Youngman P. A Homolog of CcpA Mediates Catabolite Control in Listeria monocytogenes but Not Carbon Source Regulation of Virulence Genes. J BACTERIOL. 1998;180.

7. Görke B, Stülke J. Carbon catabolite repression in bacteria: many ways to make the most out of nutrients. Nat Rev Microbiol. 2008 Aug;6(8):613–24.

8. Thomasen RSS, Jespersen MG, Jørgensen K, Dos Santos PT, Sternkopf Lillebæk EM, Skov MN, et al. The Global Regulator CcpA of Listeria monocytogenes Confers Sensitivity to Antimicrobial Fatty Acids. Front Microbiol. 2022 May 3;13:895942.

9. Christensen DP, Benson AK, Hutkins RW. Mutational Analysis of the Role of HPr in *Listeria monocytogenes*. Appl Environ Microbiol. 1999 May;65(5):2112–5.

10. Yoon CK, Lee SH, Zhang J, Lee HY, Kim MK, Seok YJ. HPr prevents FruR-mediated facilitation of RNA polymerase binding to the *fru* promoter in *Vibrio cholerae*. Nucleic Acids Research. 2023 Jun 23;51(11):5432–48.

11. Pätzold L, Brausch AC, Bielefeld EL, Zimmer L, Somerville GA, Bischoff M, et al. Impact of the Histidine-Containing Phosphocarrier Protein HPr on Carbon Metabolism and Virulence in Staphylococcus aureus. Microorganisms. 2021 Feb 24;9(3):466.

12. Antunes A, Derkaoui M, Terrade A, Denizon M, Deghmane AE, Deutscher J, et al. The Phosphocarrier Protein HPr Contributes to Meningococcal Survival during Infection. Rudel T, editor. PLoS ONE. 2016 Sep 21;11(9):e0162434.

13. Paget M. Bacterial Sigma Factors and Anti-Sigma Factors: Structure, Function and Distribution. Biomolecules. 2015 Jun 26;5(3):1245–65.

14. Gaballa A, Guariglia-Oropeza V, Wiedmann M, Boor KJ. Cross Talk between SigB and PrfA in Listeria monocytogenes Facilitates Transitions between Extra- and Intracellular Environments. Microbiol Mol Biol Rev. 2019 Nov 20;83(4):e00034-19.

15. Wang S, Orsi RH, Tang S, Zhang W, Wiedmann M, Boor KJ. Phosphotransferase System-Dependent Extracellular Growth of Listeria monocytogenes Is Regulated by Alternative Sigma Factors σ^{L} and σ^{H}. Appl Environ Microbiol. 2014 Dec 15;80(24):7673–82.

16. Oliveira AH, Tiensuu T, Guerreiro DN, Tükenmez H, Dessaux C, García-del Portillo F, et al. Listeria monocytogenes Requires the RsbX Protein To Prevent SigB Activation under Nonstressed Conditions. Mullineaux CW, editor. J Bacteriol. 2022 Jan 18;204(1):e00486-21.

17. Guerreiro DN, Wu J, Dessaux C, Oliveira AH, Tiensuu T, Gudynaite D, et al. Mild Stress Conditions during Laboratory Culture Promote the Proliferation of Mutations That Negatively Affect Sigma B Activity in Listeria monocytogenes. Henkin TM, editor. J Bacteriol [Internet]. 2020 Apr 9 [cited 2025 Apr 22];202(9). Available from: https://journals.asm.org/doi/10.1128/JB.00751-19

18. Vehkala M, Shubin M, Connor TR, Thomson NR, Corander J. Novel R Pipeline for Analyzing Biolog Phenotypic Microarray Data. Aziz RK, editor. PLoS ONE. 2015 Mar 18;10(3):e0118392.

19. Luque-Sastre L, Jordan K, Fanning S, Fox EM. High-Throughput Characterization of Listeria monocytogenes Using the OmniLog Phenotypic Microarray. In: Fox EM, Bierne H, Stessl B, editors. Listeria Monocytogenes: Methods and Protocols [Internet]. New York, NY: Springer US; 2021. p. 107–13. Available from: https://doi.org/10.1007/978-1-0716-0982-8_8

20. Wishart DS, Tzur D, Knox C, Eisner R, Guo AC, Young N, et al. HMDB: the Human Metabolome Database. Nucleic Acids Research. 2007 Jan 3;35(Database):D521–6.

21. Mertins S, Joseph B, Goetz M, Ecke R, Seidel G, Sprehe M, et al. Interference of Components of the Phosphoenolpyruvate Phosphotransferase System with the Central

Virulence Gene Regulator PrfA of *Listeria monocytogenes*. J Bacteriol. 2007 Jan 15;189(2):473–90.

22. Lauer P, Chow MYN, Loessner MJ, Portnoy DA, Calendar R. Construction, Characterization, and Use of Two Listeria monocytogenes Site-Specific Phage Integration Vectors. J BACTERIOL. 2002;184.

23. Schwardt NH, Halsey CR, Sanchez ME, Ngo BM, Reniere ML. A genome-wide screen in ex vivo gallbladders identifies Listeria monocytogenes factors required for virulence in vivo. O'Riordan MX, editor. PLoS Pathog. 2025 Mar 3;21(3):e1012491.

24. Chen GY, McDougal CE, D'Antonio MA, Portman JL, Sauer JD. A Genetic Screen Reveals that Synthesis of 1,4-Dihydroxy-2-Naphthoate (DHNA), but Not Full-Length Menaquinone, Is Required for *Listeria monocytogenes* Cytosolic Survival. Swanson MS, editor. mBio [Internet]. 2017 May 3 [cited 2021 Dec 14];8(2). Available from: https://journals.asm.org/doi/10.1128/mBio.00119-17

25. Halsey CR, Glover RC, Thomason MK, Reniere ML. The redox-responsive transcriptional regulator Rex represses fermentative metabolism and is required for Listeria monocytogenes pathogenesis. O'Riordan M, editor. PLoS Pathog. 2021 Aug 16;17(8):e1009379.

26. Argov T, Rabinovich L, Sigal N, Herskovits AA. An Effective Counterselection System for Listeria monocytogenes and Its Use To Characterize the Monocin Genomic Region of Strain 10403S. Nojiri H, editor. Appl Environ Microbiol. 2017 Mar 15;83(6):e02927-16.

27. Sun AN, Camilli A, Portnoy DA. Isolation of Listeria monocytogenes small-plaque mutants defective for intracellular growth and cell-to-cell spread. Infect Immun. 1990 Nov;58(11):3770–8.

28. Fernandez NF, Gundersen GW, Rahman A, Grimes ML, Rikova K, Hornbeck P, et al. Clustergrammer, a web-based heatmap visualization and analysis tool for high-dimensional biological data. Sci Data. 2017 Oct 10;4(1):170151.

29. Smith HB, Li TL. Listeria monocytogenes MenI Encodes a DHNA-CoA Thioesterase Necessary for Menaquinone Biosynthesis, Cytosolic Survival, and Virulence. Infection and Immunity. 2021;89(5):12.

30. Sauer JD, Sotelo-Troha K, Von Moltke J, Monroe KM, Rae CS, Brubaker SW, et al. The *N* -Ethyl- *N* -Nitrosourea-Induced *Goldenticket* Mouse Mutant Reveals an Essential Function of *Sting* in the *In Vivo* Interferon Response to *Listeria monocytogenes* and Cyclic Dinucleotides. Flynn JL, editor. Infect Immun. 2011 Feb;79(2):688–94.